

PERTURBATIONS IN
NUCLEOTIDE BIOSYNTHESIS
INHIBITS *SALMONELLA* BIOFILM
FORMATION

Anna E. J. YSSEL

Supervisors:

Em. Prof. Jos Vanderleyden, KU Leuven

Prof. Hans Steenackers, KU Leuven

Members of the Examination Committee:

Prof. Paolo Landini

Dr. Dries De Maeyer

Prof. Johan Thevelein

Prof. Abram Aertsen

Prof. Christine Kirschhock (Chair)

Dissertation presented in partial
fulfilment of the requirements
for the degree of Doctor in
Bioscience Engineering

August 2017

Doctoraatsproefschrift nr. 1446 aan de faculteit Bio-ingeneurswetenschappen van de KU
Leuven

© 2017 KU Leuven, Science, Engineering & Technology, Arenberg Doctoraatsschool, W.
De Croylaan 6, 3001 Heverlee, België

Alle rechten voorbehouden. Niets uit deze uitgave mag worden vermenigvuldigd en/of openbaar gemaakt worden door middel van druk, fotokopie, microfilm, elektronisch of op welke andere wijze ook zonder voorafgaandelijke schriftelijke toestemming van de uitgever.

All rights reserved. No part of the publication may be reproduced in any form by print, photoprint, microfilm, electronic or any other means without written permission from the publisher.

Onderzoek gefinancierd met een beurs van het Erasmus Mundus action2 South Africa
(ema2SA)

Acknowledgements

First, I must express my gratitude to my promotors. Jos, thank you for always being kind and supportive. Knowing that your door was always open and that I could go to you for advice, meant a lot to me. Hans, you are a very thorough scientist and never missed any details, thank you for many fruitful brainstorming sessions, honest feedback and for motivating me to do my best. I know that with you at the steer, the Mica group will be a great success! To Team-Technicians: You are the heart and soul of the lab. David and Ami, you have helped me so much, I can never thank you enough! If I ever had my own lab, the first thing I would do is to try find technicians that are as skilled as you and as easy to get along with, but that will not be an easy task. Tine and Serge, you are very different (especially when it comes to noise level), but one thing you have in common is your never ending optimism and that helped to maintain a great atmosphere in the lab. Anita, Jos and Andre, you do so much more than keeping the lab running. Thank you for making sure we get through each day without accidentally burning the place down or forgetting to fill in some important paperwork. You made life in the lab easy. To my fellow lab-rats from the CMPG, including the more distant ones at the Bio-Incubator and the S&P “oude zakke”. So many of you went out of your way to help me solve problems in the lab, think about experimental setups and help with the microscope and so forth, but most of all I appreciate our friendly conversations. I can only hope to have such great colleagues in the future. Elien, Mizan and Bram L, thank you for the contributions that you have made to this thesis during your masters studies. I wish you all success with your own PhDs. The other members of S&P (now Mica) and the girls from the office: Lise, Ilse, Stefanie, Kenny, Maries, Bram, Erkuden, Irina, Mariya, Xabier as well as Elke and Katie. Thank you for the “gezelligheid” and the moral support; it was fun to share a space with you. Kathleen, Dries, Aminael, Yan, Bram W, Sergio, Toon and Bram VdB it was very interesting to collaborate/ work alongside you. To the members of my supervisory committee, and the professors from the CMPG, I appreciate the comments that you have given me at various meetings and seminars. To my jury members, thank you for your willingness to serve on the committee and for the provided feedback.

I have to express my gratitude to my family. Ruan, your love and support were instrumental in helping me to reach my goals and stay sane. You have always been reliable and solid. Thank you for making sure that I get a good dose of adventure at regular intervals. Annelies, you don't understand this yet, but you just make every day so bright. Mom and Dad, without you

none of this would have been possible. You made sure that I had everything that I needed (and more). To my brothers, you are the top two brothers in the world, To my “in-laws”: Maria, Antonie, Shune and tannie Rina. I thank all of you for your encouragement and support

To Marianne and Alexandra who also did their PhDs at the same time as me. I am proud of you! To all my other friends, you are great people, I am so glad that I have you in my life!

Summary

The overall goal of this project was to investigate the molecular link between nucleotide metabolism and biofilm formation, with a particular focus on pyrimidine starvation. The potential of using nucleoside based drugs as antibacterial compounds was also explored.

In order to determine which intermediates in the *de novo* pyrimidine biosynthesis pathways are required for biofilm formation, a set of single gene knockout mutants was evaluated for its ability to form biofilms. The molecular links between nucleotide biosynthesis and biofilm formation were probed by assessing the effect of disruption of nucleotide biosynthesis pathways on the expression of a diverse set of genes. Gene expression levels were measured with RNA sequencing, GFP-promoter fusions and RT-qPCR. Transcriptome profiles were analysed using a network based approach that integrates a variety of “omics” data. Furthermore metabolite analysis and mutant phenotyping were also used.

Our results indicate that pyrimidine starvation is a limiting factor for biofilm formation and that biofilm inhibition is associated with a repression of the transcription of *csgD*. Interestingly *csgD* down-regulation occurs despite an increase in c-di-GMP, which is known to stimulate biofilm formation. We explored the possible causes behind the increased c-di-GMP level and concluded that it is propelled by an increase of the precursor GTP. In fact, not only GTP but also other purine pathway intermediates showed an increased intracellular concentration. We propose that this increase is driven by an unknown factor that prevents repression of purine and PRPP biosynthesis genes by PurR.

We also explored possible mechanisms behind the down-regulation of *csgD* despite high c-di-GMP levels. Based on transcriptome data analyzed with a network-based approach, we hypothesize that the global regulator Fis is involved. Fis negatively regulates *rpoS* expression and RpoS is known to activate *csgD* transcription. Transcription of *fis* is sensitive to nucleotide availability, providing a link between pyrimidine starvation, *csgD* down regulation and biofilm inhibition.

Our results indicate that interfering with nucleotide biosynthesis and signalling is a feasible way to combat biofilms, as demonstrated with 5-FU.

Samenvatting

Het algemene doel van dit project was het onderzoeken van de moleculaire koppeling tussen nucleotide metabolisme en biofilmvorming, met bijzondere aandacht voor pyrimidine-limitatie. Het potentieel van het gebruik van nucleoside-gebaseerde geneesmiddelen als antibacteriële verbindingen werd tevens onderzocht.

Om te bepalen welke tussenproducten in de *de novo* pyrimidine biosynthese pathways nodig zijn voor biofilmvorming, werden een reeks ‘single-gene knock-out’ mutanten geëvalueerd voor hun biofilm-vormend vermogen. De moleculaire schakels tussen nucleotidebiosynthese en biofilmvorming werden onderzocht door het effect van een verstoring in de nucleotidebiosynthese pathway te beoordelen op de expressie van een brede set van genen. Genexpressieniveaus werden gemeten met RNA-sequencing, GFP-promoter fusies en RT-qPCR. De transcriptieprofielen werden geanalyseerd met behulp van een netwerk-gebaseerde aanpak die een verscheidenheid van “omics-data” integreert. Bovendien werden metabolietanalyse en mutant fenotypen gebruikt.

Onze resultaten geven aan dat pyrimidine-limitatie een beperkende factor is voor biofilmvorming en dat de biofilm inhibitie gerelateerd is met een down-regulatie van de transcriptie van *csgD*. Een interessante bevinding is dat *csgD* down-regulatie plaatsvindt ondanks een toename in het signaalmolecule c-di-GMP, dat bekend staat om biofilmvorming te stimuleren. We hebben de mogelijke oorzaken van de verhoogde c-di-GMP concentratie onderzocht en vonden dat deze gelinkt is aan een toename van de precursor GTP. In feite, werd niet enkel voor GTP, maar ook voor andere purines een verhoogde intracellulaire concentratie aangetoond. We veronderstellen dat deze stijging wordt gedreven door een onbekende factor die de repressie van purine- en PRPP-biosynthese-genen door PurR voorkomt.

We hebben ook de mogelijke mechanismen onderzocht die de down-regulatie van *csgD* kunnen verklaren, ondanks de hoge c-di-GMP concentraties. Op grond van transcriptome data geanalyseerd met een netwerk-gebaseerde benadering, veronderstellen we dat de “globale regulator” Fis betrokken is. Fis oefent een negatieve regulatie uit op de *rpoS* expressie en RpoS staat bekend om *csgD* transcriptie te activeren. Transcriptie van *fis* is gevoelig voor nucleotide beschikbaarheid, wat een link voorziet tussen pyrimidine-limitatie, *csgD*-regulatie en inhibitie van biofilmvorming.

Onze resultaten wijzen erop dat interferentie met nucleotide biosynthese en “signalling” een haalbare manier is om biofilmen te bestrijden, zoals aangetoond met 5-FU.

.

List of abbreviations

3D	Three-dimensional
5-FC	5-Fluocytosine
5-FU	5-Fluorouracil
AI-2	Autoinducer-2
CFU	Colony forming unit
CMPG	Centre of Microbial and Plant Genetics
COG	Clusters of orthologous genes
CW	Calcofluor White
EPS	Extracellular polysaccharides
FC	Fold change
LC	Liquid chromatography
LB	Lysogeny Broth
LPS	Lipopolysaccharides
mRNA	Messenger RNA
MS	Mass Spectrometry
NNADs	Nucleoside and nucleotide analog drugs
NTS	Non-typhoidal <i>Salmonella</i>
OD	Optical density
ONC	Overnight culture
ORF	Open reading frame
PRPP	Phosphoribosyl pyrophosphate
qRT-PCR	Quantitative real-time polymerase chain reaction

rRNA	Ribosomal RNA
SAM	S-adenosyl-methionine
SD	Standard deviation
SPI	<i>Salmonella</i> pathogenicity island
sRNA	Small RNA
TF	Transcription factor
tRNA	Transfer RNA
TS	Typhoidal <i>Salmonella</i>
UTR	Untranslated region
WT	Wild type

Table of contents

Acknowledgements	i
Summary	iii
Samenvatting	v
List of abbreviations	vii
Chapter 1	1
1 A general introduction to <i>Salmonella</i> and biofilm formation and outline of the thesis ..	1
1.1 Abstract	1
1.2 Aim and scope of thesis	1
1.3 Introduction	2
1.3.1 <i>Salmonella</i> taxonomy	2
1.3.2 Clinical and economic relevance of NTS <i>Salmonella</i> infections	4
1.4 Biofilm formation	6
1.4.1 Biofilm associated problems	6
1.4.2 The switch to a biofilm mode of life	7
1.4.1 Relevance of <i>Salmonella</i> biofilms	8
1.5 Models for studying biofilm formation	10
1.5.1 Congo red Agar	10
1.5.2 Calcofluor agar	11
1.5.3 Crystal violet staining	12
1.5.4 Fluorescent probes that bind specific EPS structures	13
1.6 Regulation of <i>Salmonella</i> biofilm formation	13
1.6.1 CsgD, the master regulator	15
1.6.2 Coordinating motility, virulence and biofilm formation	16
1.7 Concluding remarks	17
Chapter 2	19
2 The importance of nucleotides in biofilm formation	19
2.1 Abstract	19
2.2 Background	19
2.2.1 Introduction to the purine and pyrimidine biosynthesis	19
2.2.2 Purine synthesis and regulation	21
2.2.3 Pyrimidine synthesis and regulation.....	26

2.3 The role of nucleotide biosynthesis in biofilm formation	34
2.3.1 Nucleotide derived second messengers	36
2.3.2 The role of c-di-GMP signaling in <i>Salmonella</i>	46
2.3.3 Regulation of biofilm formation by c-di-GMP in <i>Salmonella</i>	49
Chapter 3	55
3 Repurposing of nucleoside- and nucleobase-derivative drugs as antibiotics and biofilm inhibitors	55
3.1 Abstract	55
3.2 Introduction	55
3.2.1 Nucleobase and nucleoside analogs have been in clinical use for several decades	56
3.2.2 Repurposing NNADs could overcome hurdles in drug discovery	57
3.3 Examples of approved NNADs with activity against bacteria	61
3.3.1 5-Fluorouracil	61
3.3.2 5-Fluorocytosine	64
3.3.3 5-Azacytidine	65
3.3.4 Azathioprine and 6-Mercaptopurine	68
3.3.5 Caffeine	69
3.3.6 Azidothymidine	68
3.3.7 Gemcitabine	70
3.4 Resistance development against NNADs	71
3.4.1 NNADs can have multiple targets within the bacterial cell	72
3.4.2 Combining treatment with antibiotics can prevent the establishment of resistance against NNADs	72
3.4.3 Mutations providing resistance to NNADs are potentially disadvantageous	73
3.4.4 NNADs can inhibit biofilm formation without impacting growth	73
3.5 Conclusion	73
Chapter 4	81
4 Pyrimidine starvation inhibits biofilm formation despite high c-di-GMP levels.....	81
4.1 Abstract	81
4.2 Introduction	81
4.3 Results	84
4.3.1 Pyrimidine starvation is a limiting factor for biofilm formation	84
4.3.2 UDP glucose levels are unaffected by pyrimidine starvation	90
4.3.3 A lack of pyrimidines is associated with an increase in c-di-GMP	91

4.4 Conclusion	92
4.5 Materials and Methods	93
4.5.1 Bacterial strains and growth conditions	93
4.5.2 Construction of deletion and complementation mutants	92
4.5.3 Phenotypic switching between planktonic and biofilm mode of growth.....	96
4.5.4 Assaying biofilm formation	97
4.5.5 Microscopy	98
4.5.6 Metabolite extraction and mass spectrometry analysis	98
Chapter 5	101
5 The impact of pyrimidine starvation on the transcriptome	101
5.1 Abstract	101
5.2 Introduction	101
5.3 Results	103
5.3.1 Pyrimidine limitation affects global regulators	105
5.3.2 Pyrimidine starvation leads to an increase in c-di-GMP	112
5.3.3 Pyrimidine starvation impacts the transcription of <i>csgD</i>	121
5.3.4 Other processes that are affected by pyrimidine starvation	130
5.4 Conclusion	134
5.5 Materials and Methods	136
5.5.1 Bacterial strains and growth conditions	136
5.5.2 Construction of deletion and complementation mutants	137
5.5.3 Temporal quantification of gene transcription	137
5.5.4 Metabolite extraction	138
5.5.5 Experimental setup for RNA extraction	139
5.5.6 RNA extraction	139
5.5.7 RNA sequencing	140
5.5.8 Transcriptome assembly and analysis	140
5.5.9 Network based- analysis	140
5.5.10 Primer extension analysis	141
Chapter 6	143
6 Prevention of <i>Salmonella</i> biofilm formation by 5-FU	143
6.1 Abstract	143
6.2 Introduction	143

6.3 Results.....	144
6.3.1 5-FU inhibits <i>Salmonella</i> biofilm formation.....	144
6.3.2 Differential gene expression in response to 5-FU treatment	145
6.4 Conclusion	146
6.5 Materials and methods	147
6.5.1 Assaying biofilm formation	148
6.5.2 High throughput biofilm assay	149
6.5.3 Microscopy	149
6.5.4 Temporal quantification of gene transcription	149
6.6 Acknowledgements	150
Chapter 7	151
7 Concluding remarks	151
7.1 General conclusion	151
7.1.1 Nucleotides and biofilm formation	151
7.1.2 Possible polar effects on <i>carB</i> due to <i>carA</i> deletion	154
7.2 Future perspectives	154
7.2.1 Linking <i>fis</i> expression and nucleotide levels to biofilm formation	154
7.2.2 Regulatory interplay between the purine and pyrimidine pathways	155
7.2.3 Partitioning of nucleotide resources during biofilm formation	156
7.2.4 Screening NNADs	156
7.2.5 Effect on virulence	156
7.3 Final remarks	157
Appendix	159
List of references	191
List of publications	225

Chapter 1

1 A general introduction to *Salmonella* and biofilm formation and outline of the thesis

1.1 Abstract

Members of the *Salmonella* genus are important food borne pathogens causing gastrointestinal infections in humans and animals. Members of this genus have the ability to switch between free-living planktonic growth and multicellular biofilm-based growth. Because biofilms provide protection against various stresses, the ability to form biofilms contributes to survival inside the host as well as in the environment. In the food processing and agricultural industries, *S. Typhimurium* biofilm formation is particularly relevant with regard to food-safety. A better understanding of the processes involved in regulating *S. Typhimurium* biofilm formation facilitates the development of improved prevention methods. The process of biofilm formation is complex, and regulation involves many different components.

1.2 Aim and scope of thesis

This thesis explores the role that pyrimidine metabolism plays in the transitioning from free-living to biofilm growth. These new insights might facilitate the development of new drugs, so called anti-biofilm agents, which work by targeting the nucleotide biosynthesis pathways. Also evaluated is the potential of using nucleoside and nucleotide analog drugs as antibacterial and antibiofilm agents.

Understanding the molecular basis of phenotypes is a central problem in biology. However, revealing the underlying mechanisms has proven to be non-trivial, as changes in a specific phenotype may result from perturbations of many pathways, any of which may contribute very little to the observed phenotype on its own. Network based approaches have proven to be very useful when searching for mechanistic insights (Janga & Contreras-Moreira, 2010; Ruan *et al.*, 2010; DeMaeyer *et al.*, 2013; Mulas *et al.*, 2017). Here we have used PheNetic (available at <http://bioinformatics.intec.ugent.be/phenetic2>), a sub network inference algorithm to reconstruct the mechanistic interactions at play in inducing pyrimidine-dependent biofilm formation.

Chapter 1 introduces the importance of *Salmonella* and our current understanding of *Salmonella* taxonomy. The impact of biofilms in the clinical and industrial environments, and

the state of the-art techniques used for studying biofilms are discussed. Factors involved in regulating the switch from free-living to biofilm-based growth are also introduced. Chapter 2 introduces the role of nucleotides and nucleotide derived signalling molecules in biofilm formation and other physiological processes. In Chapter 3 the prospect of using nucleoside- and nucleotide analogues to combat biofilm formation are discussed in the form of a review article (Yssel *et al.*, 2017). Chapter 4 to 5 summarizes the results obtained during the course of the author's doctoral studies. In Chapter 4 the phenotypic effects of pyrimidine starvation on the biofilm phenotype is discussed, while Chapter 5 explores the regulatory mechanisms behind the observed effects. In Chapter 6 the potential of using 5-FU (known to disrupt nucleotide pool sizes) against *Salmonella* biofilm formation is investigated. Future perspectives, shortcomings and conclusions appear in Chapter 7.

1.3 Introduction

1.3.1 *Salmonella* taxonomy

Members of the *Salmonella* genus are characterized by their motility, rod-shape, inability to form spores and Gram-negative cell walls, furthermore they are chemotrophs and facultative anaerobes. Members of the *Salmonella* genus are often pathogenic to humans and/ or animals and can cause intestinal or systemic infections. *Salmonellae* are part of the family Enterobacteriaceae, the phylum Proteobacteria and the class γ -proteobacteria and are closely related to *Escherichia*. One of the most important differences between *Salmonella* and *Escheirchia* is that the typical *Salmonella* genome contains a large number of additional virulence genes located on pathogenicity islands. This bestows *Salmonella* with the ability to invade epithelial cells and to survive within phagocytic cells (Hensel *et al.*, 1997; Folkesson *et al.*, 1999; Ochman *et al.*, 2000; Folkesson *et al.*, 2002; Winfield & Groisman, 2004; Haneda *et al.*, 2009). The *Salmonella* genus can be divided into two species, *S. bongori* and *S. enterica*. The *S. enterica* species is further subdivided into six subspecies: (I) *enterica*, (II) *salamae*, (IIIa) *arizonae*, (IIIb) *diarizonae*, (IV) *houtenae* and (V) *indica* (Brenner *et al.*, 2000; Jenkins & Gillespie, 2006). Before the advent of PCR and DNA sequencing the subspecies were further subdivided into serovars based on the Kauffmann-White-Le Minor scheme which evaluates the presence or absence of O-, H-, and surface-antigens. More recently, genetic methods have been used to give a more accurate determination of the evolutionary relationships between serovars (Boyd *et al.*, 1996; Cai *et al.*, 2005; Dilmaghani *et al.*, 2010; Soler-Garcia *et al.*, 2014; Zhao *et al.*, 2015). Nearly all *Salmonella* isolates from homoeothermic hosts are members of the *enterica* subspecies. Only serovars of the *enterica*

subspecies are given names (for example *Salmonella enterica* subspecies *enterica* serovar Paratyphi). Serovars belonging to other subspecies are denoted by their antigen typing formulas. Based on the clinical manifestation of infection, *Salmonella* serovars can be divided into two main groups. Typhoidal *Salmonella* (TS) and non-typhoidal *Salmonella* (NTS). TS infections are systemic in nature and are characterized by high fever. TS infections are typically caused by *S. Typhi* or *S. Paratyphi*. NTS infections result in acute, self-limiting (in most cases) gastroenteritis and are usually caused by *S. Enteritidis* and *S. Typhimurium*. Strains that cause TS infection are often host-restricted and share pseudogenes that relate to genes involved in causing virulence and gastroenteritis, which supports the hypothesis that pseudogene formation occurs during adaptation to a specific niche (Jacobsen *et al.*, 2011).

The strains *S. Typhimurium* LT2, ATCC14028 and SL1344 are commonly used laboratory strains. These strains mainly differ with regard to certain prophages in their chromosomes (Figueroa-Bossi *et al.*, 2001). For this work, *S. Typhimurium* ATCC14028 is used as model organism. The complete genome sequence of this strain has been published in 2010 (Jarvik *et al.*, 2010). ATCC14028 is a descendant of CDC 60-6516, a strain isolated in 1960 from pools of hearts and livers of 4-week-old chickens. Originally, ATCC14028 has been typed as LT2, based on phage sensitivity. However, the two strains were isolated decades apart making their genealogy and relationship vague. Analysis that is more recent predicted that they diverged from each other between 3000 to 9000 years ago (Jarvik *et al.*, 2010).

1.3.2 The *Salmonella enterica* pan-genome

Changes to the *Salmonella* genome during niche adaptation can occur *via* horizontal gene transfer, rearrangement, duplication, gene excision and pseudogene formation (Bäumler, 1997; Abby & Daubin, 2007; Jacobsen *et al.*, 2011). Pan-genome analysis can provide insights into the genetics underlying host-preference and/or host-specificity of the different serovars (Abby & Daubin, 2007) .

The pan-genome/ supra-genome is defined as the full complement of genes from all the sequenced strains of the same clade (Rouli *et al.*, 2015). The pan-genome is composed of the core/universal genome (the genes common for all strains), the unique genome (the strain specific genes known as ORFans) and the periphery (genes that are present in a subset of strains) (Lapierre & Gogarten, 2009; Gordienko *et al.*, 2013). The *Salmonella* pan- and core-genomes were estimated based on 35 sequenced genomes (Figure 1 and Figure 2). The core genome of 35 sequenced *Salmonellas* contains 2,811 gene families, and the pan-genome 10,015. Hypothetically speaking, if all the genomes were of the same size and each unique

gene family occurred only once, then the unique portion of gene families would be 10% for each hypothetical strain and the core genome would make up the remaining 90%. The corresponding numbers within the *S. enterica* subsp. *enterica* are 3,224 and 9,16. Note that the core genome becomes larger for the smaller sub-group, because some of the smaller group's core genes are absent from other members of the larger group (Jacobsen *et al.*, 2011). The *Salmonellae* were found to have quite high similarity in protein sequences and the identity between the genomes within *Salmonella* subsp. *enterica* ranges from 65% to 99%. It was concluded that the *Salmonella* core-genome is quite large compared to that of other bacterial genera and that the pan-genome is relatively small. Certain pathogenicity islands were found only in specific serovars where they undoubtedly play an important role in providing the genomes that host them with characteristic phenotypes. In addition to the *Salmonella* specific genomic islands, other genomic islands were also identified. Many of these were found to be of viral-origin and were strain-specific. Thus, genomic islands are important during *Salmonella* evolution and niche-adaptation (Jacobsen *et al.*, 2011). Without a doubt, differences in the non-coding regions of strains that share very high similarity in protein coding genes would also have some impact on the phenotypic differences of closely related strains, because these differences may influence the regulation of gene expression.

1.3.3 Clinical and economic relevance of NTS *Salmonella* infections

Salmonella is of significant clinical relevance in both developing and developed countries, where it is one of the most frequent causative agents of food-borne diseases and is a major cause of gastrointestinal illness (Vaagland *et al.*, 2004; Vojdani *et al.*, 2008; Majowicz *et al.*, 2010; Kozak *et al.*, 2013; Fàbrega & Vila, 2013). According to information published on the Center for Disease Control (CDC) website (<http://www.cdc.gov/Salmonella/general/index.html>) approximately 1.2 million illnesses and approximately 450 deaths occur due to NTS annually in the United States. These numbers could be much higher if one takes into account unreported or misdiagnosed cases. Children, the elderly and those with a weakened immune system are most at risk of severe infections.

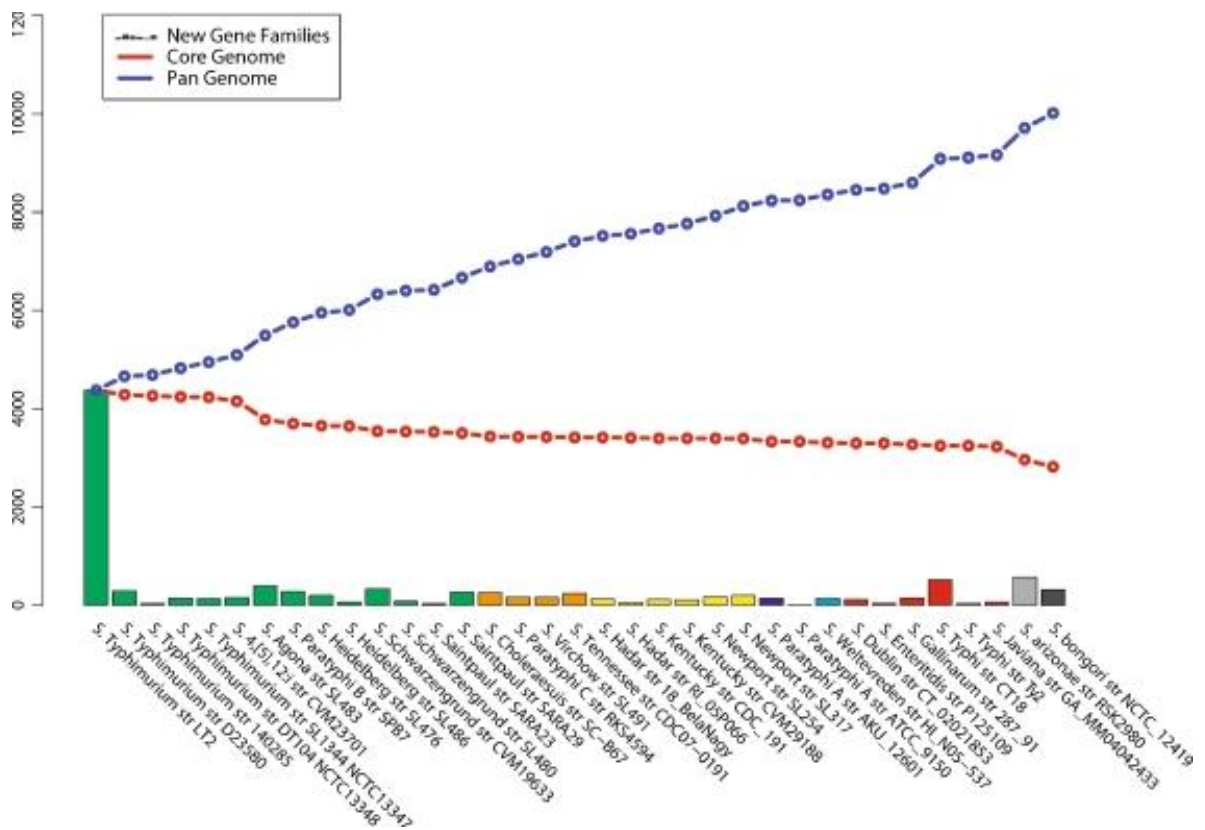


Figure 1 Pan- and core genome plot of 35 *Salmonella* strains. The red and blue lines show the progression in the core and pan genomes, as more and more genomes are considered. The columns indicate the amount of novel gene families encountered. The color of the columns represents the associated serogroup (Jacobsen et al., 2011).

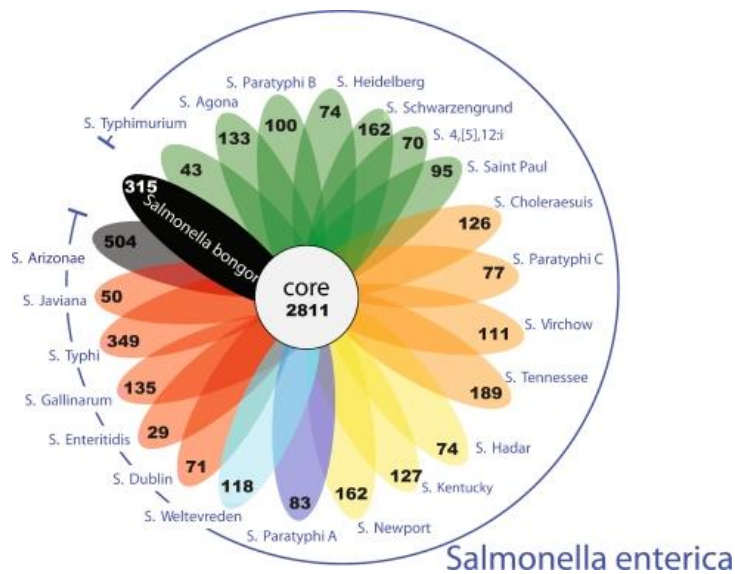


Figure 2 Flowerplot of unique gene families in each *Salmonella* serovar. The figure presents the average number of gene families found in each genome as being unique to the serovar. Also given is the size of the core genome. The colour of the petals represents the *S. enterica* serogroups (Jacobsen et al., 2011).

1.4 Biofilm formation

1.4.1 Biofilm associated problems

Bacteria can switch between a free-living planktonic lifestyle, which enables them to explore aquatic environments to a sessile multi-cellular biofilm mode of life that provides them with protection from several stressors and other advantages not associated with the planktonic lifestyle. Usually biofilms can be found on solid surfaces that are submerged or exposed to liquid, but they can also form floating mats on the surfaces of liquids. Under propitious conditions (such as in nutrient-sufficient ecosystems) bacteria are predominantly associated with biofilms (Stoodley *et al.*, 2002). Many bacterial species also form biofilms in response to various stress conditions (Lapaglia & Hartzell, 1997; Otto & Silhavy, 2002; Boehm *et al.*, 2009; Landini, 2009). Although beneficial biofilms do exist, for example the fungal and lactic acid biofilms used for making fermented Kombucha tea (Jayabalan *et al.*, 2014) or the activated sludge found in wastewater treatments (Sanz & Köchling, 2007), very often biofilms are detrimental to human health and industry. According to a public announcement by the National Institutes of Health (<https://www.nih.gov>), over 80% of microbial infections are biofilm associated. Biofilm infections include pneumonia in cystic fibrosis patients, dental caries, chronic wounds, chronic ear-infections and catheter- and implant-related infections (Costerton *et al.*, 1987; Passerini *et al.*, 1992; Costerton *et al.*, 1999; Bjarnsholt, 2013). The biofilm mode of life has been stated as a contributing cause of emerging (multi)drug-resistance to disinfectants, antibiotics and sanitizers due to the protection of the biofilm matrix and adaptation mechanisms of the bacterial cells in the biofilms, see reviews by (Gilbert & Brown, 1995; Mah & O'Toole, 2001; Stewart, 2002). Mechanisms by which biofilms can confer protection against antibiotics are summarized in Figure 3. In the food sector, biofilms are particularly problematic in green houses, breweries, meat- and dairy-processing factories. In these environments they compromise food safety and cause damage to equipment (for example by blocking pipes) and so cause significant economic losses (Simões *et al.*, 2010).

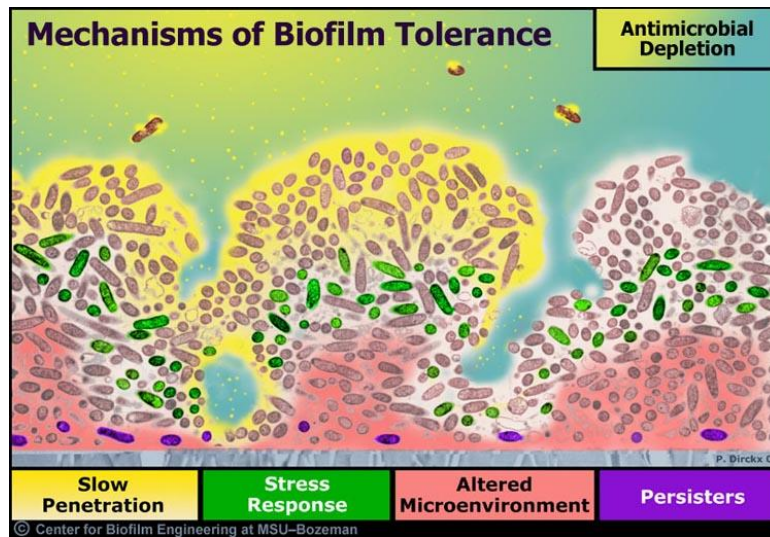


Figure 3 Diagram illustrating five mechanisms by which biofilms can contribute to antibiotic tolerance to antimicrobial agents. Image credit Phil Stewart, Peg Dirckx (2011). This image is used with permission of Montana State University Center for Biofilm Engineering.

1.4.2 The switch to a biofilm mode of life

Bacteria that are living in biofilms are substantially different to their free-living counterparts with respect to their morphological appearance, metabolic state and physiology (Valentini, Filloux 2016, JW, Z *et al.* 1995, Stoodley, Sauer *et al.* 2002). The defining feature of the biofilm mode of life is the production of an extensive extracellular matrix which includes polysaccharide components, surface-associated proteins and extracellular DNA (eDNA) (Costerton *et al.*, 1987; O'Toole *et al.*, 2000; Davey & O'Toole, 2000; Landini, 2009). The exact composition of the biofilm matrix depends on the bacterial species and environment. Biofilms can be made up of single- as well as mixed-species and the self-produced matrix can constitute up to 90% of the mature biofilm biomass (Flemming & Wingender, 2010). The biofilm matrix renders bacteria more resistant to UV stress, desiccation, antibiotic treatment, host-defenses and heat-stress amongst others. Furthermore the biofilm matrix also functions as an external digestive system by keeping extracellular enzymes in close proximity to the cells and so facilitates the metabolism of dissolved, colloidal and solid biopolymers (Flemming & Wingender, 2010). Sauer and colleagues (Sauer *et al.*, 2002) have identified 5 stages of biofilm development: (i) reversible attachment, (ii) irreversible attachment, (iii) maturation-1, (iv) maturation-2, and (v) dispersion. Each phase has a characteristic stage-specific physiology.

Van Puyvelde studied the dynamics of *Salmonella* biofilm formation in a petri-dish setup that allowed for separate analysis of free-living planktonic cells in the liquid phase and surface

attached biofilm cells (Van Puyvelde, 2014). The CFUs in each phase were determined at discrete time points over a course of 24 hours Figure 4. It was observed that the phenotypic switch from the planktonic lifestyle to biofilm based growth occurred at a distinct time interval (in this case, 8 – 10 hours post incubation). Initially the planktonic growth curve shows an exponential increase in cell numbers. Then there is a levelling off-phase, similar to the standard growth curves of shaking liquid cultures. However, after reaching a maximum, the number of planktonic CFUs starts to decrease. This coincides with a marked increase in the number of biofilm CFUs, suggesting that individual planktonic cells make the transition to the biofilm fraction. The biofilm fraction does not only increase due to additional planktonic cells that make this transition, but also because of cell division occurring within the biofilm. Inspection of the total CFUs (combination of biofilm and planktonic cells) at each time point, revealed that a fraction of cells become non-viable during the switch phase. Live-dead staining revealed that these cells belong to the planktonic fraction that does not join the biofilm fraction.

In the case of *Salmonella*, whose lifestyle is characterized by periods of host colonization followed by periods outside the host, the ability to form biofilms contributes to its resistance and persistence in both host and non-host environments, as discussed below.

1.4.3 Relevance of *Salmonella* biofilms

Salmonella can form biofilms on plastic, glass, cement, rubber, stainless steel, plant surfaces, epithelial cells and gallstones, for a review see (Steenackers *et al.*, 2012). The most important structural components that play a role during *Salmonella* biofilm formation include cellulose, curli fimbriae, BapA, flagella, fatty acids, O-antigen capsule and colanic acid. The importance and presence of these structural components vary according to the surface on which the biofilms are grown and the prevailing environmental conditions.

Typhoid fever-causing *Salmonella* have no known environmental reservoir and the chronic asymptomatic carrier state, where approximately 2-5% of typhoid patients do not fully clear the infection after recovery from acute typhoid fever, is thought to be centrally important for maintaining the presence of TS within human populations. Chronic carriers shed the bacteria into the local environment aiding the spread of the disease (Gunn *et al.*, 2014). NTS strains have also been linked to infrequent persistent human infection (between 0.15-3.9% of patients treated for acute infection continue to shed NTS bacteria after recovery), although the duration of carriage is shorter than that of TS chronic infections (Musher & Rubenstein, 1973; Gonzalez-Escobedo *et al.*, 2011; Gunn *et al.*, 2014). Evidence suggest that chronic TS- and

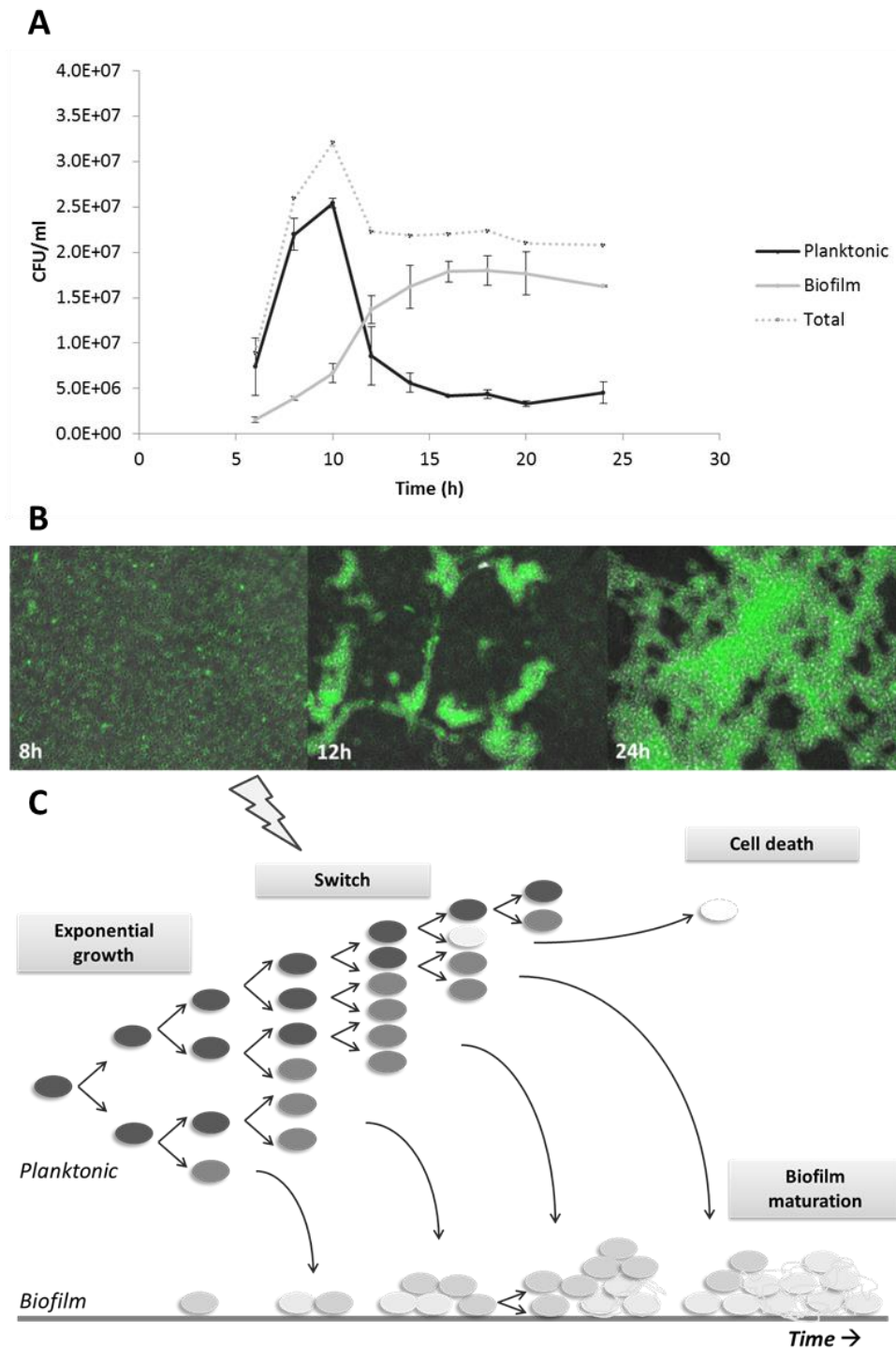


Figure 4. Panel A: This graph shows a clear switch from predominantly planktonic to biofilm growth around 8-12 h after inoculation. Panel B: Fluorescence microscopy images after 8, 12 and 24 h of *Salmonella* biofilms formation revealed the presence of no, initial and more mature biofilms at these time points. Panel C: During exponential, planktonic growth individual cells begin forming biofilm. Biofilm mass increases over time due to the transition of planktonic cells and replication of the biofilm cells themselves.

NTS-infections are both associated with biofilms on gallstones (Musher & Rubenstein, 1973; Buchwald & Blaser, 1984; Cruickshank & Humphrey, 1987).

After passing through the host's digestive system, *Salmonella*'s ability to form biofilms on abiotic surfaces enhances its survival in the often nutrient-poor hostile environment. In four out of six households where a family member recently suffered an attack of NTS, *Salmonella* cells persisted in the scaly biofilms adhering to the toilet bowls for up to four weeks, despite sanitation measures. However, *Salmonella* cells were not isolated from areas that are normally dry, such as toilet seats and flush handles. This indicates that *Salmonella* biofilms provide a considerable risk of spreading infective NTS to people who share bathroom facilities (Barker & Bloomfield, 2000). A large number of NTS outbreaks are linked to the consumption of contaminated agricultural produce (Barak *et al.*, 2008). Microscopy analyses have revealed that salad leaves harbour a high number of bacteria, typically 10^5 per square millimetre, and that the bacteria are present in complex 3D aggregations. Moreover, washing of the salad leaves had a very small effect on the number of adherent bacterial cells (Warner *et al.*, 2008). Since the survival of *Salmonella*, and other pathogens, on abiotic as well as biotic surfaces is largely reliant on their ability to produce biofilms, it is of great importance to get molecular insights into the process of biofilm formation and to use this knowledge to design effective treatments and preventative strategies. The following sections give a brief overview of various models for studying biofilm formation as well as factors involved in the regulation of *Salmonella* biofilm formation.

1.5 Models for studying biofilm formation

1.5.1 Congo red Agar

When grown at temperatures below 30°C in low salt medium *S. Typhimurium* and *E.coli* produces the exopolysaccharide components cellulose and amyloid curli fibers. The production of these components influences the colony appearance on Congo red agar (Figure 5). Colonies that produce cellulose appear pink, dry and rough (pdar). Colonies that produce curli fimbriae appear brown dry and rough (bdar). When both curli and cellulose are produced the morphology is red dry and rough, while the absence of both matrix components result in a smooth and white (saw) morphotype (Römling, 2001; Römling, 2005). In addition to curli fimbriae and cellulose, the rdar biofilm of *S. Typhimurium* is composed of other components which include the O-antigenic capsule, the large surface protein BapA, lipopolysaccharide and capsular polysaccharide (see reviews by (Steenackers *et al.*, 2012; Ahmad, 2013; Simm *et al.*, 2014). The rdar morphotype and the regulator CsgD have been shown to be important for environmental adaptation, the survival of long term desiccation, adherence to and colonization of plant- and tumour-tissue and bacterial-host interactions (Barak *et al.*, 2005; Barak *et al.*,

2008; Brandl *et al.*, 2011; Aviles *et al.*, 2013; Ahmad, 2013). The production of an ample extracellular matrix, consisting of proteinaceous and exopolysaccharide components protects enclosed bacterial cells from adverse environmental conditions and so contributes to the persistent character of bacterial biofilms. The various morphotypes on CR agar provide a convenient way to assess the production of critical biofilm components. The rdar morphotype can be divided into three distinct zones (with some further subdivision within zones) which correspond to different developmental stages within the biofilm in which curli and cellulose production varies (Serra *et al.*, 2013a; Serra *et al.*, 2013b). This characteristic of displaying different developmental zones (Figure 6) makes the rdar morphotype a practical model to study biofilm development (Ahmad, 2013; Serra *et al.*, 2013b).

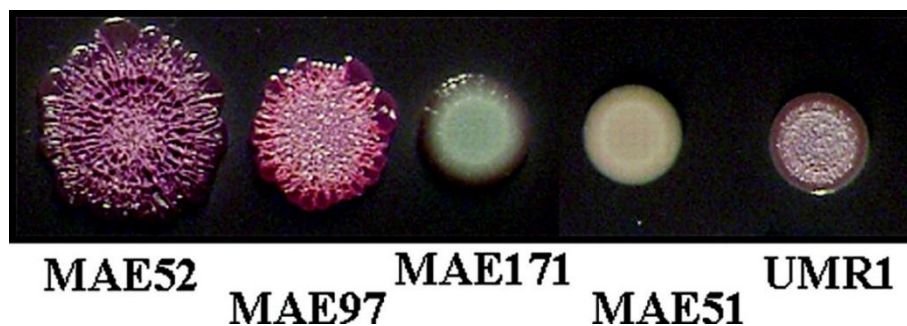


Figure 5. Morphotypes of *S. Typhimurium* expressing different matrix components from left to right: Semi-constitutive rdar morphotype (MAE52 [UMR1 P_{csgD1}]) with curli and cellulose. A pdar morphotype (MAE97 [MAE52 Δ csgBA102]) that is cellulose positive and curli negative. A bdar morphotype (MAE171 [MAE52 Δ bcsA102]) which is curli positive but cellulose negative. A saw morphotype (MAE51 [UMR1 P_{csgD2csgD101}]) that is negative for cellulose and curli fimbriae. Finally a regulated rdar morphotype (UMR1 [wild type]). Image obtained from (Simm *et al.*, 2007) is reproduced with permission of the author.

1.5.2 Calcofluor agar

Calcofluor White (CW) is a fluorescent stain that binds strongly to structures containing 1-4- β -D-glucan-based polysaccharides (Herth & Schnepf, 1980; Wood, 1980). The presence or absence of extracellular cellulose can conveniently be assessed by growing *Salmonella* on LB-no salt agar containing 0.025% CW and observing colony fluorescence under UV light (Zogaj *et al.*, 2001). *S. enterica* strains that are deficient in cellulose production, as determined by CW staining were also found to exhibit poor attachment to *Aspergillus niger* hyphae and chitin beads (Brandl *et al.*, 2011). These results are an indication that differences in cellulose production under laboratory conditions are also applicable in *in situ* conditions and that Calcofluor staining is a reliable method to measure these differences.

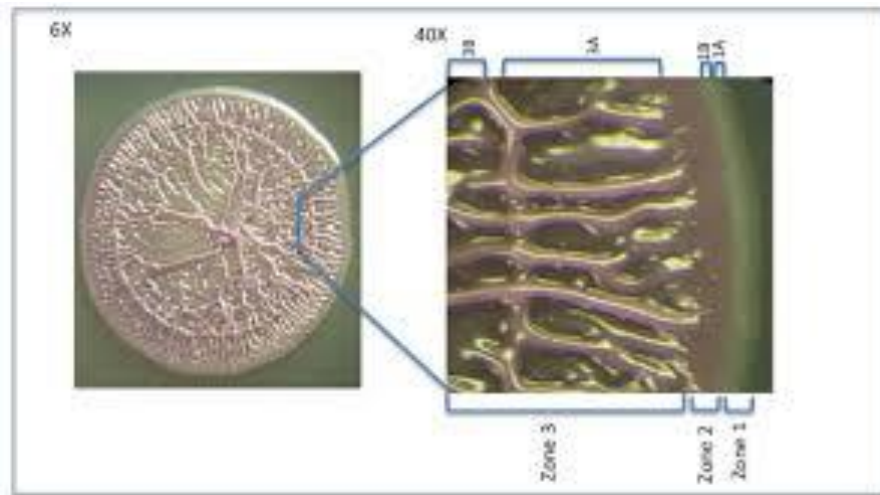


Figure 6 Stereo microscopic image of a typical rdar colony morphotype of *S. Typhimurium*. The rdar colony is surrounded by a thin white and smooth zone (zone 1), which is the zone containing the youngest generations of cells. This zone can be divided into two distinct subzones, the outer most transparent subzone 1A and inner white subzone 1B. Curli and cellulose fibers are not secreted in Zone 1. Beneath Zone 1 is a thin red region that lacks 3D structure (Zone 2) where the cells have begun to excrete the matrix components. Zone 3 (containing the most mature cells) is the largest of the regions and is characterized by a web like 3D structure. A septum divides zone 3 into two subzones (3A and 3B) which have similar but unique architectures. Figure is reproduced with permission of the author (Ahmad, 2013).

1.5.3 Crystal violet staining

The Calgary Biofilm device provides a convenient high-throughput experimental setup for biofilm formation. This system consist of 96 polystyrene pegs on a lid which fits over a microtiter plate, with each peg hanging into a separate well. Biofilm formation occurs on the pegs at the air-liquid interface (Ceri *et al.*, 1999). Crystal violet staining can be used to colour the biofilm matrix as well as cells that are present in the biofilm on the pegs. After de-staining the pegs in acetic acid, the intensity of the dissolved stain can be used to infer the degree of biofilm formation. The degree of planktonic growth can also be determined by measuring the optical density of the medium in the wells of the microtiter-plate. This high-throughput setup where biofilms and planktonic growth can be assessed simultaneously makes the Calgary setup ideal for studying inhibitory molecules and dose-responses. The observation that *Salmonella* strains which form strong biofilms on the polystyrene pegs also attach better to lettuce leaves while those that form weak biofilms also show defective attachment to lettuce leaves provides a link between *in vitro* and *in planta* biofilm formation, which is evidence that the Calgary biofilm setup is a suitable prediction model for real-life *Salmonella* biofilm formation (Kroupitski *et al.*, 2009; Patel & Sharma, 2010).

1.5.4 Fluorescent probes that bind specific EPS structures

To visualize EPS components one can make use of fluorescently marked antibodies or other probes which specifically target the desired EPS component. The antibody-based approach is particularly useful for labelling protein components of the EPS, but it is more challenging for tagging sugar components. Recently a novel biofilm imaging probe CDy11, which binds to amyloid fibers (Figure 7), was demonstrated as an *in vivo* diagnostic tool for detecting biofilms (Kim *et al.*, 2016a).

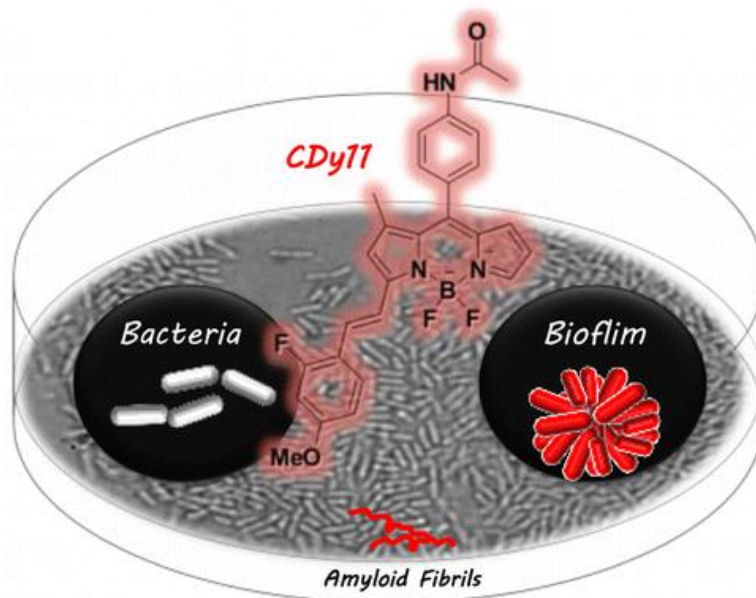


Figure 7 The fluorescent probe CDy11 targets amyloid fibers in the *P. aeruginosa* biofilm matrix. Figure reproduced with permission (Kim *et al.*, 2016a).

1.6 Regulation of *Salmonella* biofilm formation

As illustrated in Figure 8, a sophisticated and complex regulatory network controls the various biofilm components' production. In the following subsections, a brief overview is given on the current understanding of this network and the interactions between its various components, particularly the master regulator CsgD.

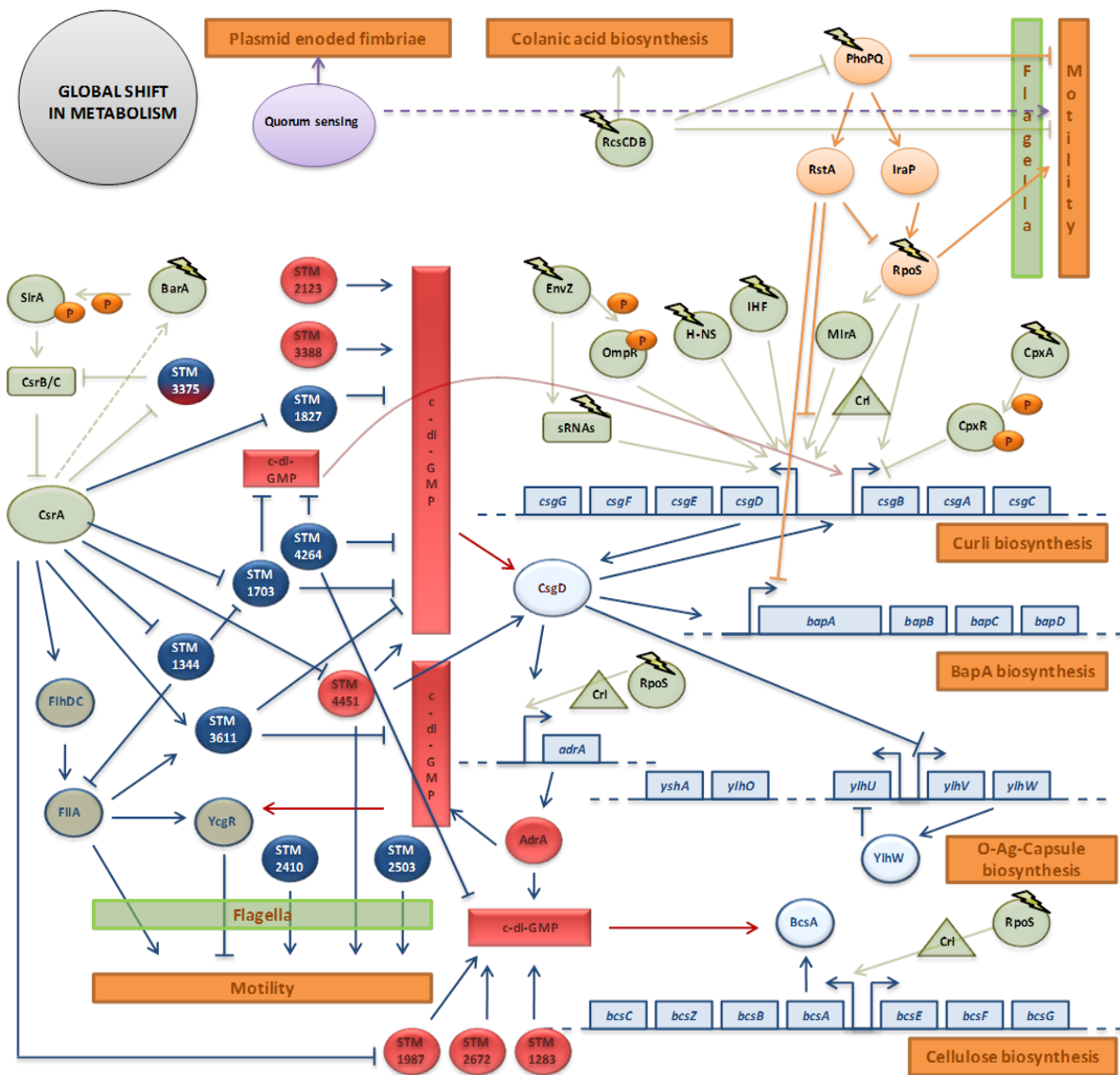


Figure 8 Overview of the transcriptional regulatory network controlling *Salmonella* biofilm formation. Arrows and flat-headed arrows represent activation and repression respectively. Broken lines indicate putative links that need to be experimentally validated or further investigated. ‘P’ symbols represent transferable phosphorus groups of two component systems. Light blue rectangles represent the genomic organization of the genes encoding the major structural biofilm components, indicated by orange rectangles. The orange ‘Motility’ rectangle is an exception as it represents a community behavior related to biofilm formation, regulated through flagellar genes (dark green circles) and flagella (green rectangle). Light blue circles represent important regulators involved in the production of the major structural biofilm components. Light green circles, triangles and rectangles represent global regulators, the Crl protein and sRNAs, respectively, and lightning bolt symbols represent the input and integration of different environmental signals into the regulatory system. Orange circles and arrows indicate the link between PhoPQ and biofilm formation. The grey and purple circles indicate the role of metabolism and quorum sensing respectively. Dark blue and red circles represent EAL and GGDEF proteins, respectively, involved in c-di-GMP turnover. Red rectangles represent the different, but interconnected c-di-GMP pools. Figure reproduced with permission of the authors (Steenackers *et al.*, 2012).

1.6.1 CsgD, the master regulator

The transcriptional regulator CsgD (previously referred to as AfgD) plays a major role in regulating biofilm formation in *E. coli* and *Salmonella*. It is a response regulator consisting of an N-terminal receiver domain with a conserved aspartate (D59) and a C-terminal LuxR-like DNA-binding motif (Römling, 2005). RpoS and MlrA activate CsgD expression in a coherent feed forward loop (Gómez-Gómez & Amils, 2014; Hosseinkhan *et al.*, 2015). CsgD directly activates transcription of the divergently transcribed *csgDEFG* and *csgBAC* operons (Römling *et al.*, 1998a; Römling *et al.*, 1998b). The *csgBAC* operon encodes the structural subunits of curli fimbriae. Furthermore it also directly activates transcription of *adrA*, which encodes the diguanylate cyclase AdrA that positively regulates post-translational activation of cellulose synthase BcsAB (Römling *et al.*, 2000; Gerstel & Römling, 2003; Kader *et al.*, 2006; Zakikhany *et al.*, 2010). Although the promoter region of the *bapABCD* operon contains a CsgD binding-site which is similar to that in the promoter region of *adrA* (Latasa *et al.*, 2006), a combined bioinformatics and transcriptomics approach did not identify *bapA* as a CsgD regulated gene (Zakikhany *et al.*, 2010). This is in contrast to another report (Latasa *et al.*, 2005) which concluded that CsgD regulates *bapA* transcription, because *bapA* mRNA levels in a $\Delta csgD$ mutant was significantly lower than in the wild type. This apparent discrepancy can be possibly attributed to the different experimental procedures that were used (Hermans, 2011). A *csgD* deletion mutant has a “saw” morphotype on CR agar, indicating the absence of cellulose and curli. Regulation of *csgD* transcription and translation is elaborate and tightly synchronized in response to a variety of environmental and intracellular cues and signals. Several global regulators affect *csgD* transcription in *Salmonella*, namely: RpoS, OmpR, H-NS, MlrA, Crl and IHF (Gerstel & Römling, 2003; Gerstel *et al.*, 2003; Robbe-Saule *et al.*, 2006; Jonas *et al.*, 2009; Simm *et al.*, 2014). Research in *E. coli* has shown that several small non-coding mRNAs play a direct role in downregulating CsgD expression on a post-transcriptional level by binding to specific regions in the 5'UTR of *csgD* mRNA, thereby suppressing translation, see review by (Boehm & Vogel, 2012). Similar regulation by small RNAs have also been confirmed in *Salmonella* (Bordeau & Felden, 2014). CsgD is also a target of transcriptional and posttranscriptional control by c-di-GMP although the exact details of this regulation remain unclear. In *E. coli* a well-defined set of DGCs and PDEs tunes *csgD* transcription (Weber *et al.*, 2006; Pesavento *et al.*, 2008; Sommerfeldt *et al.*, 2009; Römling *et al.*, 2013). CsgD expression is highly correlated with the activities of the PDE YhjH and

several DCS involved in motility regulation (Simm *et al.*, 2007; Pesavento *et al.*, 2008). In *V. cholera* VspT, a CsgD homologue, contains a c-di-GMP binding motif with the consensus W(F/L/M)(T/S)R. This motif is not present in *Salmonella* and other enterobacteria. Unlike VspT which undergoes a change in oligomerization upon c-di-GMP binding, CsgD is regulated by phosphorylation (Krasteva *et al.*, 2012). The important role of c-di-GMP during the transition between motile and sessile modes of growth is discussed in the next paragraphs and Chapter 2.

1.6.2 Coordinating motility, virulence and biofilm formation

Flagella and the chemotaxis machinery are important in the transition between motile and sessile modes of growth. *Salmonella* cells typically have between three and eight flagella per cell, the biosynthesis of which is controlled by FlhD₄C₂ (Guttenplan & Kearns, 2013). It seems rather evident that when bacteria switch to a sessile mode of growth, motility ought to be inhibited. In fact, mutations in various regulatory genes have opposing effects on biofilm formation and motility, as observed in different species (Yildiz & Schoolnik, 1999; Sauer & Camper, 2001; Yildiz *et al.*, 2001; Blair *et al.*, 2008; Verstraeten *et al.*, 2008; Pesavento *et al.*, 2008). However, intact motility is important for attachment and early stage biofilm formation, as demonstrated by the biofilm defects of strains that lack FlhD₄C₂ or FliC (the flagella filament protein) (Pratt & Kolter, 1998; Guttenplan & Kearns, 2013). The regulation of the interplay between virulence, motility and biofilm formation is discussed below.

The carbon storage regulator CsrA affects motility and biofilm formation in the following ways: (i) By promoting the expression of FlhD and FlhC by stabilizing the *flhDC* transcript and preventing it from RNaseE cleavage. (ii) By suppressing two degenerate EAL domain proteins (STM1697 and STM1344) which target FlhD₄C₂ on a posttranslational level to inhibit the expression of flagella genes. (iii) By suppressing the *rdar* morphotype and promoting motility by increasing the expression of the EAL-domain protein STM3611 (Yakhnin *et al.*, 2013; Ahmad, 2013). Nevertheless, at some stage during biofilm development the motile bacteria become sessile and embedded in a self-produced matrix. Research done on *E. coli* showed that curli production in early-stage biofilms is dependent on FlhD₄C₂ degradation by the protease CplXP (Pesavento *et al.*, 2008).

ClpXP and CsrA are also involved in regulating virulence in *Salmonella*. Deleting ClpP causes attenuation of virulence by affecting RpoS and CsrA (Knudsen *et al.*, 2013). Deleting CsrA,

as well as overexpressing, it reduces the expression of genes that are important for invasion of epithelial cells (Altier *et al.*, 2000).

In general, high levels of the signalling molecule c-di-GMP are associated with biofilm formation and lower levels are usually associated with motility and virulence. In fact 5 EAL domain proteins (which break down c-di-GMP) STM0343, STM0468, STM2215, STM3611 and STM4264 all play a role in stimulating HT-29 invasion. Nevertheless, unconventional phenotypes have been found for the DGC proteins (which make c-di-GMP) STM1283 and STM2123, which both stimulated invasion (Ahmad *et al.*, 2011). The roles of CsrA, flagella, c-di-GMP and some other components that coordinate biofilm formation, motility and virulence are summarized Figure 9.

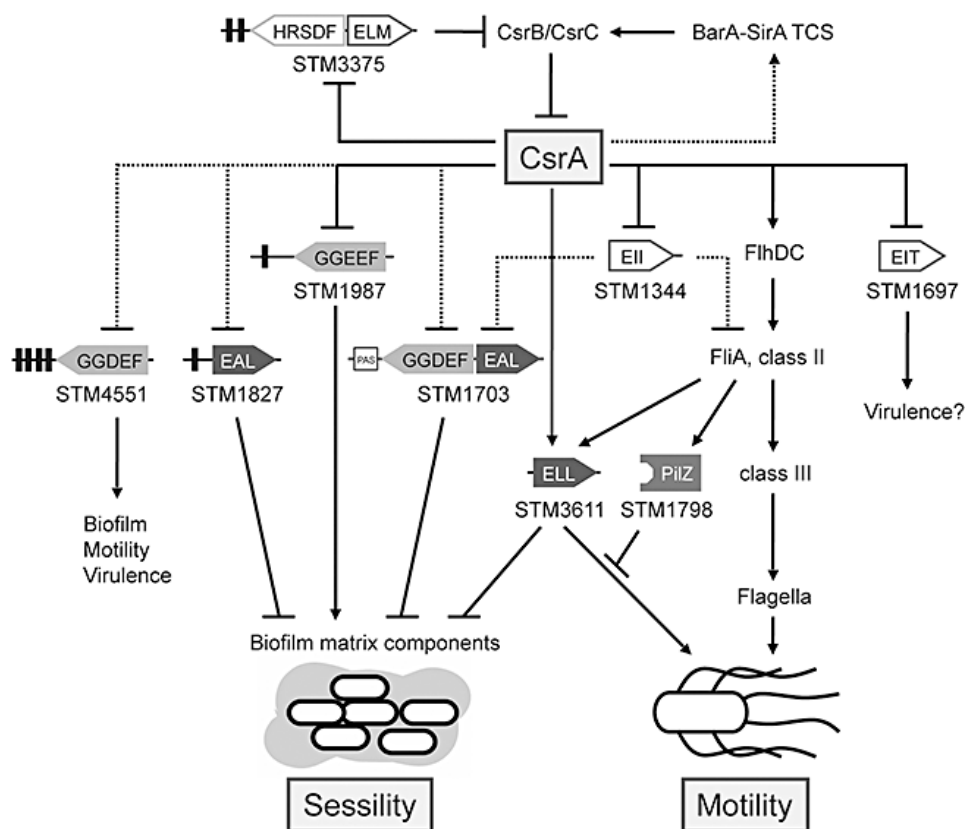


Figure 9 Schematic model illustrating the roles of various GGDEF/EAL domain proteins and CsrA in regulating invasion, motility and biofilm formation (Jonas, *et al.*, 2009).

1.7 Concluding remarks

This chapter briefly introduced the taxonomy of the pathogen *Salmonella* as well as the impact of biofilms in human health and industry. Factors regulating *Salmonella*'s ability to switch from a free-living to biofilm-based lifestyle were recapitulated. The following two chapters

Chapter 1: Introduction

are literature reviews in which the roles of nucleotides in biofilm formation and the potential of using nucleoside and nucleotide analogs as antibacterial agents are discussed.

Chapter 2

2 The importance of nucleotides in biofilm formation

2.1 Abstract

Nucleotides and their derivatives have many important functions within the bacterial cell. This chapter provides an overview on the biosynthesis pathways that produce the purine and pyrimidine nucleotides. The importance of nucleotide biosynthesis during biofilm formation is reviewed and special focus is given to the nucleotide based second messengers, particularly c-di-GMP.

2.2 Background

2.2.1 Introduction to the purine and pyrimidine biosynthesis

Nucleotides have important functions within the cell including: as the building “blocks of life” (DNA and RNA), as co-factors in sugar and lipid metabolism, polyamine biosynthesis, methylation reactions, energy transfer, signalling, and as components of co-enzymes in redox-reactions for instance NAD(P) and FAD (see review by (Jensen *et al.*, 2008)). A nucleotide consists of three main parts: a purine/ pyrimidine base (nucleobase), a pentose-sugar that can either be a ribose or deoxyribose, and one to three phosphate groups (Figure 10). A nucleoside is nucleobase with an attached pentose-sugar. DNA and RNA are polynucleotides in which the base guanine pairs with cytosine and adenine pairs with thymine or uracil (for DNA and RNA respectively). Nucleotides can be formed *de novo* or via salvage pathways (Figure 11). The *de novo* synthesis of purines and pyrimidines occurs via two separate pathways which are both tightly regulated by end-products and intermediates, as will be further explained in the rest of this chapter. The salvage pathways have several functions: (i) To utilize exogenous, preformed nucleobases and nucleoside for nucleotide synthesis. (ii) To re-use nucleobases and nucleosides that were produced endogenously by nucleotide turnover. (ii) The catabolic processing of pentoid moieties of exogenous nucleosides and the amino groups of adenine components as carbon and nitrogen sources respectively (Zalkin & Nygaard, 1996). The salvage of free nucleobases and nucleosides in the medium suppresses *de novo* synthesis by suppressing the expression of the enzymes as well as by feedback inhibition of the *de novo* reactions.

Chapter 2: Nucleotides

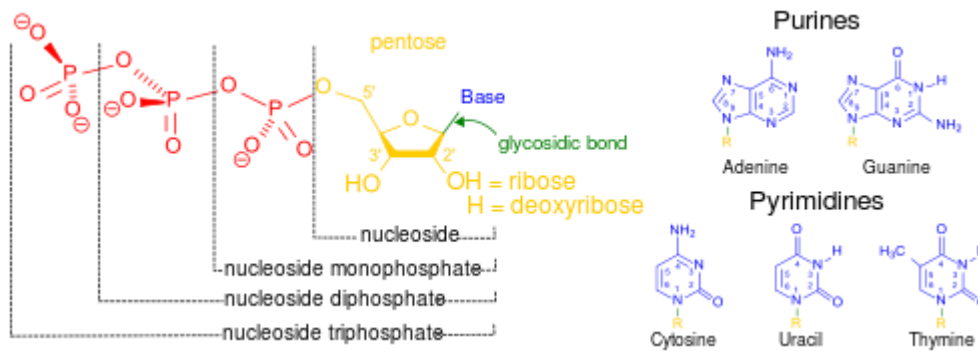


Figure 10. Structural elements of common nucleic acid constituents. Because they contain at least one phosphate group, the compounds marked nucleoside monophosphate, nucleoside diphosphate and nucleoside triphosphate are all nucleotides (<https://en.wikipedia.org/wiki/Nucleotide>).

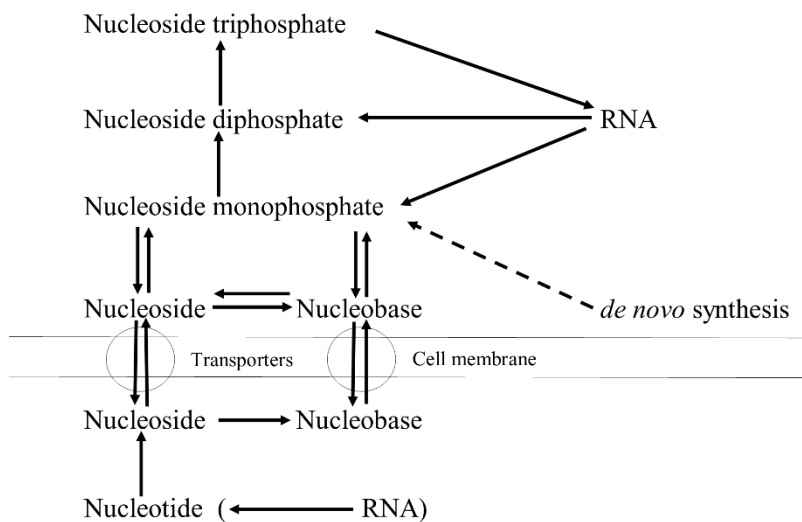


Figure 11 Schematic and simplified outline of nucleotide metabolism. The arrow, indicating breakdown of RNA outside the cytoplasm, is flanked by parentheses, because *E. coli* and *S. enterica* do not secrete RNases to the periplasm or medium. The scheme applies to the metabolism of deoxyribonucleotides with noticeable exceptions: (i) these are formed *de novo* by reduction of ribonucleoside di- or triphosphates, (ii) no PRTase attaches a 5-phosphodeoxyribosyl group to a nucleobase, and (iii) phosphorolytic breakdown of DNA, generating dNDPs, does not occur. Figure adapted from (Jensen *et al.*, 2008).

2.2.2 Purine synthesis and regulation

2.2.2.1 Enzymatic reactions for *de novo* purine biosynthesis

The *de novo* purine biosynthesis pathway (Figure 12) of *Salmonella* consists of 11 enzymatic steps which convert phosphoribosyl pyrophosphate (PRPP) to the first complete purine, inosine monophosphate (IMP). In the first step, the amide group of glutamine displaces the diphosphoryl group of PRPP. This results in the formation of PRA. The amino group of PRA (which will become N-9 of the purine ring) reacts with the carboxyl group of glycine leading to the formation of GAR. This step requires one ATP molecule (the atoms of glycine will become the C-4, C-5 and N-7 atoms of the purine ring). Next, the primary amino group of the glycylic residue becomes formylated to produce FGAR (the formyl group will become C-8 of the purine ring). There are two alternatives for catalyzing this step: A carbon atom may be provided by either 10-formyl-THF or formic acid. Subsequently, an amide group provided by glutamine is attached to the carboxyl carbon atom of FGAR yielding FGAM (the nitrogen from the amide group will become N-3). This is followed by an ATP-dependent closure of the imidazole ring of AIR. The subsequent carboxylation reaction introduces the C-6 atom of the purine ring, generating N⁵-CAIR. The carboxylation reaction requires ATP and bicarbonate. Next, the formyl moiety is transferred to the C-4 atom of the imidazole group to form CAIR. Two amination steps of CAIR then follow. In the first ATP-dependent amination step, aspartate is added to the carboxylate of CAIR to yield SAICAR. In the second amination step, fumarate is withdrawn, generating AICAR. The amination reactions are responsible for introducing the N-1 atom of the purine ring. Next, the final (C-2) atom of the purine ring is introduced when the formyl group of 10-formyl-THF is transferred to the amino group of AICAR resulting in FAICAR formation. The complete purine IMP is formed when the ring is closed in an ATP-independent dehydration step (Jensen *et al.*, 2008).

IMP is the branching point for the formation of AMP and GMP. AMP and GMP can be further converted to the di- and tri-phosphate nucleotides (Figure 12). The conversion of IMP to GMP requires ATP, and the conversion of IMP to AMP requires GTP, the energy donor requirements for these reactions probably contribute to the balancing of guanine nucleotide and adenine nucleotide pools. The conversion of IMP to AMP requires two steps with succinyl-AMP as an intermediate. The conversion of IMP to GMP also requires two steps and XMP is the intermediate (Jensen *et al.*, 2008).

2.2.2.2 Purine salvage and interconversion

The purine salvage and interconversion pathways are shown in Figure 13. Nucleobases that are assimilated from the environment are directly converted to the nucleotide level by a phosphoribosyltransferase step that is subject to feedback inhibition. Salvaged nucleosides are mostly converted to nucleobases of which the major part is excreted again while the pentose moiety is further catabolized. Exogenous nucleotides may also be used as precursors for nucleic acids; however, this requires dephosphorylation to nucleosides by periplasmic enzymes. Endogenously, mRNA turnover results in large quantities of ribonucleotide monophosphates that are reutilized directly or after conversion to nucleosides or nucleobases (Nygaard, 1983; Zalkin & Nygaard, 1996). The deoxynucleotides dATP and dGTP are synthesized via ADP and GDP under aerobic conditions and directly from ATP and GTP under anaerobic conditions (Zalkin & Nygaard, 1996). The genes and enzymes involved in purine biosynthesis are listed in Table 1.

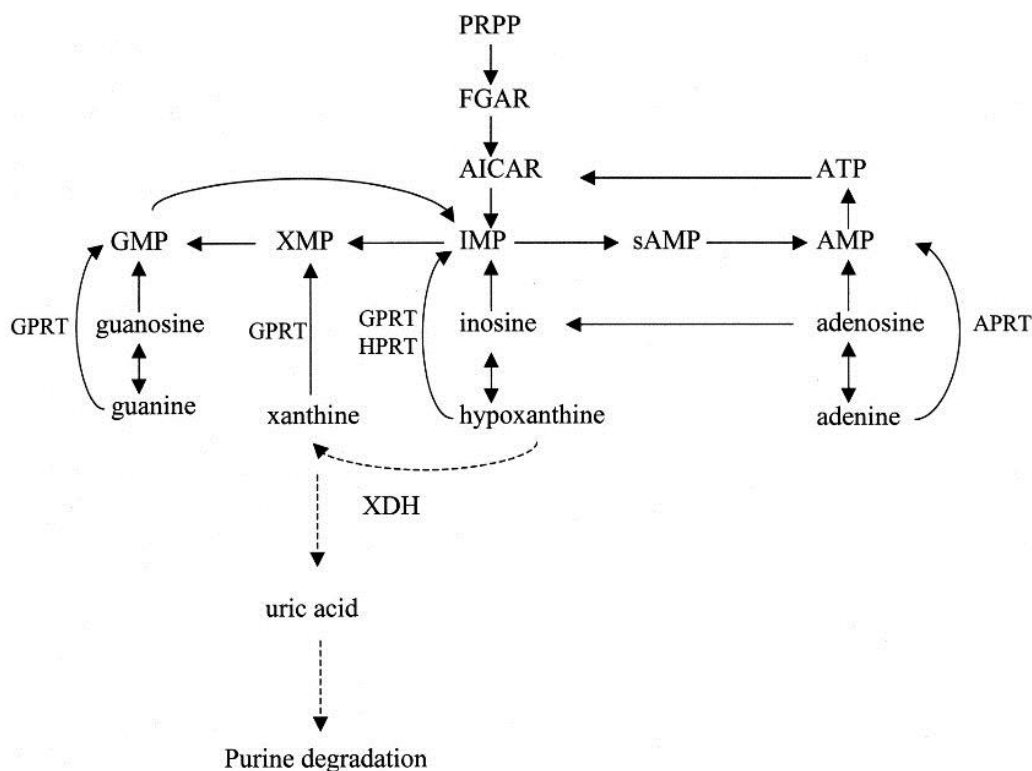


Figure 13 Purine salvage and interconversion. The solid lines show known pathways, while the dashed lines indicate reactions demonstrated by (Xi *et al.*, 2000) involving the hypothetical xanthine dehydrogenase genes. Abbreviations: PRPP, 5'-phospho- α -D-ribose-1-pyrophosphate; FGAR, 5'-phosphoribosyl N-formylglycinamide; GPRT, guanine phosphoribosyltransferase; HPRT, hypoxanthine phosphoribosyltransferase; APRT, adenine phosphoribosyltransferase; XDH, Xanthine dehydrogenase; AICAR, 5-aminoimidazole-4-carboxamide ribonucleotide; and sAMP, adenylosuccinate. Figure reproduced from (Xi *et al.*, 2000).

2.2.2.3 Regulation of the purine pathway

Purine biosynthesis is regulated on the protein level via allosteric activation and inhibition of the enzymes of various steps in the pathway, enzyme production is controlled on a genetic level as well. The genes that are responsible for the 11 steps to IMP production are not located together in a single operon. Instead, they are distributed over the chromosome. The genes *purT*, *purL*, *purC* and *purB* are in monocistronic operons; *purH* and *purD* are located next to each other but are transcribed separately; the purine operons are *purMN* and *purEK*. The gene *purF* is part of the *cvp purF dedF* operon whose other members are not involved in purine metabolism (Zalkin & Nygaard, 1996; Jensen *et al.*, 2008).

The transcriptional regulation of the genes involved in IMP synthesis requires two regulatory elements: a *purR*-encoded repressor protein and a DNA operator site (Pur box) where the repressor binds. Hypoxanthine and guanine function as co-repressors *in vivo* (Houlberg & Jensen, 1983). The Pur box has the consensus sequence ACGAAACGTTTGCGT, and is present in front of the transcription start sites of all the operons involved in *de novo* IMP production, as well as *purA*, *guaBA* and *purR* itself. The position of the Pur box varies and in some cases more than one operator site is present. PurR represses the genes specifying IMP synthesis between 10- to 17-fold, while repression of *purB*, *purA*, *guaBA* and *purR* is between two to five- fold (Meng *et al.*, 1990; Rolfes & Zalkin, 1990; Choi & Zalkin, 1992; Jensen *et al.*, 2008). This regulatory pattern may have evolved to permit purines obtained from the medium or from RNA turnover to shut down the *de novo* pathway while still permitting GMP and AMP synthesis via the salvage reactions. Except for *purA* and *guaBA*, there is no evidence for additional regulation of the *pur* genes. In the case of *purA*, an uncharacterized adenine-specific control system augments regulation by PurR (Zalkin & Nygaard, 1996). Research done on *B. subtilis* found an adenine dependent role for YabJ regulation of *purA* transcription, possibly via a YabJ-PurR interaction (Rappu *et al.*, 1999). YabJ is present in *E.coli* and *Salmonella* but to my best knowledge, its role in regulating nucleotide metabolism was not studied in these organisms. For *guaBA* the 5-fold regulation by PurR is modulated to 15-fold by DnaA, which binds to two DnaA boxes (Tesfa-Selase & Drabble, 1992). It is thought that the regulation of *guaBA* by DnaA is important for coordinating purine nucleotide production with DNA replication (Zalkin & Nygaard, 1996).

On an enzymatic level the first step in the *de novo* pathway, catalysed by glutamine PRPP amidotransferase, is inhibited by AMP and GMP. This reaction is also subject to feed-forward regulation by PRPP. The characteristics of the regulation is as follows: (i) AMP is a weaker

inhibitor than GMP. (ii) The inhibition by GMP and AMP is synergistic. (iii) Inhibition by AMP and GMP is competitive with the substrate PRPP. (iv) In the absence of inhibitors, saturation by PRPP is hyperbolic. When AMP is present saturation remains hyperbolic (i.e. the rate of the catalysis reaction depends on the substrate concentration) but is sigmoidal when GMP is present. (v) AMP and GMP exhibit positive cooperativity for inhibition (binding of one molecule increases the enzyme's affinity for the other) (Zalkin & Nygaard, 1996). When the concentrations of PRPP is very high, the normal feedback inhibition by AMP and GMP is overcome and the rate of the reaction is increased.

Table 1 Enzymes and genes of purine metabolism (Jensen *et al.*, 2008).

Enzyme name	Gene	Locus a		Proteins
		<i>E. coli</i>	<i>Salmonella</i>	
De novo synthesis of IMP				
PRPP amidotransferase	<i>purF</i>	b2312	STM2362	Tetramer 56.5 kDa
GARSynthetase	<i>purD</i>	b4005	STM4175	Monomer 45.9 kDa
GAR transformylase N	<i>purN</i>	b2500	STM2500	Monomer 23.5 kDa
GAR transformylase T (FGAR synthase)	<i>purT</i>	b1849	STM1883	Dimer 42.4 kDa
FGAR amidotransferase	<i>purL(purG)</i>	b2557	STM2565	Monomer 141.4 kDa
AIR synthase	<i>purM</i>	b2499	STM2499.S	Dimer 36.9 kDa
N5-AIR-carboxylase	<i>purK</i>	b0522	STM0533	Dimer 39.5 kDa
N5-CAIR mutase	<i>purE</i>	b0523	STM0534	Octamer 17.8 kDa
SAICAR synthetase	<i>purC</i>	b2476	STM2487	Trimer 27.0 kDa
Adenylosuccinate lyase	<i>purB</i>	b1131	STM1232	Tetramer 51.5 kDa
AICAR transformylase	<i>purH</i>	b4006		Dimer 57.3 kDa Bifunctional
IMP cyclohydrolase	<i>purH</i>	b4006	STM4176	Dimer 57.3 kDa Bifunctional
Biosynthesis of AMP				
Adenylosuccinate synthase	<i>purA</i>	b4177	STM4366	Dimer 47.3 kDa
Adenylosuccinate lyase	<i>purB</i>	b1131	STM1232	Tetramer 51.5 kDa
AMP kinase	<i>adk</i>	b0474	STM0488	Monomer 23.6 kDa
Biosynthesis GMP				
IMP dehydrogenase	<i>guaB</i>	b2508	STM2511	Tetramer 52.0 kDa
GMP synthase	<i>guaA</i>	b2407	STM2510	Dimer 58.7 kDa
GMP kinase	<i>gmk</i>	b3640	STM3740	Dimer 23.6 kDa
Purine interconversion and salvage				
GMP reductase	<i>guaC</i>	b0104	STM0141	Tetramer 37.4 kDa
Guanosine kinase	<i>gsk</i>	b0477	STM0491	48.4 kDa
Purine nucleoside phosphorylase	<i>deoD</i>	b4384	STM4570	Hexamer 26.0 kDa
Xanthosine phosphorylase	<i>xapA</i>	b2407	STM2422	Hexamer 29.8 kDa
Ribonucleoside hydrolase (Low expression)	<i>rihC</i>	b0030	STM0051	Tetramer 32.6 kDa
Hypoxanthine PRTase	<i>hpt</i>	b0125	STM0170	Tetramer 20.1 kDa

Enzyme name	Gene	Locus a		Proteins
		<i>E. coli</i>	<i>Salmonella</i>	
Xanthine/guanine PRTase	<i>gpt</i>	b0238	STM0317	Tetramer 17.0 kDa
Guanine deaminase	<i>guaD</i>	b2883	Not in <i>Salmonellae</i>	Mer? 50.2 kDa
Adenosine deaminase	<i>add</i>	b1623	SMT1463	Tetramer 36.4 kDa
Adenine deaminase (cryptic)	<i>adc</i>	b3665	Not in <i>Salmonellae</i>	Dimer 63.7 kDa
Adenine PRTase	<i>apt</i>	b0469	STM0483	Dimer 19.9 kDa
AMP nucleosidase	<i>amn</i>	b1982	STM2009	Hexamer 54.0 kDa
S-Adenosyl homocysteine hydrolase	<i>mtn</i>	b0159	STM0207	Dimer 24.3 kDa
ATP PRTase	<i>hisG</i>	b2019	STM2071	Hexamer 33.4 kDa
Purine regulatory protein				
Purine repressor	<i>purR</i>	b1658	STM1430	Dimer 38.2 kDa

^a The loci labelled bXXXX refer to the ordered gene map of *E. coli* K-12 strain MG1655, while loci designated STMxxxx refer to the ordered chromosomes map of *S. enterica* serovar Typhimurium strain LT2.

The pathway is also regulated after the IMP branch point. In *in vitro* experiments, the rate of AMP synthesis from IMP is inhibited by several nucleotides including AMP, GMP and ppGpp. The inhibition by ppGpp is very strong ($K_i = 50\mu\text{M}$), which suggests that amino-acid starvation might decrease the rate of AMP synthesis. The conversion of IMP to GMP is inhibited by GMP ($K_i = 55\mu\text{M}$) in a manner that is competitive with IMP ($K_m = 11\mu\text{M}$).

2.2.3 Pyrimidine synthesis and regulation

2.2.3.1 Enzymatic reactions for *de novo* pyrimidine biosynthesis

The *de novo* synthesis of CTP and UTP occurs via an unbranched pathway in which dTTP is the ultimate end product, and UTP, CTP and dCTP are obligatory intermediates (Figure 14). The first step in the *de novo* pyrimidine biosynthesis is the formation of carbamoylphosphate from glutamine, bicarbonate and two ATP molecule (one is required for the formation of the reaction intermediate, the other for phosphorylating the enzyme-bound carbamate). This first reaction is also required for arginine biosynthesis. The next reaction involves the condensation of carbamoylphosphate and the amino group of aspartate to yield carbamoylaspartate, also known as ureidosuccinate. The pyrimidine ring is formed by cyclization followed by oxidation. First, the ring is closed to form dihydroorotate. Next, an enzyme that is linked to the electron transport system catalyzes the oxidation of dihydroorotate to orotate. PRPP donates a ribose-5 phosphate to yield orotidine 5'- monophosphate (OMP). OMP is irreversibly decarboxylated to produce UMP. UMP is subsequently phosphorylated to UDP

and then to UTP. UTP is aminated to CTP. CMP is not an obligatory intermediate in *de novo* CTP synthesis, but *Salmonella* possesses a CMP kinase that can re-phosphorylate CMP and dCMP from mRNA and CDP-diacylglycerol turnover (Beck *et al.*, 1974; Frick *et al.*, 1990; Neuhard & Kelln, 1996). The genes and enzymes involved in pyrimidine biosynthesis are listed in Table 2.

Table 2 Genes encoding enzymes that are involved in pyrimidine nucleotide synthesis, interconversion, and salvage

Enzyme name	Gene	Locus <i>a</i>		Proteins
		<i>E. coli</i>	<i>Salmonella</i>	
Pyrimidine nucleotide biosynthesis <i>de novo</i>				
Carbamoylphosphate synthase				A/B-monomer
Glutaminase subunit	<i>carA</i>	b0032,	STM0066	41.5 kDa
Synthase subunit	<i>carB</i>	b0033	STM0067	118 kDa
Aspartate transcarbamoylase	<i>pyrBI</i>			2C3/3R2
Regulatory subunit (R)	<i>pyrI</i>	b4244	SMT4459	17.1 kDa
Catalytic subunit (C)	<i>pyrB</i>	b4245	SMT4460	43.4 kDa
Dihydroorotase	<i>pyrC</i>	b1062	STM1163	Dimer C: 39 kDa
Dihydroorotate dehydrogenase	<i>pyrD</i>	b0945	STM1058	Monomer 36.7 kDa
Orotate phosphoribosyltransferase	<i>pyrE</i>	b3642	STM3733	Dimer 26.4 kDa
OMP decarboxylase	<i>pyrF</i>	b1281	STM1707	Dimer 26.4kDa
UMP kinase	<i>pyrH</i>	b0171	STM0218	Hexamer 26.0 kDa
Nucleoside diphosphate kinase	<i>ndk</i>	b2518	STM2526	Tetramer 15.5 kDa
CTP synthase	<i>pyrG</i>	b2780	STM2953	Tetramer 60.5 kDa
Salvage reactions				
Uracil PRTase	<i>upp</i>	b2498	STM2498	Tetramer 22.5 kDa
Uridine-cytidine kinase	<i>udk</i>	b2066	STM2122	Dimer? 24.4 kDa
CMP kinase	<i>cmk</i>	b0910	STM0980	24.7 kDa
Deaminases				
Cytidine deaminase	<i>cdd</i>	b2143	STM2183	Dimer 31.5 kDa
Cytosine deaminase	<i>codA</i>	b0337	STM3334	Hexamer 47.6 kDa
Enzymes splitting the glycosyl bond nucleosides				
Uridine phosphorylase	<i>udp</i>	b3831	STM3968	Hexamer 27.2 kDa
Pyrimidine ribonucleoside hydrolase (Low expression)	<i>rihA</i>	b0651	STM0661	33.8 kDa
Pyrimidine nucleoside hydrolase (Silent)	<i>rihB</i>	b2162	Not in <i>Salmonella</i>	Tetramer 33.7 kDa
Ribonucleoside hydrolase (Low expression)	<i>rihC</i>	b0030	STM0051	Tetramer 32.6 kDa

a The loci labeled bXXXX refer to the ordered gene map of *E. coli* K-12 strain MG1655, while loci designated STMxxxx refer to the ordered chromosomes map of *S. enterica* serovar Typhimurium strain LT2 (Jensen *et al.*, 2008).

2.2.3.2 Pyrimidine salvage

The *de novo* pyrimidine biosynthesis pathway generates UTP as well as CTP. Cytidine nucleotides can only be formed *via* the reaction catalysed by CTP synthase (encoded by *pyrG*). Furthermore, cytidine and cytosine compounds can only be converted to uracil compounds by deamination (enzymes encoded by *cdd* and *codA*). Pyrimidine nucleotide products from RNA breakdown are converted to diphosphates and triphosphates by the nucleoside monophosphate kinases (UMP kinase and CMP kinase), in combination with the nucleoside diphosphate kinase. While UMP kinase (encoded by *pyrH* also known as *umk*) is an integral part of both the *de novo* as well as salvage pathways, the CMK kinase (*cmk*) is only involved in salvage. Under aerobic conditions, CDP is the major pyrimidine substrate for ribonucleotide reduction, thus the salvage reaction catalysed by CMP kinase is of major importance as reviewed in (Jensen *et al.*, 2008). See Figure 15 for a summary of the salvage pathways for uracil and cytosine.

Specific transport systems import free pyrimidine nucleosides and bases that are present in the growth medium into the cell (Jensen *et al.*, 2008). Cytosine and cytidine are generally deaminated to uracil and uridine respectively. Then uridine is converted to UMP by uridine kinase (*udk*). Uracil can be directly converted to UMP by uracil PRTase (*upp*). There is no known cytosine PRTase (nor a reversible cytidine phosphorylase) identified in any organism. Furthermore, enteric bacteria do not possess a deoxycytidine kinase. Thus, the deamination of cytosine and deoxycytosine to their corresponding uracil compounds is the only way to utilize cytosine and deoxycytosine for nucleotide synthesis. Exogenous nucleosides can only be utilized under conditions that permit their dephosphorylation prior to uptake; this ability is repressed by high phosphate concentrations in the medium (Bonekamp *et al.*, 1984; Neuhard & Kelln, 1996).

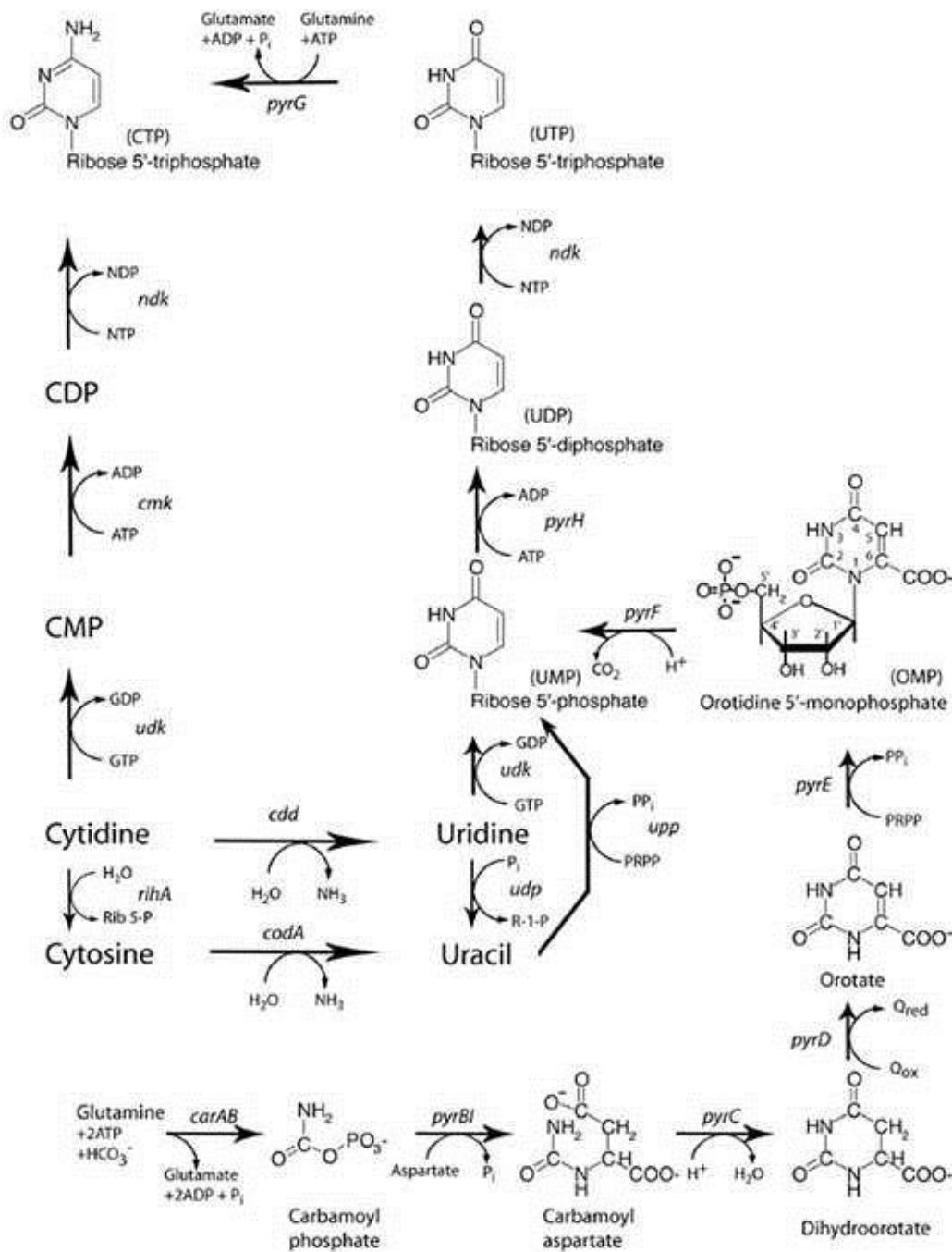


Figure 14 Biosynthesis and interconversion of pyrimidine nucleotides, nucleosides, and bases. The enzymes are indicated by their gene symbols (Jensen *et al.*, 2008). Figure copyright belongs to the American Society for Microbiology.

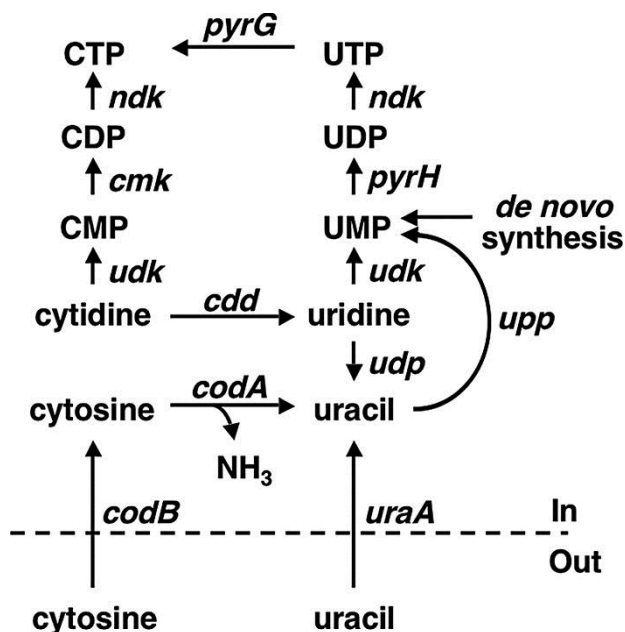


Figure 15 Salvage pathways for uracil and cytosine. Gene names are used to represent the encoded proteins. Figure replicated from (Jensen *et al.*, 2008). Figure copyright belongs to the American Society for Microbiology.

2.2.3.3 Regulation of pyrimidine biosynthesis

Like the purine pathway, the pyrimidine pathway is also subject to regulation on the enzymatic as well as transcriptional level. Generally (aside from the *carAB* operon), the addition of preformed pyrimidines to the growth medium of wild type cells has quite a small effect and does not result in significant nucleotide pool changes. However, during extended partial pyrimidine starvation (for example due to leaky mutations or slow-feeding auxotrophic mutants) the changes in the nucleotide pool sizes and enzyme levels become more pronounced. Pyrimidine starvation causes a reduction in intracellular pyrimidine nucleoside triphosphates (especially UTP), but leads to a substantial increase in the size of ATP and GTP pools as was observed by (Vogel *et al.*, 1991).

The pyrimidine biosynthesis pathway is regulated on the level of gene expression by mechanisms that control the synthesis of the six enzymes that are required for the *de novo* production of UMP and of ribonucleotide reductase, which catalyzes the crossover reaction from ribonucleotides to deoxyribonucleotides (Neuhard & Kelln, 1996). The *pyr* genes are scattered on the chromosome and are organized in single transcription units or in small operons, together with genes that are seemingly unrelated. Unlike the purine pathway, there is no common pyrimidine repressor and each gene is regulated in a unique way (Jensen *et al.*, 2008). With the exception of the *carAB* operon, regulation depends largely on the behavior of

RNA polymerase as a function of the purine-and pyrimidine-nucleoside triphosphate pools (Jensen *et al.*, 1982). Ribosome dynamics and PurR also play a role (Houlberg & Jensen, 1983; Jensen, 1988; Weissborn *et al.*, 1994). The control of gene expression of all the steps up to UMP synthesis have been studied in detail. This part of the pathway is redundant in the presence of exogenous pyrimidine sources. On the other hand, not much is known about how the expression of the genes encoding enzymes that convert UMP to UTP and CTP is controlled. These enzymes are needed regardless of the presence of pyrimidines in the growth medium (Jensen *et al.*, 2008) and as such are essential for survival. The mechanisms that regulate *pyr* gene expression can be divided into three categories: (i) Rho-independent transcriptional attenuation that is facilitated by a transcription terminator between the promoter and structural gene. Regulation depends on the distance between the elongating RNA polymerase and the first coupled ribosome a function of the UTP and GTP pools. (ii) UTP-dependent “slippery” RNA synthesis at a U-rich stretch in the ultimate 5’ end of the newly formed mRNA. When intracellular UTP concentrations are high, the RNA polymerase stays bound to the promoter and iteratively adds more U-residues, blocking productive initiation at the promoter. When intracellular UTP concentrations are low, the reiterative addition does not occur and extension completes successfully. (iii) The pool sizes of different nucleoside triphosphates influences the point from where transcription is initiated, which in turn affects mRNA translation. The three regulatory mechanisms are summarized in Figure 16, Figure 17 and Figure 18.

As if the above mechanisms of regulation are not complicated enough, evolution has conjured up an even more complex regulator mechanism for *carAB* gene expression. This mechanism involves the transcription factors IHF, PepA, RutR, PurR and ArgR as well as “slippery transcription”. Transcription can be induced from either the P1 or P2 promoter (Shimada *et al.*, 2008; Nguyen Le Minh *et al.*, 2015). Thymidine, uracil, arginine and purine molecules all act as regulatory signals. The biggest advantage of such a complicated mechanism is that regulation can be responsive to a large range of concentrations of effector molecules, with each mechanism sensitive to a different range of effector concentrations. It appears as if the IHF/PepA/RutR mediated regulation occurs when UTP levels are high. Regulation by reiterative transcription occurs when UTP levels are lower. The lowest levels of UTP occur in a pyrimidine auxotroph in limiting conditions or when a shift is made from a pyrimidine-rich to a pyrimidine poor medium (Turnbough & Switzer, 2008).

Aside from regulation on the level of gene expression, enzyme activity is also controlled. Allosteric regulation of the pyrimidine biosynthesis enzymes occurs at five strategic points: (i) the synthesis of carbamoyl phosphate; (ii) the formation of carbamoyl aspartate; (iii) the amination of UTP to yield CTP; (iv) the reduction of CTP to dCTP; and (v) the conversion of dCTP to dTTP. CPSase is inhibited by UMP and activated by ornithine, IMP and PRPP. The binding sites of IMP and UMP overlap and the result is that CPSase is feedback inhibited according to the metabolic needs of the cell. In the event that carbamoylphosphate becomes limiting for arginine biosynthesis, ornithine accumulates and prevents inhibition by UMP. In the event that an excess of arginine is present, ornithine is not produced and the enzyme is controlled by UMP alone (Piérard *et al.*, 1965). ATCase is activated by ATP and feedback inhibited by CTP. UTP alone has no effect, but it leads to synergistic inhibition with CTP. Activation by ATP probably serves the purpose of regulating pyrimidine production to match that of purine production (reviewed by (Jensen *et al.*, 2008). UMP kinase is allosterically regulated by the positive effector GTP and the negative effector UTP. CTP synthase exhibits negative cooperativity for the substrate glutamine and the effector GTP, and positive cooperativity for ATP and UTP, see review by (Jensen *et al.*, 2008).

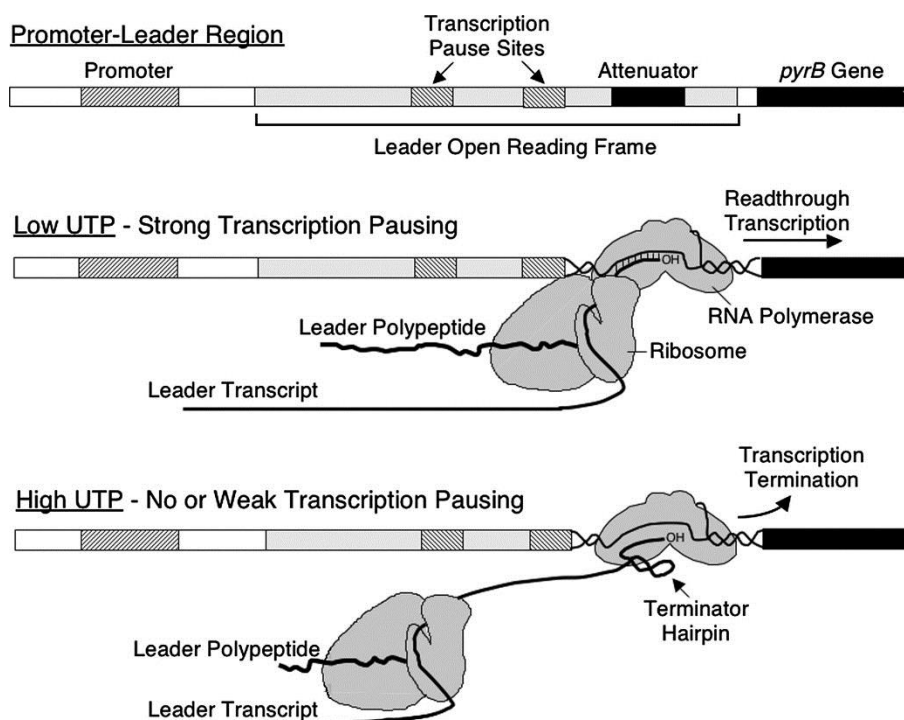


Figure 16 Model for attenuation control of *pyrBI* expression in *E. coli*. The diagram shows the relative positions of RNA polymerase and the translating ribosome within the leader region when UTP concentrations are either low or high (Turnbough & Switzer, 2008). Figure copyright belongs to the American Society for Microbiology. Figure copyright belongs to the American Society for Microbiology.

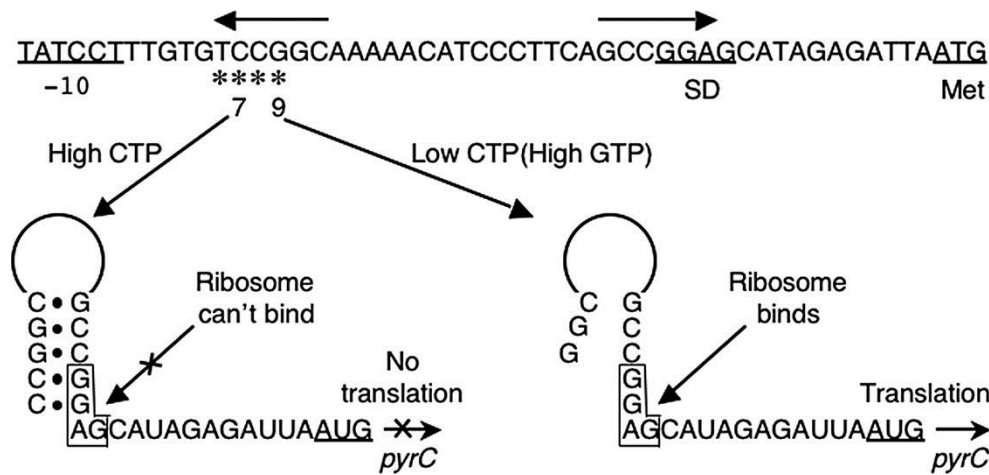


Figure 17 Model for transcription start site switching and translational control of *pyrC* expression in *E. coli* and *Salmonella*. The nucleotide sequence of the *pyrC* promoter-regulatory region of *E. coli* is shown, with the -10 region, SD sequence, and *pyrC* initiation (Met) codon underlined and labelled. Asterisks indicate the four transcription start sites at the *pyrC* promoter, and the two major start sites, C7 and G9, are indicated. Inverted horizontal arrows indicate the region of dyad symmetry. The sequence and structure of transcripts initiated at start sites C7 (high CTP) and G9 (low CTP) are shown, with the SD sequence boxed. Only C7 transcripts form the hairpin that includes the SD sequence and prevents translation initiation (Turnbough & Switzer, 2008). Figure copyright belongs to the American Society for Microbiology. Figure copyright belongs to the American Society for Microbiology.

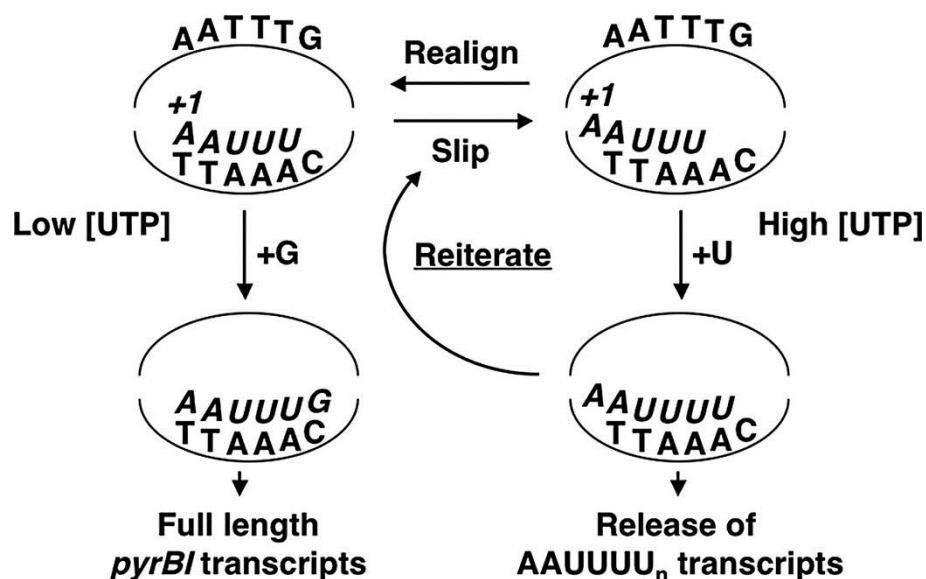


Figure 18 Model for the regulation of *pyrBI* expression by UTP-sensitive reiterative transcription. DNA sequences in the transcription bubble are shown, and the sequence of the nascent transcript, starting at position +1, is italicized (Turnbough & Switzer, 2008). Figure copyright belongs to the American Society for Microbiology.

2.2.3.4 Thymineless death

In 1954 Barner and Cohen observed that a thymine-requiring mutant of *E. coli* lost viability when grown in a medium lacking thymine (Barner & Cohen, 1954). This phenomenon has also been found in other organisms including yeast and higher eukaryotes. Thymine starvation in *E. coli* can be induced in several ways that inhibit the synthesis of thymidylate either directly by inhibiting the conversion of dUMP to dTMP and subsequently to dTTP, or indirectly by interfering with folate metabolism. Thymineless death is a unique effect, since starvation of bacteria for the other nucleotides have bacteriostatic effects that can be reversed with supplementation with the required nucleotides. On the other hand, thymine starvation is bactericidal. Although this phenomenon has been studied extensively, its exact molecular mechanisms remained obscure for many decades (Sat *et al.*, 2002). Throughout the years, thymineless death has been attributed to DNA damage and DNA recombination structures and their associated outcomes: SOS induction, filamentation, mutagenesis, loss of plasmids, or induction of suicide modules and prophages, among others. However, recent advances made by independent research groups have presented compelling evidence that the initiation of chromosome replication under thymine starvation is a key element in the phenomenon. In this scenario, degradation of the AT-rich *oriC* sequence leads to abortive attempts at replication and eventually results in cell death (Guzman & Martin, 2015).

2.3 The role of nucleotide biosynthesis in biofilm formation

Over the course of the past decade, various investigations using different bacterial models have been directed at uncovering the regulatory mechanisms that control the switch from a free-living planktonic state of growth to surface-attached biofilm growth. Some of the studies that have found roles for nucleotide biosynthesis in biofilm formation are briefly discussed next.

Sauer and co-workers characterized transitional episodes in biofilm development by *P. aeruginosa* and found roles for enzymes involved in nucleotide biosynthesis. Using direct observation by microscopy, they evaluated biofilm morphology, matrix production and the activation of quorum-sensing (QS) regulated genes. They used this information to determine optimal sampling times for protein analysis by 2-D gel electrophoresis in order to compare the physiological characteristics of different phases of biofilm formation (Sauer *et al.*, 2002). The sampling schedule for protein analysis was chosen as follows: planktonic cells from the chemostat; 8-h biofilm, reversible attachment; 1-day biofilm, irreversible attachment; 3-day

biofilm, maturation-1; 6-day biofilm, maturation-2; and 12-day biofilm, dispersion. Microscopic observations revealed that bacteria having the phenotypes from more than one biofilm phase could be present simultaneously. However, at the various sampling times the majority of bacteria displayed the same phenotypes. Protein mass-spectrometry (MS) results indicated that, after attachment proteins involved in carbon catabolism, amino-acid metabolism and co-factor biosynthesis were upregulated. Among these proteins were thioredoxin reductase and adenylate kinase, which are involved in pyrimidine- and purine biosynthesis respectively.

Beenken and co-workers used micro-arrays to compare the gene expression profiles of planktonic and biofilm *S. aureus* isolates. They found that several operons of the pyrimidine nucleotide biosynthesis pathway were induced in biofilms (Beenken *et al.*, 2004). In another study on *Pseudomonas aeruginosa*, 5850 transposon mutants were assayed for altered biofilm phenotypes (Ueda *et al.*, 2009). Mutations caused by transposon insertions in the genes from the *de novo* pyrimidine synthesis pathway resulted in complete abolishment of biofilm formation. When exogenous uracil was applied to one such a mutant, biofilm formation was restored. Furthermore, whole transcriptome analysis revealed that pyrimidine starvation affected all three known QS systems in *P. aeruginosa*. This study found that purines were not required for biofilm formation (Ueda *et al.*, 2009). Nevertheless, other research on other model systems has emphasized the importance of purine biosynthesis for biofilm formation and symbiosis with nematodes, insects or plant roots (Han *et al.*, 2006; Ge *et al.*, 2008; Kim *et al.*, 2014; Yoshioka & Newell, 2015). In these studies, defective biofilm formation and/or symbiotic interactions were observed for purine auxotrophic mutants.

Oggioni and colleagues identified two principal patterns of pneumococcal behaviour in the host during infection: during bacteraemic sepsis *S. pneumoniae* exhibits planktonic growth behaviour, while tissue infection (like meningitis or pneumonia) bacteria are in a biofilm-like state (Oggioni *et al.*, 2006). Yadav and colleagues (Yadav *et al.*, 2012b) compared the gene expression profiles of early phase biofilms to that of planktonic cells using cDNA microarrays. Genes involved in isoprenoid biosynthesis, cell-wall biosynthesis, translation and purine and pyrimidine nucleotide metabolic pathways were induced in the biofilms.

These results suggest that nucleotide biosynthesis may be a universal requirement for biofilm formation of different microbial species. There could be various reasons why intact *de novo* nucleotide biosynthesis is important for biofilm formation, including: (i) a lack of nucleotides affects growth, and biofilm inhibition may be a direct result of reduced growth. (ii) A lack of

nucleotides may inhibit eDNA production which is an important component of the biofilm matrix for some organisms. (iii) Perturbations in the nucleotide pools may lead to changes in the concentrations of nucleotide derived signalling molecules (such as cAMP or c-di-GMP) which regulate biofilm formation. The roles of nucleotide derived signalling molecules in the bacterial cell are discussed next.

2.3.1 Nucleotide derived second messengers

Prokaryotes and eukaryotes utilize cyclic and linear nucleotides to regulate a diversity of physiological processes in response to internal and external stimuli. It has become evident that in bacteria c-di-GMP, c-di-AMP, cAMP and pp(p)Gpp all play important roles as second messengers involved in the coordination of virulence factor production, biofilm formation, carbon metabolism, stress response and cell cycle progression and more. These small molecules diffuse within as well as between cells and so contribute to the regulation of biological processes at different levels. Furthermore, different nucleotide-based signalling systems are often integrated with each other. For example in *S. aureus* high levels of c-di-AMP activate the stringent response through RelA/SpoT (enzymes that metabolize (p)ppGpp), in addition the phosphodiesterase enzyme GdpP is inhibited in a dose-dependent manner by ppGpp (Corrigan *et al.*, 2013). In *P. aeruginosa* the cAMP-Vfr signaling pathway, which is involved in virulence regulation, is inhibited by c-di-GMP through a yet undiscovered mechanism (Almblad *et al.*, 2015). Evidence also points to an interaction between Quorum Sensing on the population level and c-di-GMP signalling within the individual bacterial cells. Research on this topic has been reviewed in (Srivastava & Waters, 2012). Some of the physiological processes that are regulated by nucleotide based second messengers are summarized in Figure 19 and briefly reviewed in the next sections.

2.3.1.1 cAMP

cAMP is synthesized from ATP by adenylyl cyclases and hydrolysed by cAMP specific phosphodiesterases. The catabolic gene activator protein (also known as Cap or Crp) is a well-studied cAMP receptor. Cap regulates the expression of more than 180 genes in *E. coli* (Robison *et al.*, 1998; Zheng *et al.*, 2004; Grainger *et al.*, 2005). When cAMP binds to Cap its DNA-binding domain is activated enabling it to bind to specific DNA sequences near the promoter sequences, where it enables transcription by directly interacting with RNA polymerase. No doubt, the best-studied example of the role that cAMP-CAP plays in gene expression is the mediation of the glucose response or catabolic repression in *E. coli*. cAMP is produced by the cell only when glucose levels are low. When glucose levels are high, there

is no cAMP activation of Cap and RNA polymerase cannot interact with the promoter. When glucose levels are low and cAMP levels are high, cAMP-Cap interacts with the RNA polymerase and the lactose operon can be transcribed (if the *lac* repressor protein is not blocking the operator due to the absence of lactose in the medium). cAMP has also been shown to regulate the expression of virulence genes and genes involved in biofilm formation in a wide set of bacterial pathogens including *Salmonella* and *E.coli* (information obtained from the Ecocyc webpage for *cap/crp* as well as the references listed therein (Keseler *et al.*, 2013).

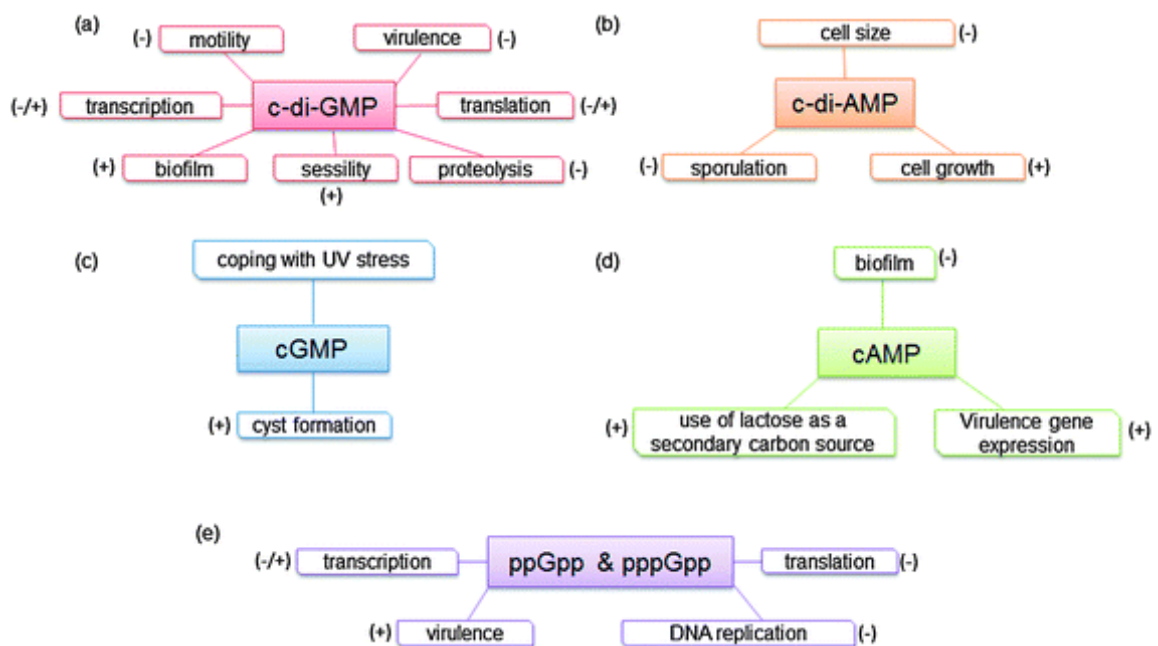


Figure 19 Phenotypes or processes that are controlled by (a) c-di-GMP. (b) c-di-AMP. (c) cGMP. (d) cAMP. (e) ppGpp and pppGpp (Kalia *et al.*, 2013). Figure reproduced with permission

2.3.1.2 (p)ppGpp

The linear nucleotides guanosine tetraphosphate and guanosine pentaphosphate, collectively referred to as (p)ppGpp, are produced in response to starvation for the following nutrients: amino acids, phosphates, fatty acids, carbon and iron (Vinella *et al.*, 2005; Battesti & Bouveret, 2006; Lapouge *et al.*, 2008; Kalia *et al.*, 2013). The so-called “stringent response” results in the inhibition of RNA synthesis during amino acid starvation. This leads to reduced translation activity, in order to conserve the amino acids that are available. (p)ppGpp also upregulates amino acid uptake genes. In the Beta- and Gamma-proteobacteria the concentration of (p)ppGpp is regulated by the activity of two homologous proteins, SpoT and RelA. SpoT is a bifunctional hydrolase-synthase, which uses ATP and GDP or GTP to

generate ppGpp or pppGpp. RelA is a mono-functional synthase, which uses GTP and ATP to produce pppGpp, which is converted to ppGpp. Furthermore, RelA or SpoT also catalyze the hydrolysis of ppGpp and pppGpp. (p)ppGpp regulates bacterial physiology on various levels including: DNA-replication, transcription and translation (Kalia *et al.*, 2013). (p)ppGpp has been implicated in the switch between the free-living lifestyle and biofilm formation by *Listeria*, *Streptococcus* and *Campylobacter* because mutants that cannot synthesize (p)ppGpp are defective in biofilm formation (Dalebroux *et al.*, 2010)

2.3.1.3 cGMP

Until recently, the involvement of cGMP in bacterial signaling was quite controversial because the findings in early reports linking cGMP to physiological functions could not be reproduced (Black *et al.*, 1980; Gomelsky & Galperin, 2013). However, that controversy has been laid to rest when Berleman and colleagues provided unambiguous evidence that *Rhodospirillum centenum* synthesizes cGMP and utilizes it for regulation of cyst formation and that it exerts its regulatory function through a specific transcription factor (Berleman *r.*, 2004). Other cyst-forming Alphaproteobacteria, *Azospirillum brasilense* and *Sinorhizobium melioli* also excrete cGMP during encystment (Marden *et al.*, 2011; Gomelsky & Galperin, 2013). Furthermore, the genomes of several other cyst-forming bacteria encode guanylyl cyclase gene clusters. Research into cGMP signaling in bacteria is still in its infancy and the details of its regulatory role is only beginning to emerge (Kalia *et al.*, 2013) therefore it remains to be seen if it plays a role in biofilm formation.

2.3.1.4 Cyclic dinucleotide second messengers

The three major types of cyclic dinucleotide second messengers discovered to date are c-di-GMP, c-di-AMP and most recently c-AMP-GMP. The first cyclic dinucleotide messenger that was discovered is c-di-GMP which serves as a regulator of diverse processes in most bacterial lineages (Römling *et al.*, 2013). Compared to the other two molecules, the c-di-GMP signaling systems are the best studied, although there are still a great many mysteries that remain to be solved. The signaling role of c-di-AMP was revealed in 2008 and was shown to be important for regulating sporulation and germination as well as the osmotic-shock response (Witte *et al.*, 2008; Oppenheimer-Shana'an *et al.*, 2011; Corrigan *et al.*, 2013; Nelson *et al.*, 2013). Very recently c-AMP-GMP was discovered to control *Vibrio cholera* virulence (Davies *et al.*, 2012), and has since been found to regulate *Geobacter* electrogenesis (Nelson *et al.*, 2015). Bacterial c-AMP-GMP is formed via two 3'5' phosphodiester linkages, however an analogue with one 2'5'-phosphodiester linkage and one 3'5'-phosphodiester linkage is

produced by metazoans (Zhang *et al.*). It is possible to vary the nucleotide composition and manner in which they are joined, thus it is expected that many additional types of cyclic dinucleotides and signaling pathways are awaiting discovery, reviewed by (Nelson *et al.*, 2015). The following sections focus on c-di-GMP mediated signaling, with special emphasis on its role in biofilm formation.

2.3.1.5 A general overview of c-di-GMP signalling

Benzinamn and colleagues first described the nucleotide based second-messenger c-di-GMP as an allosteric activator of cellulose production in *Gluconacetobacter xylinus*. (Ross *et al.*, 1986; Ross *et al.*, 1987). Over the years, it has been established that c-di-GMP is a major player in the regulation of physiology across the bacterial kingdom. For instance cell differentiation, the switch from the free-living planktonic mode of growth to the sessile biofilm mode of growth as well as the transition from acute infection to chronic infection are all regulated by c-di-GMP (see reviews by (Römling *et al.*, 2005; Hengge, 2009; Krasteva *et al.*, 2012)). Furthermore, it has become rather obvious that the c-di-GMP signalling cascades are far more complex than that of other known signal transduction systems. In canonical two-component transduction systems, a signal stimulates a histidine kinase to phosphorylate its cognate response regulator, which subsequently alters the expression of a limited set of genes (Albright *et al.*, 1989). In contrast, the c-di-GMP signalling cascades have a multilayer impact, which includes control at the transcriptional, translational and post-translational level. Proteins involved in c-di-GMP typically have a modular multi-domain architecture to allow for a diversity of regulatory inputs and/ or signal outcomes (Krasteva *et al.*, 2012). Many bacterial genomes encode several copies of GGDEF and EAL domains, however the mechanisms by which the activities of parallel c-di-GMP signalling systems are segregated to avoid potential cross talk are not well understood (Seshasayee *et al.*, 2010).

2.3.1.6 c-di-GMP metabolism and architecture of c-di-GMP metabolizing proteins

The condensation of two GTP molecules to form c-di-GMP is catalysed by diguanylate cyclase domains (DGEs) with GGDEF motif. The enzymatic degradation of c-di-GMP occurs via hydrolyses by phosphodiesterase (PDEs) with EAL or HD-GYP domains. Many of the DGE or PDE proteins contain sensory domains that integrate cellular or environmental signals into the regulation of c-di-GMP production and breakdown (Figure 20).

DGE proteins form homodimers and each monomer contributes a single bound GTP molecule to create a phosphodiester bond. Two divalent metal ions Mn^{+2} or Mg^{+2} are indispensable for the formation of the phosphodiester bond between the GTP molecules. The intermediate

product pppGpG is converted into c-di-GMP and two phosphor molecules are released (Ross *et al.*, 1987; Wassmann *et al.*, 2007; Paul *et al.*, 2007). The two glycine residues in the GGD(D/E)F motif are important for GTP binding, the glutamate/aspartate residue in the third position is required for metal ion coordination and for catalysis and the glutamate residue in the fourth position also plays a role in metal ion coordination (Chan *et al.*, 2004; Wassmann *et al.*, 2007). Approximately half of the proteins that have a GGDEF domain also contains a c-di-GMP binding site with a conserved RxxD motif. The RxxD site has an allosteric inhibitory function and is found close to the GGDEF site (Chan *et al.*, 2004). This self-inhibitory mechanism enables accurate control of the localized c-di-GMP pool and thereby avoids the diffusion of excess c-di-GMP, which could potentially interfere with other intracellular processes.

c-di-GMP can be degraded into two GMP molecules or into pGpG by the activity of either HD-GYP or EAL domain containing PDEs respectively. EAL domain PDEs are much better studied than those with HD-GYP domains. EAL domain PDEs contain the highly conserved Glu-Ala-Leu sequence motif and hydrolyse c-di-GMP into pGpG which is subsequently converted to two molecules GMP. EAL domains function as dimers and require Mg^{2+} binding for catalytic activity (Rao *et al.*, 2008). A conserved EGVE motif acts as a general base catalyst and accepts a proton from an H_2O molecule. The resulting hydroxid ion performs the nucleophilic attack, which breaks the phosphodiester bond. The EAL domain contains another conserved motif, DFG (T/A)GYSS which is also thought to be essential for catalytic activity (Rao *et al.*, 2008; Römling, 2009). Although EAL domain proteins typically function as dimers, some EAL domains can exhibit limited PDE activity as monomers (Tarutina *et al.*, 2006; Barends *et al.*, 2009; Ahmad, 2013).

HD-GYP domains are not as well studied as EAL domains, mostly because they are difficult to crystalize. By 2015 only the third structure of this class have been solved by X-ray diffraction and a recent search of the Protein Data Bank (<http://www.rcsb.org>) has not revealed any new structures (date of access 13 July 2016). The first high resolution HD-GYP domain that was studied by crystallography is BD1817 from *B. bacteriovorus* which lacks the active-site tyrosine that is conserved between most HD-GYP domains (Lovering *et al.*, 2011). For a few years, BD1817 was the best available model to deduce the catalytic mechanism of c-di-GMP cleavage by HD-GYP domains. Sequence alignment with other HD-GYP containing proteins revealed that the majority of residues that make contact with the phosphate moiety of c-di-GMP, are conserved. However, it could not reveal the strategy that HD-GYP domains use

to cleave the two phosphate moieties of c-di-GMP (Kalia *et al.*, 2013). PA478 from *P. aeruginosa* was the third HD-GYP domain PDE to be solved. It exhibited significant differences with its homologues in both the nature and the binding mode of the coordinated metals. This is an indication that HD-GYP domains have the ability to fine-tune their function, which would help to increase the chances of the bacterial cell to adapt to different environmental needs (Rinaldo *et al.*, 2015).

The catalytic GGDEF, EAL and HD-GYP domains can be organized in separate subunits or together in the same polypeptide. The tandem “GGDEF-EAL” domain arrangement is found in almost a third of proteins that contain a GDEF motif. On the other hand, the “GGDEF-HD-GYP” arrangement is less common (Römling *et al.*, 2013; Kalia *et al.*, 2013). Interestingly, most of the studied proteins that possess hybrid GGDEF-EAL domains typically show either DGE activity or PDE activity, proteins with both activities are comparatively rare. Bioinformatics analysis of 11248 GGDEF and EAL domain-containing proteins from 867 prokaryotic genomes revealed that a higher proportion of GGDEF domain proteins (23%) have lost their catalytic motif compared to only 16.8% of EAL domains. Out of all the proteins analysed, 5674 were GGDEF-only, 1805 were EAL-only and 3769 were hybrids (Seshasayee *et al.*, 2010). In some instances, the catalytic inactive domain of the hybrid proteins function as an allosteric regulator. For example, the hybrid protein CC3396 from *C. crescentus* contains a catalytically inactive GGDEF domain which binds GTP leading to the allosteric activation of the EAL domain and enhanced PDE activity (Christen *et al.*, 2005).

2.3.1.7 c-di-GMP effectors

Following the production of c-di-GMP in response to an environmental stimulus, the signal must be relayed to the downstream c-di-GMP effectors. These effectors are highly diverse and include riboswitches, transcription factors with a variety of domain architectures, divergent c-di-GMP turnover domains, and allosteric sites on active or degenerate DGCs (see review by (Krasteva *et al.*, 2012)). Moreover, the structural diversity of c-di-GMP is not limited to the nucleotide-sensing modules, but c-di-GMP itself can adopt a number of different stable conformations. For example dimeric c-di-GMP bound to Alg44 is required for alginate polymerization by *Pseudomonas aeruginosa* (Whitney *et al.*, 2015), whereas c-di-GMP binds in a monomer form to FimX to regulate twitching motility in the same organism (Huang *et al.*, 2003).

Among the different groups of c-di-GMP effector modules, the PilZ family (named after a type IV pilus control protein in *P. aeruginosa*) was the first to be identified. In certain

instances, the PilZ domain is directly attached to the C-terminus of the GGDEF, EAL and/ or HD-GYP domains. In other cases it is linked to a domain that generates a molecular output, such as alginate production, cellulose synthesis or twitching motility, see review (Hengge, 2009). When c-di-GMP binds to a RxxxR and DXSXXG motifs on the PilZ domain, conformational changes occur which affect the affinity for the protein to its interacting protein partner(s) (Amikam & Galperin, 2006; Habazettl *et al.*, 2011).

Some c-di-GMP effector proteins are members of protein families that generally sense or metabolize other small nucleotide signalling molecules. For example VpsR (of *V. cholera*) and FleQ (of *P. aeruginosa*) are members of the AAA+ superfamily of ATPases, but apparently function as c-di-GMP effectors independently of ATP binding or hydrolysis. When FleQ is not bound to c-di-GMP it functions as a transcriptional repressor of the *pel* operon, which encodes enzymes for PEL polysaccharide synthesis. In the presence of c-di-GMP, FleQ binding to the *pel* promoter DNA is relieved and transcription can continue (Hickman & Harwood, 2008; Baraquet *et al.*, 2012).

Although degenerate GGDEF or EAL domains are enzymatically inactive as DGCs/ PDEs, they can bind c-di-GMP and thereby regulate downstream proteins. For example, the LapD protein (from *P. fluorescens*) which is an inner-membrane protein with both degenerate EAL and GGDEF domains, can bind c-di-GMP with high affinity. Binding to c-di-GMP occurs on the EAL domain. The formation of a c-di-GMP-LapD complex leads to the sequestration of LapG. LapG is a periplasmic protease and once it is interacting with LapD it loses its proteolytic activity towards the large adhesion protein LapA. As a result, LapA remains in the outer membrane, which stabilizes the biofilm matrix. Conversely, when c-di-GMP levels are low, LapG is released from LapD into the periplasm. LapG can then cleave LapA from the cell surface leading to biofilm dispersal (Newell *et al.*, 2011). Another example is PelD (from *P. aeruginosa*), which contains a degenerate GGDEF domain and an I-site with an RxxD motif. When c-di-GMP binds to the I-site, which normally serves as an allosteric inhibition site for active DGCs, the production of PEL polysaccharide is activated and in turn biofilm formation is upregulated (Lee *et al.*, 2007b). The activation probably occurs via PelD interaction with PelF, which is predicted to assemble the PEL polysaccharide from an unidentified sugar nucleotide precursor (Whitney *et al.*, 2012). Figure 21 provides a summary of the modes of function of some c-di-GMP effector proteins.

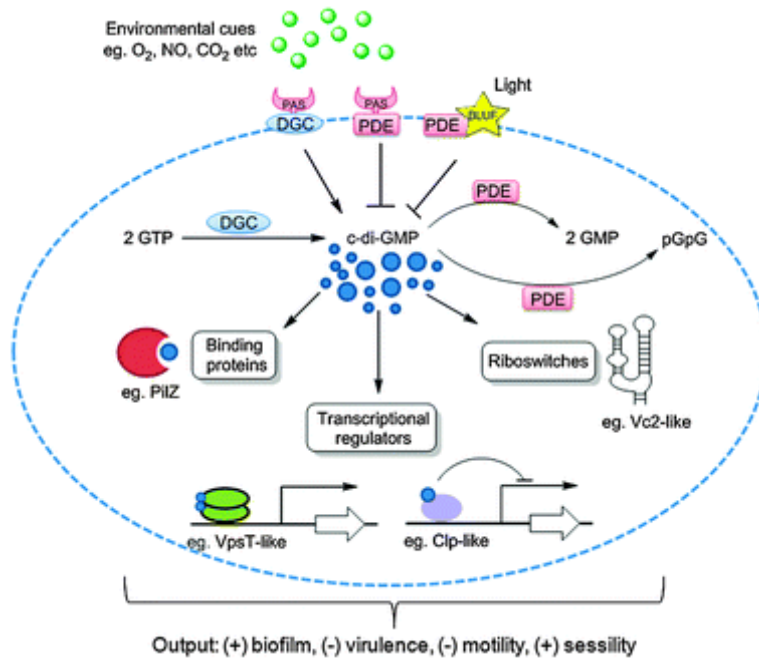


Figure 20 c-di-GMP synthesis, degradation and signalling. Two molecules of GTP are converted to c-di-GMP by DGC proteins containing the GGDEF domain and c-di-GMP is degraded by PDE proteins with EAL or HD-GYP domains. Multiple numbers of DGCs and PDEs are often associated with sensor domains such as PAS for sensing gaseous ligands such as O₂, CO₂, NO etc. and BLUF for sensing light. c-di-GMP binds to receptor proteins such as PilZ or riboswitches or transcriptional regulators to regulate bacterial “lifestyle”. Figure reproduced from (Kalia *et al.*, 2013)

The regulation of cellular functions by c-di-GMP does not only involve allosteric regulation of protein functions or the regulation of gene expression via modulation of transcription factors. But, it also occurs via direct interaction with noncoding RNA molecules known as riboswitches (Valentini & Filloux, 2016). So far two classes of riboswitches that sense c-di-GMP have been discovered (Lee *et al.*, 2010; Nelson *et al.*, 2013). Riboswitches are structured noncoding RNA domains that selectively bind a small molecule or ion and thereby trigger a change in the expression of associated genes (Breaker, 2011; Serganov & Patel, 2012; Nelson *et al.*, 2015). See Figure 22 for the general architecture of Class I and Class II riboswitches and Figure 23 for a description of their function. These riboswitches are typically located upstream of the open reading frame (ORF) of DGC and PDE encoding genes or genes that are controlled by c-di-GMP. Binding of c-di-GMP can affect transcription or translation (Lee *et al.*, 2010; Kalia *et al.*, 2013; Nelson *et al.*, 2013). Binding of c-di-GMP to a Class I riboswitch regulates gene expression *via* structural rearrangement of RNA molecules (Sudarsan *et al.*, 2008; Kalia *et al.*, 2013). Binding of c-di-GMP to a Class II riboswitch stimulates the self-splicing activity of the adjacent ribozyme, which renders the ribosomal binding site in the RNA molecule accessible. On the other hand, when c-di-GMP is absent, the ribosomal binding

site is inaccessible (Lee *et al.*, 2010; Kalia *et al.*, 2013). A subset of the Class I riboswitches are now known to bind the newly discovered signalling molecule c-AMP-GMP (Nelson *et al.*, 2015).

Attempts to reveal undiscovered c-di-GMP-binding proteins are ongoing, and both deductive and inductive (or targeted) approaches are being used (Valentini & Filloux, 2016). Deductive approaches are based on affinity pulldown assays using whole cell lysates in combination with a c-di-GMP-conjugated Sepharose resin, biotin, or a tripartite c-di-GMP capture compound to detect c-di-GMP-binding proteins (Düvel *et al.*, 2012; Nesper *et al.*, 2012; Laventie *et al.*, 2015; Valentini & Filloux, 2016). The differential radial capillary action of ligand assay (DRaCALA) is a systematic screening protocol, which assesses protein expression libraries for their c-di-GMP binding activity (Roelofs *et al.*, 2011; Valentini & Filloux, 2016). On the other hand, the inductive approaches are based on “educated guesses”. Several biochemical assays, such as isothermal titration calorimetry, DRaCALA, and a peptide array approach are used to test the c-di-GMP binding capacity of potential targets, which are functionally associated with c-di-GMP regulated processes (Roelofs *et al.*, 2011; Whitney *et al.*, 2015; Düvel *et al.*, 2016; Valentini & Filloux, 2016).

2.3.1.8 Controlling the intracellular levels of c-di-GMP

The intracellular pools of c-di-GMP can be regulated in response to environmental stimuli. This precise spatial and temporal regulation is made possible by the sensory domains that are often located at the N-terminus of GGDEF or EAL domains. The sensory domains are typically PAS/PAC, MASE or GAF domains. DGEs or PDEs containing such sensory domains can monitor cytoplasmic or periplasmic levels of their respective ligands, and alter the synthesis or hydrolysis of c-di-GMP in response to ligand binding. Some DGEs and PDEs can respond to the redox state, nitric oxide, light and oxygen (Chang *et al.*, 2001; Barends *et al.*, 2009; Wan *et al.*, 2009; Tuckerman *et al.*, 2009; Qi *et al.*, 2009; Cao *et al.*, 2010). The carbon storage regulator, CsrA, is another major role player and controls c-di-GMP metabolism on a post-transcriptional level. CsrA is a RNA binding protein, which functions as a homodimer with two RNA binding surfaces located on opposite sides (Schubert *et al.*, 2007). It regulates the expression of its target genes by binding to its mRNA transcripts. In *E.coli*, CsrA regulates the expression of at least seven of the 29 encoded GGDEF and/or EAL domain proteins (Simm *et al.*, 2014) and has been shown to regulate some of the GGDEF and/or EAL domain proteins in *Salmonella*, directly or indirectly.

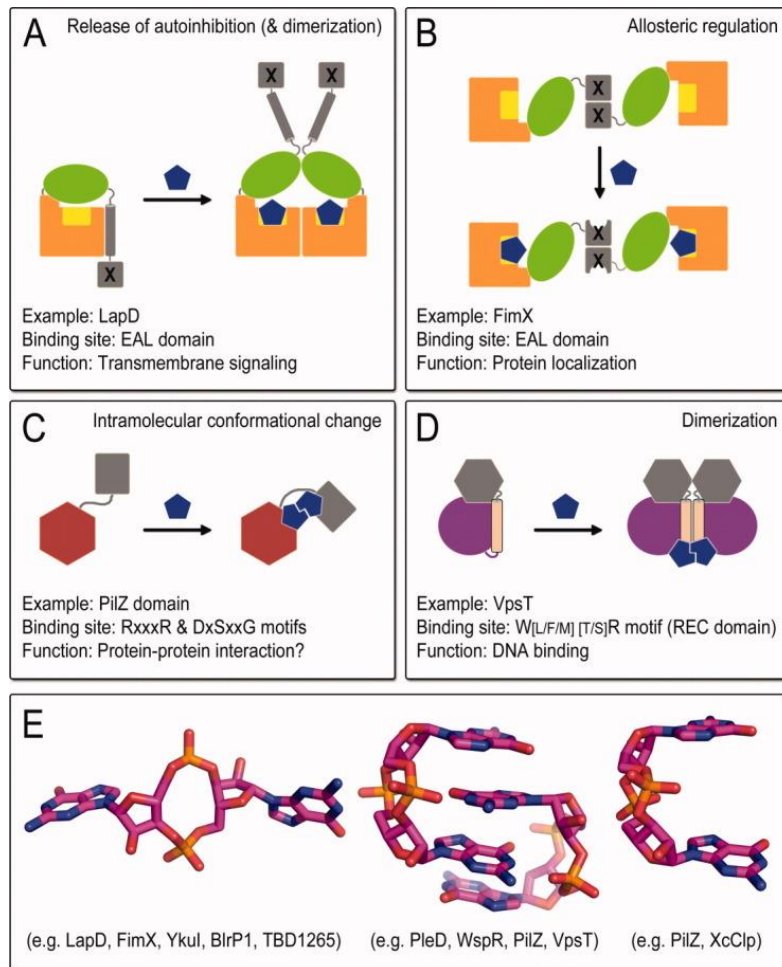


Figure 21. Modes of c-di-GMP effector function. Based on structural studies several modes of c-di-GMP action on effector proteins have been described, including the release of auto-inhibitory interactions (A), allosteric regulation (B), major structural rearrangements (C) and/or dimerization (D). In addition, c-di-GMP itself can adopt several distinct conformations when bound to proteins. Figure obtained from (Krasteva *et al.*, 2012)

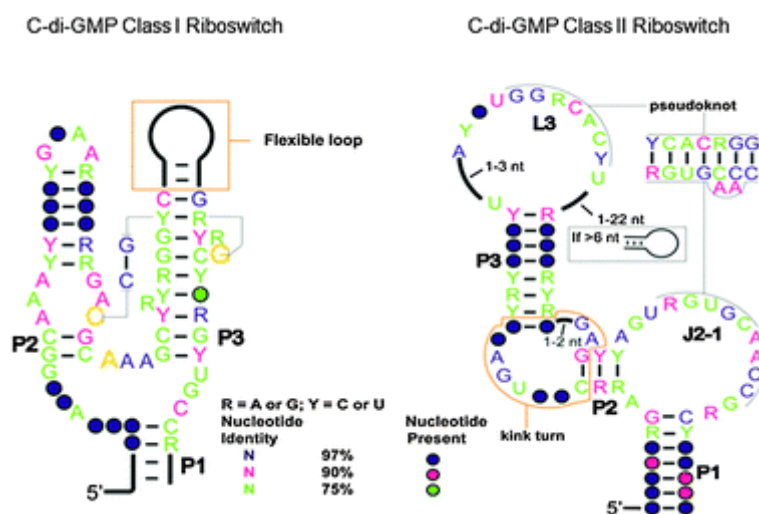


Figure 22 Comparison of c-di-GMP Class I and Class II riboswitches (reproduced from (Kalia *et al.*, 2013).

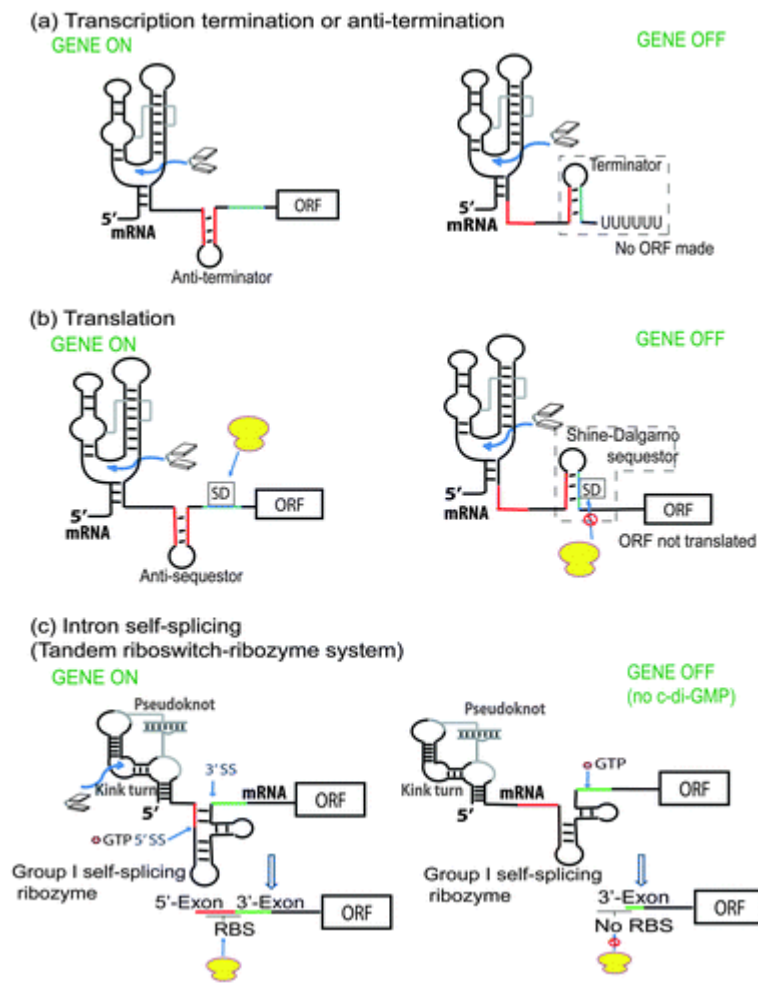


Figure 23 Mechanism of c-di-GMP riboswitch function. Image reproduced from (Kalia *et al.*, 2013).

2.3.2 The role of c-di-GMP signaling in *Salmonella*

The *S. Typhimurium* genome contains twenty-two proteins with GGDEF and/or EAL domains and no HD-GYP domain proteins (Jonas *et al.*, 2009; Ahmad *et al.*, 2017). The GGDEF/EAL domains can be divided into classes based on their catalytic activity and conserved residues. Class I GGDEF domain proteins contain all residues that are required for catalytic activity, while Class II GGDEF domain proteins are catalytically inactive. The *S. Typhimurium* 14028 genome encodes eight Class I and four Class II GGDEF domain proteins. The EAL domain proteins are divided into 3 groups: In Class I EAL domains all residues required for c-di-GMP dependent phosphodiesterase activity are conserved. Class 2 EAL domain proteins lack the conserved loop 6, nevertheless some of these proteins have been demonstrated to possess PDE activity. Class 3 EAL domain proteins are predicted to be catalytically inactive. For the classification of GGDEF/ EAL domain proteins of *Salmonella* see Table 3. At least eight of

the GGDEF/EAL domain proteins in *S. Typhimurium* have been shown to contribute directly or indirectly to rdar biofilm formation. There are only two PilZ domain containing c-di-GMP receptors in *S. Typhimurium*, BcsA and YcgR; both of them influence motility. YcgR affects flagellar rotational switching and speed in response to c-di-GMP (Ryjenkov *et al.*, 2006; Paul *et al.*, 2007; Boehm *et al.*, 2010). BcsA produces cellulose, which hinders swimming by sterically interfering with the flagella (Zorraquino *et al.*, 2013; Le Guyon *et al.*, 2015).

The roles that the various GGDEF/EAL domain proteins play in *S. Typhimurium* biofilm formation, virulence and motility are summarised in Table 3. Redundancy of function for some GGDEF/EAL domain proteins has been reported (Ahmad *et al.*, 2011). For example, four DGCs were found to be functionally redundant with regard to the induction of cellulose biosynthesis when single DGCs were re-inserted into the genome of a strain that contained no DGCs (Solano *et al.*, 2009). Unfortunately c-di-GMP levels were not measured for the re-insertion mutants, and thus no conclusion about the relationship between the phenotypic output and the c-di-GMP levels could be drawn (Massie *et al.*, 2012).

Nevertheless, Ahmad and colleagues (Ahmad *et al.*, 2011) and Le Guyon and colleagues (Le Guyon *et al.*, 2015) performed complementation and mutation studies to systematically couple GGDEF/EAL domain proteins to virulence, motility and biofilm phenotypes. Their results confirm that certain c-di-GMP signalling pathways are dedicated to the regulation of specific cellular functions, or to the regulation of similar cellular functions on different levels. For example, STM2672 inhibits motility through YcgR, while STM1987 appeared to work solely through BcsA (Le Guyon *et al.*, 2015). These findings give support to the hypothesis that there exist a spatial and temporal compartmentalization of c-di-GMP and effector proteins (Christen *et al.*, 2010).

2.3.3 Regulation of biofilm formation by c-di-GMP in *Salmonella*

The regulation of biofilm formation in *Salmonella* is quite complex and involves the master regulator CsgD as well as c-di-GMP which activates several steps in the biofilm regulatory network (Kader *et al.*, 2006). In its unphosphorylated form, CsgD activates *csgB* and *adrA* transcription (Zakikhany *et al.*, 2010). CsgB is a major subunit of curli, which is an important component of the EPS matrix. AdrA is a DGC which synthesizes c-di-GMP to activate the cellulose biosynthesis complex subunit BcsA. Because transcription of the *bcsABC* operon is not affected by AdrA, cellulose production is regulated by AdrA on a post-transcriptional level. Furthermore, cellulose biosynthesis on CR agar relies on AdrA, but does not require CsgD to activate *adrA* expression (Zogaj *et al.*, 2001; Simm *et al.*, 2004). Deletion of AdrA

caused a reduction in the intracellular c-di-GMP pool and furthermore resulted in white and non-fluorescent colonies on CR agar plates and Calcofluor plates respectively, which is typical of impaired cellulose production. Expressing AdrA from the pBAD30 plasmid in the *adrA* knockout strain led to the activation of cellulose biosynthesis as monitored by pdar colonies on CR agar as well as fluorescent colonies on Calcafluor plates (Simm *et al.*, 2004). These results clearly showed that CsgD regulates cellulose production indirectly via affecting c-di-GMP production by AdrA.

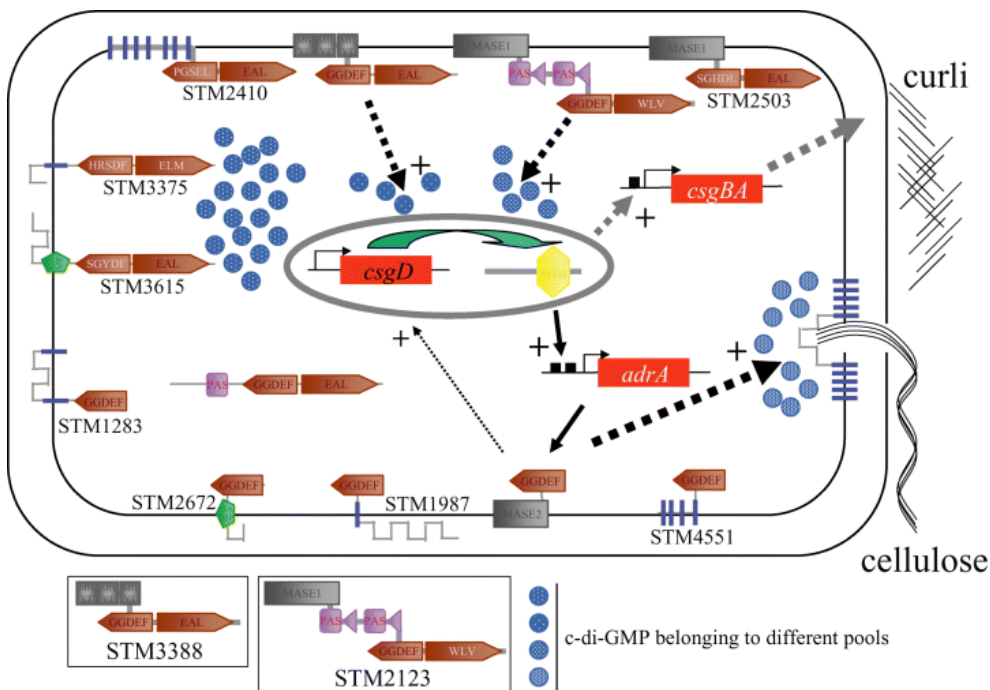


Figure 24 Schematic model showing the role of various GGDEF domain proteins in *S. Typhimurium* UMR1. STM3388 and STM2132 have an additive effect on CgsD expression levels. AdrA primarily activates cellulose biosynthesis through the creation of a different c-di-GMP pool. The feedback regulation by c-di-GMP produced by AdrA on CsgD expression is observed in strain MAE52 but not in strain UMR1. Domain abbreviations are: HAMP (histidine kinases, adenine cyclase, methyl binding protein, phosphatases), HTH (helix tur helix), MASE1 and MASE2 (membrane associated sensors 1 and 2), MHYT (integral membrane sensory domain containing a conserved motif), PAS/PAC (periodic clock protein, Ah receptor transnuclear translocator protein, single-minded protein). Deviations from the GGDEF or EAL motifs are also shown. Figure reproduced from Kader *et al.*, 2006.

CsgD itself is also regulated by c-di-GMP on a transcriptional and post-transcriptional level. Elevated concentrations of c-di-GMP mediated by the overexpression of plasmid encoded AdrA in *S. Typhimurium* UMR1 lead to enhanced expression of curli fimbria (detected on CR and Calcafluor agar plates) by inducing expression of CsgA and CsgD as measured by Western

blot (Figure 24). Furthermore overexpression of YhjH (STM3611 a PDE) using plasmid pRGS1 led to an almost white phenotype on CR agar indicating that a reduction in the c-di-GMP pool negatively impacts cellulose and curli production. The effect of c-di-GMP on curli production was further confirmed by changes in the rdar morphotype of strain MAE222 which only expresses curli but not cellulose. It was determined by Northern blotting that high levels of c-di-GMP positively control CsgD production on a transcriptional level, while low levels of c-di-GMP have a negative effect (Simm *et al.*, 2004; Kader *et al.*, 2006). The post-transcriptional effect of c-di-GMP on CsgD production was verified by expressing CsgD from an arabinose inducible promoter while expressing YhjH (STM3611) from an IPTG inducible promoter in a strain containing a double deletion of *csgD* and *bcsA*. When YhjH levels were high, CsgD levels were lowered. Because the native Shine Dalgarno sequence of *csgD* was cloned into the plasmid it was concluded that post-transcriptional events from increased ribosome binding to diminished protein degradation could be responsible for controlling CsgD levels. AdrA and YhjH are not the only c-di-GMP metabolizing proteins to affect rdar biofilm formation. Reducing the intracellular c-di-GMP pool by deleting the DGCs STM2123 and STM3388 also negatively affected CsgD expression (measured by Western blot), and a double knockout mutant showed an additive effect (Kader *et al.*, 2006). Although AdrA has a large impact on the generation of elevated c-di-GMP levels, chromosomally encoded *adrA* was not required for the expression of CsgD and curli fimbriae in strain UMR1. STM2123 was found to be important for early rdar morphotype development while STM3388 contributed later. Single gene knockouts of STM2123 or STM3388 showed reduced *csgD* transcript levels as measured by Northern blot analysis; however the *adrA* knockout did not have an effect. On the other hand, all three single gene knockouts displayed a downregulation of *csgA* transcript levels. This indicates that although AdrA does not influence CsgD expression under native conditions, it does play a role in curli-biosynthesis, downstream of CsgD expression (Kader *et al.*, 2006). Based on the above results it was concluded that c-di-GMP acts transcriptionally and post-transcriptionally on CsgD and that different GGDEF domain proteins have specific effects on CsgD expression at specific growth phases. By 2015 it was known that out of the twenty-two GGDEF and/ or EAL domain proteins in *S. Typhimurium*, 10 affect rdar biofilm formation or cellulose production. Of those that affect CsgD levels specifically, two GGDEF domains upregulate *csgD* expression while four EAL domains down-regulate *csgD* expression. Very recently another two GGDEF domain proteins were found to contribute to optimal *csgD* expression (Ahmad *et al.*, 2017). The EAL domain protein STM4264 (*yjcC*) is the only protein that has been shown to regulate the rdar morphotype on both the level of *csgD*

expression and cellulose synthesis. This is not surprising, given that STM4264 downregulates the cellular c-di-GMP concentration approximately five-fold (Simm *et al.*, 2007). The exact mechanism by which c-di-GMP regulates CsgD expression is not known. Although it has been found that the regulation of CsgD expression and rdar biofilm formation, by GGDEF/EL domain proteins, is mainly mediated by the enzymatic activities of the proteins. This is not the exclusive mechanism. The GGDEF/EAL domain protein ST1730 suppresses the transcription of *csgD* by acting on the promoter upetram region from -208 to -340. It is hypothesized that STM1703 forms a complex with a high affinity c-di-GMP receptor. Furthermore it is thought that STM1703 degrades c-di-GMP produced from its own GGDEF domain, acting locally as a diguanylate cyclase. STM4264 exerts its inhibitory effect on *csgD* by acting on a post-transcriptional level (Figure 25).

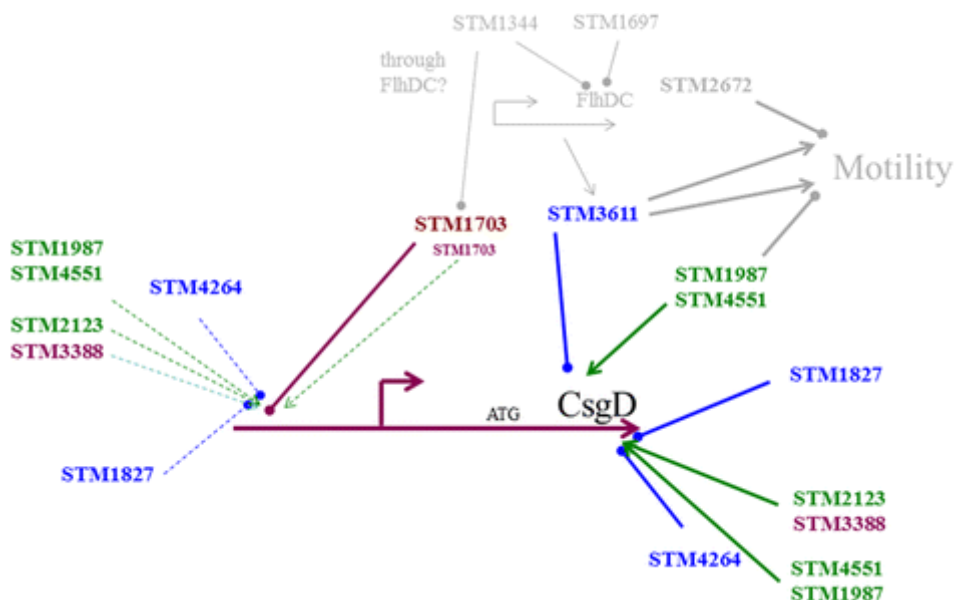






















Figure 25 A model of c-di-GMP regulation proposed by Ahmad *et al* (2017). Green represents a diguanylate cyclase, blue a phosphodiesterase and magenta represents a diguanylate cyclase/phosphodiesterase; light grey not directly investigated by Ahmad *et al* (2017). There are at least three distinctive groups of c-di-GMP turnover proteins that regulate *csgD* expression. Regulation by STM1703 occurs on the transcriptional level. Regulation by the other group occur on unknown levels and are drawn arbitrarily. The group consisting of STM1987, STM4551 and STM3611 inversely regulate motility. EAL-like proteins STM1344 and STM1697 affect the c-di-GMP signalling network through post-translational inhibition of FlhD4C2, the regulator of the flagellar cascade and regulation of STM1703. Image reproduced from (Ahmad *et al.*, 2017). Open access address, DOI: 10.1186/s12866-017-0934-5.

Table 3: GGDEF and EAL domain proteins of *Salmonella*.

Gene ID and name	Domain organization	GGDEF/EAL ^b	Enzyme activity ^c (class)	Cellular function and regulation	Reference
STM0343		EAL	PDE (I)	Stimulates invasion of the HT-29 cell line	(Ahmad <i>et al.</i> , 2011)
STM0385 (<i>adrA/yaiC</i>)		GGDEF	DGC (I)	Stimulation of cellulose biosynthesis and rdar development; upregulation of biofilm formation under LB (but not ATM) conditions; downregulation of motility; restoring cellulose production in a c-di-GMP lacking strain. Direct upregulation by <i>csgD</i>	(Zogaj <i>et al.</i> , 2001; Simm <i>et al.</i> , 2004; García <i>et al.</i> , 2004; Solano <i>et al.</i> , 2009; Zakikhany <i>et al.</i> , 2010)
STM1283 (<i>yeaJ/dgcI</i>)		GGDEF	DGC (I)	Invasion of HT-29 cells. Inhibition of IL-8 phenotype. Assuming role of STM1987 under ATM conditions	(Ahmad <i>et al.</i> , 2011)
STM1344 (<i>cdgR</i>)		EAL	No PDE (III)	Indirect upregulation of <i>csgD</i> and rdar expression; downregulation of motility; role in virulence (survival in mice, antioxidant defense, macrophage killing). Direct repression by CsrA	(Hisert <i>et al.</i> , 2005; Simm <i>et al.</i> , 2007; Simm <i>et al.</i> , 2009; Jonas <i>et al.</i> , 2009; Wozniak <i>et al.</i> , 2009)
STM1697		EAL	No PDE (III)	Possible role in virulence, no obvious role in motility or biofilm formation	(Ahmad <i>et al.</i> , 2011)
STM1703 (<i>yciR</i>)		GGDEF /EAL	PDE, DGE (I, I)	Strong downregulation of <i>csgD</i> (temperature suppressive effect), <i>csgA</i> and rdar expression, biofilm formation and cellulose synthesis. Negatively regulated by STM1344 and CsrA	(García <i>et al.</i> , 2004; Simm <i>et al.</i> , 2007; Simm <i>et al.</i> , 2009)
STM1827		EAL	PDE (I)	Slight downregulation of cellulose biosynthesis, <i>csgD</i> , rdar development and biofilm formation; very little	(Simm <i>et al.</i> , 2004; Simm <i>et al.</i> , 2007; Jonas <i>et al.</i> , 2009)

Gene ID and name	Domain organization	GGDEF/EAL ^b	Enzyme activity ^c (class)	Cellular function and regulation	Reference
				upregulation of swarming. Negatively regulated by CsrA	
STM1987		GGEEF	DGC (I)	Upregulation of cellulose production and biofilm formation under ATM conditions (<i>csgD</i> independent); assume role of <i>adrA</i> under LB conditions; restoring cellulose production and ATM biofilm formation in a c-di-GMP lacking strain. Negatively regulated by CsrA	(García <i>et al.</i> , 2004; Jonas <i>et al.</i> , 2009; Solano <i>et al.</i> , 2009)
STM2123 (<i>yegE</i>)		GGDEF /WLV	DGC (I)	Assuming role of <i>adrA</i> and STM1987 under LB and ATM conditions respectively; upregulation of <i>csgD</i> and <i>rdar</i> expression; restoring cellulose production and ATM biofilm formation in a c-di-GMP lacking strain	(García <i>et al.</i> , 2004; Kader <i>et al.</i> , 2006; Solano <i>et al.</i> , 2009)
STM2215 (<i>rtm</i>)		EAL	PDE (II)	Involved in fitness in mice. Does not affect motility, expressed on plates, and in liquid media at late exponential and early stationary phase. Stimulates invasion of HT-29 cells.	(Ahmad <i>et al.</i> , 2011; Zheng <i>et al.</i> , 2013)
STM2410 (<i>yfeA</i>)		EA GGDEF /EAL	No DGC activity, putative PDE (I, II)	Reinstating swimming in a c-di-GMP lacking strain	(Solano <i>et al.</i> , 2009)
STM2503		SGHDL /EAL	Probably PDE-like (I)	Reinstating swimming in a c-di-GMP lacking strain. STM4264 and STM2503 degrade the c-di-GMP produced by STM1283 dedicated to inhibition of IL-8 induction.	(Solano <i>et al.</i> , 2009; Ahmad <i>et al.</i> , 2011)

Gene ID and name	Domain organization	GGDEF/EAL ^b	Enzyme activity ^c (class)	Cellular function and regulation	Reference
STM2672 (<i>yfiN/dgcN</i>)		GGDEF	DGC (I)	Unable to assume role of <i>adrA</i> and STM1987 under LB and ATM conditions respectively; restoring cellulose production and ATM biofilm formation in a c-di-GMP lacking strain	(García <i>et al.</i> , 2004; Solano <i>et al.</i> , 2009)
STM3375 (<i>yhdA/csrD</i>)		HRSDF /ELM	No PDE or DGC activity (in <i>E. coli</i>) (III, II)	Upregulation of motility (swimming) and biofilm formation (in liquid LB without salt); destabilizing activity of sRNA <i>csrB</i> and <i>csrC</i> along with RNase E, (in <i>E. coli</i>). Negatively regulated by CsrA	(Simm, Morr <i>et al.</i> 2004, Simm, Lusch <i>et al.</i> 2007, Jonas, Edwards <i>et al.</i> 2009)
STM3388		GGDEF /EAL	DGC (I)	Assuming role of <i>adrA</i> and STM1987 under LB and ATM conditions respectively; upregulation of <i>csgD</i> and <i>rdar</i> expression	(García <i>et al.</i> , 2004; Kader <i>et al.</i> , 2006; Solano <i>et al.</i> , 2009)
STM3611 (<i>yjhH</i>)		ELL	PDE (II)	Downregulation of cellulose biosynthesis, <i>csgD</i> , <i>rdar</i> and biofilm formation; upregulation of motility (antagonized by <i>ycgR</i>); involved in growth competition between different <i>S. enterica</i> strains. Negatively regulated by STM1344; positively regulated by CsrA and FlhDC via FliA	(Simm, Morr <i>et al.</i> 2004, Simm, Lusch <i>et al.</i> 2007, Jonas, Edwards <i>et al.</i> 2009)
STM3615 (<i>yhkK/pdeK</i>)		SGYDF /EAL	Probable PDE (I)	Invasion of murine intestine.	(Ahmad <i>et al.</i> , 2011)
STM4264 (<i>yjcC</i>)		EAL	PDE (I)	Strong downregulation of <i>csgD</i> (slight temperature suppressive effect), <i>csgA</i> and <i>rdar</i> expression, biofilm formation and cellulose (also <i>csgD</i> independent) synthesis. STM4264 and STM2503 degrade the c-di-GMP produced by	(Simm <i>et al.</i> , 2007; Simm <i>et al.</i> , 2009; Ahmad <i>et al.</i> , 2011)

Gene ID and name	Domain organization	GGDEF/EAL ^b	Enzyme activity ^c (class)	Cellular function and regulation	Reference
				STM1283 dedicated to inhibition of IL-8 induction	
STM4551		GGEEF	DGC (I)	Assuming role of <i>adrA</i> and STM1987 under LB and ATM conditions respectively; regain motility, curli (rdar) production, virulence and long-term survival in a c-di-GMP lacking strain. Negatively regulated by CsrA	(Solano, García <i>et al.</i> 2009, García, Latasa <i>et al.</i> 2004)
STM0468 (<i>ylaB</i>)		EAL	No PDE activity (III)	Stimulates invasion of the HT-29 cell line	(Ahmad <i>et al.</i> , 2011)

Chapter 3

3 Repurposing of nucleoside- and nucleobase-derivative drugs as antibiotics and biofilm inhibitors

3.1 Abstract

There is an urgent need for new antibacterial drugs that are robust against the development of resistance. Drug repurposing is a cost effective strategy to fast track the drug development process. Here we motivate why the nucleoside and nucleobase analog drugs in particular present an attractive class for repurposing. Some of these drugs have already been evaluated for their potential as antibacterial agents. In addition to inhibiting bacterial growth and survival, some also work synergistically with antibiotics, and as such can enhance the therapeutic spectrum of currently available antibiotics. Furthermore nucleoside and nucleobase analog drugs can inhibit bacterial virulence and biofilm formation. Biofilms are known to impart antibiotic tolerance and are associated with chronic infections. Targeting biofilm formation thus renders pathogens more susceptible to antibiotic treatment and host immune defenses. Moreover, specific analogs have properties which make them less susceptible to the development of resistance. Thus, nucleoside and nucleobase analog drugs ought to be considered as new weapons in our fight against pathogenic bacteria.

3.2 Introduction

The discovery of antibiotics is without doubt one of the greatest medical achievements and proved to be a turning point in human history by saving countless lives and placing infectious diseases under control. However, there is a growing concern that we are approaching a post-antibiotic era in which common infections or minor injuries might become life-threatening (Alanis, 2005). The widespread use of antibiotics in medicine, agriculture and other anthropogenic activities has been followed with the emergence and rapid dissemination of antibiotic-resistant pathogens (Aminov, 2009; Aminov, 2010; Davies & Davies, 2010). Most worrisome, in clinical environments there are increasing reports of extensive drug resistant infections (Falagas *et al.*, 2005; Zhi-Wen *et al.*, 2015). Indeed, the recent discovery of an *E.coli*

strain harbouring resistance genes to colistin and 14 other antibiotics on a plasmid is thought to herald the emergence of true pan-drug resistance (McGann *et al.*, 2016). It is estimated that 700 000 people die of resistant infections every year, that number is feared to increase to 10 million per year by 2050 (O'Neill, 2014). Aside from the tragic human cost, the economic impact of antibiotic resistance is enormous. The cost in terms of lost global production between now and 2050 is predicted to be 100 trillion USD (O'Neill, 2014).

To continue our fight against pathogenic bacteria it is absolutely imperative that there should be no abatement in the quest for new antimicrobial agents. An emerging strategy is to repurpose drugs that are already approved for other uses. The antibiotic, anti-biofilm and anti-virulence activities of diverse drugs including gallium compounds, alkylating agents, hormonal modulators and antimetabolites were recently reviewed (Younis *et al.*, 2015; Rangel-Vega *et al.*, 2015; Soo *et al.*, 2016). Here we will examine the striking antibacterial properties of nucleoside and nucleobase analog drugs (abbreviated as 'NNADs'). These drugs are important anti-proliferative therapies used against cancer and viral diseases. Although, application of these NNADs for antibacterial therapy has only been poorly evaluated (Landini *et al.*, 2010) We, and others are of the opinion that these drugs could also have a significant impact on the clinical treatment of bacterial infections, with potentially a lower risk of resistance development, and that they could be a financially viable option for pharmaceutical companies. We argue that repurposing approved NNADs as bactericidal, bacteriostatic or anti-biofilm agents could have potential to circumvent important hurdles related to traditional antimicrobial discovery and illustrate this with recent experimental evidence. Finally, factors that need to be taken into account to assess the likeness of resistance development against NNADs are discussed.

3.2.1 Nucleobase and nucleoside analogs have been in clinical use for several decades

Nucleotides are the basic structural units of DNA and RNA, which direct and control the production of proteins. Nucleotides serve as cofactors in a wide range of metabolic pathways including lipid- and polyamine biosynthesis. Furthermore they function as energy carriers and are constituents of signaling molecules such as (p)ppGpp, cGMP and cAMP to name but a few. Because of this, NNADs' that target enzymes of nucleotide metabolism constitute important parts of current anticancer and antiviral therapies. NNADs that are used for the treatment of cancer inhibit DNA replication and repair while antiviral NNADs inhibit replication of the viral genome (Van Rompay *et al.*, 2003). In addition, certain analogs can

inhibit the enzymes that are involved in nucleotide biosynthesis and cause chain termination by depleting dNTP pools. There is also potential for other enzymatic cross-reactivity when analogs bind to regulatory sites where they cause activation or inhibition of enzymes (Ewald *et al.*, 2008; Egeblad *et al.*, 2012; Jordheim *et al.*, 2013). Table 4 (at the end of this chapter) provides an overview of the 45 currently FDA approved NNADs. Some NNADs have been in clinical use for over 50 years, however these compounds are not routinely used against bacteria and only limited small scale investigations into their antibacterial properties have been.

3.2.2 Repurposing NNADs could overcome several hurdles in traditional antimicrobial discovery

Just as cancer cells and viruses, bacteria are fast proliferating entities (O'Donnell *et al.*, 2013), making them good candidate targets for drugs that interfere with DNA or RNA replication. Moreover, nucleotides and derived compounds have important functions as signalling molecules and cofactors in bacterial processes associated with biofilm formation, virulence and persistence (Römling *et al.*, 2005; Lamprokostopoulou *et al.*, 2010; McDonough & Rodriguez, 2012; Garavaglia *et al.*, 2012), suggesting that NNADs might have interesting cross-activities against bacteria. Consistently, in recent years the bactericidal, anti-biofilm or anti-virulence activity of a subset of FDA approved NNADs has been demonstrated (Casado *et al.*, 1999; Sandrini *et al.*, 2007a; Attila *et al.*, 2009; Antoniani *et al.*, 2013), while other NNADs were shown to enhance the efficiency of classic antimicrobials (Nyhlén *et al.*, 2002; Krishnan *et al.*, 2009; Jordheim *et al.*, 2012; Lele *et al.*, 2016). However, the antibacterial effect of the majority of approved NNADs remains to be tested. Already reported activities against bacteria are listed in Table 4 (at the end of this chapter) and discussed in more detail in the following sections. Here we describe important hurdles associated with classical antimicrobial discovery and how repurposing of NNADs could overcome these.

3.2.2.1 NNADs are synthetic compounds without prior evolutionary history in ecological settings

In ecological settings, natural antibiotics are thought to be “weapons” that are used during microbial competition (Abrudan *et al.*, 2015). Antibiotic resistance mechanisms are considered to be akin to “shields” that protect target organisms, or detoxifying systems that protect antibiotic producers from their own weapons (Fajardo & Martínez, 2008). Antibiotics may also have a role in intra and inter domain communication, where they can act as cues/coercions in complex microbial communities (Linares *et al.*, 2006; Aminov, 2009; Bernier & Surette, 2013). In this scenario, antibiotic resistance may serve as a mechanism to

attenuate signal intensity (Linares *et al.*, 2006; Davies, 2006a; Martínez, 2008; Aminov, 2009; Davies & Davies, 2010; Romero *et al.*, 2011).

Regardless of their exact role in nature, it is now appreciated that resistance-conferring genes are the result of ancient evolution and not merely of the modern pressures of anthropogenic antibiotic use (Hall & Barlow, 2004; Garau *et al.*, 2005; Song *et al.*, 2005; Allen *et al.*, 2008). This is worrying, as the majority of antibiotic resistance mechanisms seen in clinical settings are acquired through horizontal gene transfer from taxonomically unrelated bacteria (Aminov, 2012; Nazaret & Aminov, 2014; van Schaik, 2015; von Wintersdorff *et al.*, 2016).

Given the ecological importance of natural antibiotics and the presence of ancient resistance mechanisms it seems sensible to focus on identifying new, synthetic compounds, such as synthetically modified NNADs, that do not have a microbial origin. Because bacteria do not have an ancient history of exposure to synthetic antibiotics, resistance development is expected to be less prominent. However, it should be noted that efflux systems that have evolved to protect bacteria from diverse natural toxic small molecules in certain cases offer cross-protection against products of a synthetic origin. For example shortly after the introduction of fluoroquinolones into clinical practice in the 1980s, it became apparent that efflux systems provided Gram-negative bacteria with high levels of resistance (Poole, 2000). Thus care should be taken since bacterial genomes, and mobile genetic elements, can harbour protection against toxic agents even without a requirement for past exposure.

3.2.2.2 NNADs have potential as anti-virulence drugs, reducing the risk of resistance development

Exposure to any compound that kills or inhibits growth of bacteria creates a strong selection pressure for resistance (Lipsitch & Samore, 2002). Even though resistance mechanisms are often costly to the bacterium in the absence of antibiotic, compensatory mutations that mitigate this cost rapidly spread so that the frequency of resistance does not decline when antibiotic use is cut down (Andersson & Hughes, 2010). Instead of targeting growth, emerging strategies focus on targeting virulence-associated phenotypes and/ or behaviours that affect the susceptibility of pathogenic bacteria to the host's immune system or antibiotic treatment (Rasko & Sperandio, 2010; Rogers *et al.*, 2012). It has been argued that targeting virulence without affecting bacterial growth, under certain circumstances, could generate much weaker selection for resistance than current antibiotics, while at the same time transforming pathogenic populations into a state that is less harmful to the host (Clatworthy *et al.*, 2007; Cegelski *et al.*, 2008; Imperi *et al.*, 2013; Allen *et al.*, 2014). As exemplified below, certain

NNADs have concentration ranges at which they inhibit the production of virulence factors without negative effects on growth (Attila *et al.*, 2009; Ueda *et al.*, 2009; Imperi *et al.*, 2013).

3.2.2.3 Specific NNADs are expected to have activity against antibiotic-tolerant biofilms

Most antibiotics have been developed to target free-living bacteria, however, it is now widely accepted that bacteria grow in multicellular communities that are encased in self-produced matrixes, called biofilms (Costerton *et al.*, 1987). Biofilm-associated growth can enhance tolerance to antibiotics by 10 to 1000 times (Nickel *et al.*, 1985; Williams *et al.*, 1997; Costerton *et al.*, 1999; Ceri *et al.*, 1999). To date there are no drugs in clinical use that were developed specifically for targeting biofilm-formation (Max V. Ranall *et al.*, 2012; Bjarnsholt *et al.*, 2013; Park *et al.*, 2016). Anti-biofilm strategies can be directed at prevention of surface adhesion, colonization and matrix production by targeting specific cellular processes, as well as by interfering with quorum sensing (Blackledge *et al.*, 2013; Wu *et al.*, 2015). *In vitro* studies have shown that combining anti-biofilm treatments with antibiotics can lower the tolerance of antibiotic resistant pathogenic bacteria (Janssens *et al.*, 2008; Reffuveille *et al.*, 2014). Thus targeting biofilm formation is an attractive strategy that would render bacteria more vulnerable to host defences and enhance the therapeutic spectrum of currently available antibiotics (Rogers *et al.*, 2012; Hänsch, 2012; Bjarnsholt *et al.*, 2013; Alhede *et al.*, 2014; Roilides *et al.*, 2015). Given the fact the major biofilm signalling molecule c-di-GMP is a nucleotide derivative, perturbations in the nucleotide pools due to the action of some NNADs are thought to cause reduced c-di-GMP levels and inhibition of biofilm formation (Antoniani *et al.*, 2013).

3.2.2.4 The defined activity spectrum of NNADs could reduce microbiome disruption and resistance development

NNAD based prodrugs have potential to be activated in a species-specific manner by bacteria, thus they can be used as species-specific antibiotics (Sandrini *et al.*, 2007a).

Sandrini and colleagues (2007) have shown that bacterial deoxyribonucleosides kinases (dNKs) activate certain nucleoside prodrugs in a species specific manner (Sandrini *et al.*, 2007a; Sandrini *et al.*, 2007b). The differences in susceptibility to these drugs were attributed to variations in the presence of kinase encoding genes between the different taxonomic groups (Sandrini *et al.*, 2007a). It is worthwhile to investigate whether other enzymes which are also involved in nucleotide metabolism (such as ribonucleotide reductases, thymidylate synthases, guanine deaminases and adenine deaminases) have species-specific interactions with nucleoside and nucleobase analog drugs. The specific affinity that different bacterial species

have towards the various analog drugs can be exploited for designing antibacterials that are effective against a narrow range of bacteria which would likely reduce microbiome disruption and resistance development.

3.2.2.5 Repurposing of NNADs is less costly and time-consuming than *de novo* drug discovery

In addition to the problem of antibiotic resistance and tolerance in the clinical environment, there has been a reduction in new antibiotic approvals over the past decades (Center for Disease Control and Prevention, 2013). Other than rapid emergence of resistance, factors that hamper antibiotic development include the high cost of *de novo* drug discovery; and stringent regulatory requirements. The combination of these factors contributed to the reluctance of pharmaceutical companies to invest in the development of new antimicrobials (Projan, 2003; Davies, 2006b). Screening of already approved compounds to find those with desirable antibiotic, anti-biofilm or anti-virulence activities provides an interesting solution. This approach of drug repurposing takes less time than *de novo* drug discovery and is not associated with the same high costs and risks that typically accompany drug innovation. The drug repurposing strategy has already been proven to be useful for identifying compounds with desirable antibacterial activities. Some of the drugs were shown to alleviate infections in animal models (Chong & Sullivan, 2007; Younis *et al.*, 2015; Rangel-Vega *et al.*, 2015; Thangamani *et al.*, 2015), and specific drugs, such as 5-fluorouracil, are now being used in human clinical tests (Rangel-Vega *et al.*, 2015).

3.2.2.6 The safety profiles of NNADs are well established and risk factors associated with toxicity are known

Because the safety profiles of approved drugs have already been established, and potential side-effects are already known, this information can be taken into account during drug repurposing studies. When considering the approved uses of NNADS, their narrow therapeutic margins are incontestable. Most healthy adult cells are quiescent, therefore targeting cancer cells with nucleoside analogs provides some level of selectivity. Nonetheless, certain tissues such as hair follicles, bone marrow and intestinal epithelium that are in a replicative state are vulnerable to the cytotoxic effects (Parker, 2009). Due to their lower activity on mammalian enzymes, antiviral NNADs typically have better tolerance profiles than those used for treating cancer (Jordheim *et al.*, 2013). Nevertheless, long-term exposure to certain antiviral NNADs is associated with mitochondrial toxicity (Anderson *et al.*, 2004). However, it is important to note that the mechanisms of toxicity for NNADs are selectivity/specificity problems. As such,

toxicity is strongly dependent on dosage and intracellular concentration (as reviewed) (Anderson *et al.*, 2004). In addition, the duration of treatment is an important factor in cumulative toxicity (Lo *et al.*, 2005). The antibacterial effects of the various NNADs reviewed in the following sections occur at concentrations that are extremely low compared to those of their approved uses and treatment of bacterial infections are typically shorter than for chronic viral infections, chronic inflammatory diseases and cancer. Moreover, even though the cytotoxic effects of NNADs may have hindered their utilization as antibiotics in the past, we are now faced with the threat of increasing antibiotic resistance. In certain cases, the risks of minor cellular injury by cytotoxic agents might be lower than the risks associated with infections that do not respond to conventional antibiotics.

3.3 Examples of approved NNADs with activity against bacteria

Here we describe approved NNADs and summarize the recent advances that have been made in evaluating their potential as antibacterial agents or biofilm and virulence inhibitors. Special emphasis is on how the specific NNADs contribute to solving the antimicrobial discovery hurdles described above.

3.3.1 5-Fluorouracil

5-Fluorouracil is widely used in clinical settings as a systemic treatment for a variety of cancers as well as a topical treatment cancerous skin conditions. 5-Fluorouracil is analogous to uracil but contains a fluorine atom at the C-5 position instead of a hydrogen atom (Heidelberger *et al.*, 1957). After entering the eukaryotic cell via the same facilitated transport mechanisms as uracil, 5-fluorouracil is converted into three main metabolites: FdUMP, FdUTP and FUTP (Longley *et al.*, 2003). The major activation product, FdUMP, is a suicide inhibitor of thymidylate synthase (TS). TS inhibition causes dTMP starvation and thus affects DNA synthesis (Longley *et al.*, 2003; Rangel-Vega *et al.*, 2015). Furthermore, depletion of dTMP also causes perturbations in the levels of the other deoxynucleotides leading to severely disrupted DNA synthesis and repair. Another 5-FU metabolite FdUTP, causes point mutations when it is incorporated into DNA, as it base pairs with guanine instead of adenine. The combination of disrupted DNA repair and repeated nucleotide misincorporation ultimately results in DNA strand breaks and cell death. The third mode of 5-fluorouracil toxicity is due to the activation product FUTP which is incorporated into RNA. This negatively affects many aspects of RNA processing and functioning, including the formation of mature rRNA, the post-transcriptional modification of tRNA and the assembly and activity of snRNA/protein complexes, as reviewed in (Longley *et al.*, 2003). In bacteria 5-fluorouracil is also converted

to FdUMP, FdUTP and FUTP (Figure 26) with similar mutagenic and cytotoxic outcomes as described for eukaryotic cells. The potent bactericidal effects of 5-fluorouracil against several bacterial pathogens was first established three decades ago. It was confirmed to inhibit the growth of *S. aureus* and *S. epidermidis* with an $MIC_{50} \leq 0.8$ mg/L, and it was found to act synergistically with beta-lactams against Gram-negative strains (Ueda *et al.*, 1983; Gieringer *et al.*, 1986). The Fractional inhibitory concentration indexes (abbreviated as ‘FICs’, a FIC index lower or higher than 1 indicates synergy or antagonism, respectively) of 5-fluorouracil and cefazolin, piperacillin and carbenicillin against *E. coli* were 0.61, 0.68 and 0.64, respectively (Ueda *et al.*, 1983). More recently, it was found that 50 mg/L 5-fluorouracil acts synergistically with sub-MIC concentrations of tobramycin against *S. aureus* leading to a >100-fold decrease in viable bacterial count after 3 hours of treatment compared to tobramycin alone (Nyhlén *et al.*, 2002).

Some bacteria show deviations from the canonical reactions. For example in *M. tuberculosis* the most likely route for 5-fluorouracil metabolism would be through its conversion to FUMP which is further processed into FUTP and FdUTP, while other pathways are considered unlikely given the absence of the enzymes thymidine kinase (*tdk*), uridine phosphorylase (*udp*) and uridine kinase (*udk*) (Singh *et al.*, 2015).

Recent investigation into the antimycobacterial action of 5-fluorouracil revealed that 5-fluorouracil becomes incorporated into sugar nucleotides. Fluorinated versions of UDP-Gal, UDP-GlcNAc and UDP-MurNAc-pentapeptide were identified (Singh *et al.*, 2015). The presence of 5-fluorouracil in sugar nucleotides interferes with their role to serve as activated sugar donors for the mycobacterial mycolyl arabinogalactan peptidoglycan complex production. These findings support earlier studies which provided evidence for inhibition of cell wall biosynthesis in *E. coli* and *S. aureus* by 5-fluorouracil (Rogers & Perkins, 1960; Tomasz, 1962; Stickgold & Neuhaus, 1967). Thus, in addition to DNA and RNA damage, 5-fluorouracil also exerts its bactericidal effect via the inhibition of cell wall biosynthesis (Singh *et al.*, 2015). The proposed pathways for 5-fluorouracil and 5-fluorocytosine metabolism in bacteria are summarized in Figure 26.

The first evidence that 5-fluorouracil can inhibit biofilm formation by *S. epidermidis* was provided by (Hussain *et al.*, 1992). More recent studies demonstrated that 5-fluorouracil inhibits biofilm formation and virulence in *P. aeruginosa* (Ueda *et al.*, 2009) and enterohemorrhagic *E. coli* (Attila *et al.*, 2009). The biofilm inhibitory effect of 5-fluorouracil is concentration dependent and influenced by the nutrient composition of the growth medium

with higher activity in lower nutrient conditions. In nutrient rich Lysogeny Broth medium, 3.25 mg/L 5-fluorouracil decreased *P. aeruginosa* PA14 biofilm formation with about 70% while the specific growth rate was only decreased by 20% and 26.02 mg/L 5-fluorouracil inhibited biofilm production by more than 90% with a 50% reduction in the specific growth rate. In nutrient-poor M9 glucose medium, 1.3 mg/L 5-fluorouracil inhibited biofilm formation by 56% without affecting growth. The following quorum sensing regulated virulence factors were also inhibited: LasB elastase activity, pyocyanin production, rhamnolipid production, swarming motility and quinolone signal production. At higher concentrations (3.25 mg/L) 5-fluorouracil, biofilm formation was inhibited by 61%, but growth was also inhibited (Ueda *et al.*, 2009). In *E. coli* 5-fluorouracil reduced biofilm formation 5-fold with about 42% toxicity at 3.25 mg/L. The anti-biofilm activity of 5-fluorouracil relies on the presence of AriR (also known as YmgB), a regulatory protein which is upregulated in response to indole (Figure 26). The importance of indole in various bacterial processes including virulence induction, cell cycle regulation, acid resistance and biofilm formation is reviewed in (Hu *et al.*, 2010). AriR, which is a repressor of biofilm formation (Lee *et al.*, 2007a) was upregulated 3.7-fold in the presence of 1.3 mg/L 5-fluorouracil in LB medium. When 5-fluorouracil was added to an *ariR* deletion mutant, biofilm inhibition did not occur (Attila *et al.*, 2009). Studies conducted by our own research group indicate that 5-fluorouracil also has potential as an anti-*Salmonella* treatment. At concentrations of ≥ 1.3 mg/L, 5-fluorouracil causes near complete inhibition of planktonic and biofilm growth, however at a concentration of 0.156 mg/L biofilm formation is reduced by 80% without affecting planktonic growth (Yssel *et al.*, unpublished). Interestingly, AriR is not present in *Salmonella* and therefore 5-fluorouracil's mechanism of biofilm inhibition in this genus is probably different than in *E. coli*. Perhaps the most significant finding regarding the use of 5-fluorouracil as antibacterial comes from large-scale randomized human trails, in which 5-fluorouracil was applied as a coating on central venous catheters. The aforementioned study by Walz *et al.* (2010) showed that the anti-infective properties of 5-fluorouracil exceeded that of silver sulfadiazine and chlorhexidine. The approximate cumulative dose of 5-fluorouracil eluted over 28 days was 1 mg, which is below the lowest toxic dose in humans (6mg/kg/3days), which is associated with cardiac and respiratory side effects (Pottage *et al.*, 1978). 5-Fluorouracil was undetectable when plasma samples from goats implanted with a 5-fluorouracil coated central venous catheters for a period of up to 21 days were analyzed by means of liquid chromatography/tandem mass spectrometry. Furthermore, histopathologic examination of the catheter/host tissue interface did not reveal any evidence of local tissue toxicity. Together these results strongly indicate

that using 5-fluorouracil as an anti-biofilm coating on medical implant devices would be safe (Walz *et al.*, 2010).

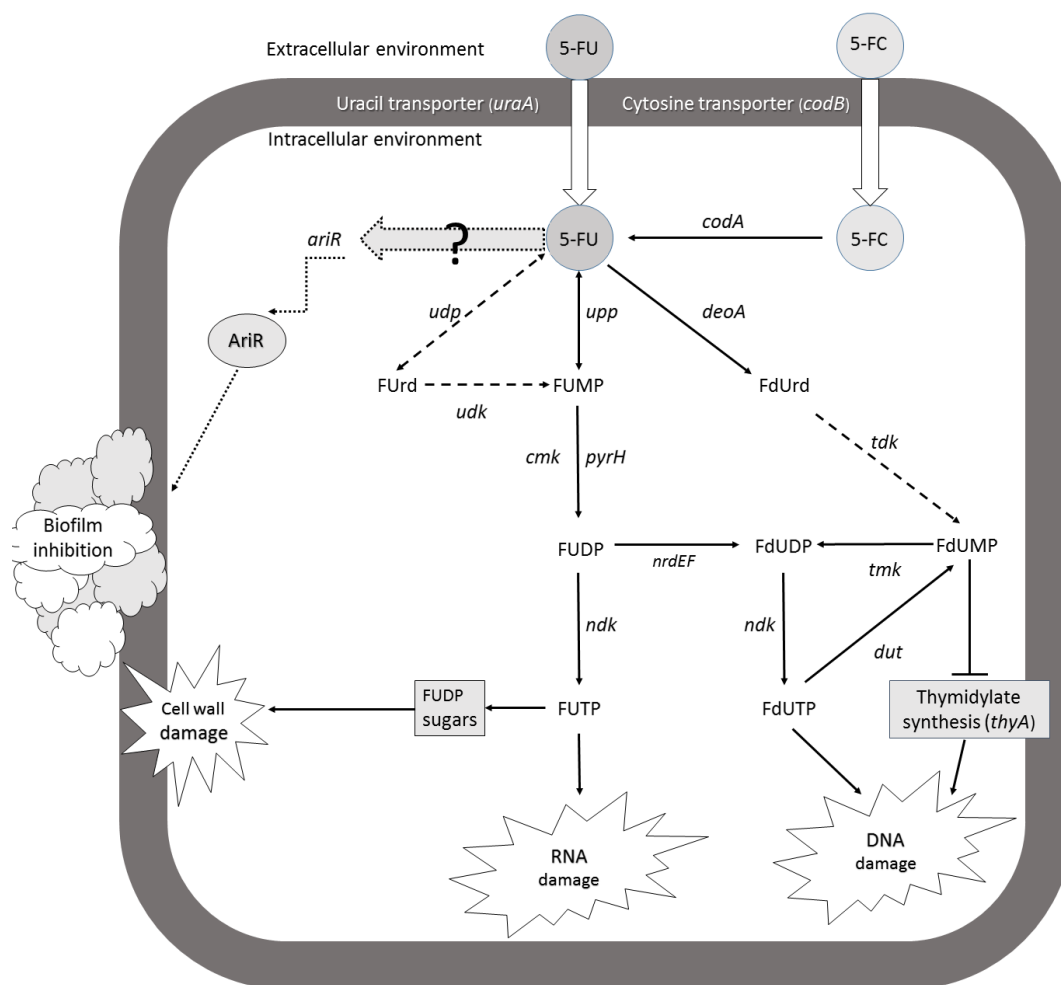


Figure 26 Proposed pathway for 5-FU and 5-FC metabolism in bacteria and the effects of these compounds on DNA, RNA, the cell wall and biofilm formation. Dashed lines indicate enzymes that are absent in *M. tuberculosis* but that are present in *E. coli*. Dotted lines indicate processes that have been observed in *E. coli* (Attila *et al.*, 2009). Information on enzymatic reactions were obtained from literature (Warner & Rockstroh, 1980; Vilella *et al.*, 2011; Warner *et al.*, 2014; Singh *et al.*, 2015). Genes encoding enzymes responsible for 5-FU and 5-FC uptake and metabolic conversion are indicated in *italic*.

3.3.2 5-Fluorocytosine

5-Fluorocytosine is a synthetic anti-mycotic compound with the brand name Ancobon and is used for treating serious infections caused by *Candida* or *Chryptococcus neoformans*. 5-Fluorocytosine is a prodrug of 5-fluorouracil. 5-Fluorocytosine is not intrinsically toxic to fungi, but once taken up into susceptible fungal cells it is converted to 5-FU by cytosine deaminase (Vermes *et al.*, 2000). Thereafter it is further metabolized to FUTP, FdUTP and FdUMP leading to disturbed protein and DNA synthesis as described before Figure 26.

Imperi and colleagues studied the effect of 5-fluorocytosine on *P. aeruginosa* pathogenicity. They found that 5-fluorocytosine did not affect *P. aeruginosa* growth (MIC > 1291mg/L) (Imperi *et al.*, 2013). However it had a very high inhibitory activity against pyoverdine production (IC₅₀ values of 0.3873 mg/L). In addition to pyoverdine inhibition, other critical virulence factors such as exotoxin A and protease PrpL were also inhibited. Using a mouse model of pulmonary infection they showed that an intraperitoneal dose of 30 mg/kg/day suppressed virulence without affecting the viability of the bacterial cells (Imperi *et al.*, 2013). This dose is far below the mouse LD₅₀ of 1190 mg/kg and below the dosage range of 50 to 150 mg/kg/day recommended for humans (<http://www.drugs.com/dosage/flucytosine.html>). (Grunberg *et al.*, 1963; Drugs.com, 2017). Although the exact molecular mechanism by which 5-fluorocytosine inhibits *P. aeruginosa* virulence factors is unknown, it was shown that 5-fluorocytosine toxicity relies on its metabolic conversion to 5-fluorouracil by cytosine deaminase (encoded by *codA*). Mammals and other higher eukaryotes do not have counterparts for cytosine deaminase, making 5-fluorocytosine an ideal drug for selectively targeting organisms capable of assimilating and activating the prodrug (Imperi *et al.*, 2013). Aside from its low toxicity in humans, other clinically desirable characteristics of 5-fluorocytosine include its ready absorption after oral administration, high bioavailability and efficient penetration throughout the body (Vermes *et al.*, 2000). Moreover, the dosing levels that are currently recommended for treating fungal infections lead to serum levels that are 40-fold higher than the levels needed to inhibit *P. aeruginosa* virulence. This suggests that typical doses are sufficiently potent for use in treating *P. aeruginosa* infection (Imperi *et al.*, 2013). The *in vitro* and *in vivo* activity of 5-fluorouracil and 5-fluorocytosine against a variety of bacterial species paves the way for further clinical trials on the anti-virulence and anti-biofilm efficacy of these compounds in humans.

3.3.3 5-Azacytidine

5-Azacytidine is an analog of cytidine, which is sold under the trade name Vidaza and is mainly used in the treatment of myelodysplastic syndrome. It possesses cytotoxic, antineoplastic, abortive, and mutagenic activity (von Hoff *et al.*, 1976). The cytotoxic effect of 5-azacytidine proceeds via two mechanisms: at low doses it interferes with gene regulation by inhibiting DNA methylation by methyl transferases (MTases), leading to inappropriate gene activation (Glover & Leyland-Jones, 1987). It is also an inhibitor of RNA methylation (Schaefer *et al.*, 2009). At higher doses its derivatives, 5-azacytidine triphosphate and 5-azadeoxycytidine triphosphate, get incorporated into RNA and DNA respectively (Dapp *et al.*,

2009). The hypomethylating effect of 5-azacytidine depends on the altered C5 position (Gowher & Jeltsch, 2004). Other cytidine analogues such as 6-azacytidine or gemcitabine do not have this property. In fact gemcitabine prevents demethylation of DNA leading to hypermethylation which also affects gene regulation and DNA repair (Schäfer *et al.*, 2010).

The Activated Methyl Cycle (AMC) is an important biosynthesis pathway that produces L-methionine for protein synthesis as well as S-adenosyl-L-methionine (SAM), the major methyl donor in the cell. When SAM donates its methyl group, it is converted to S-adenosyl-L-homocysteine (SAH). SAH can be recycled back to SAM via the AMC (Figure 27). In bacteria, the quorum sensing molecule, AI-2, which is an important regulator of biofilm formation, (Vidal *et al.*, 2011) is formed as a by-product of the AMC. Because of the inhibitory effect of 5-azacytidine on DNA MTases and the involvement of MTases in the AMC, Yadav and colleagues were interested in the effect of 5-azacytidine on AI-2 production and biofilm formation by *S. pneumoniae* (Yadav *et al.*, 2012a). They found that the inhibitory effect of 5-azacytidine is higher for biofilm growth than for planktonic growth. At 24.42 mg/L 5-azacytidine, the degree of biofilm inhibition nearly doubled that of planktonic growth inhibition. Scanning electron microscopy revealed that 5-azacytidine disrupted biofilm organization, since the treated biofilms were thin, cells were scattered in clumps, and micro-colonies were absent. Expression analysis of 11 genes involved in AI-2 synthesis, competence and DNA repair and synthesis was conducted. Genes that were found to be downregulated by 5-azacytidine include: *luxS*, *metK*, *pfs* and *cmk* (Yadav *et al.*, 2012a). The enzymes encoded by *luxS* and *pfs* are both involved AI-2 biosynthesis and detoxification of methylthioadenosine/S-adenosylhomocysteine (MTA/SAH) which are toxic byproducts of the AMC and *metK* is involved in SAM production (Figure 27). Cytidylate kinase (encoded by *cmk*) catalyses the transfer of a phosphoryl group from ATP to CMP or dCMP, thus its downregulation would interfere with DNA synthesis. The authors indicated that it is unclear whether the biofilm inhibition by 5-azacytidine is due to the downregulation of AI-2 production, changes in SAM levels, or due to the accumulation of toxic by-products of the AMC (Yadav *et al.*, 2012a). Although insightful, the gene expression analysis of the above study was limited to a small set of genes analysed with RT-qPCR. Further comprehensive transcriptome analysis would likely yield additional insights into how interfering with the AMC affects *S. pneumoniae* biofilm growth and quorum sensing. Some compelling supplementary information was obtained in a very recent investigation into the effect of 5-azacytidine on the transcriptome of *E. coli*. Expression changes for 63 genes were observed, the majority of which were up-regulations. It was found that transcription was affected by two

mechanisms, one involving loss of DNA methylation, and the other involving a DNA-damage response mechanism that is independent of methylation loss (Militello *et al.*, 2016). Because 5-azacytidine impacts the transcription of many genes the possibility that biofilm related processes which are unrelated to AI-2 production and the AMC are affected certainly exists.

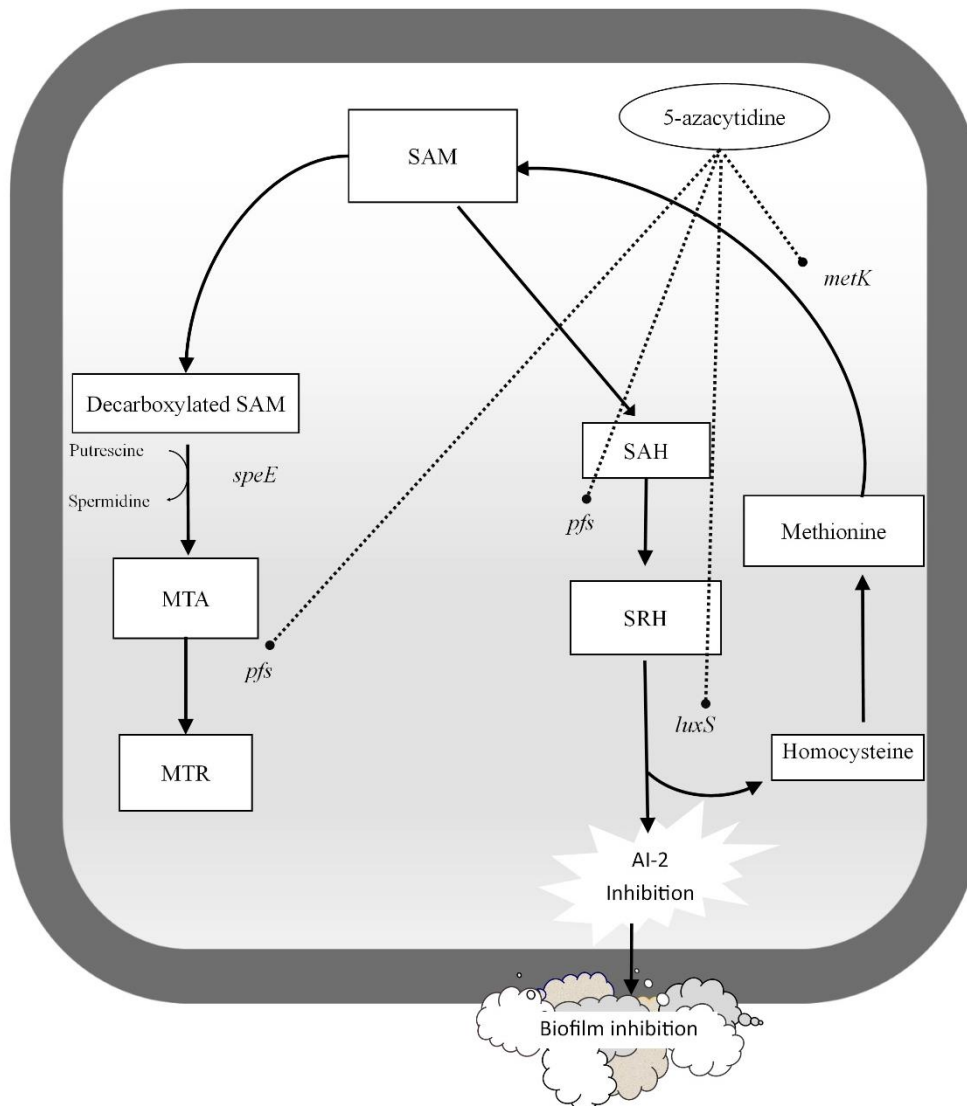


Figure 27 Diagram showing the activated methyl cycle (AMC) of *S. pneumoniae*. Black text in white rectangles denote pathway intermediates and black solid arrows indicate enzymatic reactions. Abbreviations for pathway intermediates are: S-adenosylmethionine (SAM), 5-Methylthioadenosine (MTA), 5-Methylthioribose (MTR), S-adenosylhomocysteine (SAH), S-ribosylhomocysteine (SRH). The effects of 5-azacytidine (white oval) on AI-2 production and biofilm formation are shown with dashed arrows indicating genes that are downregulated in the presence of 5-azacytidine.

Further encouraging results were obtained with the non FDA-approved compounds 1-(4-bromophenyl)-5-(2-furylmethylene)-3-phenyl-2-thioxodihydro-4,6(1H,5H)-pyrimidinedione (from here on simply referred to as pyrimidinedione) and sinefungin. Pyrimidinedione is a potent inhibitor of DNA adenine methyltransferase (DAM), an enzyme unique to bacteria. It was found that pyrimidinedione significantly inhibits pneumococcal biofilm growth at concentrations that are not cytotoxic to human epithelial cells (Yadav *et al.*, 2015). Sinefungin which is an experimental drug, is structural analog of SAM. Sinefungin reduces the production of AI-2, affecting cell-to-cell connections and disrupting pneumococcal biofilm formation (Yadav *et al.*, 2014). The results obtained with azacytidine, pyrimidinedione and sinefungin highlight the potential of interfering with biofilm formation and AI-2 production via disrupting the AMC (Yadav *et al.*, 2014) and give strong support for testing other methyltransferases, such as decitabine, for the treatment of pneumococcal infections.

3.3.4 Azathioprine and 6-Mercaptopurine

Azathioprine (brand name Imuran, originally developed as an anti-cancer drug) and its derivative 6-Mercaptopurine (brand name Purinethol) are widely used immunosuppressive drugs for treatment of ulcerative colitis, Crohn's disease, myasthenia gravis, atopic dermatitis and intractable pruritus (Kim *et al.*, 1999; Timmer *et al.*, 2007; Maley & Swerlick, 2015; Lee *et al.*, 2015; Rae *et al.*, 2016).

Studies published almost a decade ago revealed that azathioprine and 6-mercaptopurine inhibit the growth of *Mycobacterium avium* subspecies *paratuberculosis* (MAP), a bacterium that is associated with Crohn's disease (Greenstein *et al.*, 2006; Shin & Collins, 2007). Interestingly other rapidly growing mycobacteria, *M. avium* and *M. smegmatis* were resistant to azathioprine and 6-mercaptopurine (Shin & Collins, 2007). Synergy between 6-mercaptopurine and the antibiotics azithromycin, clarithromycin, rifampicin, rifabutin and ethambutol was also reported (Krishnan *et al.*, 2009). More recently it was demonstrated that azathioprine inhibits biosynthesis of c-di-GMP (a signal molecule that plays an important role in regulating biofilm formation), by interfering with intracellular nucleotide pool availability. Exposure to 25 mg/L azathioprine resulted in 50 % reduction of intracellular c-di-GMP levels in *E.coli* and prevented biofilm formation. *In silico* docking experiments suggested that azathioprine has high affinity to the cyclohydrolase domain of AICAR transformylase (a key enzyme in the purine biosynthesis pathway). Binding of azathioprine to AICAR transformylase might interfere with purine nucleotide biosynthesis by inhibiting the enzyme's activity. It is possible that even a slight reduction in GTP pools can negatively impact c-di-

GMP synthesis by directing available GTP towards transcription and translation instead of signal molecule production (Antoniani *et al.*, 2013). c-di-GMP is ubiquitous in bacteria, where it regulates multiple cellular processes including motility biofilm formation and virulence (Römling *et al.*, 2005; Hengge, 2009; Lamprokostopoulou *et al.*, 2010; Ahmad *et al.*, 2011; Römling *et al.*, 2013). Thus, drugs that interfere with c-di-GMP signalling could have activity against diverse bacterial species.

3.3.5 Caffeine

Caffeine is a methylated xanthine analog which is not only consumed in copious amounts by coffee lovers, but is also used to prevent and treat bronchopulmonary dysplasia and apnea in premature babies (Schmidt, 1999; Schmidt, 2005). Methylated xanthine analogues act as adenosine receptor antagonists in humans (Biaggioni *et al.*, 1991).

In bacteria methylated xanthine analogues affect bacterial physiology by interfering with the following processes: (i) inhibition of thymidine uptake; (ii) inhibition of the conversion of thymidine to dTTP; (iii) inhibition of DNA synthesis and repair; (iv) reduction of RNA and protein synthesis; (v) increase in cAMP levels due to inhibition of cAMP phosphodiesterase (Lieb, 1961; Grigg, 1968; Sideropoulos & Shankel, 1968; Sandlie *et al.*, 1980; Kawamukai *et al.*, 1986; Selby & Sancar, 1990).

The first evidence that caffeine can disrupt quorum sensing was put forth by Norizan and colleagues in 2013 (Norizan *et al.*, 2013). They showed that 100 to 1000 mg/L caffeine inhibited short-chain AHL production by *P. aeruginosa* PA01 in a concentration-dependent manner with only trace amounts of AHLs produced at 1000 mg/L. The reduction in AHLs was not due to degradation by caffeine and the applied concentrations did not affect bacterial growth. The mechanism by which caffeine inhibit the synthesis of AHLs remains unsolved. Given the importance of AHLs in the regulation of virulence and biofilm formation, it could be interesting to investigate the anti-virulence or anti-biofilm properties of caffeine and other xanthine analogs, such as aminophylline and pentoxifyline.

3.3.6 Azidothymidine

Azidothymidine (also known as AZT or zidovudine) is an analog of thymidine in which the 3' hydroxy group is replaced with an azido group. Upon entry into an HIV infected cell it is phosphorylated. The triphosphorylated form acts as an HIV-reverse transcriptase inhibitor by inducing DNA chain termination due to the absence of the 3'-OH group.

The antibacterial activity of azidothymidine has already been demonstrated three decades ago (Elwell *et al.*, 1987; Lewin *et al.*, 1990a). It was shown that the antibacterial activity relies on the presence of a thymidine kinase with the ability to phosphorylate azidothymidine. Azidothymidine is active against Gram-negative bacteria while it has no effect on Gram-positive bacteria. Recent research by Sandrini and colleagues provided strong evidence that species specific activation of azidothymidine by bacterial thymidine kinases is important for the drug's selective activity (Sandrini *et al.*, 2007a). A comprehensive investigation by Doléans-Jordheim and colleagues into the mechanism of azidothymidine's effect against several bacterial species showed that it is particularly active against the enterobacteria (Doléans-Jordheim *et al.*, 2011). These results are in agreement with observations that HIV-positive patients that are treated with azidothymidine are less likely to develop *Salmonella* infections (Casado *et al.*, 1999). It was demonstrated that azidothymidine acts in synergy with aminoglycosides. The most effective association is with gentamicin (mean FIC value of 0.40). With regards to side-effect, azidothymidine is quite well tolerated in an anti-HIV setting, however the effective doses for treating bacterial infection remain to be established (Doléans-Jordheim *et al.*, 2011).

3.3.7 Gemcitabine

Gemcitabine is a pro-drug used for the treatment of various cancers. It is an analog of deoxycytidine in which the hydrogen atoms on the 2' carbon are replaced by fluorine. When transported into the human cell, it is activated by deoxycytidine kinase. Both gemcitabine diphosphate (dFdCDP) and gemcitabine triphosphate (dFdCTP) inhibit processes required for DNA synthesis. Incorporation of dFdCTP instead of dCTP into DNA is thought to be the major mechanism by which cell death is induced. Following incorporation of dFdCTP on the end of the elongating DNA strand, one more deoxynucleotide is added and thereafter, the DNA polymerases are unable to proceed. Proofreading enzymes are unable to remove gemcitabine from this position. Furthermore, the unique actions that gemcitabine metabolites exert on cellular regulatory processes serve to enhance the overall inhibitory activities on cell growth (Plunkett *et al.*, 1995).

The activity of Gemcitabine against bacteria was recently investigated by Sandrini and colleagues. It was found that gemcitabine is active against Gram-positive bacteria and inactive against Gram-negative bacteria (Sandrini *et al.*, 2007a; Sandrini *et al.*, 2007b). Although the exact mechanisms of action of gemcitabine in bacteria is not yet clearly understood, the

enzyme deoxyadenosine kinase was shown to be responsible for species specific activation of the drug (Sandrini *et al.*, 2007a; Sandrini *et al.*, 2007b).

Adult mice that were infected intraperitoneally with lethal doses of *Streptococcus pyogenes* (a beta-haemolytic bacterium) did not develop systemic infection if they received 100 µg gemcitabine after infection. It was determined that exponential growth is a prerequisite for the efficacy of gemcitabine and that stationary phase profoundly diminishes the susceptibility of bacterial cells. *In vitro* concentrations that can effectively kill *S. aureus* and *S. pyogenes*, are 0.002 mg/L and 0.2 mg/L respectively (Sandrini *et al.*, 2007b). This is a clinically achievable range which is much lower than the plasma concentrations (2.99~5.99 mg/L) produced by the standard treatment dose for acute leukaemia (Wang *et al.*, 2007), with potentially lower side effects. Jordheim and colleagues performed pre-clinical investigation into the antibacterial activity against MRSA strains and the association with gentamicin. Their experiments showed that gemcitabine and gentamicin act synergistically (Jordheim *et al.*, 2012). Their results provide strong support for the use of nucleoside analogs in hospital settings, where multidrug-resistant nosocomial infections are increasingly problematic. Implant associated osteomyelitis caused by *S. aureus* is a significant complication for orthopaedic patients following surgery. Given that the number of total hip and knee replacements are projected to grow significantly, by 2030 in the United States alone (Kurtz *et al.*, 2007), we propose that gemcitabine be added to gentamicin impregnated cement spacers to reduce complications associated with infection.

3.4 Resistance development against NNADs

When bacteria are exposed to agents that kill them or inhibit their growth there is a positive selection of bacteria that have acquired resistance mechanisms. Both strategies that reduce acquisition of resistance mechanisms or that reduce positive selection pressure on resistant strains are expected to result in lower resistance development.

Reduced acquisition of resistance can be achieved when multiple genes determine the structures of the molecular targets. In this case multiple mutations are required to offer high-level resistance, reducing the likelihood of high-level endogenous resistance (Silver, 2007).

If a resistance mechanism were to arise, the trade-off between the cost and benefit of resistance is an important factor in determining whether resistance becomes established (Andersson & Hughes, 2010). Emerging strategies aim to circumvent the spread of resistance by not directly targeting growth but rather targeting virulence or biofilm related factors (so called anti-virulence-drugs). In the opinion paper by Allen and colleagues (2014), key predictions on the

direction of selective pressure on strains resistant to anti-virulence drugs are discussed (Allen *et al.*, 2014). It is hypothesized that anti-virulence drugs will generate weaker selection for resistance or even select against resistance under the following circumstances: (i) the targeted factor confers no benefit to the pathogen at the site of treatment; (ii) the targeted factor confers collective benefits to a well-mixed population; (iii) the targeted factor is conditionally beneficial and/or conditionally expressed; (iv) the drug reduces the supply of quorum-sensing signals in a well-mixed population (Allen *et al.*, 2014). In the following paragraphs we argue that, based on the above criteria, NNADs may have properties which make them less susceptible to the development of resistance:

3.4.1 NNADs can have multiple targets within the bacterial cell

Nucleotides have a multitude of roles within the bacterial cell and interact with many enzymes. NNADs (or their activation products) may thus have multiple enzymatic targets with which they can potentially cross-react to disrupt cellular functioning. As such, they could be more robust against acquisition of resistance mechanisms and resistance development. Although there are potential sources for endogenous resistance, as is discussed below, the use of drug combinations with diverse targets could reduce the likelihood of its emergence.

3.4.2 Combining treatment with antibiotics can prevent the establishment of resistance against NNADs

Combination therapy is a widely used strategy to combat the emergence of resistance not only in bacteria, but also during treatment of HIV and cancer. Combination therapies that have multiple molecular targets would require multiple mutations to achieve resistance. Synergistic combinations can also reduce the evolution of resistance by clearing the infection faster so that resistant mutations have less time to arise in the population. However, if resistance to one drug provides collateral resistance to the other drug, the combination will not be very effective in preventing the evolution of resistance. In the case of enteric bacterial resistance against azidothymidine, resistance was conferred by changes in the thymidine kinase enzyme, and no cross protection against other antibiotics was observed. Combination with gentamicin therefore completely prevented re-growth of azidothymidine resistant bacteria (Doléans-Jordheim *et al.*, 2011). The framework provided by Munck and colleagues (Munck *et al.*, 2014) for aiding the rational selection of antibiotic combinations that limit resistance evolution can be applied to NNADs to reveal suitable combinations with antibiotics.

3.4.3 Mutations providing resistance to NNADs are potentially disadvantageous

Endogenous resistance mechanisms against NNADs can occur amongst others by alteration of enzyme activity or uptake mechanisms. For example, several NNAD pro-drugs are activated by nucleotide salvage enzymes, and these enzymes have been implicated in resistance development (Lewin *et al.*, 1990a; Lewin *et al.*, 1990b; Sandrini *et al.*, 2007a; Doléans-Jordheim *et al.*, 2011). However, mutations in nucleotide salvage pathways may become quite costly under conditions where salvage is required. In addition to inactivation of salvage pathways, increased activity of analogue-degrading enzymes or reduced nucleoside uptake could also reduce susceptibility but may negatively affect the fitness or competitive ability of mutants by causing imbalances in the pools of pathway intermediates or by placing more strain on the *de novo* pathways (Sandrini *et al.*, 2007a).

3.4.4 NNADs can inhibit virulence and/ or biofilm formation without impacting *in vitro* growth

Several drugs discussed in this work have concentration ranges in which they affect quorum sensing, virulence and/or biofilm formation without impacting *in vitro* growth. According to Allen *et al.* (2014), a good understanding of the *in vivo* fitness benefits and costs of the affected virulence factors and their group-beneficial character is required to evaluate the potential of resistance development (Allen *et al.*, 2014). Pyoverdine, for example, which is targeted by 5-fluorocytosine, is a well-known group-beneficial virulence trait (Lamont *et al.*, 2002), therefore it is expected that there will be selection against resistance. Indeed, resistant cells are expected to share the advantage of resistance, i.e. access to pyoverdine, with surrounding susceptible cells, but not the production cost, resulting in inferior performance of resistant cells. Sinefungin and 5-azacytidine on the other hand inhibit AI-2 production, while caffeine inhibits AHL production. These substances are thus quorum sensing signal supply inhibitors. Selection is expected to be neutral because susceptible and resistant cells will likely equally sense and respond to signals produced by resistant strains, and thus experience the same benefits and costs.

3.5 Conclusion

On average, it takes about 15 years from discovery before a drug becomes available for clinical use, and only a small fraction of identified novel molecules pass the clinical trial phases (Freeman & Dervan, 2011). Since 1962 only two new classes of antibiotics have made it onto

the market (Coates *et al.*, 2011). Given the high attrition rates of pharmaceutical development, repurposing may be the only feasible approach to treat recalcitrant bacterial infections in the near future.

Although efforts to utilize NNADs for the inhibition of bacterial growth, virulence and biofilm formation are relatively new, we have exemplified some feasible candidates with promising *in vitro* (and in some cases *in vivo*) activities. The antibacterial actions of the drugs that we have discussed are diverse and range from interfering with methylation activity, inhibiting c-di-GMP biosynthesis by disturbing nucleotide pool concentrations, to interfering with quorum signaling. More extensive searches will likely continue to yield new, promising drugs that target a variety of processes. Differences between target enzymes in bacteria and mammals can be taken into account during the selection process in order to single out specific inhibitors with low host-toxicity. Egeblad and colleagues have developed an approach for identifying interactions between NNADs and human enzymes involved in nucleotide metabolism. A thermal shift assay based on light scattering was used to measure enzyme-ligand binding between the purified enzymes and 45 FDA approved NNADs (Egeblad *et al.*, 2012). To facilitate the identification of NNADs that act selectively against bacteria or specific groups of bacteria, the protocol developed by Egeblad *et al.* could be modified to include bacterial enzymes. Moreover, the family of NNADs is expected to grow with the anticipated approval of additional drugs in the near future. The review by Jordheim and colleagues (2013) focussed on 53 such new compounds which are in various phases of development. The new agents are expected to have reduced long-term toxicity, amongst other improved properties (Jordheim *et al.*, 2013).

Following the identification of compounds with promising antibacterial properties, their potential therapeutic applications need to be considered. Topically applied NNADs can, for example, be used to treat infected skin ulcers or burn-wounds, while intravenously administered NNADs can be useful against systemic infections. Because pharmacokinetics, pharmacodynamics, safety and adverse effects have already been determined, certain steps in the drug development path can be skipped. Typically, drug repurposing reduces the drug development process with 5 or more years (Chakraborty & Trivedi, 2015). In order to facilitate the repurposing of NNADs as antibacterial agents it is vital to move from small scale *in vitro* studies to *in vivo* proof of concept experiments and finally phase II and III clinical trials. Given that various animal models for studying a wide variety of bacterial infections are already established (Siebenhaar *et al.*, 2007; DeLeon *et al.*, 2009; Malachowa *et al.*, 2013; Watson *et*

al., 2016), preclinical tests ought to be relatively straightforward. The most progress towards clinical implementation of NNADs as antibacterial agents were made with 5-FU. Indeed, catheters coated with 5-FU were shown to prevent implant associated biofilm formation in human trials (Walz *et al.*, 2010) and Angiotech received FDA approval to manufacture them commercially in 2008 (FDA, 2008).

We hope that this short review will encourage others to evaluate yet untested NNADs for their potential as antibacterial compounds, either on their own or in combination with antibiotics that are currently on the market. Furthermore, we hope that (pre-) clinical investigations aimed at verifying the efficacy of these compounds will become a priority.

Table 4 Summary of FDA approved NNADs and their activities. Information on mechanisms of action were obtained from the National Center for Biotechnology Information PubChem Compound Database (<https://pubchem.ncbi.nlm.nih.gov>)(Kim *et al.*, 2016b)

Type of agent	Drug	Analog of	Mechanism of action	Approved	Report on antibacterial activity
Anticancer agents	Fludarabine	deoxyadenosine	Inhibits DNA synthesis.	1991	
	Clofarabine	deoxyadenosine	Inhibits DNA synthesis and repair.	2004	
	Nelarabine	deoxyguanosine	Incorporates into DNA leading to fragmentation and apoptosis.	2005	
	Gemcitabine	deoxycytidine	Metabolic products inhibit DNA synthesis, synthesis of dNTPs and are incorporated into DNA.	1996	Active against <i>M. pneumoniae</i> , <i>Listeria</i> , <i>Bacillus</i> , <i>Enterococcus</i> and <i>Staphylococcus</i> (Sandrini <i>et al.</i> , 2007a; Sun & Wang, 2013).
	Cytarabine	deoxycytidine	Not clearly understood, but may involve inhibition of DNA polymerase.	1969	
	Capecitabine	uracil	Converted to fluorouracil, inhibits DNA synthesis and RNA processing.	1998	
	Cladribine	deoxyadenosine	Converted into 2-chloro-2'-deoxyadenosine 5'-triphosphate, which is incorporated into DNA resulting in breakage.	1993	
	Floxuridine	deoxyuridine	Blocks enzymatic conversion of cytosine nucleosides to deoxy-derivatives.	1970	Active against <i>M. pneumoniae</i> , <i>Listeria</i> , <i>Bacillus</i> , <i>Enterococcus</i> and <i>Staphylococcus</i> (Sandrini <i>et al.</i> , 2007a; Sun & Wang, 2013).
	Thioguanine	guanine	Interferes with the synthesis of guanine nucleotides. Incorporated into DNA and RNA.	1996	Inhibits <i>M. pneumoniae</i> growth (Sun & Wang, 2013).
	5-Fluorouracil	uracil	Blocks the conversion of deoxyuridylic acid to thymidylic acid, interfering with DNA synthesis.	1962	Synergism with beta-lactams and tobramycin. Inhibits <i>Staphylococcus</i> growth. Inhibits biofilm formation by <i>S. epidermis</i> , <i>P. aeruginosa</i> and <i>E.coli</i> (Gieringer <i>et al.</i> , 1986; Nyhlén <i>et al.</i> , 2002; Attila <i>et al.</i> , 2009; Ueda <i>et al.</i> , 2009).

Type of agent	Drug	Analog of	Mechanism of action	Approved	Report on antibacterial activity
	Pemetrexed	folic acid, deoxyuridine*	Inhibits folate-dependent enzymes involved in purine and thymidine synthesis..	2008	
	Mercaptopurine	guanine, adenine	Inhibits several enzymatic reactions related to purine synthesis.	2004	Increases susceptibility of <i>Mycobacterium</i> to antibacterials (Krishnan <i>et al.</i> , 2009).
Demethylating agents	Azacytidine	Cytidine	Disrupt transcription and translation after incorporation into DNA/RNA.	2004	Inhibits <i>S. pneumoniae</i> biofilm formation. (Yadav <i>et al.</i> , 2012a)
	Decitabine	deoxycytidine	Incorporated into DNA resulting in hypomethylation.	2006	
Antiviral agents	Ganciclovir	2'-deoxy-guanosine	Incorporation into the DNA strand prevents chain elongation.	1989	
	Acyclovir	guanosine	Inhibits DNA synthesis.	1982	
	Vidarabine	deoxyadenosine	Inhibits replication of viral DNA.	1976	
	Trifluridine	deoxyuridine	Inhibits viral replication by a mechanism that is not yet fully understood.	1995	Inhibits <i>M. pneumoniae</i> growth (Sun & Wang, 2013).
	Ribavirin	guanosine	Diverse effects involving nucleotide biosynthesis, RNA synthesis and translation.	1998	
	Idoxuridine	deoxyuridine	Inhibits viral replication by substituting thymine.	1963	
	Zidovudine	deoxythymidine	After metabolic conversion to its active 5-'triphosphate form it inhibits the activity of HIV-1 reverse transcriptase via chain termination.	1987	Active against <i>M. pneumoniae</i> , <i>Listeria</i> , <i>Bacillus</i> , <i>Enterococcus</i> and <i>Staphylococcus</i> (Sandrini <i>et al.</i> , 2007a; Sun & Wang, 2013).
	Didanosine	deoxyadenosine	Active metabolites incorporate into viral DNA terminating synthesis.	1991	

Type of agent	Drug	Analog of	Mechanism of action	Approved	Report on antibacterial activity
	Abacavir	guanosine	Active metabolites incorporate into viral DNA terminating synthesis	1998	
	Lamivudine	deoxycytidine	Terminates viral DNA synthesis.	1995	
	Valacyclovir	guanosine	Inhibits viral DNA replication by competitive inhibition of viral DNA polymerase, and by incorporation into the growing viral DNA chain.	1996	
	Cidofovir	acyclic dCMP	Selectively inhibits viral DNA polymerase.	1996	
	Stavudine	deoxythymidine	Active metabolites incorporate into DNA, terminating synthesis.	1994	Inhibits <i>M. pneumoniae</i> growth (Sun & Wang, 2013).
	Zalcitabine	deoxycytidine	Interferes with viral RNA-directed DNA polymerase.	1992	
	Valganciclovir	guanosine	Prodrug for ganciclovir.	2001	
	Emtricitabine	deoxycytidine	Competes with deoxycytidine 5'-triphosphate and incorporates into nascent viral DNA, inhibiting reverse transcription of viral RNA.	2003	
	Adefovir	acyclic deoxyadenosine monophosphate	Competes with deoxyadenosine triphosphate for incorporation into viral DNA.	2003	
	Tenofovir	acyclic deoxyadenosine monophosphate	Inhibits HIV reverse transcriptase by competing with deoxyadenosine 5'-triphosphate and, by causing DNA chain termination.	2001	
	Entecavir	deoxyguanosine	Inhibits all three steps in the viral replication process.	2004	
	Famciclovir	guanine	Prodrug for penciclovir.	2007	

Type of agent	Drug	Analog of	Mechanism of action	Approved	Report on antibacterial activity
	Penciclovir	guanosine	Triphosphate form inhibits viral DNA polymerase by competing with deoxyguanosine triphosphate	2002	
	Telbivudine	L-isomer thymidine	of Causes chain termination during DNA synthesis.	2006	
Antifungal	5-Flucytosine	cytosine	Prodrug of 5-fluorouracil.	2011	Inhibits virulence factor production in <i>Pseudomonas</i> (Imperi <i>et al.</i> , 2013).
Other uses	Azathioprine	guanine	Prodrug of mercaptopurine.	2007	Inhibits <i>Mycobacterium</i> growth, affects production of extracellular structures in <i>E. coli</i> (Shin & Collins, 2007; Antoniani <i>et al.</i> , 2013).
	Pentoxifyline	Xanthine	Inhibits erythrocyte phosphodiesterase, non-selective adenosine receptor antagonist.	1997	
	Theophylline	Xanthine	Phosphodiesterase inhibitor, adenosine receptor blocker, and histone deacetylase activator.	1982	Causes abnormal cell growth in <i>E. coli</i> (Kawamukai <i>et al.</i> , 1986).
	Caffeine	xanthine	Inhibits cyclic nucleotide phosphodiesterases, antagonises adenosine receptors, and modulates intracellular calcium handling.	1987	Retards growth of <i>E.coli</i> , <i>Enterobacter aerogenes</i> , <i>Proteus vulgaris</i> , <i>Pseudomonas aeruginosa</i> and <i>B. subtilis</i> . Interferes with quorum sensing in <i>P. aeruginosa</i> , inhibits AHL production (Dash & Gummadi, 2008; Norizan <i>et al.</i> , 2013).
	Theobromine	xanthine	Inhibits cyclic nucleotide phosphodiesterases and antagonises adenosine receptors.	No label, generally recognized as safe	Lowers MIC of antibiotics against <i>Burkholderia cepacia</i> (Rajyaguru & Muszynski, 1998).
	Dyphylline	xanthine	Inhibits phosphodiesterase causing an increase in cyclic AMP.	1951	

Type of agent	Drug	Analog of	Mechanism of action	Approved	Report on antibacterial activity
	Allopurinol	hypoxanthine	Inhibits xanthine oxidase, blocking the conversion of oxypurines to uric acid.	1986	
	Adenosine	adenosine	Activates purine receptors and inhibits calcium uptake.	2007	

Chapter 4

4 Pyrimidine starvation inhibits biofilm formation despite high c-di-GMP levels

4.1 Abstract

We studied the role of pyrimidines during the initiation of biofilm formation by *S. enterica* serovar Typhimurium. When the *de novo* pathway for UMP production was disabled, planktonic growth and biofilm formation were abolished. Planktonic growth was restored at lower concentrations of exogenous uracil than biofilm growth, indicating a special role of pyrimidines in biofilm formation. Remarkably, quantification of intracellular metabolites revealed an increase in c-di-GMP concentration under pyrimidine starved conditions. This is in contrast to the standard paradigm of high levels of c-di-GMP being associated with high levels of biofilm formation.

4.2 Introduction

Salmonella enterica serovar Typhimurium is a frequent colonizer of animal hosts. During its complex lifestyle it comes across a great variety of conditions inside and outside of its host such as exposure to acid, bile, increased osmolarity, peroxide, anoxia, and nutrient limitation amongst others (Kröger *et al.*, 2013). To survive in such vastly different conditions, evolution has endowed bacteria like *Salmonella* with elaborate mechanisms to sense and respond to the multitude of environmental cues that they encounter. Typical responses involve the regulation of gene expression and the modulation of protein activity. Cross-talk can occur between the various response systems of a cell. Therefore, to prevent undesirable reactions, sophisticated regulatory networks evolved (Filloux, 2012).

An effective response to environmental stress is the production of multicellular biofilms (O'Toole & Stewart, 2005; Gotoh *et al.*, 2010). In the case of *Salmonella*, biofilm formation plays a crucial role in survival outside as well as inside the host (Steenackers *et al.*, 2012). Induction of biofilm formation is coordinated by the master regulator CsgD which controls the production of curli and cellulose (Römling, 2005). The regulatory role of CsgD has been extensively reviewed recently and will only be briefly summarized here (Simm *et al.*, 2014). In its unphosphorylated form, CsgD directly facilitates curli production by initiating transcription of the *csgBAC* operon (Hammar *et al.*, 1995; Brombacher *et al.*, 2003; Kader *et*

al., 2006) and indirectly stimulates cellulose biosynthesis by initiating transcription of *adrA* (Römling *et al.*, 2000; Gualdi *et al.*, 2008). AdrA in turn produces cyclic diguanylic acid (c-di-GMP) which relieves auto-inhibition of the cellulose synthase BcsAB (Römling *et al.*, 2000; García *et al.*, 2004; Kader *et al.*, 2006; Morgan *et al.*, 2014). Regulation of CsgD itself is quite complex and involves various mechanisms acting from the transcriptional to post-translational level. These mechanisms include: various transcriptional regulators, sRNAs and the c-di-GMP signalling system (Boehm & Vogel, 2012). The c-di-GMP-mediated inverse regulation of adhesion and motility has been the subject of rigorous study, for an overview see the review by Hengge (Pesavento & Hengge, 2009). It was reported in 2009 that in *Salmonella*, CsgD production is induced at the transcriptional and post-transcriptional level by the activity of at least two diguanylate cyclases (DGCs) and inhibited by at least four phosphodiesterases (PDEs) (Schmidt *et al.*, 2005; Kader *et al.*, 2006; Simm *et al.*, 2007; Simm *et al.*, 2009). Five years later, ten DGC/PDEs have been proven to regulate processes associated with matrix production, but despite the advances in the field the exact molecular mechanism by which c-di-GMP regulates CsgD expression remains uncertain (Simm *et al.*, 2014).

Ueda and colleagues (Ueda *et al.*, 2009) revealed the important role that pyrimidine availability plays in *Pseudomonas* aggregation. They demonstrated that transposon insertions in genes encoding enzymes of the *de novo* synthesis pathway (*carA*, *carB*, *pyrB*, *pyrC*, *pyrD* or *pyrE*) lead to decreased biofilm formation, and that the wild type phenotype can be restored by addition of uracil to the medium. Moreover, certain uracil analogues used as anti-cancer drugs, were shown to possess potent biofilm inhibitory activity (Ueda *et al.*, 2009; Attila *et al.*, 2009). In *Escherichia coli*, transcription of the curli operon was shown to be downregulated under low pyrimidine nucleotide availability. Inactivation of *de novo* UMP production of *E. coli* MG1655 impaired biofilm formation in LB 1/4 medium, and the addition of 0.25 mM uracil restored the wild type phenotype. Furthermore cellulose production was shown to be triggered by exogenous uracil via the DGC, YedQ (Garavaglia *et al.*, 2012). It was postulated that perturbations in the nucleotide pools, caused by mutations in the pyrimidine biosynthesis pathway, could lead to changes in c-di-GMP production which in turn would explain the effects on curli and cellulose production. However, no significant changes in c-di-GMP levels were observed when *carB* (encoding the large subunit of carbamoyl phosphate synthetase, which catalyzes the first reaction in the *de novo* pyrimidine biosynthesis pathway) was deleted (Garavaglia *et al.*, 2012), leaving the link between pyrimidine synthesis and matrix production open for further exploration.

The *de novo* pyrimidine biosynthesis pathway can be considered a linear series of enzyme-catalysed reactions in which orotidine monophosphate (OMP) is the first pyrimidine nucleotide that is formed (Supp. Figure 1). The first reaction in the pathway is catalysed by carbamoyl phosphate synthetase, encoded by *carAB*, and yields carbamoyl phosphate, which is also a precursor for arginine biosynthesis. The second step of pyrimidine biosynthesis, which converts carbamoyl phosphate to carbamoyl aspartate, is catalysed by aspartate carbamoyltransferase, encoded by *pyrBI*. Another three steps (enzymes encoded by *pyrC*, *pyrD* and *pyrE*) lead to the formation of OMP which is sequentially converted to UMP, UDP and UTP (respective enzymes encoded by *pyrF*, *pyrH* and *ndk*). Finally, CTP is formed by ATP-dependent amination of UTP using glutamine as an amino group donor (enzyme encoded by *pyrG*). Additionally, *Salmonella* possesses salvage enzymes which allow the *de novo* synthesis of pyrimidines to be bypassed when exogenous pyrimidine nucleoside and nucleotides are present in the environment and also enables the reutilization of nucleic acid fragments generated by nucleic acid turnover. For a more detailed review of the pyrimidine biosynthesis pathway the reader is referred to EcoSal (Jensen *et al.*, 2008).

Building on prior work done at the CMPG using a $\Delta carA$ mutant that is defective in the first step of pyrimidine biosynthesis, and inspired by the research of other groups as described above, we aimed to further unravel the link between pyrimidine biosynthesis and the regulation of biofilm-associated processes. We were particularly interested in the earliest stage of biofilm formation, known as the “switch-phase” (*vide supra*, Chapter 1).

We first studied the effect of pyrimidine limitation on the ability of *Salmonella enterica* subsp. *enterica* Typhimurium 14028 to produce biofilm on plastic surfaces. We observed that under our experimental conditions, limited pyrimidine availability causes reduced biofilm formation and changes in the c-di-GMP pools of *Salmonella*. Surprisingly, it was not a reduction but an increase in c-di-GMP that was detected. Thus, inhibition of biofilm formation under conditions of pyrimidine starvation occurs despite high levels of c-di-GMP. These results indicate that the established paradigm of low c-di-GMP levels being equated with reduced biofilm formation, while high c-di-GMP levels being associated with increased biofilm formation, needs to be nuanced and underscores the importance of other mechanisms that regulate adhesion and matrix production.

4.3 Results

4.3.1 Pyrimidine starvation is a limiting factor for biofilm formation of *S. Typhimurium*

To test the effect of pyrimidine starvation on the ability of *S. Typhimurium* 14028 to form biofilms on hydrophobic surfaces, mutants containing single-gene deletions of *carA* and *pyrB* or kanamycin insertions in *pyrI*, *pyrC*, *pyrD*, *pyrE* or *pyrF*, were complemented with a dilution series of uracil. Their biofilm and planktonic growth were measured after 24 hours of incubation in the Calgary biofilm device (Ceri *et al.*, 1999). With the exception of strain *S. Typhimurium* 14028 *pyrI::Km*, lacking the regulatory subunit of ATCase which renders the enzyme insensitive to feedback-inhibition by CTP and UTP, all mutants had a growth defect and required the addition of uracil to the growth medium (Figure 28). Addition of 17.5 μM uracil was sufficient to restore planktonic growth (determined by measuring OD₆₀₀ of the liquid phase) to $\geq 50\%$ of wild type levels. Despite the restoration of planktonic growth, biofilm formation (as measured by crystal violet staining of bacteria and matrix adhering to the plastic pegs) was still severely impaired when 17.5 μM uracil was applied. Only upon addition of 35 μM uracil or more, biofilm formation could be restored to near wild type levels (Figure 28). For further experiments 70 μM uracil was used to study the biofilm restorative effects of uracil. When the wild type strain was grown in the presence of exogenous uracil, no changes in planktonic growth or biofilm formation were observed. Crystal violet staining of biofilms formed on the bottom of petri-dishes gave results, which were comparable to observations from the Calgary biofilm setup. It should be noted that the $\Delta carA$ mutant is also auxotrophic for arginine, however the TSB 1/20 growth medium can supply this need as it is a complex medium containing various amino acids, including arginine. Furthermore, because *carA* and *carB* form an operon, disrupting the *carA* gene by replacing it with a kanamycin-resistance cassette (and removing it), may cause downstream effects on *carB* transcription as well, this will be discussed in Chapter 7.

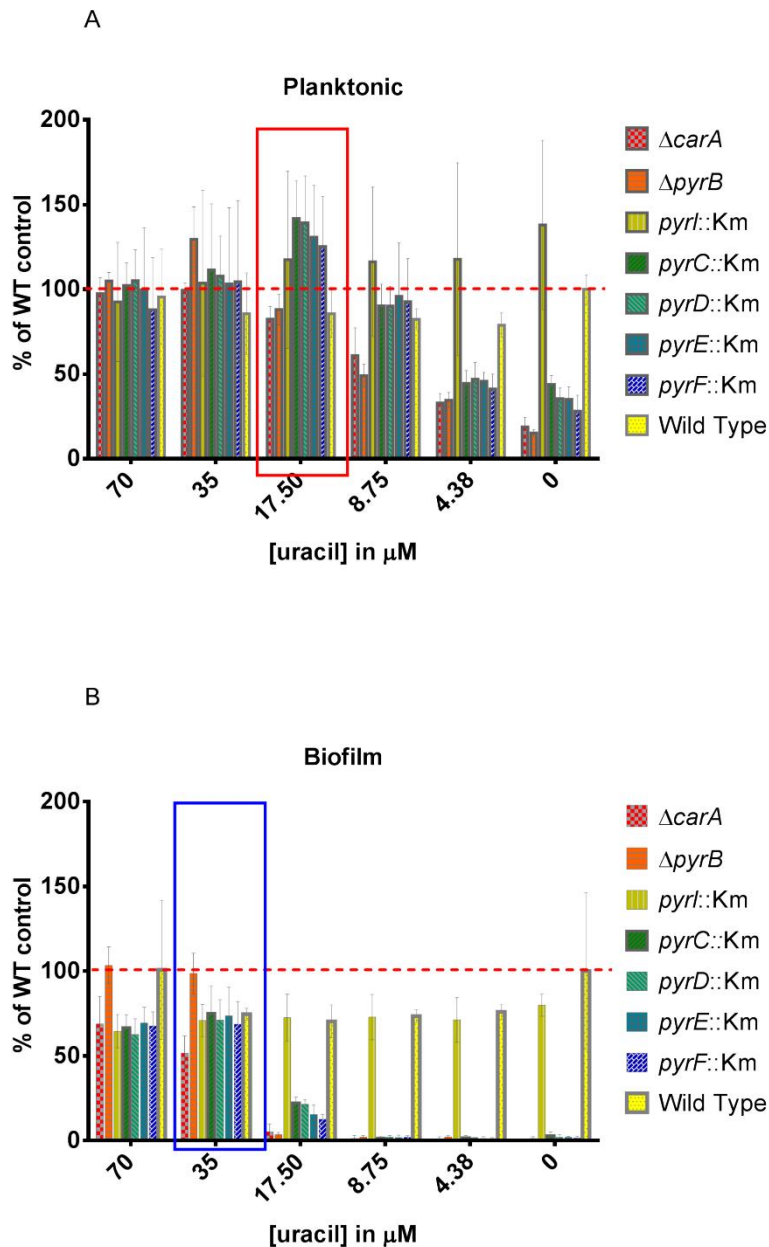


Figure 28 Panels A and B show the concentration dependent restoration of planktonic growth and biofilm formation for various mutants of the *de novo* pyrimidine biosynthesis pathway of *S. Typhimurium*. The results are represented here as percentages of the wild type grown in TSB1/20 without added uracil (red dotted lines). Without addition of uracil, all mutants (excluding *pyrI::Km*) are defective in planktonic growth and biofilm formation. Restoration of planktonic growth (panel A; red box) to more than 50% of wild type levels requires the addition of $\geq 17.5 \mu\text{M}$ uracil to the medium. Restoration of biofilm formation to near wild type levels (panel B, blue box) requires a higher concentration ($\geq 35 \mu\text{M}$ uracil) than what is needed for restoring planktonic growth. Data are represented as means \pm standard deviations ($n = 3$ to 6).

Confocal laser scanning microscopy of biofilms grown on the surfaces of petri-dishes revealed that wild type biofilms were thick, heterogeneously organized and cells were interconnected with each other in clusters. In the case of the pyrimidine starved $\Delta carA$ mutant, the number of cells were greatly reduced, the thin layer of cells were disorganized and scattered over the

Chapter 4: Pyrimidine starvation and biofilm inhibition

surface. When grown in the presence of 70 μM uracil, the mutant displayed a biofilm phenotype that was similar to that of the wild type (Figure 29). These results, together with those from the Calgary assay, indicate that an inadequate supply of pyrimidines is a limiting factor for biofilm formation in *S. Typhimurium* 14028. On the other hand, the availability of excess uracil has no noteworthy effect on biofilm formation by the wild type.

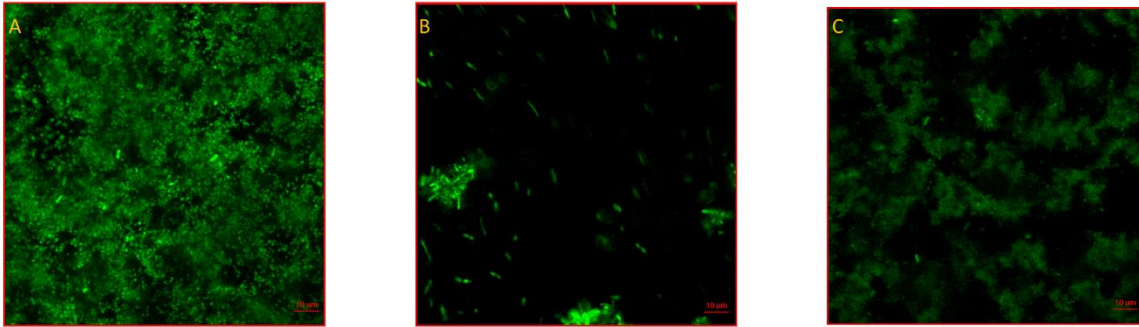


Figure 29 Confocal laser scanning microscope images (500x) of 24 hour old biofilms from: (A) wild type; (B) $\Delta carA$ with 17,5 μM uracil; and (C) $\Delta carA$ with 70 μM uracil. The wild type biofilm is thick with an organized three-dimensional structure, while the pyrimidine starved mutant has a limited number of cells on the surface which lacks organization and only a few clumps are present. The addition of 70 μM uracil to the mutant increases the number of surface attached cells as well as the three-dimensional organization

To determine the time point at which the switch between the motile and sessile lifestyles occurs, we used the petri-dish setup and plated out serial dilutions onto LB agar at regular intervals (every 2 or 3 hours). In the case of the wild type, it was clear the cells undergo a switch from the free-living planktonic mode to a biofilm-based lifestyle 8 to 10 hours post inoculation. Because the $\Delta carA$ mutant has a growth defect on LB agar, we used crystal violet staining and optical density measurements for quantification. The severely inhibited biofilm formed by the pyrimidine starved $\Delta carA$ mutant, 10 hours post-inoculation, indicates that this switch does not occur (Figure 30).

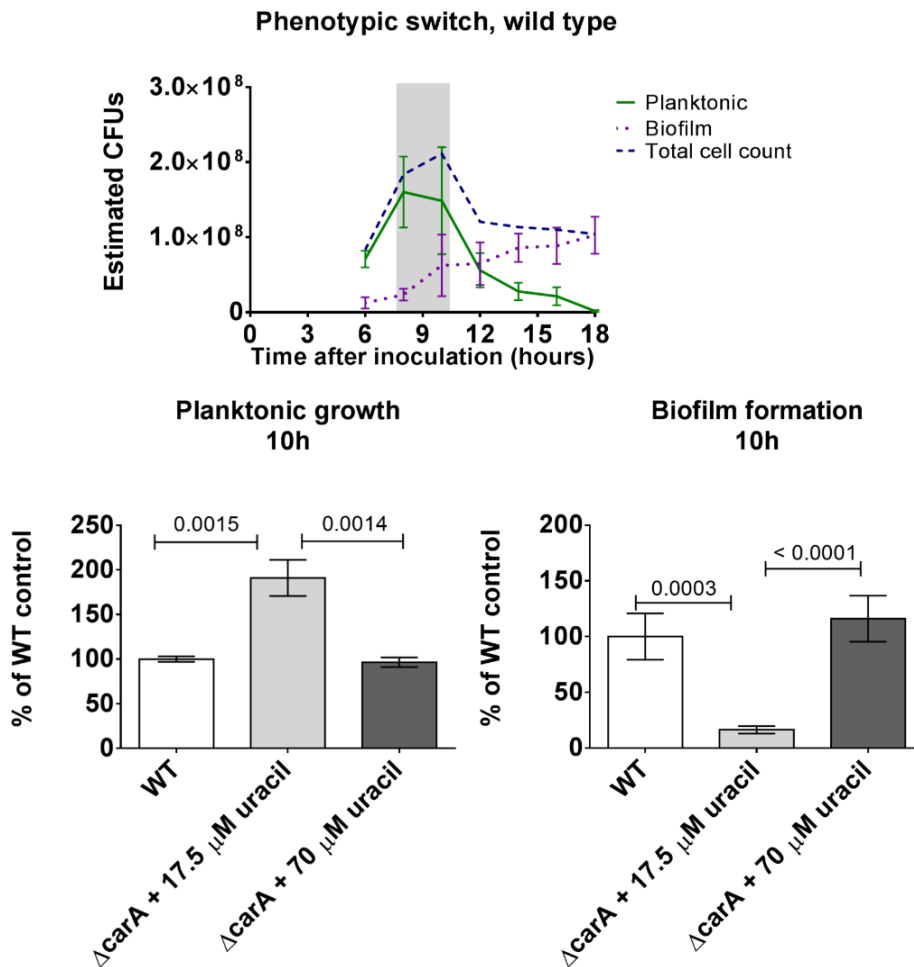


Figure 30 Graph showing the pattern of planktonic growth (solid green line) and biofilm formation (dotted purple line) of *S. Typhimurium* 14028 wild type based on estimated colony forming units (CFUs). Between 8 and 10 hours (shaded period), there is a decline in the number of viable planktonic phase cells. This coincides with an increase in the number of viable biofilm cells, indicating that a phenotypic switch occurs. The total cell count (indicated as a dashed blue line) shows a deceleration of exponential growth between 8 to 10 hours. This is followed by a reduction in the number of viable cells (a dying off phase) which stabilizes at around 14 hours. Error bars represent the standard deviations of 3 technical repeats. The bottom images indicate planktonic and biofilm growth of wild type, $\Delta carA$ 10 hours post inoculation, determined by optical density and crystal violet staining. The data represents the mean values and standard deviations ($n=3$ to 6), p-values for t-tests are indicated above the strains that were compared.

In order to compare the role of pyrimidines in biofilm formation in *Salmonella* and *E. coli* under our experimental conditions, we tested the effect of complementing various deletion mutants of the *de novo* and salvage pathway of *E. coli* BW25113 (Supp. Table 1). Our findings were complementary to the results of previously published work also done in *E. coli* (Supp. Figure 2). It should be noted that, like other *E. coli* K12 strains, BW25113 is a poor biofilm former due to disrupted expression of curli (Hammar *et al.*, 1995; Brombacher *et al.*, 2003)

and cellulose (Zogaj *et al.*, 2001; Da Re & Ghigo, 2006). We observed that addition of 27 μM uracil enhanced biofilm formation of the wild type 4-fold. Interestingly this strain (and other K12 variants) carries a mutation that causes low frequency of transcription of *pyrE*, resulting in dysregulated nucleotide metabolism during growth on a pyrimidine-free medium and perpetually reduced pyrimidine pools (Jensen, 1993; Jensen *et al.*, 2008). Restoration of the pyrimidine pools by exogenous uracil could thus explain the observed increase in biofilm formation. As in the case of *S. Tyhimurium*, the pyrimidine deletion mutants of *E. coli* were affected in free-living growth and biofilm formation in TSB 1/20. Addition of 17.5 μM uracil could restore the free-living growth defects of the mutant strains and concentrations above 35 μM uracil enhanced biofilm formation to 200 - 600% of the parental control levels. We hypothesize that the addition of uracil to the growth medium helps to overcome both the negative effects on biofilm formation of the deletion mutation and the low transcription of *pyrE*, which is also present in wild type strain.

Upon uptake into the cell, uracil is converted to UMP by the action of uracil phosphoribosyltransferase (encoded by *upp*). The forward directions of the *de novo* pathway are thermodynamically favoured, thus UMP cannot be converted to OMP or upstream intermediates of the *de novo* pathway. The fact that exogenously applied uracil could restore biofilm formation in the deletion mutants thus indicates that uracil, UMP or another downstream intermediate is required for biofilm formation. To elaborate on this we then tested the biofilm formation of a *Salmonella* double mutant *carA::Km- Δ upp*. The enzyme UPRTase encoded by *upp* is responsible for converting uracil taken up from the medium to UMP. Thus, the double mutant cannot make its own UMP *de novo*, nor can it utilize uracil from the medium. We compared this mutant to the Δ *carA* strain, Δ *upp* and the wild type. The Δ *upp* mutant formed the same amount of biofilm (50% of wild type levels) regardless of the concentration of added uracil. The Δ *carA* strain responded as already described. The double mutant consistently had less than 5% biofilm regardless of the presence of uracil in the medium (Figure 31). However, the double mutant also had a severe growth defect, no doubt due to a lack of pyrimidines, and thus it was hard to draw a conclusion from these results. Therefore we also tested an *E. coli* BW25113 *upp::Km* mutant and found that it is not responsive to stimulation of biofilm formation by 30 μM uracil, whereas the amount of biofilm formed by the parental strains was nearly quadrupled (Supp. Figure 3). This suggests that UMP as opposed to uracil is the effector that influences the switch to biofilm formation in *E. coli*, and probably in *Salmonella* as well. Based on our results for *Salmonella* and *E. coli* we conclude that in a pyrimidine deficient environment, an intact *de novo* UMP synthesis pathway is

required for biofilm formation. When the *de novo* pathway is disrupted, biofilm formation is dependent on the presence of extracellular uracil that can be taken up and converted to UMP.

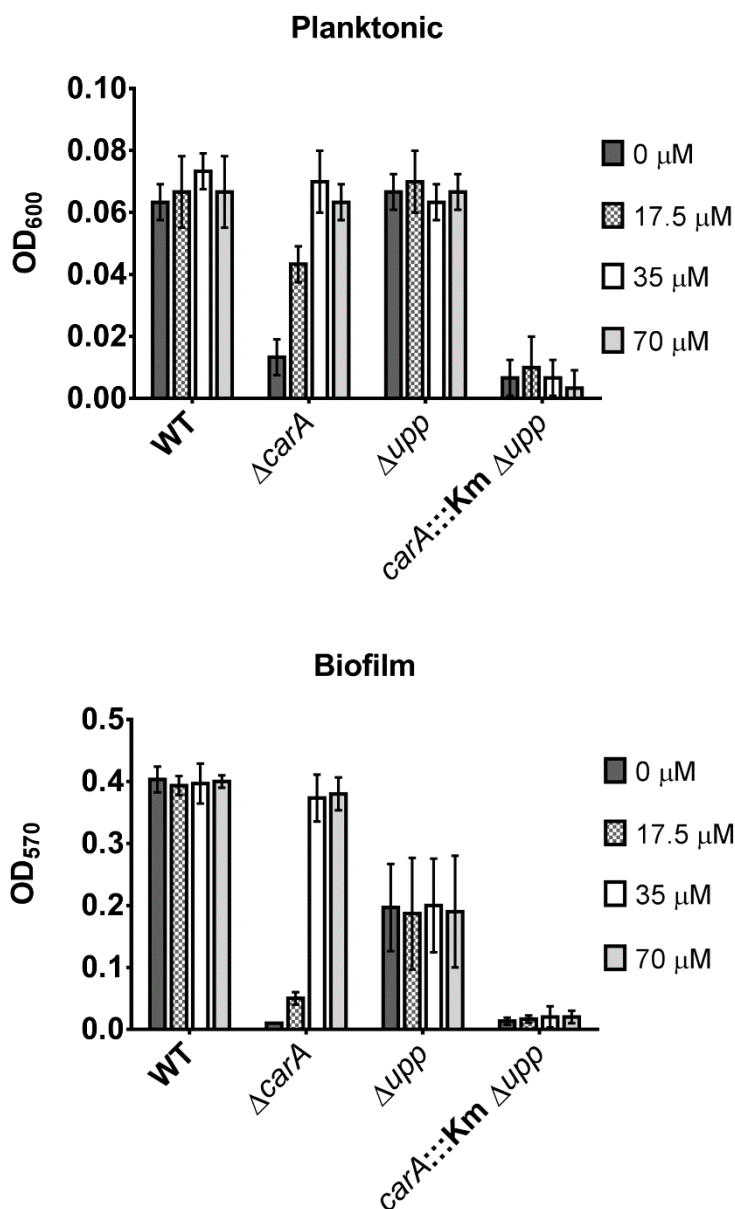


Figure 31 Biofilm formation and planktonic growth of *S. Typhimurium* WT, ΔcarA , Δupp and $\text{carA}::\text{Km}-\Delta\text{upp}$ in different concentrations of uracil. Data are represented as means \pm standard deviations (3 biological repeats were further divided into 3 technical repeats each).

In the following sections, we attempt to elucidate the mechanisms by which pyrimidine levels affect biofilm formation by measuring the levels of key nucleotide derived metabolites. Previous work in *E. coli* has shown that pyrimidine availability affects both cellulose and curli

biosynthesis. It was hypothesized that these effects may be due to changes in nucleotide pool levels, which may in turn have an influence on intracellular c-di-GMP concentrations and cellulose and curli production (Garavaglia *et al.*, 2012). To test whether changes in pyrimidine availability influences the intracellular concentrations of c-di-GMP and UDP-glucose (the substrate for cellulose biosynthesis), we measured their levels in planktonic samples at the time point where free-living cells switch to biofilm based growth.

4.3.2 UDP glucose levels are unaffected by pyrimidine starvation

Cellulose is synthesized by the cellulose synthase complex (BcsA-BcsB) which links UDP- α -D-glucose units into long polymers. UDP- α -D-glucose is formed by the addition of UTP to α -D-glucose 1-phosphate in a reaction catalysed by uridylyl transferase, encoded by *galU* (Weissborn *et al.*, 1994). Since cellulose (and thus by association, UDP-glucose), is of high importance for matrix production by *Salmonella* as well (Steenackers *et al.*, 2012), we wanted to determine whether disruptions in the pyrimidine pathway can lead to altered UDP-glucose levels and so impair biofilm formation.

HPLC-MS/MS analysis was performed on cellular extracts from planktonic *S. Typhimurium* wild type and $\Delta carA$ cultures, at the time point where early biofilm formation occurs for the wild type (~10 hours). These measurements indicated that the UDP-glucose levels for the $\Delta carA$ mutant complemented with 17.5 or 70 μ M uracil were not different than those of the wild type (Supp. Figure 4). This suggests that reduced biofilm production is likely not attributable to a lack of substrate for the cellulose synthase complex (BcsA-BcsB), as the intracellular UDP-glucose levels are at least within the concentration range of the wild type strain. However, it should be kept in mind that the sizes of the UDP-glucose pools are determined by the balance between synthesis and utilization, although the pool sizes for the different strains were similar their fluxes might differ.

As a control experiment, we were interested in determining the extent to which cellulose and curli contribute to biofilm formation under our experimental conditions. Therefore, we compared the biofilm phenotypes of a curli-deficient mutant (*csgB::Km*), a cellulose deficient-mutant (*bcsA::Km*) and a mutant deficient in both components (*csgD::Km*). Based on these results it appears that cellulose biosynthesis does not make a noteworthy contribution to biofilm formation, and that curli plays the most important role (Supp. Figure 5). Therefore, pyrimidine starvation probably affects curli biosynthesis rather than cellulose production. The signalling molecule c-di-GMP is known to affect both cellulose and curli production in *Salmonella*, by affecting the transcription of *csgD* (Ahmad *et al.*, 2017). Thus, in an attempt

to uncover the cause of the biofilm defect of the pyrimidine starved $\Delta carA$ mutant we next determined the intracellular concentrations of c-di-GMP.

4.3.3 A lack of pyrimidines is associated with an increase in c-di-GMP

Given the fact that c-di-GMP plays a central role in biofilm formation by regulating the expression of CsgD at the transcriptional and posttranscriptional level (Kader *et al.*, 2006), we were interested in quantifying c-di-GMP levels at the time of the switch between lifestyles. Intracellular c-di-GMP concentrations were determined from extracts of wild type and $\Delta carA$ mutants complemented with various concentrations of uracil. Extractions were performed on planktonic and biofilm cells during the early stages of biofilm formation in petri-dishes, as described above. The pyrimidine-starved mutant did not form sufficient biofilm on the bottom to allow for the extraction and detection of metabolites. The c-di-GMP concentration from each sample was determined by mass spectrometry and normalized according to the sample's optical density for planktonic samples (Figure 32) and protein content for biofilm and planktonic samples (Supp. Figure 6). The different normalization methods did not give the same fold changes for the pyrimidine-starved mutant compared to the wild type; however the general patterns were similar as explained below and in the Supplemental section.

There was no significant increase in c-di-GMP concentration of the wild type biofilm cells compared to the wild type planktonic cells (Supp. Table 2). However, we were surprised to find that the c-di-GMP levels of the $\Delta carA$ mutant complemented with 17.5 μM uracil (sufficient to restore planktonic growth but not biofilm formation) were 20-fold higher than those of the wild type. On the other hand, when complemented with 70 μM uracil (enough to also restore biofilm formation), c-di-GMP concentrations were reduced again to a level similar to that of the wild type (Figure 32). Results for *E. coli* also showed an increase in c-di-GMP concentration during pyrimidine starvation (Supp. Figure 6). Together, these results suggest that a lack of pyrimidines inhibits biofilm formation, despite high levels of c-di-GMP. It is well known that the complex interplay between c-di-GMP, *csgD*, the alternative sigma factor *rpoS* and other regulators controls aggregative behavior, with high c-di-GMP levels usually associated with biofilm formation and reduced motility. However, this paradigm does not always hold true. Sanchez-Torres *et al.* (2010) reported that early-stage biofilm formation occurs only when motility is not inhibited by the activity of certain DGCs (Sanchez-Torres *et al.*, 2010). In that particular study no differences in total intracellular concentrations of c-di-GMP were detected upon deletion of these DGCs, accentuating the possibility that there may be various segregated c-di-GMP pools within the cell. Here we report a measured increase in

total c-di-GMP concentration, which is associated with a defective biofilm phenotype. Our results support the notion that there is an ambiguous relationship between biofilm formation and intracellular c-di-GMP concentration.

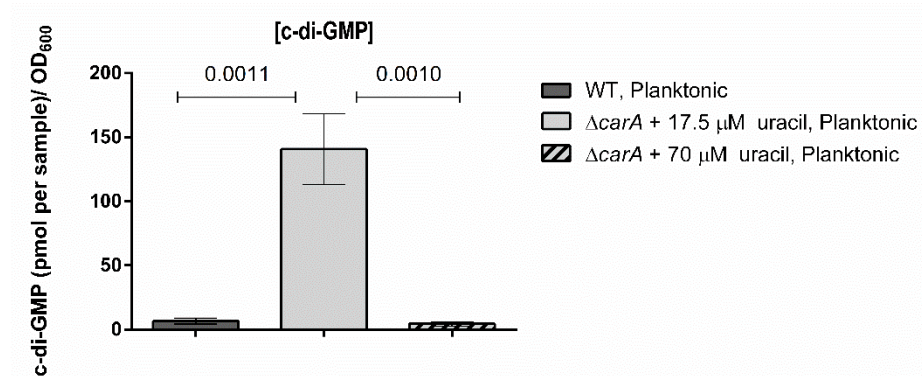


Figure 32 Concentration of c-di-GMP from cellular extracts of *S. Typhimurium* 14028 wild type and $\Delta carA$ strain as determined by LC-MS/MS. Metabolites were extracted from biologically independent cultures and normalized according to sample optical density. The error bars represent standard deviations of the three independent experiments. When the $\Delta carA$ strain was grown in the presence of 17.5 μ M uracil (enough to restore planktonic growth but not biofilm formation) the c-di-GMP concentration differed significantly from that of the wild type planktonic phase (unpaired t test, 95% confidence interval, p value = 0.0011). There was also a significant difference in c-di-GMP concentration of the $\Delta carA$ strain grown in 17.5 μ M versus 70 μ M uracil (unpaired t-test, 95% confidence interval, p value = 0.0010). The experiment was repeated for a second time on a different day and a similar pattern was observed.

4.4 Conclusion

Salmonella species are a leading cause of acute gastroenteritis and are estimated to be responsible for more than 2.8 billion cases of diarrheal illnesses per year (Majowicz *et al.*, 2010). Biofilms are known to be associated with chronic infections and environmental persistence of *Salmonella*, as this mode of life facilitates enhanced surface colonization and host transmission (Gonzalez-Escobedo *et al.*, 2011). *Salmonella* biofilm formation is particularly problematic in the agricultural and food industry (Marin *et al.*, 2009; Schonewille *et al.*, 2012). Prompted by the need to develop new methods to combat biofilm formation, we investigated the role of the *de novo* pyrimidine biosynthesis pathway as a potential anti-biofilm target. With this work we showed that pyrimidine availability affects a diversity of processes in *Salmonella* that are linked to matrix production. Although a similar work has been published for *E.coli* (Garavaglia *et al.*, 2012), we were of the opinion that the role of pyrimidine biosynthesis in biofilm formation by *Salmonella* needed to be clarified as well. It is clear from

our study that in the absence of intact *de novo* biosynthesis, extracellular pyrimidines are a requirement for biofilm formation in *S. Typhimurium* 14028 and *E. coli* BW25113 (similar to the previous publication). However, in wild type *S. Typhimurium*, the addition of exogenous uracil did not enhance biofilm formation, indicating that the presence of extracellular uracil has effects that are distinct from those in *E. coli*.

We showed that pyrimidine metabolism has an effect on the c-di-GMP pool size of *S. Typhimurium*, albeit in an unexpected way, as a lack of pyrimidines coincides with reduced biofilm formation in spite of increased levels of c-di-GMP. This suggests either that pyrimidine availability regulates biofilm production in a manner that is decoupled from regulation by c-di-GMP, or that local c-di-GMP pools are affected differently. Although it is established that the relationship between c-di-GMP concentration and biofilm formation is not perfectly linear and that low c-di-GMP levels are important for motility and initial attachment (Wood *et al.*, 2010; Sanchez-Torres *et al.*, 2010), to our knowledge this is the first time that defective biofilm formation is linked to a measured increase in total c-di-GMP production. From a clinical perspective, the prevention of biofilm formation is an important step to treat pathogens. Our results complement and expand observations that advocate the therapeutic potential of interfering with pyrimidine biosynthesis to prevent the transition from free-living growth to growth as part of matrix-embedded communities. Furthermore, we shed more light onto the different effects that pyrimidine starvation has on biofilm formation by *Salmonella* compared to *E. coli*.

Nevertheless, key questions remained unanswered. Therefore further investigation was needed to shed light on the following: (i) The link between pyrimidine starvation and increased c-di-GMP production. (ii) The mechanism of biofilm inhibition, despite increased c-di-GMP levels. (iii) The global effect of pyrimidine starvation on cellular processes. To address these questions we used a network based approach to analyse the effects of pyrimidine starvation on the transcriptome in the next chapter.

4.5 Materials and Methods

4.5.1 Bacterial strains and growth conditions

Bacterial strains and plasmids used in this study are listed in Table 5. Prior to experiments strains were stored at -80°C and inoculated onto Lysogeny broth (LB) agar plates, containing the relevant antibiotics if needed. Once inoculated, LB agar plates were incubated at 37°C overnight, and subsequently stored at 4°C. Single colonies were used to inoculate liquid LB

cultures (containing antibiotics if needed), and were incubated overnight at 37°C with shaking. Antibiotics used were ampicillin (100 µg/ml) and kanamycin (50 µg/ml). Antibiotics and uracil were obtained from Sigma. Biofilm formation and reporter fusion assays were performed using 1:20 diluted tryptic soy broth (TSB) from Becton Dickinson.

4.5.2 Construction of deletion and complementation mutants

Deletion mutants *S. Typhimurium* 14028 $\Delta carA$ and *S. Typhimurium* 14028 $\Delta pyrB$ were constructed using the Datsenko and Wanner procedure (Datsenko & Wanner, 2000). The entire coding regions (plus ~10bp before and after the coding regions) were replaced by kanamycin or chloramphenicol resistance cassettes which were subsequently removed by FLP recombinase. Plasmids used in Chapter 4 and 5 are listed in Table 5 and Table 6.

Table 5 *Salmonella* strains and plasmids used in this study. *Salmonella* promoter fusions used in this study were published by . More detailed descriptions of the various genes listed can be found in the review by (Steenackers *et al.*, 2012)

Strain	Relevant genotype	Source	Reference
S. Typhimurium14028	Wild type	ATCC strain collection	
	$\Delta carA$	This work	
	$\Delta pyrB$	This work	
	$\Delta csgD$	In house strain collection	
	$\Delta csgD\Delta carA$	This work	
	$\Delta csgD\Delta upp$	This work	
S. Typhimurium14028	Wild type	Parental strain of McClelland collection	
	<i>pyrD</i> ::Km	(Porwollik <i>et al.</i> , 2014)	
	<i>pyrC</i> ::Km	(Porwollik <i>et al.</i> , 2014)	
	<i>pyrF</i> ::Km	(Porwollik <i>et al.</i> , 2014)	
	<i>pyrI</i> ::Km	(Porwollik <i>et al.</i> , 2014)	
	<i>uraA</i> ::Km	(Porwollik <i>et al.</i> , 2014)	
	<i>purR</i> ::Km	(Porwollik <i>et al.</i> , 2014)	
Plasmids for constructing knockout mutants (datsenko; wanner, 2000)			
pKD4			
pKD3			
pKD46			
pCP20			
pFPV25 promoter-<i>gfp</i> fusions*			
pFPV25	Promoterless <i>gfpmut3</i>	(Addgene plasmid # 20668)	(Valdivia; Falkow, 1996)
pFPV25.1	<i>rpsM</i>	Constitutive <i>gfpmut3</i>	
pCMPG10408	<i>bcsA</i>	Component of cellulose synthase	
pCMPG10405	<i>adrA</i>	c-di-GMP production, regulates cellulose biosynthesis	

Strain	Relevant genotype	Source	Reference
pCMPG5539	<i>csgB</i>	Minor curlin subunit	(Hermans <i>et al.</i> , 2011)
pCMPG5521	<i>csgD</i>	Master regulator of biofilm formation	
pCMPG10433	<i>purA</i>	Purine synthesis, adenylosuccinate synthetase	
pCMPG10434	<i>purF</i>	Purine synthesis, amidophosphoribosyltransferase	
pCMPG11011	<i>prsA</i>	Synthesis of PRPP	This work
Overexpression from plasmid			
pFAJ1708-CSGD		<i>csgD</i> expression from the <i>nptii</i> promoter	(Hermans, 2011)

*For each fusion, the corresponding gene of the promoter sequence, inserted into the pfpv25 vector, is indicated. Promotor sequences are all from *S. Typhimurium* 14028.

Table 6. Primers used for constructing deletion mutants and quantifying mRNA levels. ^a STM numbers refer to the locus tags of the gene from the *Salmonella* LT2 genome, ^b STM14 numbers are the locus tags in the 14028 genome

PCR Target for gene deletion		Nucleotide sequences of primers		
<i>carA</i>		GGGTGTTTTGATTAAGTCAGCGCTATTGGTTCTGGAGTGTAGGCTGGAGC TGCTTC TCCTGATTATTCGCGGACTGACGGTATTGCTCAATCATATGAATATCCT CCTTAG		
<i>pyrB</i>		AGAGCTGAGTATAATCGCGACAATTTGCCGGGAGGAAGCGTGTAGGCT GGAGCTGCTTC CAACCTGCAGTTTGTATCGTGTGTCATCGTTTTTCTCCCATATGAATAT CCTCCTTA		
<i>upp</i>		TCCGGCGATTTTTTTTGTGGTTGCCAGTCATCTGAGGATAGGAGAAGAGT GTGTAGGCTGGAGCTGCTTC TATTCAAAAAAAGCCGACTCTTAAAGTCGGCTTTTAATTATTTATTCAC CATATGAATATCCTCCTTA		
Primer extension		Nucleotide sequences of primers		
<i>dusB-fis</i> 5'-UTR fragment determination		5'-Hex TTCCCACTTGC GGTTAGAAGACATCATCTCGGATACTG		
<i>dusB -fis</i> promotor region sequencing		TTCCCACTTGC GGTTAGAAGACATCATCTCGGATACTG GTCATATCCGTCTGGATAAACAGCTGCTACCAGCGGAC		
RT-qPCR Target ^a	Locus tag ^b	Nucleotide sequences of primers	Source	Amplicon size (base pairs)
<i>adrA</i>	STM14_0455	GAAGCTCGTCGCTGGAAGTC CGAACAGAAGCGGATACAACATAAT	In house	63
<i>csgD</i>	STM14_1306	ACGCTACTGAAGACCAGGAACAC GCATTCGCCACGCAGAATA	In house	62
<i>csgB</i>	STM14_1309	TCAGGCGGCCATTATTGGT TTGATCCTTCCTGGCGTACTCT	(Hermans <i>et al.</i> , 2011)	66
<i>bcsA</i>	STM14_4358	AGTTGTAGCCCGACCTCATT GGAAGGGCAGAAAGTGAATC	In house	102
<i>gcpA/STM1987^a</i>	STM14_2408	CGGCGTGCGGTGGTT GTCATTTTTTCTGCTCGTCAGTAAC	In house	60

PCR Target for gene deletion		Nucleotide sequences of primers		
STM16 97 ^a	STM14_2 047	GCCATTAGTTTGC GG GTGTT TGAGACAAAAAGCTGCGATCA	(Jonas <i>et al.</i> , 2009)	58
STM18 27 ^a	STM114_ 2209	GCGCGAGCTGCATCGT TCCTGTGCCAAAATCATCG	(Jonas <i>et al.</i> , 2009)	55
STM33 88 ^a	STM14_4 086	CCGTACCGCACTACTTGCT CGTGT TTTCCCGATTGCT	(García <i>et al.</i> , 2004)	151
<i>yjiR</i> / STM17 03 ^a	STM14_2 058	CCAACGCCTGTTCTATTTCG GCCGGTGACGGTGTCTGTAT	(García <i>et al.</i> , 2004)	151
<i>ydiV</i> / STM13 44 ^a	STM14_1 632	TTGATACTGAGGCGATGTTTG CCCTGGAATGCGCTAAAC	(Jonas <i>et al.</i> , 2009)	58
<i>yegE</i> / STM21 23 ^a	STM14_2 620	CTGTTGATGTGGAGTGCGGT GCAGCCACGGCATATTGAC	(García <i>et al.</i> , 2004)	151
<i>yhdA/c</i> <i>srD</i> / STM33 75 ^a	STM14_4 070	CCGATGATGTACGCGACCTT TGGACCGCGACTTTATCAAA	(Jonas <i>et al.</i> , 2009)	58
<i>yhjH</i> / STM36 11 ^a	STM14_4 346	CTGCTGCTGCAACTGATGAAC CTCCACGCCCTCGACAAT	(Rouf <i>et al.</i> , 2011)	57
<i>yjcC</i> / STM42 64 ^a	STM14_5 126	AAAAACGCGTCAGCATTTCAGT CCGCGCTCAGTCACTTCAA	(Rouf <i>et al.</i> , 2011)	60
<i>yjiE</i> /STM4 551 ^a	STM14_5 467	ATCCGGCGTTAGGCCATTAT TTACCGTTCAGCCACAGGC	(García <i>et al.</i> , 2004)	151
<i>yfiN</i> / STM26 72	STM14_3 275	TGGCAGTGCTGACAGGATGT GGTACCCGGCGTGAAAAATT	(García <i>et al.</i> , 2004)	151
<i>yeaJ</i> / STM12 83 ^a	STM14_1 553	CAACCTGACCCGGCATAATT CCCGTGACTATGGTCTGCTCT	(García <i>et al.</i> , 2004)	151
STM25 03 ^a	STM14_3 068	GCGTTGGAGCACGATCATT CATGGTAAACGTCCCCACGA	In house	70
<i>rfaH</i>	STM14_4 783	GTCAGGCAACTTACCGCTTGT AAACGCGGGCAACTTCAG	In house	62
<i>recA</i>	STM14_3 417	ACGGCGCGGCGATT TGTCGTGGGTAGCGAAACG	In house	56
<i>gyrA</i>	STM14_2 804	CGCACGGCCAACAATGA CAACATTGAGGAGGAGCTGAAGA	In house	67
16S rRNA gene	STM14_4 686	CGGGGAGGAAGGTGTTGTG GAGCCCGGGGATTTACATC	(Tabak <i>et al.</i> , 2007)	178

4.5.3 Phenotypic switching between planktonic and biofilm mode of growth of *S. Typhimurium* 14028 wild type

The optical densities of overnight cultures were determined at 595 nm. Following centrifugation at 3000 × g for 5 minutes, the optical densities of the overnight cultures were normalized to an OD₅₉₅ of 1.5 by suspending the pellets in the appropriate amount of TSB

1/20. Petri-dishes containing 20 ml TSB 1/20 were inoculated with 200 μ L bacterial cells and incubated at 25 °C. Colony forming units (CFUs) of the planktonic cells from the liquid phase, as well as the biofilm on the bottom of the petri-dishes, were determined by plating out serial dilutions onto LB agar plates at regular intervals over a course of a day. Planktonic cells were harvested by carefully pouring off the liquid phase and removing the remaining liquid with a pipette. Biofilm encased cells on the bottom of the plate were harvested by adding 10 ml medium to the petri-dish and scraping the biofilm off the plate. Clumps were dispersed by passing the harvested cells through a needle with a diameter of 0.9 mm, fitted to a syringe.

4.5.4 Assaying biofilm formation

The optical densities of overnight cultures were determined at 595 nm and normalized as described above. High-throughput biofilm assays were performed using the Calgary biofilm device, which is a standard 96-well plate with a lid that has pegs which fit into the wells (Ceri *et al.*, 1999). All experiments were performed using TSB 1/20 as growth medium to which additional compounds were added if required (see main text for details). Wells were filled with 200 μ l medium and inoculated with 1 μ l bacteria from the normalized overnight cultures. Biofilm plates were incubated statically at 25°C. After 24 hours, the lids were removed and stained with a crystal violet solution consisting of 0.1% crystal violet dissolved in isopropanol, methanol and phosphate buffered saline (PBS) in a (1:1:18) ratio (modified protocol (Fletcher, 1977)). The pegs were de-stained with acetic acid and biofilm formation was quantified by measuring the optical density at 575 nm of the resolubilized stain using a Synergy Multimode reader. The optical density of the planktonic phase was determined at 600 nm. Experiments were performed in triplicate using biologically independent overnight cultures, with two to three technical repeats each, as indicated in the relevant results section. Data processing was done using Microsoft Office Excel 2013 and GraphPad Prism 6.

The average values of biofilm formation and planktonic growth of the reference strain were calculated per biologically independent experiment after subtraction of the blank. The reference values of each 96-well plate were then used to calculate the percentage of planktonic growth and biofilm formation at a given concentration for each mutant from the same plate. The mean growth percentages and standard deviations for each concentration were calculated from the values of the biologically independent experiments.

Low-throughput biofilm assays were performed using standard petri-dishes containing 20 ml of the appropriate growth medium. After pouring off the planktonic phase, biofilms on the bottom of the plate were quantified by CFU counting (after scraping off the biofilm) or staining

with crystal violet. After de-staining with acetic acid, biofilm formation was quantified as described above.

4.5.5 Microscopy

Biofilms formed on the bottoms of petri-dishes for 24 hours, as described above, were visualized with a Zeiss confocal laser scanning microscope (LSM 700), with digital camera (AxioCam MRm) and the associated Zen 2011 software. Strains used for microscopy expressed GFP constitutively from plasmid pFPV25.1.

4.5.6 Metabolite extraction and mass spectrometry analysis

Prior to metabolite extraction, the optical densities of overnight cultures were determined as described above and normalized to an OD₅₉₅ of 1.5 by suspension of pelleted cells in the appropriate volume of TSB1/20. Petri-dishes containing 20 ml TSB1/20 (with the appropriate amounts of uracil added) were inoculated with 200 µl overnight culture. Petri-dishes were incubated statically at 25°C for 8 to 10 hours before cells were harvested by pouring off the liquid growth medium (containing the free-living planktonic cells). This time point was selected because it corresponds to the time when *S. Typhimurium* enters late exponential phase and switches from a planktonic lifestyle to early biofilm formation. A 15 ml fraction of the harvested planktonic cells was used for metabolite extraction. The remaining 5 ml fraction was used for determining culture optical density, colony forming units and protein content by bicinchoninic acid (BCA) assay. When applicable, cells attached to the bottom of the plate (biofilm cells) were harvested by adding 10 ml TSB 1/20 to the petri-dish, scraping the biofilm off the plate and dispersing the clumps by passing them through a needle as described before. The harvested biofilm cells were divided into two aliquots of 5 ml, which were subsequently used for metabolite extraction, colony forming unit determination and protein quantification by BCA assay.

An extraction method with cold acetonitrile was used for c-di-GMP (Burhenne; Kaeffer, 2013). The extraction solution contained HPLC grade acetonitrile, methanol and water in a 2:2:1 volume ratio. For the extraction UDP-glucose 0.1 M formic acid was added to the extraction solution, and the heat-inactivation step was omitted to prevent dephosphorylation of the triphosphates. Final extracts were evaporated with Speed-Vac. Prior to mass spectrometric analysis, residues were dissolved in 200 µL H₂O.

The concentration of c-di-GMP was determined with LC-MS/MS as described in (28). A different LC-MS/MS method was applied for the quantitation of linear nucleotides and UDP-

glucose. Briefly, a Hypercarb 30 x 4.6 mm 5 μ m column (ThermoFisher) protected by a 2 μ m column saver (Supelco Analytical) and a C18 security guard (Phenomenex) was applied. Eluent A was 10 mM ammonium acetate in HPLC-gradient grade water adjusted to pH 10.0 with ammonium hydroxide. Eluent B was acetonitrile. A linear gradient from 4% B (v,v) up to 60% B (v,v) over 8 min was applied, followed by an equilibration phase of further 4 min at 4% B (v,v). The injection volume was 20 μ l per sample and the flow rate was constantly held at 0.6 ml/min. Specific mass transitions (UDP and UTP in negative ionization mode, all other analytes in positive ionization mode) were recorded by a tandem mass spectrometer (5500QTRAP, ABSCIEX). All experiments were conducted in triplicate starting from biologically independent overnight cultures. Data were processed with Microsoft Office Excel 2013 and GraphPad Prism 6.

Concentrations of metabolites were normalized according to optical density (for planktonic samples) and protein content (for planktonic and biofilm samples taken at the time of c-di-GMP extraction). Due to impaired growth of the $\Delta carA$ mutant on LB agar, CFU determination was not considered a reliable method for quantification.

Chapter 5

5 The impact of pyrimidine starvation on the transcriptome and the switch to biofilm growth

5.1 Abstract

This chapter studies the mechanisms behind reduced biofilm formation and increased c-di-GMP levels, using a network based approach to analyse transcriptome data. RNAseq data are verified with the use of GFP-promoter fusions and RT-qPCR. We found that the increase in c-di-GMP levels are probably driven by an increase in purine biosynthesis. Furthermore, biofilm inhibition occurs via inhibition of *csgD* transcription, possibly through the action of Fis and RpoS.

5.2 Introduction

As described in chapter 1, Van Puyvelde (2014) showed that *Salmonella* SL1344 biofilm development in nutrient-poor liquid media could be divided into three distinct phases: (i) The planktonic pre-switch phase, (ii) the interphase-switch and (ii) post-switch biofilm growth. In this thesis it was reported that the same pattern was observed for strain wild type strain ATCC14028, and that a pyrimidine starved $\Delta carA$ mutant does not undergo such a switch.

Transcriptome analysis by Van Puyvelde indicated that core biofilm genes (such as *csgDCBA* and *bapABCD*) were already activated in the planktonic phase. In some cases, there was a time-shift in the activation/repression of genes when comparing biofilm and planktonic samples at the time points 7, 8, 9 and 10 hours (the pre-switch and switch timepoints). In other words, biofilm cells had gene expression levels at a certain time-point that were comparable to expression levels in planktonic cells at a later time-point. Van Puyvelde concluded that genes which were differentially expressed in this fashion might be necessary for sub-populations of planktonic cells to switch to biofilm mode (in other words, some planktonic cells switch to a biofilm lifestyle before others, and this switch happens after the genes' expression levels change). The set of regulatory genes that were predicted to play a role in this switch consist of PrpR, PhoB, BaeR, KdgR RpoE, OmrA and OmrB (Van Puyvelde, 2014). What is striking is that some of these genes are part of the outer membrane (OM) stress systems. OM remodelling and biofilm formation are related processes, due to the role that the cell surface plays in biofilm formation. Many of the biofilm components, such as curli,

fimbriae and lipopolysaccharides are associated with the OM. Several components involved in environmental signalling are also shared between the OM and biofilm regulatory pathways. Thus, one can conclude that the aforementioned regulators probably play a role in changing the OM in a way that enables bacteria to attach to the surface and produce a biofilm matrix. During the post-switch phase, pathways involved in oxidative stress, carbohydrate metabolism, starvation-related systems, virulence genes and iron-sulphur cluster assembly are activated (Van Puyvelde, 2014).

Based on our observations that pyrimidine starved cells have impaired biofilm formation, we were interested in determining how pyrimidine starvation prevents the switch to biofilm-based growth. Although a number of insights were obtained in the previous chapter, some very important questions remained unanswered: (i) Why are c-di-GMP levels increased in the $\Delta carA$ mutant supplemented with low levels of uracil (17.5 μM)? (ii) By which mechanism is biofilm formation down regulated? (iii) What are the other effects of pyrimidine starvation? Thus, to get a global overview of the transcriptional differences between the pyrimidine starved cells compared to the wild type planktonic cells that are preparing to enter the biofilm-mode, we sampled RNA 10 hours past inoculation when planktonic phase cells switch to biofilm based growth. Further validations were done using GFP-promoter fusions, RT-qPCR and mutant studies.

5.3 Results

In order to study the transcriptional changes that affect the switch from free-living to biofilm growth in the wild type and pyrimidine starved $\Delta carA$ mutant, RNA samples were taken from the planktonic phase at the time of the switch between lifestyles. The optical densities of the planktonic phases were determined and the biofilms on the surface of the plates were coloured and measured (to verify that the pyrimidine starved mutant did not make biofilm and that it does not have a growth defect). As expected, the pyrimidine-starved samples exhibited a severely reduced biofilm phenotype and slightly increased planktonic culture densities.

RNA sequencing of the planktonic samples was performed by BGI. Reads were mapped to the *S. Typhimurium* LT2 genome and gene expression levels were quantified using Rockhopper (McClure *et al.*, 2013). More than 96% of the reads coming from each sample aligned to the *S. Typhimurium* LT2 chromosome and approximately 1% of the reads aligned to the LT2 plasmid (Supp. Table 3, Supp. Table 4). We defined genes that are significantly up/down-regulated as those with a \log_2 fold change of 1 or -1 (expression levels are 2x higher/lower compared to the wild type control) and a q value smaller than 0.05. According to

these selection criteria, 849 genes are significantly differentially regulated (roughly 20% of the genome) with 450 being up-regulated and 399 being down-regulated. The LT2 genome was used as a reference for assembly because subsequent analyses were done on a publicly available LT2 interactions network. As a control the ATCC14028 genome was also used as a reference: assembly results and gene expression predictions were similar. Genes with very high differential expression (absolute \log_2 fold change >2 and low q-values) are listed in (Supp. Table 5).

The expression data were analysed using a network-based approach. The networks that were generated by PheNetic (DeMaeyer *et al.*, 2013) were visualised in Cytoscape (Shannon *et al.*, 2003). PheNetic predicts the most probable interaction and regulatory networks that lead to the observed transcriptional changes. For analysis, a reduced gene list (size 427) was submitted to PheNetic after increasing the \log_2 fold cutoff to 1.5. Due to the way in which the algorithm works, genes that do not appear in the gene list but that are part of the connection path between other genes in the list are also added as nodes in the network. Thus, important interactions involving genes with smaller absolute \log_2 fold changes were also visible. To identify downstream pathways that are triggered by differentially repressed/ activated in the pyrimidine starved strain, PheNetic was run in “Downstream” mode. The network produced by the “Downstream mode” mostly contains genes with similar functionalities or that are involved in the same pathways and are together differentially up or down regulated. From these results, it was possible to identify affected pathways which include, purine metabolism, pyrimidine metabolism, curli biosynthesis, chemotaxis, invasion, the TCA-cycle and lipopolysaccharide biosynthesis amongst others.

In order to identify and prioritize the regulatory mechanisms potentiating the observed differential expression of genes in the pyrimidine starved $\Delta carA$ strain, PheNetic was run in “Upstream mode” to identify the regulatory mechanisms behind the global transcription profile. Some of the most interesting/relevant pathways and their regulatory mechanisms are discussed in the rest of this Chapter. Figure 33 presents a global view of both networks produced with PheNetic.

In the following sections, we will first discuss the effects that pyrimidine starvation has on the highest hierarchical levels of the gene regulatory networks and the processes that are affected, and then we will shed more light on the mechanisms behind the increase in c-di-GMP and biofilm inhibition.

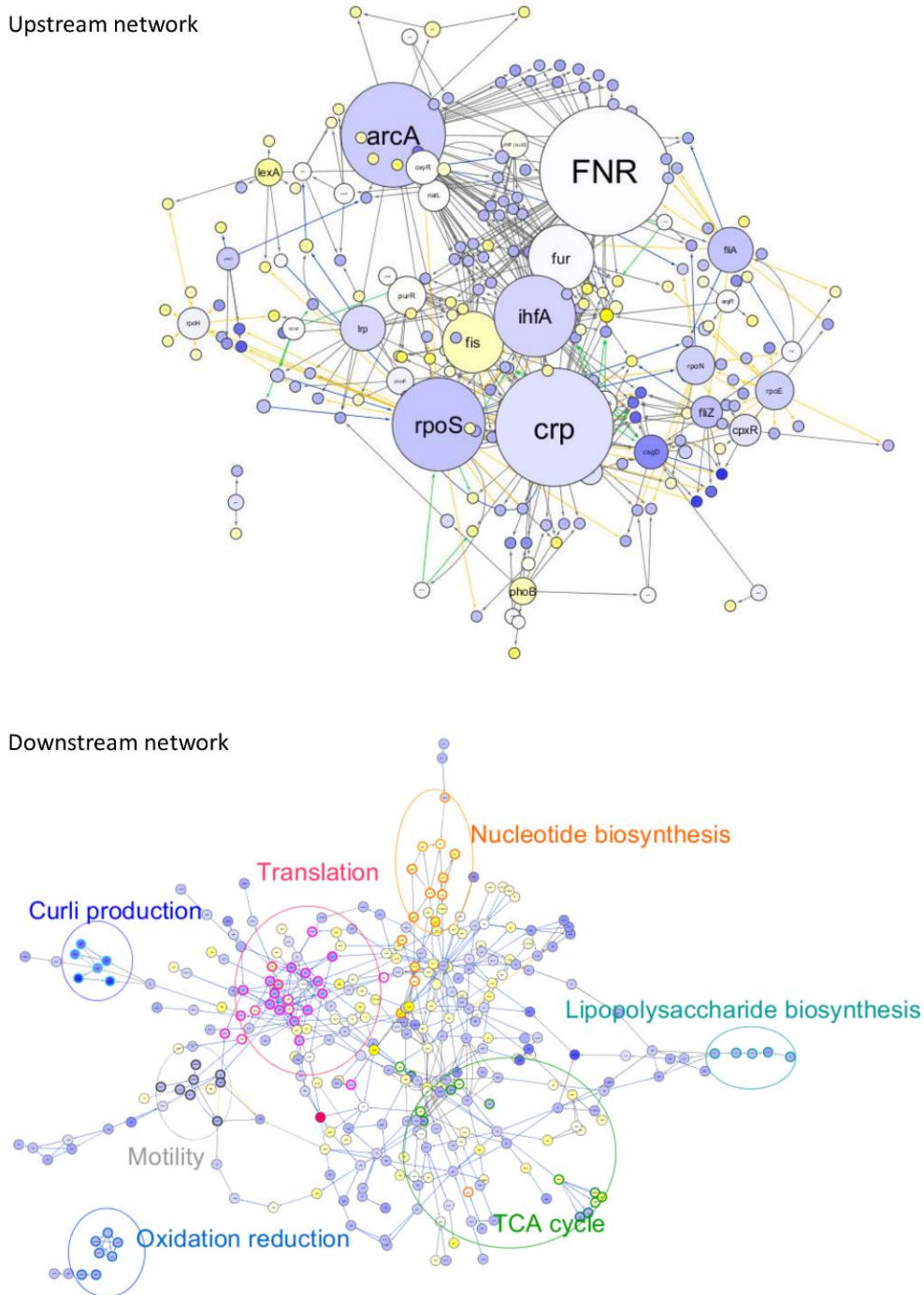


Figure 33 Global overviews of the upstream and downstream networks predicted by Phenetic. Networks were visualized in Cytoscape. The upstream network shows regulator pathways that can explain the observed changes in transcription. The size of a node correlates to the amount of targets connected to that particular node. The downstream network shows pathways that are activated or deactivated because of changes in transcription. Genes that are down-regulated are shown in blue and genes that are upregulated are shown in yellow.

5.3.1 Pyrimidine limitation affects global regulators

The mechanisms that co-ordinate the regulation of gene expression are complex and hierarchic. This co-ordination is critical for sustaining a balanced gene expression profile in response to varying environmental conditions while maintaining cellular homeostasis. Two different, yet complimentary means are used to achieve this balance. On the one hand transcription factors compete with other regulators to redirect the RNAP to transcribe a set of genes. Transcription factors can also prevent the transcription of certain genes. On the other hand, sigma factors compete with other sigma factors for the scarce RNAP core. The fact that total RNAP is a limited resource in the cell, is a pivotal aspect for the successful functioning of this regulatory mechanism through competence. The alternate activation of different sigma factors leads to an efficient reprogramming of global gene expression in response to sudden changes in the environment. The specificity that sigma factors confer to the RNAP for certain promoters allows it to “bypass” the transcriptional regulatory proteins currently active (in response to a previous condition), thereby enabling a specific and efficient response to the new condition. The availability of sigma factors is managed at multiple levels by specific signal transduction pathways that are activated in response to distinct environmental conditions or stresses. Anti-sigma factors bind to sigma factors to inhibit their activity; as such anti-sigma systems provide the cell with a negative feedback system to silence the expression of genes that are not required in a particular biological context (Trevino-Quintanilla *et al.*, 2013). For example, Rsd mediates the transition from exponential growth, where RpoD is the most important sigma factor, to stationary phase where RpoS is the most abundant. Rsd’s main function is to allow for the redistribution of RNAP to RpoS-specific promoters by sequestering RpoD. Thus Rsd plays a vital role in maintaining cellular homeostasis (Jishage; Ishihama, 1998; Mitchell *et al.*, 2007; Campbell *et al.*, 2008).

By running Phenetic in the upstream mode it was possible to extract and visualize a regulatory network that is involved in processes that were differentially regulated between the pyrimidine starved strain and the wild type. The network consists of a large- and a small subnetwork. The large regulatory network consists of 240 nodes. The smaller network has three nodes. From the large network, it was possible to identify a number of regulatory hubs, many of which are known to be involved in matrix production and other biofilm related processes. Other regulators with delineated functions in bacterial metabolism are also visible. At the highest hierarchical layer of the network are the global transcription factors and sigma factors. The most highly connected hubs (with between 52 to 10 target nodes) are *fnr*, *ihfA*, *fis*, *arcA*, *crp*,

Chapter 5: Mechanisms behind biofilm inhibition

lrp, *rpoS*, *fliA*, *rpoN*, *rpoE*, *fur*, *purR*, *csgD* and *oxyR* (Table 7). It should be noted that the primary sigma factor RpoD was not included in the interaction network because its high connectivity would mask other interactions. However, expression of *rpoD* was down-regulated with a log₂ fold change of -1.27.

Table 7. Summary of regulators identified with the network based approach. Regulators identified to be involved in controlling the observed gene expression patterns. The value in the “Out-degree” column is an indication of how many targets a particular node has. The column showing changes in transcription level is colour coded. Blue genes are down-regulated in the mutant, while yellow genes are up-regulated. The intensity of the colour corresponds to the log₂ fold change. *H-NS was not in the regulatory network produced by PheNetic (perhaps because its q value did not meet the cut-off criteria). **RpoD was not included in the interactomic network used as input for PheNetic because it is so highly connected it would mask other interactions. Information on function was obtained from ecocyc.org and uniprot.org

Classification	Process/Role	Gene name	STM identifier	Out-degree	log ₂ fold change
Global transcriptional regulators					
	DNA supercoiling, affects replication, recombination and expression	ihfA	STM1339	31	-0.83
	DNA-binding and bending. Modulates transcription, replication, DNA inversion, phage integration/excision	fis	STM3385	22	1.87
	Respiration mode, anoxic redox control	arcA	STM4598	41	-1.12
	Respiration mode, transition from aerobic to anaerobic metabolism, acid resistance, chemotaxis, cell structure and other processes	fnr	STM1660.S	52	0.73
	Condensing and supercoiling DNA, transcriptional silencer of genes with high AT content	*H-NS	STM1751	*	0.13
	Regulator of Carbon metabolism	crp	STM3466	47	-0.36
	Regulator of amino acid metabolism, nutrient transport and other cellular functions. Induces many genes on entry into stationary phase	lrp	STM0959	15	-0.61
Sigma factors					
	Primary Sigma factor, exponential growth	**rpoD	STM3211	*	-1.27
	General stress response.	rpoS	STM2924	36	-1.45
	Cytoplasmic stress, heat shock	rpoH	STM3568	9	0.36
	Motility and flagellar genes synthesis, implicated in virulence	fliA	STM1956	15	-1.42
	Nitrogen metabolism	rpoN	STM3320	12	-0.90
	Extra cytoplasmic stress, extreme heat shock	rpoE	STM2640	12	-0.93
Other transcriptional regulators					
	Transcriptional dual regulator controls genes involved in iron homeostasis, flagellum chemotaxis, purine metabolism, gluconeogenesis, respiration and other processes.	fur	STM0693	24	0.68
	Controls expression of genes involved in purine biosynthesis.	purR	STM1430	12	0.92
	Transcriptional regulator, biofilm components. May respond to starvation and high cell density	csgD	STM1142	10	-3.74

Chapter 5: Mechanisms behind biofilm inhibition

Classification	Process/Role	Gene name	STM identifier	Out-degree	log ₂ fold change
	Regulates the expression of antioxidant genes in response to oxidative stress.	oxyR	STM4125	10	0.81
	Regulates expression of anaerobic electron transport genes and fermentation-related genes in response to nitrate or nitrite.	narL	STM1767	9	0.75
	Regulates expression of curli and motility. Abundant during post-exponential growth phase.	fliZ	STM1955	9	-1.54
	Controls genes involved in envelope stress response, pilus assembly, secretion, motility, biofilm formation and others.	cpxR	STM4059	9	-0.22
	Activates expression of genes in response to environmental Pi	phoB	STM0397	7	1.92
	Member of the two-component regulatory system phoQ/phoP involved in adaptation to low Mg ²⁺ environments and the control of acid resistance	phoP	STM1231	7	0.31
	Pyrimidine sensor regulates degradation of pyrimidines, glutamate transport, glutamine synthesis, pyrimidine synthesis and degradation of purine and arginine	ompR	STM3502	7	-0.77
	Regulates the expression of the components of a secondary pathway of iron-sulfur cluster assembly, iron-sulfur proteins, anaerobic respiration enzymes, and (<i>E.coli</i>) biofilm formation	yfhP (iscR)	STM2544	7	0.96
	SOS response	lexA	STM4237	7	2.30
	Controls expression of genes of diverse functions such as acid tolerance, curli fimbria formation and anaerobic respiration.	rstA	STM1475	6	-0.39
	Repressor of genes involved in arginine biosynthesis, histidine transport. Activator of genes involved in arginine catabolism.	argR	STM3360	5	0.60
	McbR: MqsR-controlled colanic acid and biofilm regulator.	yncC (mcbR)	STM1588	5	-1.12
	Activates expression of invasion genes	hilA	STM2876	5	2.00
	FlhD and FlhC forms a complex that regulates flagellum biogenesis and swarming migration.	flhD	STM1925	4	0.51
	Transcriptional activator, response to superoxide and nitric oxide	soxS	STM4265	4	0.77
	repressor of the glycine cleavage enzyme system, which is a secondary pathway for production of C1 units	gcvA	STM2982	3	0.81
	Target genes are involved in antibiotic resistance, tolerance to organic solvents and heavy metals.	rob	STM4586	3	0.87
	The principal regulator that controls the transcription of operons involved in the transport of molybdenum and synthesis of molybdoenzymes and molybdate-related functions, among others	modE	STM0779	3	-1.15
	The DcuR/DcuS two-component regulatory system regulates genes involved in C4-dicarboxylate	dcuR	STM4303	2	0.79

Chapter 5: Mechanisms behind biofilm inhibition

Classification	Process/Role	Gene name	STM identifier	Out-degree	log ₂ fold change
	metabolism as well as some genes for lipopolysaccharide biosynthesis, anaerobic nitrate and nitrite respiration.				
	Transcription factor involved in disaccharide melibiose degradation	melR	STM4297	2	0.55
	Transcription factor that controls expression of genes involved in propionate catabolism.	prpR	STM0367	2	0.65
	The BasS/R system regulates expression of genes involved in lipopolysaccharide modification to prevent excessive Fe(III) binding.	basR	STM4292	2	0.35
	Controls expression of genes involved in transport and catabolism of L-lactate.	lldR	STM3693	2	2.05
	Controls transcription of genes involved in arginine transport and DNA replication. Regulates DNA opening at OriC.	iciA (argP)	STM3064	1	0.61
	Pyrimidine sensor regulates degradation of pyrimidines, glutamate transport, glutamine synthesis, pyrimidine synthesis and degradation of purine and arginine	rutR (ycdC)	STM1122	1	-0.81
	Transcriptional repressor and chaperone. Involved in gluco-side utilization	stpA	STM2799	1	2.21
	Transcriptional regulator for the expression of type II secretion system SPII effector proteins.	invF	STM2899	1	1.00
Effect via protein-protein interaction, metabolism and other means					
	Involved in the biosynthesis of iron-sulfur clusters, thio-nucleosides in tRNA, thiamine, biotin, lipoate and pyranopterin (molybdopterin).	nifS	STM2543	2	0.84
	Chaperone protein, interacts with RpoH to control the heat shock response.	dnaK	STM0012	1	-1.39
	Synthetase component of the carbamoyl synthase complex.	carB	STM0067	1	4.87
	ATP-dependent protease that degrades misfolded proteins and regulatory proteins	lon	STM0450	1	-1.03
	Substrate-binding component of maltose ABC transporter.	malE	STM4229	1	1.87
	Citrate synthase	gltA	STM0730	1	1.55
	Cell invasion protein, stimulates actin polymerization and counteracts F-actin destabilizing proteins.	sipA	STM2882	1	2.17
	Bifunctional hydroperoxidase I (HPI) with catalase and peroxidase activity.	katG	STM4106	1	-1.66
	UDP-3-O-acyl-N-acetylglucosamine deacetylase (LpxC) catalyzes the second reaction and the first committed step in lipid A biosynthesis.	lpxC	STM0134	1	0.62
	DNA-damage inducible gene of SOS regulon.	yebG	STM1882	1	1.62
	AdhE is a homopolymeric protein with three Fe ²⁺ -dependent catalytic functions: alcohol dehydrogenase, coenzyme A-dependent acetaldehyde dehydrogenase, and pyruvate formate-	adhE	STM1749	1	-1.45

Classification	Process/Role	Gene name	STM identifier	Out-degree	log ₂ fold change
	lyase deactivase (the latter is called into question due to lack of reproducibility).				
	AHL receptor*	srgC	PSLT008	1	-0.57
small regulatory RNAs					
	Regulates protein composition of outermembrane by effect on <i>ompT</i> , <i>cirA</i> , <i>fecA</i> , <i>fepA</i> , <i>ompR</i> , <i>csgD</i> and <i>flhD</i> mRNAs	omrA		6	
	Regulates outermembrane composition by negative effect on levels of <i>ompT</i> , <i>cirA</i> , <i>fecA</i> , <i>gntP</i> , <i>ompR</i> , <i>csgD</i> and <i>flhD</i>	omrB		6	
	Postranscriptional control of <i>csgD</i> and genes involved in amino acid biosynthesis	gcvB		5	
	Mediates positive Fur-regulon response	rhyB		2	
	Effect on transcription and translation. Overcomes transcription silencing by H-NS. Promotes translation of RpoS.	drsA		2	
	Targets include <i>ompA</i> , <i>phoPQ</i> , <i>ompX</i> and other mRNA's	micA		2	

Some of the anti-sigma factors and adaptor proteins that regulate sigma factor activity were also differentially expressed (Table 8). The role of anti-sigma factors in regulating biofilm formation and swarming motility has been studied in *Pseudomonas*. It is possible that the interplay between sigma factors and anti-sigma factors can also contribute to the impaired ability of the pyrimidine starved *carA* strain to switch to a biofilm mode of life, by affecting the expression of genes that are part of the RpoS regulon. However this possibility was not explored further in this thesis. Portions from the upstream network showing the various sigma factors and the netto effect on expression of their direct targets are in the supplemental section (Supp. Figure 7, Supp. Figure 8, Supp. Figure 9, Supp. Figure 10 and Supp. Figure 11)

Two of the most highly connected regulatory hubs are the global regulators **FNR (STM1660.S)** with 52 targets and **ArcA** with 41 targets (Figure 34). These two global transcription factors regulate the adaptation to changes in O₂ availability. FNR is a fast-reacting direct O₂ sensor, whereas the ArcBA two-component system senses O₂ indirectly by monitoring the redox state of the quinone pool and is slow reacting. (Khoroshilova *et al.*, 1997; Georgellis *et al.*, 2001; Partridge *et al.*, 2007). FNR and ArcBA cooperate to regulate some operons such as *cydAB* (encoding cytochrome bd) and *focA-pflB* (encoding pyruvate formate-lyase)(Sawers, 1993; Govantes *et al.*, 2000). The expression of *arcA* is regulated by FNR (Compan; Touati, 1994).

The ability of FNR to sense and respond to cellular O₂ levels depends on its [4Fe-4S](2+) cluster. In the presence of O₂, the [4Fe-4S](2+) cluster is converted to a [2Fe-2S](2+) cluster, which inactivates FNR as a transcriptional regulator (Khoroshilova *et al.*, 1997). Thus, when O₂ is limited enzymes involved in aerobic respiration are repressed and the synthesis of enzymes required for anaerobic respiration is increased (Salmon *et al.*, 2003; Kang *et al.*, 2004). FNR also regulates the transcription of many genes with other functions, such as acid resistance, chemotaxis, cell structure, and molecular biosynthesis, among others (Salmon *et al.*, 2003; Kang *et al.*, 2004).

In the case of the pyrimidine starved mutant, 41 of FNR's targets (visualized on our upstream network) are down-regulated significantly while 10 are upregulated. FNR itself was only modestly upregulated (log₂ fold change 0.73). The transcription patterns of some of the genes that are directly regulated by FNR, suggest that the response to oxygen limitation (which one would expect in our petri-dish setup, and according to Van Puyvelde might be a trigger for the switch between phenotypes) is not induced. For example, *yfiD* should be highly induced under anaerobic conditions (Scott *et al.*, 2003). Incidentally, *yfiD* is known to be upregulated in biofilms. However, in the *carA* mutant *yfiD* is down regulated (log₂ fold change -2.95). A very interesting observation is that *arcA* is downregulated as well. As can be expected, the genes under the control of ArcA are down-regulated too. The above observations indicate that the switch from aerobic metabolism to micro-aerobic/anaerobic metabolism is not taking place. A possible explanation is that O₂ is not limiting in the growth medium of the $\Delta carA$ strain, which is unlikely however since the mutant did not have a growth defect under the tested conditions that would have accounted for lower oxygen consumption. A second possibility is that the wild type cells have a pre-emptive response in anticipation of oxygen limitation that would occur in a biofilm, and that this pre-emptive response is not taking place in the mutant. A third possibility is that iron-sulphur cluster biogenesis or transport is affected, which would have an effect on FNS activity. This possibility will be elaborated on in later paragraphs when the ***suf* system** is discussed.

The nucleoid associated protein **FIS** (factor for inversion stimulation) is also a highly connected hub with 24 connections in our upstream network(Figure 35). The *fis* gene shows an upregulation of transcription in the *carA* mutant (log₂ fold change 1.87). Our subnetwork extraction of genes that are directly controlled by FIS showed that out of 10 genes that are known to be activated by FIS, 3 were upregulated. Out of 11 genes that are known to be repressed by FIS, 7 were down-regulated. The above results indicate that pyridine starvation

affects transcription regulatory networks on the highest hierarchical levels. Some of the downstream processes that are affected will be discussed in the following sections. In particular, we seek to explain the increase in c-di-GMP and the inhibition of biofilm production.

Table 8. Sigma factors and the anti-sigma factors and adaptor proteins that control their activity. The expression patterns of the anti-sigma factors resemble those of the sigma factors, because anti-sigma factors are regulated by their own sigma factors, creating a negative feedback circuit. A notable exception is *rsd* whose transcription is regulated by both RpoD and RpoS. RpoN does not have a cognate anti-sigma factor; instead, activity depends on ATP-dependent bacterial enhancer binding proteins.

Sigma factor	log ₂ fold change	anti-sigma factor/ adaptor protein	log ₂ fold change
<i>rpoD</i>	-1.27	<i>rsd</i>	-1.06
		<i>hscC</i>	0.13
<i>rpoS</i>	-1.45	<i>rssB (hnr)</i>	-0.56
<i>rpoE</i>	-0.93	<i>rseB</i>	-0.81
		<i>rseA</i>	-1.45
<i>rpoN</i>	-0.90		
<i>rpoH</i>	0.35	<i>dnaK</i>	-1.40
<i>fliA</i>	-1.42	<i>flgM</i>	-1.45

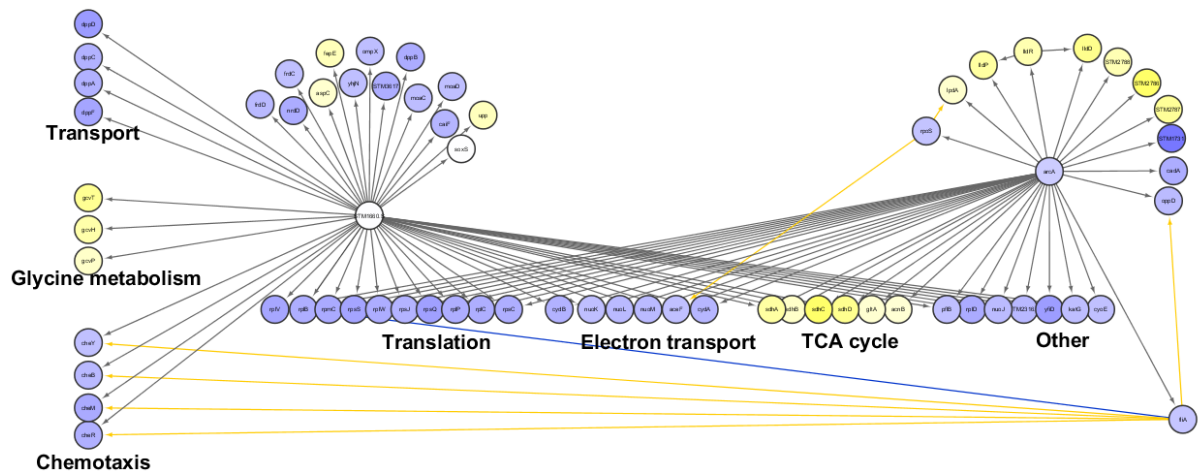


Figure 34 Sub-network extraction from our upstream-regulatory network, showing genes regulated by FNR(STM1660) and ArcA. Most of the genes are down-regulated. The TCA cycle genes are up-regulated. Genes that are down-regulated are shown in blue and genes that are upregulated are shown in yellow.

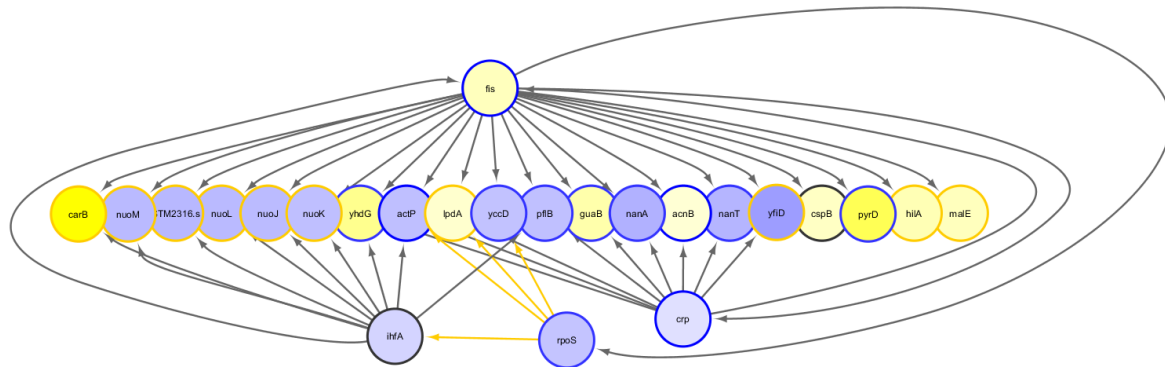


Figure 35 Subnetwork extraction of genes regulated by FIS. The colour of nodes indicate whether the genes are up or down regulated under our experimental conditions (yellow and blue respectively). The colour of the circles surrounding the nodes indicate whether the genes are activated or repressed by Fis, according to RegulonDB and other sources. Genes that are down-regulated are shown in blue and genes that are upregulated are shown in yellow.

5.3.2 Pyrimidine starvation leads to an increase in c-di-GMP by influencing gene expression levels in key pathways

In the next paragraphs, we aim to unravel the cause for increased c-di-GMP levels during pyrimidine starvation. We will explore two possibilities: (i) That the increase in c-di-GMP might be caused by imbalances in the nucleotide pools which leads to an increase in GTP, the substrate for c-di-GMP synthesis. (ii) That the increase in c-di-GMP may be driven by a combination of increased levels of DGCs and decreased levels of PDEs.

5.3.2.1 The effect of pyrimidine starvation on the nucleotide biosynthesis pathways

The transcriptomics results indicate that the pyrimidine starved $\Delta carA$ mutant exhibits changes in the regulation of genes involved in nucleotide metabolism (Table 9). CytoKegg was used to import the metabolic pathways into Cytoscape; expression data were mapped onto the nodes. Genes involved in *de novo* pyrimidine metabolism, pyrimidine salvage and pyrimidine uptake are highly up-regulated. Genes for *de novo* purine biosynthesis, salvage and interconversion are also up-regulated. Genes involved in deoxyribonucleotide metabolism are down-regulated. The *pur* genes are all under control of the repressor PurR, however the pyrimidine genes are not regulated by a single repressor and have regulatory mechanisms that differ between the genes, as discussed in Chapter 1.

The up-regulation of the *de novo* **pyrimidine biosynthesis** genes can be interpreted as a futile attempt to make more UMP (Figure 36). However, since the first enzymatic step of this pathway that starts with the conversion of glutamine is not functioning, not enough UMP can be made via this pathway. The expression results also seem to indicate that a pathway to convert cytidine to CMP (via the enzyme encoded by *udk*) is upregulated, perhaps in an attempt to maintain CXP nucleotide levels. The same enzyme will also enable the conversion of uridine to UMP. The downregulation of *cdd* could lower conversion of cytidine to uridine and so also contribute to the maintenance of CXP nucleotide levels. The expression of *cdd* is induced by cytidine and inhibited by CytR (Pedersen *et al.*, 1991; Gerlach *et al.*, 1991). The expression of *udk* is activated by RbsR and D-Ribose (Shimada *et al.*, 2013). To clarify the effect that fluctuations in nucleotide pools have on the regulation of pyrimidine pathway genes, further studies are needed.

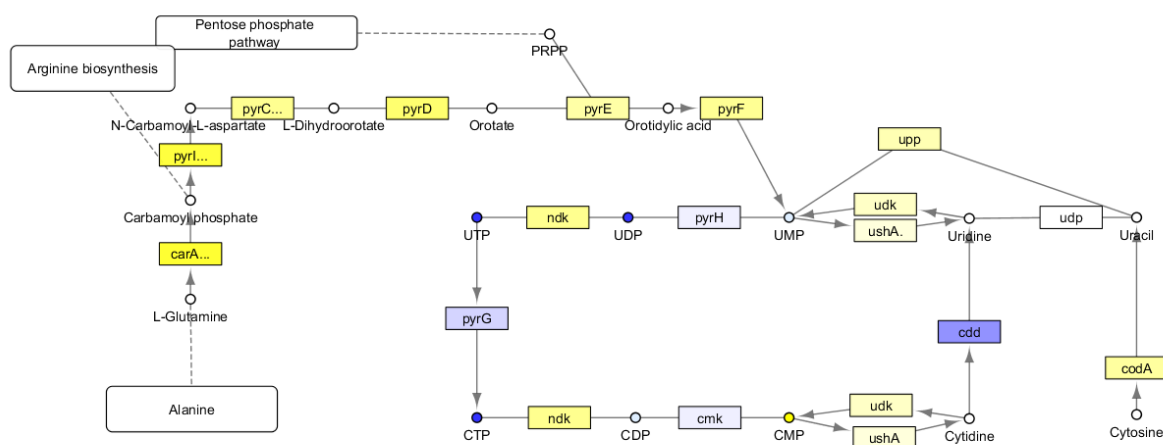


Figure 36 Pyrimidine biosynthesis pathway indicating changes in gene regulation. Gene names are written in rectangles, yellow indicates up regulation and blue indicates down regulation. Metabolites are indicated in circles. The levels of the nucleotides were measured by LC-MS/MS (see previous chapter). Dark blue means a compound has a significant decrease in levels in the *carA* mutant, yellow means levels are significantly increased. Light blue means that there is a slight, but non-significant decrease.

The **purine *de novo* synthesis** genes are up-regulated, while the salvage genes are down-regulated. The genes encoding purine salvage enzymes are down-regulated, which can be interpreted as an indication that there is an ample supply of purines produced by the *de novo* pathway. Another gene that shows increased expression is *prsA* (encodes the 5-Phosphoribosyl-1- α -diphosphate synthase, \log_2 fold change of 1.15), which plays an important role in nucleotide biosynthesis by supplying 5-Phosphoribosyl-1- α -diphosphate (PRPP). We

Chapter 5: Mechanisms behind biofilm inhibition

were able to verify the expression results for some nucleotide biosynthesis genes by using our own *in-house* collection of promoter-GFP fusions (Supp. Figure 12 and Figure 39).

Table 9. Gene expression results of enzymes of purine and pyrimidine metabolism. Genes with significant changes in their regulation are underlined and shown in bold.

Pathway	Gene	Locus in LT2	Product	q-val	log ₂ FC
<i>De novo</i> synthesis of IMP	<i>purF</i>	STM2362	amidophosphoribosyltransferase	1	0.27
	<i>purD</i>	STM4175	phosphoribosylamine--glycine ligase	0.00	1.09
	<i>purN</i>	STM2500	phosphoribosylglycinamide formyltransferase	0.00	1.02
	<i>purT</i>	STM1883	phosphoribosylglycinamide formyltransferase 2	0.00	1.00
	<i>purG</i>	STM2565	phosphoribosylformylglycinamide synthase	0.000	2.02
	<i>purM</i>	STM2499.S	phosphoribosylformylglycinamide cyclo-ligase	0.00	1.48
	<i>purK</i>	STM0533	N5-carboxyaminoimidazole ribonucleotide synthase	0.002	0.95
	<i>purE</i>	STM0534	N5-carboxyaminoimidazole ribonucleotide mutase	0.001	1.01
	<i>purC</i>	STM2487	phosphoribosylaminoimidazole-succinocarboxamide synthase	0.066	0.69
	<i>purB</i>	STM1232	adenylosuccinate lyase	0.000	0.99
<i>purH</i>	STM4176	bifunctional phosphoribosylaminoimidazolecarboxamide formyltransferase/IMP cyclohydrolase	0.00	1.77	
Biosynthesis of AMP	<i>purA</i>	STM4366	adenylosuccinate synthetase	0.000	1.46
	<i>purB</i>	STM1232	adenylosuccinate lyase	0.000	0.99
	<i>adk</i>	STM0488	adenylate kinase	0.000	1.14
Biosynthesis of GMP	<i>guaB</i>	STM2511	inosine 5'-monophosphate dehydrogenase	0.00	2.16
	<i>guaA</i>	STM2510	GMP synthase	0.05	0.12
	<i>gmk</i>	STM3740	guanylate kinase	0.000	0.90
Purine interconversion/salvage	<i>guaC</i>	STM0141	GMP reductase	0.000	1.98
	<i>gsk</i>	STM0491	inosine-guanosine kinase	0.000	1.69
	<i>deoD</i>	STM4570	purine nucleoside phosphorylase	0.000	-0.92
	<i>rihC</i>	STM0051	ribonucleoside hydrolase RihC	1.000	0.52
	<i>hpt</i>	STM0170	hypoxanthine phosphoribosyltransferase	0.269	0.73
	<i>gpt</i>	STM0317	xanthine phosphoribosyltransferase	0.004	0.83
	<i>add</i>	STM1463	adenosine deaminase	0.646	0.34
	<i>apt</i>	STM0483	adenine phosphoribosyltransferase	0.000	-1.16
	<i>amn</i>	STM2009	AMP nucleosidase	0.000	-0.31
	<i>mtn</i>	STM0207	5'-methylthioadenosine/S-adenosylhomocysteine nucleosidase	0.000	1.21
<i>(pfs)</i>					
<i>hisG</i>	STM2071	ATP phosphoribosyltransferase	1.000	-0.18	
Purine repressor	<i>purR</i>	STM1430	HTH-type transcriptional repressor PurR	0.000	0.92
<i>De novo</i> pyrimidine biosynthesis	<i>carB</i>	STM0067	carbamoyl phosphate synthase large subunit	0.000	4.87
	<i>pyrI</i>	STM4459	aspartate carbamoyltransferase regulatory subunit	0.000	4.74
	<i>pyrB</i>	STM4460	aspartate carbamoyltransferase catalytic subunit	0.000	4.83
	<i>pyrL</i>	STM4461	pyrBI operon leader peptide	0.000	4.20
	<i>pyrC</i>	STM1163	Dihydroorotase	0.000	2.71
	<i>pyrD</i>	STM1058	dihydroorotate dehydrogenase 2	0.000	3.52
	<i>pyrE</i>	STM3733	orotate phosphoribosyltransferase	0.000	2.18
	<i>pyrF</i>	STM1707	orotidine 5'-phosphate decarboxylase	0.000	2.64
	<i>pyrH</i>	STM0218	uridylylase	0.000	-0.18
	Pyrimidine salvage	<i>ndk</i>	STM2526	nucleoside diphosphate kinase	0.000
<i>pyrG</i>		STM2953	CTP synthetase	0.011	-0.53
<i>upp</i>		STM2498	uracil phosphoribosyltransferase	0.00	1.87
<i>udk</i>		STM2122	uridine kinase	0.000	1.42
<i>cmk</i>		STM0980	cytidylate kinase	0.046	-0.20

Chapter 5: Mechanisms behind biofilm inhibition

Pathway	Gene	Locus in LT2	Product	q-val	log ₂ FC
Deaminases	<i>cdd</i>	STM2183	cytidine deaminase	0.000	-1.34
	<i>codA</i>	STM3334	cytosine deaminase	0.000	2.36
Enzymes splitting glycosyl bond of nucleotides	<i>udp</i>	STM3968	uridine phosphorylase	0.234	0.01
	<i>rihA</i>	STM0661	pyrimidine-specific ribonucleoside hydrolase RihA	1.000	0.33
	<i>rihC</i>	STM0051	ribonucleoside hydrolase RihC	1.000	0.52
Pyrimidine regulator	<i>rutR</i> (<i>ycdC</i>)	STM1122	transcriptional repressor	0.000	-0.81
Genes and enzymes of deoxyribonucleotide metabolism	<i>nrdA</i>	STM2277	ribonucleotide-diphosphate reductase subunit alpha	0.000	-1.15
	<i>nrdB</i>	STM2278	ribonucleotide-diphosphate reductase subunit beta	0.000	-1.30
	<i>nrdH</i>	STM2805	glutaredoxin-like protein	1.000	-2.17
	<i>nrdI</i>	STM2806	ribonucleotide reductase stimulatory protein	1.000	-2.00
	<i>nrdE</i>	STM2807	ribonucleotide-diphosphate reductase subunit alpha	1.000	-0.94
	<i>nrdF</i>	STM2808	ribonucleotide-diphosphate reductase subunit beta	1.000	0.70
	<i>nrdG</i>	STM4451	anaerobic ribonucleotide-triphosphate reductase-activating protein	1.000	-0.53
	<i>nrdD</i>	STM4452	anaerobic ribonucleoside-triphosphate reductase	0.000	-2.37
	<i>nrdR</i>	STM0415	transcriptional repressor NrdR	0.032	0.85
	<i>dut</i>	STM3731	deoxyuridine 5'-triphosphate nucleotidohydrolase	1.000	0.60
	<i>dcd</i>	STM2121	deoxycytidine triphosphate deaminase	1.000	0.50
	<i>thyA</i>	STM3001	thymidylate synthase	0.000	-0.25
	<i>tdk</i>	STM1750	thymidine kinase	1.000	0.49
	<i>tmk</i>	STM1200	thymidylate kinase	0.000	-0.62
	<i>deoA</i>	STM4568	thymidine phosphorylase	0.000	-0.65
	<i>ybjR</i>	STM0931	aminidase	0.021	0.03
<i>yjjG</i>	STM4559.S	nucleotidase	0.000	1.26	
“SILENT GENES”	<i>ushA</i>	STM0494	silent protein UshA	0.002	0.85
Pyrimidine base transporters	<i>codB</i>	STM3333	cytosine permease	0.000	3.35
	<i>uraA</i>	STM2497	uracil transporter	0.03	0.86
	<i>dctA</i>	STM3614	C4-dicarboxylate transporter	0.012	0.69
Purine base transporters	<i>purP</i> (<i>yieG</i>)	STM3851.S	xanthine/uracil permease	0.000	1.72
	<i>yicE</i>	STM3747	NCS2 family purine/xanthine transport protein	1.000	-1.05
Nucleoside transporters	<i>nupC</i>	STM2409	NUP family nucleoside transport protein	0.003	-0.60
	<i>nupG</i>	STM3113	nucleoside transport	1.000	0.42
	<i>yegT</i>	STM2142	MFS family transport protein	1.000	-0.51
	<i>xapB</i>	STM2421	MFS superfamily xanthosine permease	1.000	0.00
	<i>nepI</i>	STM3776	purine ribonucleoside efflux pump NepI	1.000	1.14
Outer membrane protein, porin	<i>tsx</i>	STM0413	nucleoside-specific channel-forming protein	0.000	1.47
Proteins regulating Nucleoside transport and catabolism	<i>deoR</i>	STM0864	DeoR family transcriptional repressor	0.322	0.66
	<i>cytR</i>	STM4094	GalR/LacI family transcriptional repressor	1.000	0.42
	<i>crp</i>	STM3466	cAMP-activated global transcriptional regulator	0.029	-0.36
	<i>xapR</i>	STM2420	DNA-binding transcriptional activator XapR	1.000	-0.26

The transcriptome results clearly suggest that the nucleotide levels in the *carA* mutant are perturbed. Thus we determined the intracellular pyrimidine nucleotide levels of planktonic $\Delta carA$ cells grown in petri-dishes under the conditions of impaired biofilm formation by performing LC-MS/MS. Metabolites were extracted from planktonic cells at the time point where early biofilm formation of the wild type is initiated (~10 hours after inoculation). It was found that the pyrimidine nucleotide pools (CDP, CTP, UMP, UDP and UTP) in the $\Delta carA$ mutant were reduced to less than three quarters of the wild type control levels (Figure 37 and Supp. Table 6), suggesting a possible role in the biofilm inhibition. CMP levels were found to be increased, which is consistent with the observation that *udk* transcription is upregulated. This could possibly be explained by the fact that CMP is not an intermediate in the *de novo* production of CTP and can be formed by metabolizing lipopolysaccharides and phospholipids, as well as RNA turnover (Jensen *et al.*, 2008). However, this suggestion needs to be verified.

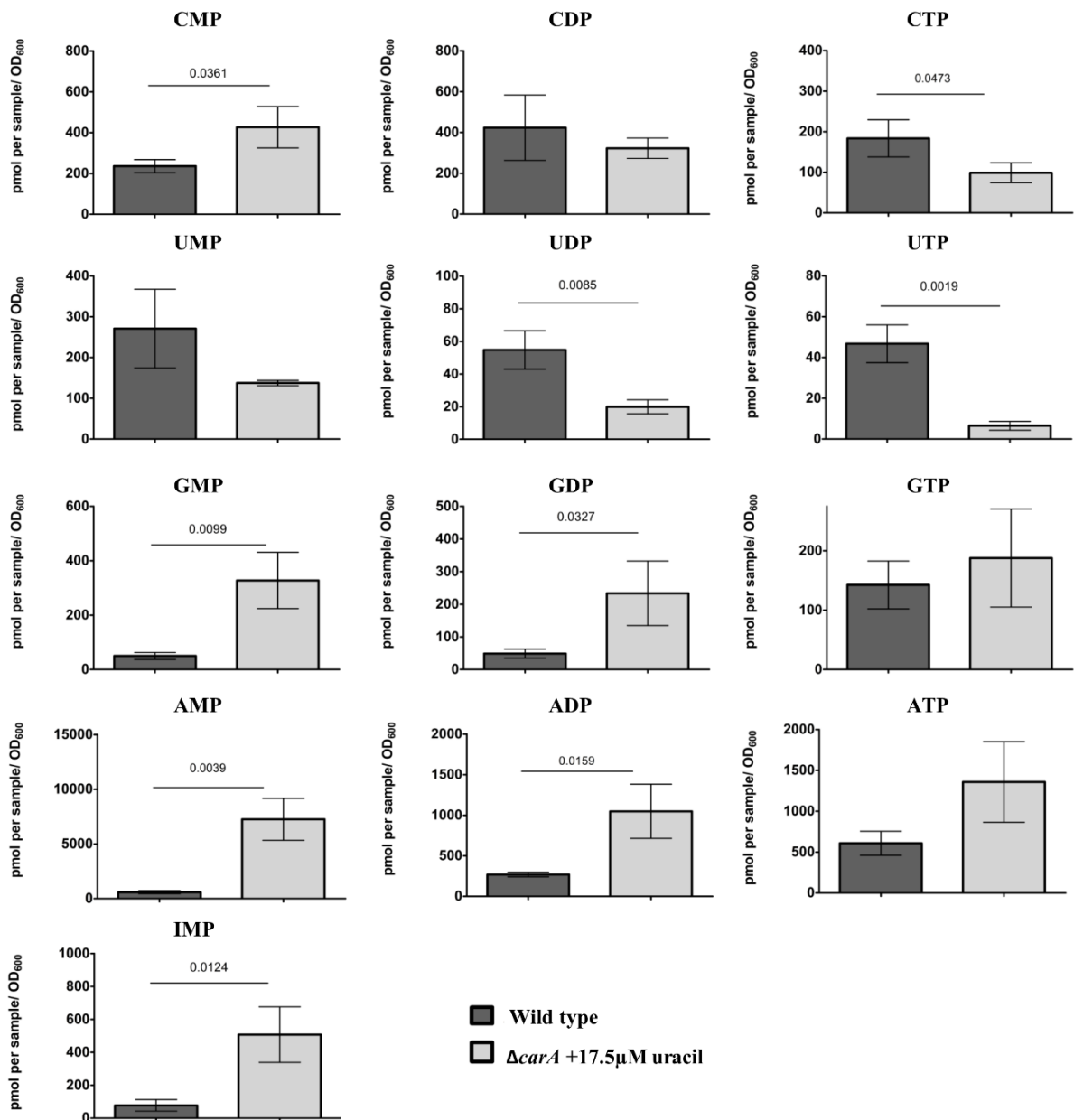


Figure 37 Intracellular levels of pyrimidine and purine nucleotides of *S. Typhimurium* 14028 wild type (dark grey bars) and the pyrimidine starved $\Delta carA$ mutant (light grey bars). The p-values of statistically significant differences (using an unpaired t-test with a 95% confidence interval) are indicated on the relevant graphs. Bars represent the means of three independent experiments and the error bars represent the standard deviations.

In the case of the purines all nucleotide levels were markedly increased (Figure 37). More specifically, IMP, AMP, ADP, GMP and GDP showed a significant increase in concentration in $\Delta carA$ compared to the wild type strain. ATP and GTP levels were also enhanced in the $\Delta carA$ strain, but not in a statistically significant manner. Similar findings were published in 1991 by Vogel and colleagues (Vogel *et al.*, 1991), who observed increased ATP and GTP levels in the pyrimidine requiring *E. coli* B AS19 *leu pyrB5 rel⁺* strain, under conditions of

partial pyrimidine starvation, which were induced by slow growth on orotate. This increase in purine nucleotides could thus be responsible for driving the increased production of c-di-GMP. Of note is that it was previously shown that the triphosphates, rather than the di- or monophosphates, are the primary nucleotides in *Salmonella* cells (Bochner; Ames, 1982). Although we reported the same here for the wild type strain, the pyrimidine starved Δ *carA* mutant exhibits a deviation in which [AMP]>[ATP]>[ADP] and [GMP]>[GDP]>[GTP]. The possibility that the higher concentrations of AMP and GMP might be caused by a shortage of P_i in the medium is worthy of further investigation.

Based on our observations we propose a hypothesis for the up-regulation of the *pur* genes (and the subsequent increase in purine nucleotides). It is already well established that expression of the *pur* genes (including *purR* itself) is negatively regulated by the transcriptional repressor PurR in combination with the co-repressor guanine. However, since the concentrations of guanine and hypoxanthine were found to be increased in the pyrimidine starved mutant (Supp. Table 6), reduced activation of PurR is unlikely. Also reduced transcription of *purR* is certainly not the cause since our transcriptome results do not indicate a down-regulation of *purR* (in fact there is a modest up-regulation with \log_2 fold change of 0.92 and a q-value smaller than 0.05). Other genes that would normally be repressed by PurR are also upregulated (Figure 38). For example, the gene *cvpA* (encoding an enzyme for colicin production) is up regulated (\log_2 fold change 1.56). The fact that these genes are also up regulated indicates that that an unidentified factor may prevent PurR and its co-repressors from binding to the upstream DNA and inhibiting *pur* gene transcription. This possibility that an unknown factor interferes with regulation by PurR was not pursued as part of this thesis due to time-constraints; however we are of the opinion that this is a very exciting topic for further research.

In addition to the upregulation of the *pur* genes, the observed increase in purine nucleotides could be explained by elevated levels of PRPP which could drive purine nucleotide production. The first enzymatic step in purine biosynthesis (catalysed by Glutamine PRPP amidotransferase/ PurF) is subject to synergistic inhibition by AMP and GMP and feed forward regulation by PRPP (Jensen *et al.*, 2008). PRPP and AMP compete for the same binding site and both exhibit positive cooperativity with GMP (Messenger; Zalkin, 1979; Muchmore *et al.*, 1998). Thus when PRPP concentrations are high, inhibition by AMP can be overridden. Furthermore, increased levels of PRPP synthase (encoded by *prsA*) have been observed in a pyrimidine requiring mutant. Although the exact mechanism remains unsolved, it seems to involve a uridine nucleotide other than UMP (White *et al.*, 1971; Olszowy; Switzer,

1972; Jensen *et al.*, 2008). Pyrimidine mediated *prsA* gene regulation occurs by an increase of transcription from the P2 promotor (Post *et al.*, 1993). Based on the available information we postulated that an increase in PRPP production, induced by a low uridine nucleotide pool in the pyrimidine starved $\Delta carA$ mutant (*vide supra*), could be responsible for driving purine biosynthesis, leading to an unchecked inflation of the purine nucleotide pools. This hypothesis is supported by our observation that the transcription of a *prsA* P2 promoter GFP fusion is increased in the pyrimidine starved $\Delta carA$ mutant as compared to the wild type, and that complementation with 70 μ M uracil restores the mutant's expression levels to the wild type norm (Figure 39). The RNAseq results also show an increase of *prsA* transcription (\log_2 fold change of 1.16, q-value < 0.05). Due to the resolution of RNAseq it is not possible to see if transcripts originate from the P1 or P2 promotor. Interestingly, the *prsA* P2 promoter is regulated by PurR (Choi; Zalkin, 1992). Thus if the *prsA* induction under pyrimidine starvation is caused by a reduced activity of PurR, the same mechanism would likely also affect *pur* gene transcription because they are also regulated by PurR, providing a potential link between the observed induction of all the genes involved. Given the above results we were curious to see whether exogenously applied purine pathway intermediates might have an inhibitory effect on biofilm formation, however this was not the case (Supp. Figure 13).

To summarize, our RNAseq results indicate that pyrimidine starvation causes an increase in purine nucleotides, including GTP, which is a substrate for c-di-GMP production. In the next section we will focus on the role of c-di-GMP metabolizing proteins and their gene expression levels.

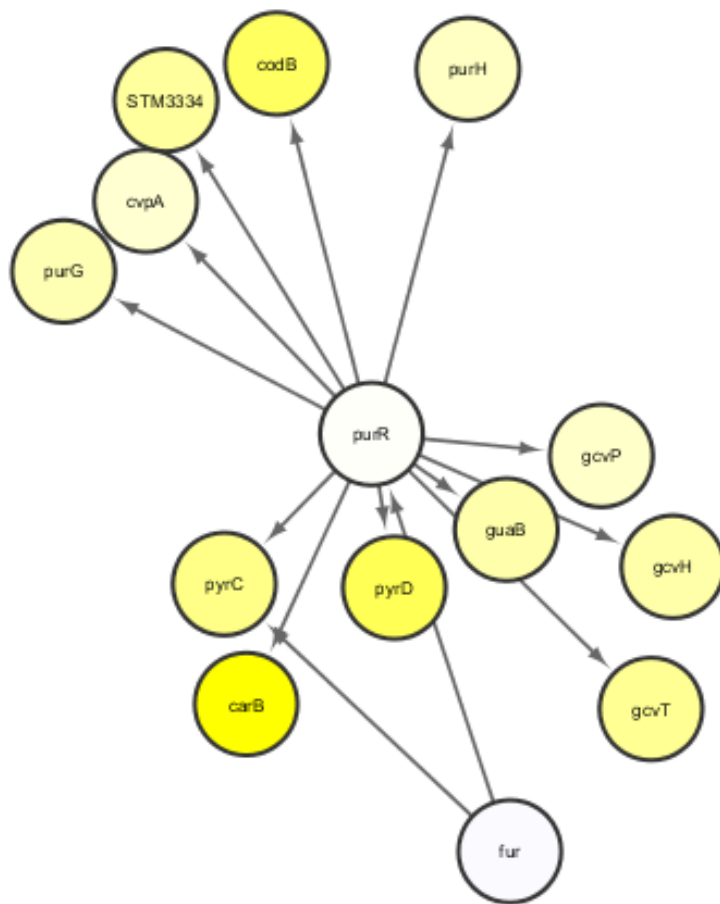


Figure 38 Genes regulated by PurR are all up-regulated

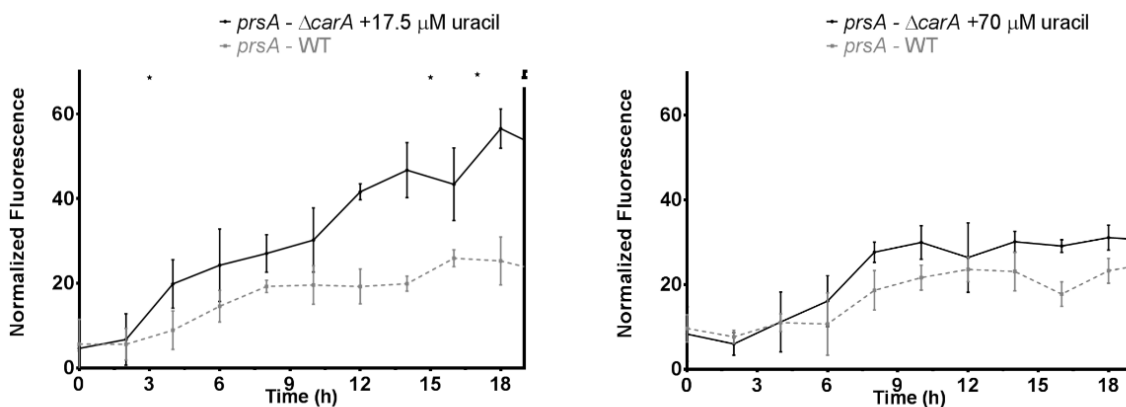


Figure 39 Normalized fluorescence of the *prsA* promoter in the *S. Typhimurium* 14028 wild type (grey lines) and the Δ *carA* mutant (black lines). Under conditions of pyrimidine starvation there is an increase in *prsA* promoter activity in the Δ *carA* mutant (left). When the concentration of extracellular uracil is increased to 70 μ M (right) *prsA* promoter activity in the Δ *carA* mutant returns to wild type levels. Stars indicate a significant difference in the slope of the two conditions between two time points (as determined by an unpaired t-test with a confidence interval of 95%) indicating that there is a significant difference in transcription from the promoters. The error bars represent the standard deviations between 3 technical repeats (corresponding to three wells in a multi-well plate). The experiment was repeated for a second time on a different day and similar profiles were obtained.

5.3.2.2 Transcription of genes encoding c-di-GMP metabolizing enzymes

When considering the individual differential expression patterns of 21 c-di-GMP metabolizing enzymes, only 3 had notable changes in their expression (Supp. Table 6) based on the RNA sequencing results. The DGC *adrA* was downregulated, while the DGC STM1987 (*gcpA*) and the PDE STM1697 were up-regulated in the *carA* mutant. qRT-PCR results did not indicate noteworthy changes in regulation in any of the DGC or PDE encoding genes that we analysed (Supp. Table 7). These results are clearly not conducive to explaining the observed increase in the global intracellular c-di-GMP pool.

Studies on the contribution of individual PDEs or DGCs on the global c-di-GMP pool in *Salmonella* are lacking. Indeed, very often c-di-GMP levels are not even measured, but changes to the global c-di-GMP pool are assumed based on phenotypic changes.

We can only assume that the increase in c-di-GMP is not driven by changes in the number of DGC or PDE proteins in the cell, but rather by a change in their activity. The high levels of the substrate GTP available in the *carA* mutant, may drive the production of c-di-GMP by DGCs, or perhaps inhibit c-di-GMP breakdown by PDEs. The inhibition of biofilm formation despite high levels of c-di-GMP is an indication that other regulatory mechanisms have a higher priority in determining this particular phenotypic outcome.

In the next section, we seek to clarify how biofilm inhibition is achieved, despite high levels of c-di-GMP.

5.3.3 Pyrimidine starvation impacts the transcription of key biofilm determinant *csgD*

In the following paragraphs we explore the mechanisms by which pyrimidine starvation impairs biofilm formation. To this end we consult the upstream and downstream networks produced by PheNetic to find the biofilm related pathways that are affected and identify the regulator mechanisms behind the effects. RNAseq results were verified with GFP-promoter fusions, and in some cases RT-qPCR. Knockout and complementation mutants were also used to further confirm that specific genes are involved.

5.3.3.1 Transcription of *csgD* and downstream pathways are affected

The transcriptome analysis indicated that genes involved in curli-production were strongly down-regulated in the *carA* mutant (\log_2 fold changes ranging between -7.0 to -3.7). Genes further downstream in the biofilm regulatory pathway, that are regulated by CsgD were also affected. These genes include the *csgBAC* and *csgDEF* operons (involved in curli production),

adrA (c-di-GMP synthesis for activation cellulose production by BcsA), *wraB* (oxidation-reduction process) and *yccJ* (unknown function). The cellulose producing gene *bcsA* itself, which is not part of the CsgD transcription regulon, was not differentially regulated. Given that the expression of *adrA* and *csgBAC* is under direct control of CsgD (Ogasawara *et al.*, 2011), their down-regulation can likely be attributed to reduced transcription of *csgD*. The *bcsABZC* operon, on the other hand, is constitutively transcribed and does not require CsgD (Gualdi *et al.*, 2008) or AdrA for transcription. BcsA-BcsB is however post-translationally activated by c-di-GMP produced by AdrA (Simm *et al.*, 2004; García *et al.*, 2004).

Based on “the “upstream” network produced by PheNetic (Figure 40) we see that various regulators are implicated in changes in *csgD* transcription. These regulators include *fliZ*, *crp*, *rpoS*, *cpxR*, *ompR*, *ihfA*, *fis*, *hilA* OMRA, OMRB. Based on their log₂fold values it is clear that the majority of regulators involved in regulating the expression patterns of *csgD* are not significantly differentially transcribed themselves. However, the gene encoding positive regulator RpoS is down regulated with a log₂ fold value of -1.5. The *fis* gene, encoding a global regulator that represses *rpoS* transcription, is upregulated (log₂ fold change = 1.87). Thus they may provide a possible mechanism explaining the down regulation of *csgD* proceeding via *fis* and *rpoS* (including effect on *rsd* that impacts interplay between RpoD and RpoS). Nevertheless, it should be kept in mind that transcriptional activators and repressors of *csgD* function in parallel to control its induction. Small non-significant effects on the transcription levels of the regulators coupled with post-transcriptional and post-translational effects can induce highly amplified effects downstream in their cascade, as is visible in the expression levels of *csgD*, the other curli genes and *adrA*.

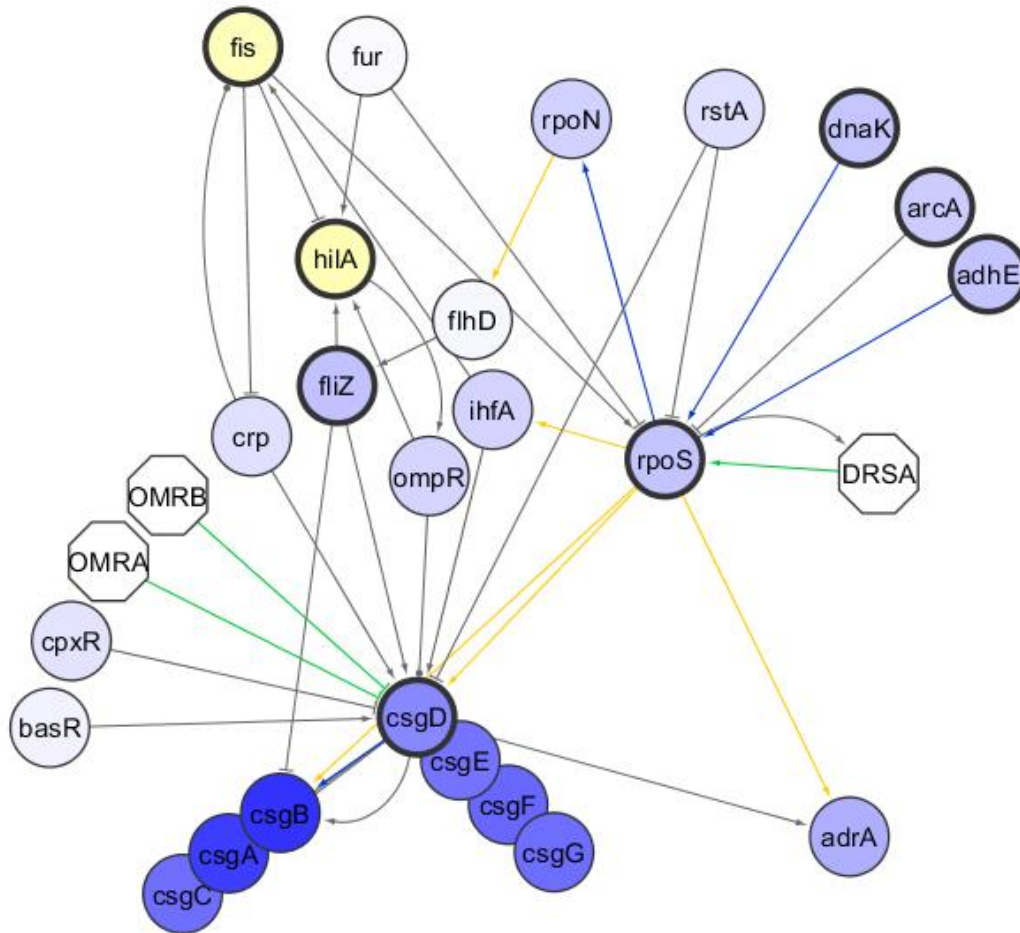


Figure 40 Sub-network extraction from our “upstream” network showing the curli genes and *adrA* as well as their regulators. PheNetic does not indicate whether interactions are repressive or activating; this information was added in Cytoscape (triangular arrowhead means activation, blunt arrow indicates repression, round arrowhead indicates a dual function). Information on nature of interactions came from EcoCyc and literature (Cabeza *et al.*, 2007). Regulators with thick black borders are those with \log_2 fold values < -1.0 or > 1 . Grey arrows indicate protein DNA interactions, yellow arrows indicate sigma factor regulation, and green arrows indicate sRNA regulation that occurs on a post transcriptional level.

Chapter 5: Mechanisms behind biofilm inhibition

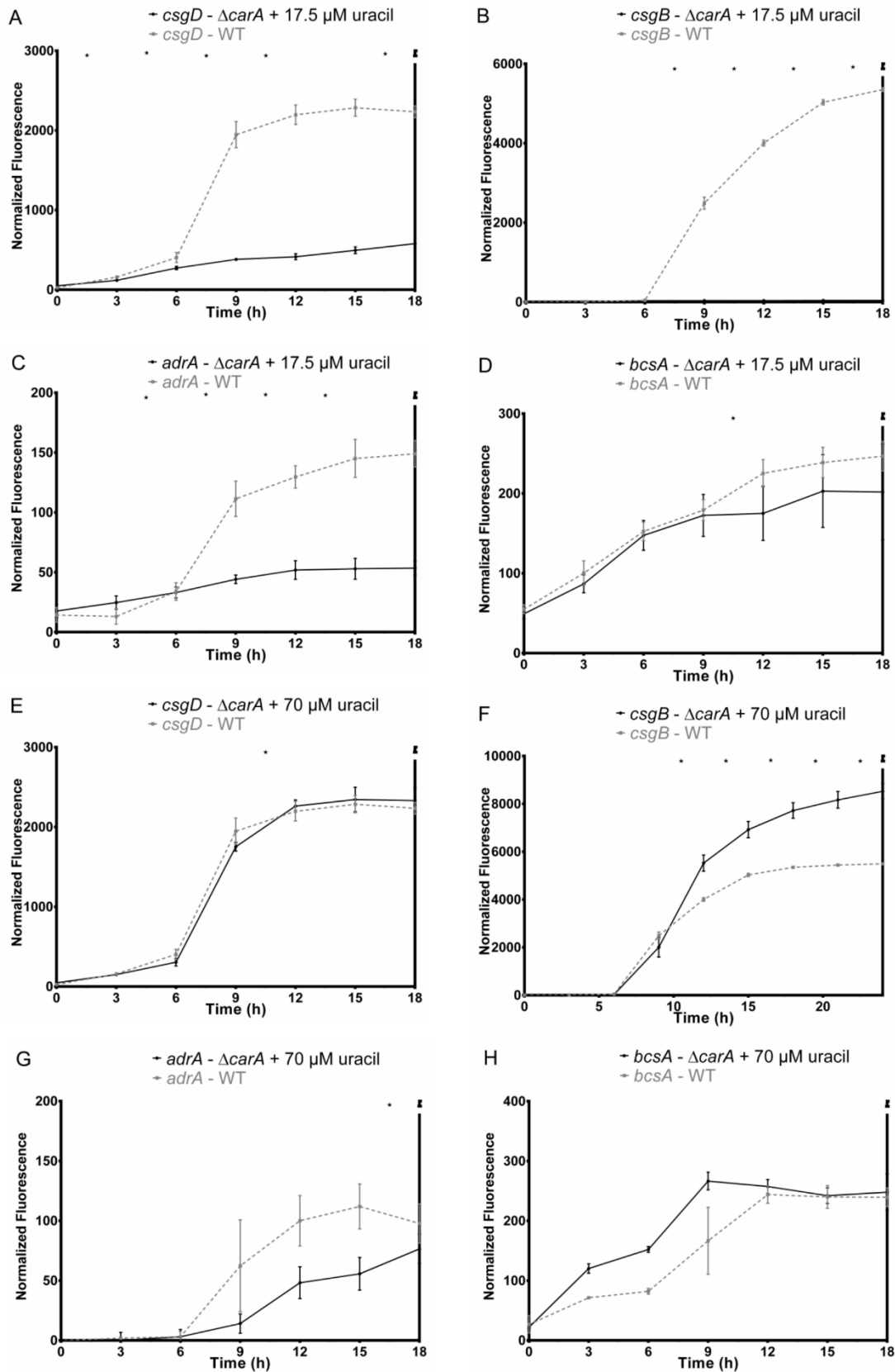


Figure 41 Panels A to D depict the normalized fluorescence of *csgD*, *csgB*, *adrA* and *bcsA* promoter fusions in the *S. Typhimurium* 14028 wild type control (WT) (light grey line) and the *S. Typhimurium* 14028 Δ *carA* mutant complemented with 17.5 μ M uracil (black line), showing a clear down-regulation in the mutant. Expression was measured over 24 hours at 25°C. Stars indicate a significant difference

in gene expression (slope of the curve). Panels E to G: Addition of 70 μM uracil to the mutant (grey line) enhanced the expression of genes to levels similar to that of the wild type (grey dotted line), in the case of *csgB* transcription is upregulated in the mutant. The error bars represent the standard deviations of the technical repeats (n=3). The experiments were repeated two to four times on different days and showed similar patterns.

Results from GFP promoter fusion studies verified the RNAseq results. When the $\Delta\textit{carA}$ mutant was complemented with sufficient uracil (17.5 μM) to restore planktonic growth but not biofilm formation, the expression of *adrA*, *csgBAC* and *csgDEFG* was found to be significantly lower than in the wild type, while *bcsABZC* transcription was not notably affected (Figure 41).

Since a $\Delta\textit{csgD}$ mutant shows a similarly decreased level of biofilm formation as the pyrimidine starved $\Delta\textit{carA}$ mutant (Figure 42), these results suggest that pyrimidine limitation reduces biofilm formation by downregulating *csgD* and its regulon members. Consistently, the expression from the *csgD* fusion was restored to wild type levels when 70 μM uracil (enough to also restore biofilm formation) was added to the growth medium, while *adrA* expression was partially reinstated (Figure 41) and *csgB* expression was slightly upregulated compared to the wild type (Figure 41). Plasmid based expression of *csgD* could partially restore biofilm formation of a *carA* mutant complemented with 17.5 μM uracil. Furthermore deletion of *csgD* in the $\Delta\textit{carA}$ background caused severe inhibition of biofilm formation (Figure 42), despite the addition of 70 μM uracil, indicating that uracil can only restore biofilm formation if chromosomally encoded CsgD is present, highlighting its important role.

Adding extra uracil (17.5 and 70 μM) to the wild type strain did not affect transcription from the *csgD*, *csgB*, *adrA* or *bcsA* promoters (Supp. Figure 14). These results are consistent with the observation that exogenous uracil did not cause any changes in biofilm formation of the wild type strains as determined by crystal violet staining.

It should be noted that the above time-lapse experiments were performed in multi-well plates. Measurements are the sum of the fluorescence originating from free-living cells in the growth medium and cells adherent to the surface. To make sure that the observed changes in gene expression were the cause of reduced biofilm formation rather than the consequence we aimed at measuring gene expression in the separate growth phases. Hereto, biofilm and planktonic samples were taken in the petri-dish setup (described above) at the 10 hour time point and transcription levels of the genes of interest were determined by RT-qPCR (Supp. Figure 15 and Supp. Table 7). Although *csgD*, *csgB* and *adrA* were expressed in the wild type when

grown in the planktonic phase, their expression was, as expected, at least two times higher in the biofilm phase. *BcsA* mRNA levels on the other hand were similar in both phases. In the pyrimidine starved $\Delta carA$ mutant (17.5 μM uracil), the *csgD* and *csgB* mRNA levels were significantly lower than in the wild type, both in the planktonic cells and the “biofilm” cells that were loosely associated with the surface (RQ values of 0.2 for *csgD* and 0.02 for *csgB*). Also, transcription of *adrA* was moderately reduced, with RQ values of 0.77 and 0.55 for the free-living and attached samples respectively, while *bcsA* transcription was only slightly affected (RQ values of 0.85 and 0.73 for free living and attached respectively). Again complementation with the higher, biofilm-restoring concentration of uracil (70 μM) resulted in a partial or complete restoration (or even induction) of *csgD*, *csgB* and *adrA* expression, in both the planktonic and biofilm phase. These results are in agreement with the results obtained from RNAseq and the GFP-reporter assay and indicate that pyrimidine starvation represses the expression patterns of genes involved in matrix production already in the planktonic phase and as such impairs adhesion and the switch from free-living to biofilm mode of growth. Moreover, this repression persists after the pyrimidine-starved bacteria encounter the surface. In the next sections of this chapter we will elaborate on the link between pyridine starvation, *csgD* down-regulation and biofilm inhibition.

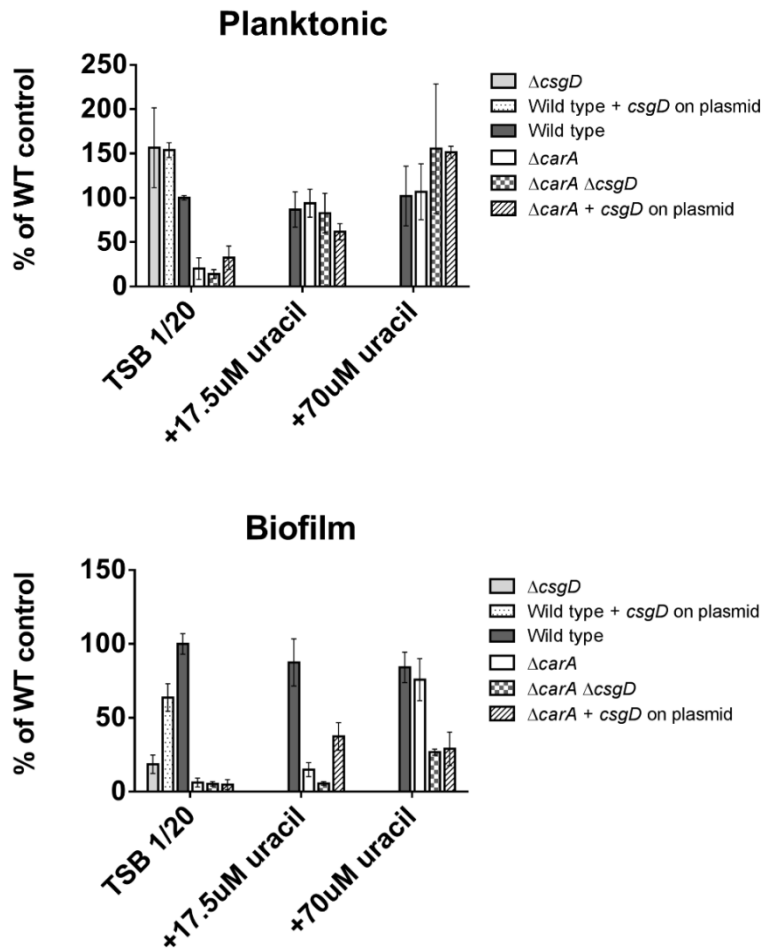


Figure 42 The effects of uracil on the planktonic phase (top image) and biofilm formation (bottom image) of *S. Typhimurium* ATCC14028 wild type, $\Delta carA$, $\Delta carA \Delta csgD$ and $\Delta csgD$ strains after 24 hours, using the Calgary setup. Plasmid based expression (on pFAJ1708) of *csgD* in the $\Delta carA$ background increases biofilm formation in the presence of 17.5 μ M uracil from 15% to almost 40%. Furthermore, the restoration of biofilm formation (bottom image) of a $\Delta carA$, by 70 μ M uracil requires the presence of CsgD as deduced from the observation that a double mutant cannot make adequate biofilm despite uracil addition. In strains that have a sufficient supply of pyrimidines (either due to *de novo* synthesis or complementation with 70 μ M uracil) and that are able to express chromosomally encoded *csgD*, the presence of *csgD* on a plasmid has a negative effect on biofilm formation. 3 to 10 biological repeats were used and were divided into 3 technical repeats each. Experiments were conducted on 2 different days. Error bars represent the standard deviations.

5.3.3.2 Attempt to link perturbations in intracellular nucleotide levels to changes in *csgD* expression and biofilm formation via *fis* and *rpoS*

Based on the RNAseq results, combined with measurements of intracellular nucleotides we propose that a regulatory mechanism involving PRPP, PrsA and PurR is responsible for the increase in purine nucleotides, as described earlier in this chapter. The increase in GTP, which is the substrate for c-di-GMP production, may be a possible cause for the increase in intracellular concentration of this signaling molecule. However, the mechanisms by which

csgD transcription is repressed despite high c-di-GMP concentrations were not yet revealed, and we aim to do so in this section.

Various regulatory pathways act on the regulation of *csgD* expression. Although many known regulators did not display significant changes in their expression levels, some possible pathways by which they could impact curli-production were identified by PheNetic. One pathway that did show changes in the expression levels of the regulators proceeded via Fis and RpoS. The mRNA levels of Fis are known to be under the control of nucleotide availability. This could provide a link between the nucleotide starvation that the *carA* mutant is subjected to, and the subsequent defect in curli production. The gene encoding positive regulator RpoS is down regulated with a log₂ fold value of -1.5. The *fis* gene encoding a global regulator that represses *rpoS* transcription is upregulated (log₂ fold change = 1.87).

Expression of *fis* in *E. coli* is controlled at the transcriptional level in accordance with nutrient availability. Normally it is highly expressed during early logarithmic phase (when cells are grown in rich medium it is the most abundant protein in the cell) but it is poorly expressed in late logarithmic phase and stationary phase (Ball *et al.*, 1992; Walker; Osuna, 2002). A single promoter (conserved between *E. coli* and *Salmonella*) is responsible for the expression of the *dusB-fis* operon and expression regulation *Salmonella* is similar to that in *E. coli* (Osuna *et al.*, 1995). As is typical for a gene involved in the modulation of many cellular processes, Fis is regulated at different levels and by several systems. At the transcription level, Fis is negatively-autoregulated, positively controlled by IHF and also regulated by both growth rate-dependent (only indirect evidence) and stringent control systems (negative regulation by ppGpp(p)). A very interesting mechanism of growth-phase dependent transcriptional regulation relies upon the availability of the nucleotide triphosphate CTP, which is the nucleotide with which transcription of *fis* is initiated and whose largest concentration is seen during log phase, a fact that correlates with the pattern of *fis* expression. Walker and colleagues made the following very interesting observation: in a *E. coli* strain that has a mutation in its pyrimidine biosynthesis pathway, which leads to an excess of purines and a lack of CTP and UTP (similar to what we see in the *carA* mutant) transcription is not initiated by CTP at position +1C anymore (in other literature indicated as 8C, based on its position, 8bp relative to the -10 box). Instead, GTP is used at an otherwise unfavourable position -2G (also sometimes referred to as 6G). In such abnormal conditions, transcription of *fis* is upregulated despite a reduced growth rate (Walker, Osuna 2002, Walker, Mallik *et al.* 2004). Walker and colleagues postulated that the switch from +1C to -2G can be attributed to the following

combined effects: (a) An increment in the GTP/CTP ratio which favors the kinetics of initiation at -2G over +1C and (b) a decrease in UTP pools which tends to hinder the kinetics of the first phosphodiester bond formation with +1C and possibly lower the efficiency with which initiation from +1C results in productive transcripts. A similar mechanism has been suggested for *rrnB* P1, see review (Turnbough 2008). Another mechanism of *fis* upregulation, that was not predicted by PheNetic, could involve DksA. DksA, which is a protein that is associated with RNA polymerase in regulating transcription, inhibits transcription of *fis* by increasing the inhibitory effects of ppGpp, decreasing the lifetime of the RNA polymerase-*fis* promoter complex, and increasing the sensitivity to the CTP nucleotide concentration (Mallik, Paul *et al.* 2006). In the *carA* mutant *dksA* is downregulated (log₂ fold change -1.25). Given that our *carA* mutant has an increase in purine nucleotides and a lack of pyrimidine nucleotides, it might be the case that the transcription start site differs between the *carA* and the wild type strain.

Thus we propose the following: Fis levels in the cytoplasm are increased, because high purine levels combined with low pyrimidine levels favours transcription from -2G. Fis represses transcription of *rpoS*. Due to lower intracellular RpoS levels, *csgD* transcription is reduced.

In an attempt to verify this hypothesis we collaborated with the group of professor N. Buys where they performed primer extension analysis to determine the fragment sizes of the 5'-UTR region of the *dusB-fis* operon. We expected to see a larger fragment for the pyrimidine starved $\Delta carA$ strain (2bp longer than the wild-type fragment or the fragment from $\Delta carA$ with 70 μ M uracil). Initial results were promising and the fragments did indeed differ with ~2 bp in length when comparing pyrimidine starved with pyrimidine sufficient conditions (wild type or mutant with 70 μ M uracil). Peak locations were: wild type (124.36bp), $\Delta carA$ + 17.5 μ M uracil (122.98 bp), $\Delta carA$ + 70 μ M uracil (123.65 bp). However, it appeared that the *dusB* gene and promoter region contained a deletion of about 40bp, because the fragments were shorter than expected by this number of nucleotides. However, during a second attempt (using the same primer), longer fragments were detected. Peaks were found at: wild type (163.63 bp), $\Delta carA$ + 17.5 μ M uracil (160.74 bp), $\Delta carA$ + 70 μ M uracil (no peak, however the negative control sample had a peak at 162.42 bp indicating that they might have been swapped) We performed a PCR on genomic DNA from the wild type and mutant strains, and loaded the samples on a gel. We found two fragments in each strain, which differed about 50bp from each other (Supp. Figure 16). BLAST searches against the ATCC14028 reference genome (NC_016856) revealed that both fragment sets matched the same region in the genome and no

other region, suggesting that a this section of the genome was duplicated (which is not present in the reference genome assembly). Due to this complication and time-constraints we did not pursue the primer extension analysis any further, however we believe that it is worthy of further investigation . In the next subsections we discuss other processes that are also affected by pyrimidine starvation and their possible links to biofilm formation.

5.3.4 Other processes that are affected by pyrimidine starvation and their possible links to biofilm formation

Aside from effect on nucleotide biosynthesis and curli production, multiple other processes were also differentially regulated in response to pyrimidine starvation, as can be expected given that various global regulators were affected. Some of these processes are discussed below:

5.3.4.1 Motility genes are affected in the pyrimidine starved state

Motility and biofilm formation are often inversely regulated (Pesavento *et al.*, 2008), however motility has also been shown to be a requirement for surface attachment. (Guttenplan; Kearns, 2013). The chemotactic sensory machinery, together with the motor complex and flagellum endows bacteria with the capacity to move up and down chemical gradients. The absence of different *che* genes has been shown to affect the rotational bias of the flagella locking it either in a mode that favors “smooth swimming” or “tumbling”(Kuo; Koshland, 1989; Conley *et al.*, 1989).

Our transcriptome results show that chemotactic genes *cheM*, *cheR*, *cheY*, *cheB*, *cheA*, *cheW*, *cheV* are down regulated in the $\Delta carA$ strain. Their \log_2 fold changes are between -2.43 and -1.45. The motor complex gene *motA*, flagellar genes *flgK* and *fliC* have \log_2 fold changes of -2.5, -1.94 and -3.28 respectively. The transcription results suggest that the pyrimidine starved mutant has defective chemotaxis sensory transduction which would impact its capability to recognize and respond to concentration gradients of attractants or repellents in its extracellular environment. In addition, some of the structural components of the motor and flagellum are inhibited as well, suggesting impaired motility. However, the results from our swimming assays showed that the mutant is able to swim (Supp. Figure 17); in fact, its diameter on the swimming plate is larger than that of the wild type, so the exact way in which motility is affected is not clear. It is possible that factors such as adaptation time and tumbling frequency are affected in a manner that still allows the bacteria to swim, but this has to be confirmed with three-dimensional tracking.

5.3.4.2 Translation machinery is affected during pyrimidine starvation

A comprehensive study on global gene expression in *E. coli* biofilms conducted by Schembri and colleagues (2003) found a significant increase in the transcription of ribosomal protein genes when comparing biofilm cells to free living cells in the stationary phase (Schembri *et al.*, 2003). Increases in ribosomal proteins in biofilms produced by other bacteria have also been identified, suggesting that it is a conserved response of bacterial cells to biofilm formation (Whiteley, 2001; Southey-Pillig *et al.*, 2005).

In our dataset a cluster of ribosomal subunit protein(r-protein) genes are downregulated (\log_2 fold changes between -2.8 to -1.7) in the pyrimidine starved mutant. The majority of the downregulated r-protein genes belong to the same operon (*rspJ*, *rplC*, *rplD*, *rplW*, *rplB*, *rpsS*, *rplV*, *rpsC*, *rplP*, *rpmC* and *rpsQ*), which is predicted to be transcriptionally activated by FNR and inhibited by DksA-ppGpp and ArcA-p^{asp54}. The downregulation of r-protein genes can be interpreted in the following ways. (i) There is a reduction in the growth rate. (ii) There is a reduction in protein synthesis. (iii) Ribosome synthesis is halted due to limiting aminoacyl tRNA (amino acid starvation). Since the growth medium contains amino acids and since planktonic growth was not affected, the first and third explanations are unlikely under our experimental conditions. Thus, the downregulation of translation machinery is possibly due to reduced protein synthesis in the *carA* mutant, compared to the wild type, which is synthesizing extra proteins that are required for making biofilms.

5.3.4.3 Iron-sulfur metabolism

Iron/sulfur centers are key cofactors of proteins intervening in multiple conserved cellular processes, such as gene expression, DNA repair, RNA modification, central metabolism and respiration (Py; Barras, 2010). The expression of the *suf* operon has been shown to be induced by oxidative stress (Yeo *et al.*, 2006; Lee *et al.*, 2008). In bacteria such as *E. coli*, where both Isc and Suf systems are present, it is thought that Isc system plays a primary role to assemble Fe-S cluster whereas the Suf system serves as a back-up and/or a specified system adapted to pro-oxidative and iron-depleted conditions.

It has been reported that changes in Fe/S homeostasis influenced mucoidity, motility and biofilm formation in *E. coli* and *Thermotoga maritima* (Beloin *et al.*, 2004; Pysz *et al.*, 2004; Giel *et al.*, 2006; Trotter *et al.*, 2009; Wu; Outten, 2009), however the link between Fe/S homeostasis and cell surface properties is yet to be unraveled.

Genes *sufA*, *sufB*, *sufC*, *sufD*, *sufS* and *ynhA(sufE)* from the iron-sulfur cluster assembly group (GO:0016266) are all downregulated in the pyrimidine starved strain (log₂ fold values of -1.5 to -2.00). This cluster is positively regulated by OxyR, IHF and IscR (YfhP) and is negatively regulated by NsrR and Fur. It is unclear whether these changes are a cause or a consequence of impaired biofilm capabilities.

5.3.4.4 Arginine metabolic genes

Our gene expression results indicate that a gene (*artJ*) with a role in L-arginine uptake is upregulated (Table 10). Furthermore out of the 8 genes involved in arginine biosynthesis, 3 (*argI*, *argC* and *argA*) are significantly upregulated and 1 (*argE*) is significantly downregulated (ArgR and the co-repressor arginine regulate all of these genes).

The gene *artJ* encodes the periplasmic binding protein of an L-arginine ABC transporter. Previous work by others showed that overexpression of *artJ* from a plasmid stimulated arginine uptake (Wissenbach *et al.*, 1995). The observation that this gene is upregulated in the *carA* mutant, is not unexpected, because the mutant has an increased reliance on extracellular arginine compared to the wild type. Nevertheless, it is unlikely that the requirement for exogenous arginine affects biofilm formation, which we verified later (Supp. Figure 18). The addition of various concentrations of arginine did not improve the $\Delta carA$ mutant's ability to make biofilm indicating that its ability to make biofilm depends mostly on uracil and not so much on arginine. Although changes in the expression of some of the arginine biosynthesis genes is a clear indication that the mutant cells are attempting to replenish their arginine supplies it appears that this does not affect biofilm formation because addition of arginine to the *carA* mutant does not increase its ability to form biofilm, however addition of uracil does. Furthermore, a *pyrB* deletion mutant (which is only impaired in pyrimidine biosynthesis but not arginine biosynthesis) also has a biofilm defect and *csgD*, *csgB* and *adrA* down-regulation (Supp. Figure 19).

5.3.4.5 Other processes

From the downstream network it was possible to see that genes involved lipid-A biosynthesis (*lpxB* and *lpxA*) and lipopolysaccharide biosynthesis (*rfbG*, *rfbJ*, *rfbI*, *rfbJ*) were down regulated (log₂ fold changes -2.56 and -1/35). Lipopolysaccharides make up an important component of the outer membrane and the biofilm matrix and the downregulation of these genes may thus also contribute to lower biofilm formation, or it could be an effect of less biofilm formation.

Table 10 Genes involved in arginine biosynthesis and uptake

Role	Gene	Locus	q-val	log ₂ fold change
Biosynthesis of arginine	<i>argD</i>	STM1303	0.05	0.32
	<i>argA</i>	STM2992	0.00	1.55
	<i>argR</i>	STM3360	0.66	0.60
	<i>argE</i>	STM4120	0.00	-1.36
	<i>argC</i>	STM4121	0.00	1.53
	<i>argB</i>	STM4122	1.00	0.31
	<i>argH</i>	STM4123	0.00	-0.54
	<i>argI</i>	STM4469	0.00	2.70
Arginine uptake	<i>artJ</i>	STM0887	0.00	1.82
	<i>artM</i>	STM0888	0.00	-0.96
	<i>artQ</i>	STM0889	0.00	-0.50
	<i>artI</i>	STM0890	0.52	0.06
	<i>artP</i>	STM0891	0.00	-0.02

5.3.4.6 The PhoBR two-component pathway

We see that PhoB is upregulated (log₂ fold change of 1.93) in the pyrimidine starved mutant. Studies on *E. coli*, *P. fluorescens*, *Pseudomonas aureofaciens*, and *V. cholera* reported that PhoB activation inhibits biofilm formation (Pratt *et al.*, 2009; Grillo-Puertas *et al.*, 2016).

The two-component system PhoBR regulates the response to extracellular P_i concentrations. Furthermore the Pho regulon also plays an important adaptive role in bacterial stress response and virulence (Lamarche *et al.*, 2008; Marzan; Shimizu, 2011). A recent publication Grillo-Puertas and colleagues (2016) showed that PhoB activation by inorganic polyphosphate (polyP) in non-limiting phosphate conditions inhibits *E. coli* biofilm formation. Their key findings were: (i) The wild type strain makes biofilm under conditions where extracellular P_i was low or sufficient, but not under high extracellular P_i conditions (high P_i inhibits biofilm formation). (ii) PhoB suppresses biofilm formation under high P_i conditions, but not under P_i sufficient or low P_i conditions. (iii) When polyP degradation is inhibited, biofilm formation is also inhibited under all extracellular P_i conditions (in other words, polyP degradation is a requirement form biofilm formation). (iv) In the absence of PhoB, polyP degradation is no longer a requirement for biofilm formation and biofilm can be made even under high extracellular P_i concentrations. Based on these findings they concluded that activation of PhoB (and biofilm inhibition) is linked to the maintenance of polyP levels under conditions where extracellular P_i is high. Although they did not report a mechanism they hypothesized that polyP level fluctuations control the intracellular P_i levels. And also that an intracellular P_i deficiency

could be generated when polyP was maintained or not degraded during the stationary phase, with consequent PhoB activation (Grillo-Puertas *et al.*, 2016). Our transcription results indicated an upregulation of PhoB (\log_2 fold change 1.92). It would be interesting to further investigate the possible role of PhoB in regulating *Salmonella* biofilm formation.

5.3.4.7 Genes with unknown roles in biofilm formation

Among the genes that are the most highly up/down regulated in the pyrimidine starved mutant are a few genes for which very little is known about their functions. Two such genes are *yciE* and *yciF* which are members of the RpoS regulon (Ibanez-Ruiz *et al.*, 2000). Their transcription is activated by YncC (Beraud *et al.*, 2010). In *E. coli* they are induced under osmotic stress imposed by NaCl in both anaerobic and aerobic conditions (reference webber). In *Salmonella*, *yciF* is induced by bile in a manner independent of RpoS (Prouty *et al.*, 2004). Transcription is repressed by H-NS (Yoshida *et al.*, 1993). The amino acid sequences of these genes are conserved between *Salmonella* and *E. coli* (86% identity for both genes). According to our transcriptome results, expression of *yciE* and *yciF* is repressed in the $\Delta carA$ strain (\log_2 fold changes -5.38 and -4.62). The gene *yncC* is downregulated (\log_2 fold change -1.13). This gene encodes a putative regulator that is part of the RpoS sigmulon (Beraud *et al.*, 2010). The gene *ymdF* is also a target of YncC regulation and is also not well characterized. It has been shown to have a role in resistance to oxidative stress in *Klebsiella pneumoniae* (Tu *et al.*, 2009). In our mutant strain *ymdF* is down-regulated (\log_2 fold change -3)

5.3.4.8 Anti-sense transcription

Among the most highly differentially expressed regions are anti-sense to coding sequences. The prevalence of antisense transcription has been noted by others, and it is believed that this provides another layer in regulatory networks by controlling gene expression (Sallet *et al.*, 2013; Brophy & Voigt, 2016). The interaction network that we used as input for PheNetic did not contain any antisense interactions. However, as more information on this phenomena becomes available, it can also be included into the interaction network.

5.4 Conclusion

In the previous chapter, we showed that pyrimidine starvation is associated with reduced biofilm formation in spite of increased levels of c-di-GMP. Here we used a network based approach to analyse transcriptome data in order to gain more insight into how c-di-GMP levels are upregulated, biofilm formation is down-regulated and what the other effects of pyrimidine starvation are on homeostasis.

indicate putative links. The global pool of c-di-GMP (red ovals) is increased under conditions of pyrimidine starvation. The lightning bolt indicates that the effect of high intracellular levels of c-di-GMP on CsgD expression under pyrimidine starved conditions is unclear. Relevant literature: (Vogel *et al.*, 1991)^a, (Olszowy; Switzer, 1972)^b and (Jensen *et al.*, 2008)^c.

5.5 Materials and Methods

5.5.1 Bacterial strains and growth conditions

Bacterial strains and plasmids used in this study are listed Chapter 4. Prior to experiments strains were stored at -80°C and inoculated onto Lysogeny broth (LB) agar plates, containing the relevant antibiotics if needed. Once inoculated, LB agar plates were incubated at 37°C overnight, and subsequently stored at 4°C. Single colonies were used to inoculate liquid LB cultures (containing antibiotics if needed), and were incubated overnight at 37°C with shaking. Antibiotics used were ampicillin (100 µg/ml) and kanamycin (50 µg/ml). Antibiotics and uracil were obtained from Sigma. Biofilm formation and reporter fusion assays were performed using 1:20 diluted tryptic soy broth (TSB) from Becton Dickinson.

5.5.2 Construction of deletion and complementation mutants

Plasmids used are listed in Chapter 4. A complementation plasmid was constructed by cloning the PCR amplified *csgD* coding sequence, as XbaI/BamHI fragment downstream of the constitutive *nptII* promoter into the RK2-based plasmid pFAJ1708 (Dombrecht *et al.*, 2001). This plasmid is stably inherited even in the absence of antibiotic selection due to the presence of a toxin anti-toxin system. For each complementation construct ~50 nt upstream and downstream the ORF were included. Cloning steps were performed using *E. coli* TOP10F². All plasmids were verified by PCR and sequencing analysis.

5.5.3 Temporal quantification of gene transcription with plasmid based GFP fusions

To obtain a comprehensive picture of the gene expression dynamics, caused by an excess or a shortage of uracil, we made use of an in-house collection of GFP fusions to promoters of genes that are important in biofilm formation (Robijns *et al.*, 2014). Three sets of comparisons were done: (i) *S. Typhimurium* 14028 wild type without added uracil vs wild type with 70 µM uracil (excess uracil), (ii) wild type without uracil vs $\Delta carA$ with 17.5 µM uracil (enough to restore planktonic growth but not biofilm formation) and (iii) wild type without uracil vs $\Delta carA$ with 70 µM uracil (enough to restore biofilm formation).

Overnight cultures of the *S. Typhimurium* 1402m8 wild type and $\Delta carA$ strains, containing reporter fusion plasmids, were grown in LB medium with ampicillin₁₀₀ at 37°C whilst shaking. 2 µl overnight culture of each reporter fusion was transferred in triplicate (i.e. 3 wells per reporter fusion) to black polystyrene 96-well plates (Greiner bio-one 655096) containing 200 µl TSB 1/20 per well (with uracil if needed). Ampicillin was omitted to minimize effects on gene transcription; the omission of antibiotics did not negatively impact plasmid maintenance during the timeframe of the experiments (the expression of GFP from a constitutive promoter was assayed in the presence and absence of ampicillin, see Supplemental Figure 20). The multi-well plates were incubated at 25°C with shaking. A Synergy MX multimode reader was used to measure absorbance and fluorescence at regular intervals over a course of 18, 24 or 48 hours. Absorbance was measured using a wavelength of 600 nm, followed directly by fluorescence measurement with excitation at 488 nm and emission at 511 nm.

Time-dependent changes in transcription profiles were obtained from the OD and fluorescence values as described (Robijns *et al.*, 2014) using a custom Microsoft Office Excel template and GraphPad Prism. In short, the effects of growth rate on the accumulation of fluorescence were normalized and first derivatives were determined in order to give a measure of gene expression at each time point. Significant differences in the first derivative of the control *vs* the test condition were calculated using a two-tailed heteroscedastic t-test with a significance level of 0.05.

5.5.4 Metabolite extraction and mass spectrometry analysis

Prior to metabolite extraction, the optical densities of overnight cultures were determined as described above and normalized to an OD₅₉₅ of 1.5 by suspension of pelleted cells in the appropriate volume of TSB1/20. Petri-dishes containing 20 ml TSB1/20 (with the appropriate amounts of uracil added) were inoculated with 200 µl overnight culture. Petri-dishes were incubated statically at 25°C for 8 to 10 hours before cells were harvested by pouring off the liquid growth medium (containing the free-living planktonic cells). This time point was selected because it corresponds to the time when *S. Typhimurium* enters late exponential phase and switches from a planktonic lifestyle to early biofilm formation. A 15 ml fraction of the harvested planktonic cells was used for metabolite extraction. The remaining 5 ml fraction was used for determining culture optical density, colony forming units and protein content by bicinchoninic acid (BCA) assay. When applicable, cells attached to the bottom of the plate (biofilm cells) were harvested by adding 10 ml TSB 1/20 to the petri-dish, scraping the biofilm off the plate and dispersing the clumps by passing them through a needle as described before.

The harvested biofilm cells were divided into two aliquots of 5 ml, which were subsequently used for metabolite extraction, colony forming unit determination and protein quantification by BCA assay.

The extraction solution contained HPLC grade acetonitrile, methanol and water in a 2:2:1 volume ratio as well as 0.1 M formic acid. Final extracts were evaporated with Speed-Vac. Prior to mass spectrometric analysis, residues were dissolved in 200 μ L H₂O.

The concentrations of nucleotides were determined with LC-MS/MS. Briefly, a Hypercarb 30 x 4.6 mm 5 μ m column (ThermoFisher) protected by a 2 μ m column saver (Supelco Analytical) and a C18 security guard (Phenomenex) was applied. Eluent A was 10 mM ammonium acetate in HPLC-gradient grade water adjusted to pH 10.0 with ammonium hydroxide. Eluent B was acetonitrile. A linear gradient from 4% B (v,v) up to 60% B (v,v) over 8 min was applied, followed by an equilibration phase of further 4 min at 4% B (v,v). The injection volume was 20 μ l per sample and the flow rate was constantly held at 0.6 ml/min. Specific mass transitions (UDP and UTP in negative ionization mode, all other analytes in positive ionization mode) were recorded by a tandem mass spectrometer (5500QTRAP, ABSCIEX). All experiments were conducted in triplicate starting from biologically independent overnight cultures. Data were processed with Microsoft Office Excel 2013 and GraphPad Prism 6.

Concentrations of metabolites were normalized according to optical density.

5.5.5 Experimental setup for RNA extraction

Overnight cultures of *S. Typhimurium* ATCC14028 wild type and Δ *carA* were normalized to similar optical densities (OD₆₀₀ of 1.5) and re-suspended in TSB 1/20. Petri-dishes, containing 20 ml TSB 1/20, were inoculated with bacteria to a final dilution of 1/200. Inoculated petri-dishes were put into a 25°C incubator for approximately 10 hours. After incubation the planktonic fractions were poured off, their optical densities (OD₆₀₀) were recorded and the samples were prepared for RNA extraction. The amount of biofilm at the bottom of the plates was coloured with Crystal Violet, carefully rinsed with water to remove unattached bacteria, and de-stained with 30% acetic acid. The optical densities (OD₅₇₀) of the liquid was measured to get an indication of the amount of biofilm at the bottom of each plate. Four biological repeats were used for each strain.

5.5.6 RNA extraction

In the petri-dish biofilm assay, bacteria were harvested from both the planktonic 10h incubation. Samples of 20 ml were taken from the liquid, planktonic fraction, added to 2.5 ml icecold phenol/EtOH (5%/95%) solution and flash frozen in liquid N₂.

Prior to RNA purification, samples were thawed on ice and centrifuged. Cell pellets were treated with 5 mg lysozyme (from chicken egg white, 40000 u/mg, Sigma Aldrich). RNA was purified with a Promega SV Total RNA Isolation kit according to the manufacturer's instructions, except for the on-column DNase treatment, which was omitted. DNA remainders were removed using the Ambion Turbo DNA-free™ kit. The absence of DNA was verified with PCR amplification, where RNA is unable to amplify, with taq polymerase (NEB). RNA was concentrated and purified by adding 1/10 volume NaOAc (3M, pH 5.2) and 2.5 volume isopropanol. After 20 minutes precipitation at -80°C and centrifugation, pellets were washed with one volume of EtOH, centrifugated and air-dried. The quality and concentration of RNA samples were verified with a Nanodrop™ 1000 Spectrometer (Thermo Scientific) and via capillary gel electrophoreses (Experion Automated Electrophoresis station & Experion RNAStdSens Analysis chips, both from Bio-Rad).

5.5.7 RNA sequencing

Total RNA samples were sent to BGI (Hong Kong) for sequencing. According to the BGI project report, rRNA was removed with a kit (manufacturer information was not provided by the sequencing facility). Fragmentation buffer was added for interrupting mRNA to short fragments. Taking these short fragments as templates, random hexamer-primer were used to synthesize the first-strand cDNA. The second-strand cDNA was synthesized using buffer, dATPs, dGTPs, dCTPs, dUTPs, RNase H and DNA polymerase I respectively after removing dNTPs. Short fragments were purified with a QiaQuick PCR extraction kit and resolved with EB buffer for end reparation and adding poly (A). After that, the short fragments were connected with sequencing adapters. Then, the UNG enzyme was used to degrade the second-strand cDNA, and the product was purified by MiniElute PCR Purification Kit before PCR amplification. The TruSeq RNA-seq libraries, of about 160 bp short-inserts were sequenced in 101bp paired-end fashion, on the same lane, using an Illumina HiSeq4000 platform. The sequencing images were translated into text-based sequencing data via base calling software as FASTQ documents. Data processing performed by BGI included removing adaptor contamination and low-quality reads from raw read.

5.5.8 Transcriptome assembly and analysis

The Rockhopper package was used to assemble clean reads and quantify gene expression. The algorithms used by Rockhopper (McClure *et al.*, 2013) have been developed specifically for analysis of bacterial transcriptome data and support various stages of bacterial RNA-seq data analysis, including aligning sequencing reads to a genome, constructing transcriptome maps, quantifying transcript abundance, testing for differential gene expression, determining operon structures and visualizing results.

The \log_2 fold changes in gene expression of the test condition *versus* the control condition were calculated with the formula $\log_2\left(\frac{1+test}{1+control}\right)$. A list of gene names, the q-values calculated by Rockhopper and the log fold changes were used as input for PheNetic. The predicted genes were removed from the list and kept separately for future analysis (might be useful for gene prediction in unannotated regions of the genome).

5.5.9 Network based- analysis

A physical interaction network for *Salmonella enterica* LT2, compiled from publicly available interaction data, was downloaded from the PheNetic website.

Protein-protein interactions from *E. coli* were obtained from Peregrin-Alvarez and colleagues (Peregrín-Alvarez *et al.*, 2009), whereas regulatory interactions came from RegulonDB (Salgado *et al.*, 2012). *E. coli* data was converted to *Salmonella* using orthology mapping (Altenhoff *et al.*, 2011). Also included in the network are *Salmonella* metabolic interactions described by the KEGG interaction database (Kanehisa; Goto, 2000). Furthermore, information on interactions obtained with text mining, as identified by EVEX, (Hakala *et al.*, 2015) and small molecule interactions derived from the literature, reviewed by Robijns (2013), are also included in the network. The complete network consists of 2699 genes/gene products linked by 15709 interactions. This interaction network, as well as the list containing gene expression data were used as input for PheNetic's "upstream" and "downstream" analysis algorithms. PheNetic extracts the sub-network that best explains genes prioritized through a molecular profiling experiment. Depending on its run mode, PheNetic searches either for the pathways (in)activated in the molecular phenotype (downstream analysis) or for a regulatory mechanism that explains the observed molecular phenotype (upstream analysis)(DeMaeyer *et al.*, 2013; DeMaeyer *et al.*, 2015). Phenetic can be accessed at <http://bioinformatics.intec.ugent.be/phenetic2/#/home>.

The parameter settings were as follows: q-value cut-off: 0.05 (default setting), log₂ fold cut-off of 1.5. The number of genes in list (determined by q-value and log₂ fold cut-offs) was 427. Path length: 4 (default setting based on results from original PheNetic publication). k-best paths: 50 (maximum search space allowed by PheNetic). Resulting network size: 220. Resulting networks were downloaded and viewed in Cytoscape (Shannon *et al.*, 2003).

5.5.10 Primer extension analysis

In order to determine the transcription start site of *fis* in the wild type and $\Delta carA$ mutant under various conditions, RNA was extracted as described before. cDNA was synthesized using a kit as described before, however a fluorescently labelled primer that specifically binds near the 5' end of the *dusB-fis* operon was used to amplify the 5'-UTR. The resulting fragments were analysed with an ABI 3001 sequencer. The regulatory region in front of the operon was verified with Sanger sequencing.

5.6 Acknowledgements

We like to thank the following people: Annette Garbe for excellent technical assistance in LC-MS/MS analysis. Kai Waldrant for his skilful help with various experiments. Rene De Mot for reading and commenting on the manuscript. Elio Rossi for valuable discussions. Ruan De Clercq for taking photos. I am most grateful towards Ami, David, Elien, Bram L and Mizan for the work that they did. Susanne Tinel from the lab of prof. Buys for the primer extension analysis. EcoCyc was used as a starting point for obtaining information on genes and biological processes.

Chapter 6

6 Prevention of *Salmonella* biofilm formation by 5-FU

6.1 Abstract

In this chapter we demonstrate that 5-FU can inhibit *Salmonella* biofilm formation at concentrations that are low enough not to impact planktonic growth. The production of curli fimbriae is strongly inhibited by 5-FU, which is a very likely explanation for the observed biofilm inhibition. Higher concentrations of 5-FU can dramatically inhibit planktonic growth as well. Biofilm inhibition appears to occur via down-regulation of curli production.

6.2 Introduction

As exemplified in the previous two chapters and by others, intact nucleotide biosynthesis plays an important role in biofilm formation (Attila *et al.*, 2009; Ueda *et al.*, 2009; Garavaglia *et al.*, 2012), and therefore drugs that disrupt nucleotide metabolic processes can potentially be useful as biofilm inhibitors.

Nucleoside and nucleotide analog (pro-)drugs can enter the cell by way of similar mechanisms used for the salvage of their natural counterparts. One of the ways in which nucleotide analog drugs interfere with normal cellular processes is by causing imbalances in the NTP pools (Ingraham *et al.*, 1982; Weigel *et al.*, 1999; Wyatt; Wilson, 2009).

As mentioned in Chapter 3 the potential of using these drugs to inhibit bacterial growth, biofilm formation and virulence has been the subject of recent review (Soo *et al.*, 2016; Yssel *et al.*, 2017). Out of the various available FDA approved nucleoside and nucleobase analog drugs, the antibiofilm properties of 5-FU has been the subject of the most thorough investigation. Nevertheless, the mechanism by which 5-FU inhibits biofilm formation is not well understood, and the only detailed investigation into its mode of action comes from whole transcriptome analysis in *E. coli* (Attila, Ueda *et al.* 2009). In *E. coli* 5-FU acts on biofilm formation through AriR as demonstrated by the observation that a Δ *ariR* mutant is not sensitive to the inhibitory effects 5-FU. To our knowledge the effects of 5-FU on *Salmonella* biofilm formation have, however, not been tested before. AriR is not present in the *S. Typhimurium* genome, it is not known whether and how this affect the activity of 5-FU on *Salmonella* biofilm formation. In the following sections we hope to shed more light onto the effects of 5-FU against *Salmonella* biofilms.

6.3 Results

6.3.1 5-FU inhibits *Salmonella* biofilm formation

5-FU uracil inhibits *Salmonella* planktonic growth and biofilm formation in a concentration dependent manner (Figure 44). The IC₅₀ and BIC₅₀ values were respectively 2.00 and 0.75 μ M. We found that the addition of 1.25 μ M 5-FU to the TSB 1/20 growth medium reduced biofilm formation to 7% of untreated levels while planktonic growth remained at 81% of wild type untreated levels.

6.3.2 Differential gene expression in *Salmonella* in response to 5-FU treatment

To explore the mechanism by which 5-FU represses *Salmonella*'s ability to form biofilm, a GFP-promotor fusion library was used to analyze changes in the transcriptional profiles of 131 genes over a period of 18 hours. 12 genes showed differential regulation between treated and untreated samples at 3 or more time-points over the 18 hour period (Figure 45).

Genes involved in putrescine transport (*potF*) and cellular response to DNA damage (*asnA*) were downregulated in the first 9 hours and upregulated thereafter. Genes that were repressed by 5-FU are: *csgD* and *csgB* (curli formation), *adrA* (c-di-GMP production for activation of cellulose synthesis), *yciG* (flagellum-dependent swarming), *nark* (nitrate transport), *virK* (virulence), *aroQ* (amino acid biosynthesis) and *ybeL* (unknown functions).

Genes that were induced by 5-FU are: *carA* (pyrimidine biosynthesis), *hisG* (histidine biosynthesis), *tig* (protein folding) and *cysJ* (sulfite reduction). Although the CysJ protein has been identified as the NADPH:flavin oxidoreductase component of the CysJI sulfite reductase complex, it has been shown that CysJ functions together with YcbX to detoxify mutagenic base analogs (Kozmin *et al.*, 2010), also by reduction. Our GFP library also included promoters from *cysB* and *cysD*, which showed no change in promoter activity between the treated and untreated conditions suggesting that other parts of the sulfate assimilation pathway are not affected by 5-FU. Thus it is an open question whether the upregulation of *cysJ* is related to its role in detoxification of modified base analogs rather than sulfate metabolism. Although CysJ and YcbX would not actually be able to detoxify 5-FU (it detoxifies N-hydroxylated base analogs which cause double strand breaks), their transcription could be upregulated by DNA damage. The downregulation of *csgB* by 5-FU may explain the reduction in adhesion as curli fibers are major constituents of the exopolysaccharide matrix (Steenackers *et al.*, 2012).

6.4 Conclusion

Given recent successful demonstrations of the anti-biofilm properties of 5-FU against *E.coli* and *Pseudomonas* we were interested in determining if it also works against *Salmonella*. Although 5-FU was already demonstrated to be effective in the clinical setting with regards to preventing biofilm formation on catheters, not much is known about how it affects biofilm regulatory pathways. The proposed mechanism of action in *E.coli* that depends on the presence of AriR is not possible in *Salmonella*, because there is no AriR homolog in this species. We found that 5-FU is a very strong inhibitor of *S. Typhimurium* biofilm formation, and that it can effectively abolish biofilm formation without affecting planktonic growth at low concentrations. The production of curli is strongly inhibited by 5-FU, which is a very likely explanation for biofilm inhibition. Chronic carriage of *Salmonella* by individuals or even pets is an important source of gastroenteritis outbreaks and is often associated with biofilms (Buchwald; Blaser, 1984; Costerton *et al.*, 1999; Gonzalez-Escobedo *et al.*, 2011; Gunn *et al.*, 2014). Removal of the gallbladder (cholecystectomy) is the most common treatment for chronic typhoid carriers; however, this treatment is both costly and invasive (Gonzalez-Escobedo *et al.*, 2011). Thus there is incentive for further research into-, and development of anti-*Salmonella* biofilm strategies using 5-FU. For example, 5-FU treatment could be combined with antibiotic treatment in cases where a person is infected with a strain that is associated with chronic carriage. However, this would also require knowledge on factors that are associated with chronic carriage as well as strain identification techniques. Aside from the anti-biofilm properties of 5-FU, at higher concentrations it is very effective at inhibiting planktonic growth as well, and thus may be a viable option for treating antibiotic resistant *Salmonella* infections. Fluoroquinolone resistant *Salmonella spp* were recently listed by the WHO organization as a high-priority pathogen, requiring urgent new R&D strategies for antibiotic development (WHO, 2017).

Chapter 6: Biofilm inhibition by 5-FU

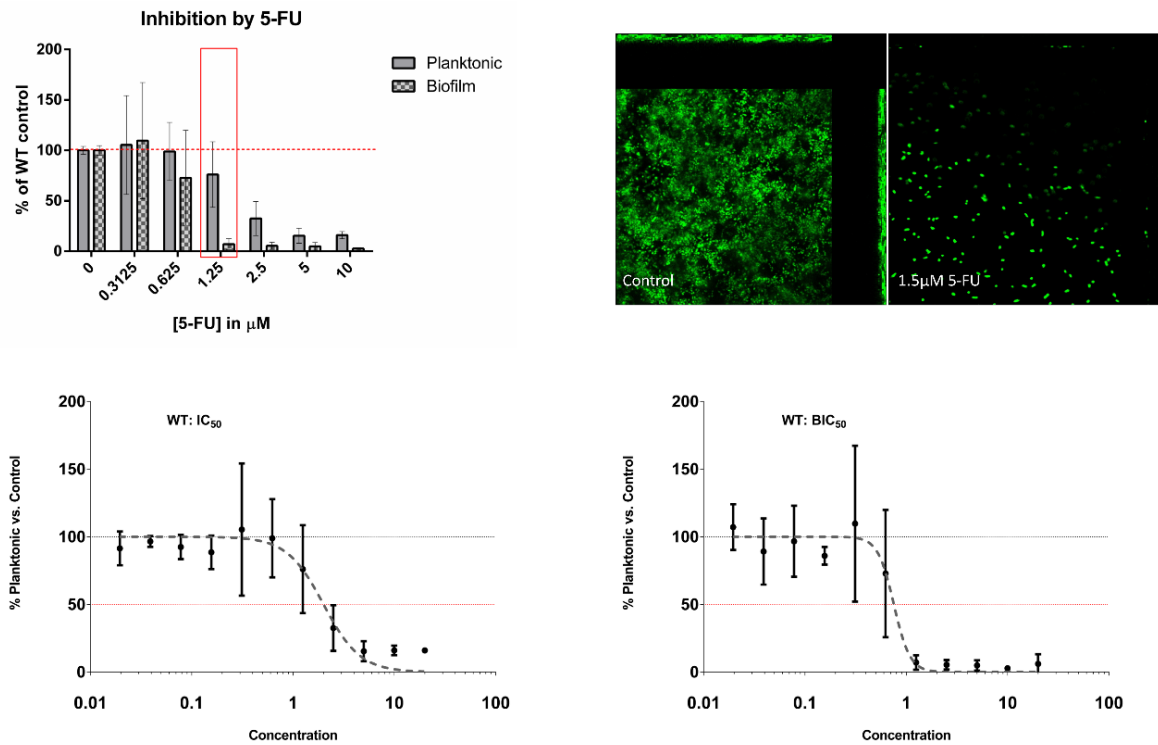


Figure 44 (Top left) 5-FU inhibits *Salmonella* biofilm formation and planktonic growth in a concentration dependent manner. (Bottom left and right) IC₅₀ and BIC₅₀ values were also calculated (bottom left and right respectively). Error bars represent standard deviations from 15 samples (3 biological repeats from 5 different days). (Top right) Biofilms were grown on the bottom of petri dishes for 24 hours at 25°C in TSB1/20 (treated and untreated). The wild type strain ATCC14028 was fluorescently labelled with a constitutively expressed GFP on plasmid pFPV25.1. The untreated biofilm shows heterogeneously distributed biofilm structures while the treated sample contains scattered cells that are not connected to each other. The figures show one layer from a Z-stack through the biofilm.

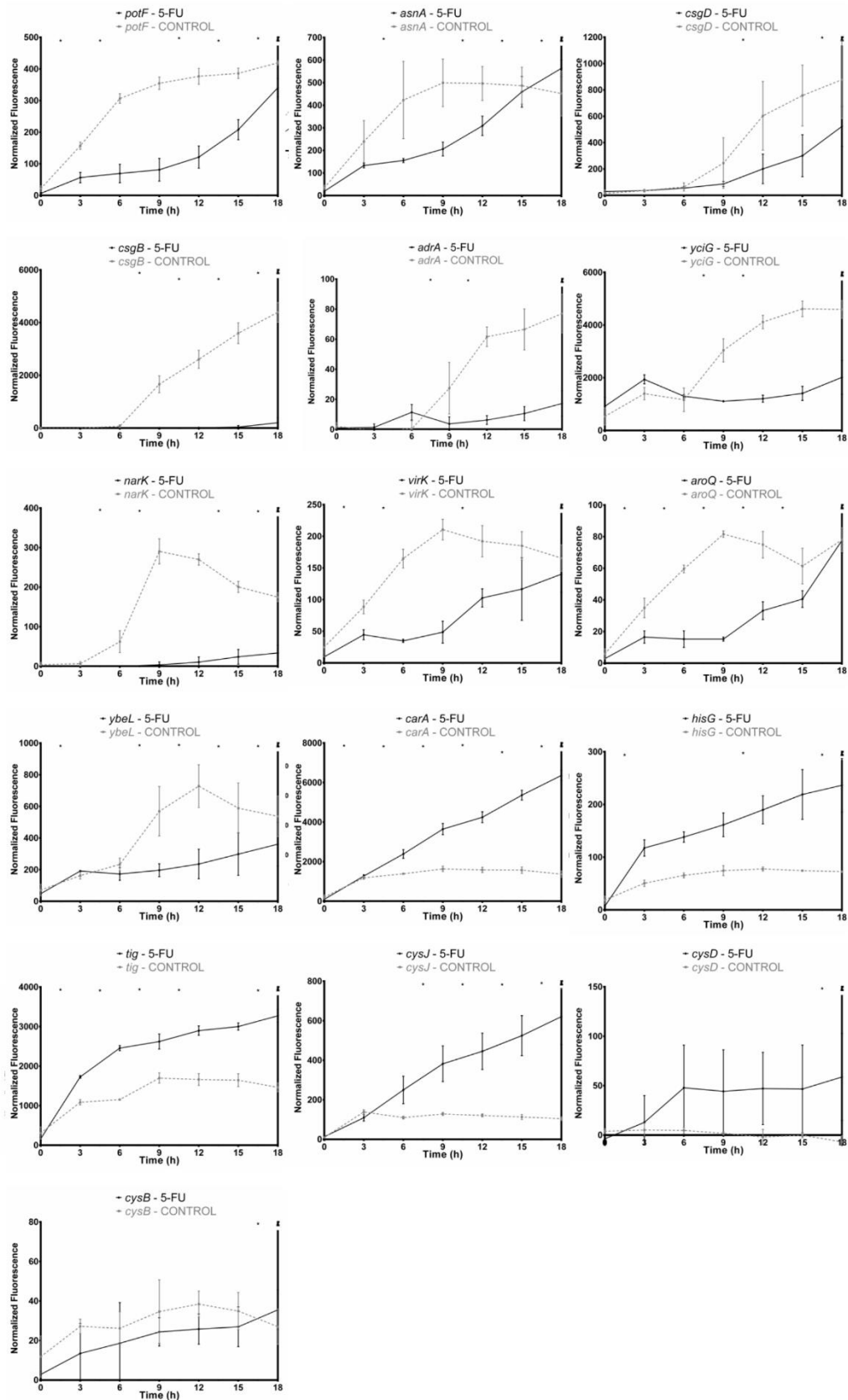


Figure 45 Promotor activity of various genes involved in biofilm formation. Measurements were made every 3 hours over a period of 18 hours. Stars indicate a significant change in promotor activity between two time points when comparing the untreated and treated samples.

6.5 Materials and methods

6.5.1 Assaying biofilm formation

Biofilm formation in the presence of various concentrations of 5-FU (obtained from Sigma) were done using the Calgary setup described in previous chapters.

6.5.2 High throughput biofilm assay

Single colonies of *S. Typhimurium* 14028 containing promotor-GFP fusions for various genes associated with biofilm formation (Robijns *et al.*, 2014) were used to inoculate liquid LB cultures, and were incubated overnight at 37°C with shaking. The optical densities (OD) of overnight cultures (ONCs) were determined at 595 nm and normalized to an OD of 1.5 before centrifugation at $3000 \times g$ for 5 minutes and resuspension in 1:20 diluted tryptic soy broth (TSB) from Becton Dickinson. High-throughput biofilm assays were performed using the Calgary biofilm device, which consists of a standard 96-well plate and a lid that has polystyrene pegs which fit into the wells (Ceri *et al.*, 199). All experiments were performed using TSB 1/20 as growth medium to which 5-FU was added in a dilution series. Wells were filled with 200 μ l medium and inoculated with 1 μ l bacteria from the normalized overnight cultures. Plates were incubated statically at 25°C. After 24 hours, the lids were removed and the biofilms that formed on the pegs at the surface-liquid interface were stained with a solution consisting of 0.1% crystal violet dissolved in isopropanol, methanol and phosphate buffered saline (PBS) in a (1:1:18) ratio (modified protocol (Fletcher, 1977)). The pegs were de-stained with 30% acetic acid and biofilm formation was quantified by measuring the optical density of the resolubized stain at 575 nm using a Synergy Multimode reader. The optical density of the planktonic phase was determined at 600 nm. Experiments were repeated 3 to 15 times using biologically independent overnight cultures, with two to three technical repeats per 96-well plate, as indicated in the relevant results section. Data processing was done using Microsoft Office Excel 2013 and GraphPad Prism 6.

The average values of biofilm formation and planktonic growth of the control conditions were calculated per biologically independent experiment after subtraction of the blank. The control values of each 96-well plate were then used to calculate the percentage of planktonic growth and biofilm formation at a given concentration for each strain from the same plate. The mean growth percentages and standard deviations were calculated from the values of the biologically independent experiments. IC_{50} and BIC_{50} values were also calculated.

6.5.3 Microscopy

Overnight cultures of *S. Typhimurium* 14028 containing a constitutively expressed *gfpmut3* gene (encoded on plasmid pFPV25.1) were inoculated, incubated and normalized as described in the previous section. Ampicillin100 was added to the LB medium before overnight incubation. Petri-dishes containing 10ml TSB 1/20 and Amp100 were inoculated in duplicate with 100 μ L bacteria from the ONCs. No additional compounds were added to the control samples, while 1.5 μ M 5-FU was applied to the treated samples. Samples were incubated for 24 hours at 25 °C. After incubation the liquid planktonic phase was poured off, and the remaining liquid was removed with a pipette. Samples were rinsed with TSB 1/20 to remove non-attached cells from the bottom of the petri-dish. The washing liquid was removed by careful pouring and pipetting.

Images were taken with a Zeiss confocal laser scanning microscope (LSM 700), with digital camera (AxioCam MRm), and the associated Zen 2011 software.

6.5.4 Temporal quantification of gene transcription

To obtain a comprehensive picture of the gene expression dynamics, caused by treatment with 5-FU at a concentration that inhibits biofilm formation, we made use of an in-house collection of GFP fusions to promoters of genes that are important in biofilm formation (Robijns *et al.*, 2014). Overnight cultures of the *S. Typhimurium* 14028 wild type containing reporter fusion plasmids, were grown in LB medium with Amp100 at 37°C whilst shaking. 2 μ l overnight culture of each reporter fusion was to black polystyrene 96-well plates (Greiner bio-one 655096) containing 200 μ l TSB 1/20 per well. Untreated and treated (1.5 μ M 5-FU) samples were inoculated in triplicate. Antibiotics were omitted to minimize effects on gene transcription; the omission of antibiotics does not negatively impact plasmid maintenance during the timeframe of the experiments. The multi-well plates were incubated at 25°C with shaking. A Synergy MX multimode reader was used to measure absorbance and fluorescence at regular intervals of 3 hours over a course of 18 hours. Absorbance was measured using a wavelength of 600 nm, followed directly by fluorescence measurement with excitation at 488 nm and emission at 511 nm.

Time-dependent changes in transcription profiles were obtained from the OD and fluorescence values as described (Robijns *et al.*, 2014). In short, the effects of growth rate on the accumulation of fluorescence were normalized and first derivatives were determined in order to give a measure of gene expression at each timepoint. Significant differences in the first

Chapter 6: Biofilm inhibition by 5-FU

derivative of the control vs the treated condition were calculated using a two-tailed heteroscedastic t-test with a significance level of 0.05.

6.6 Acknowledgements

Lise Dieltjens for kindly helping with overnight measurements. David De Coster and Ami De Weerdts for various technical assistance. Tine Verhoeven, Mariya Petrova and Stefanie Roberfroid: Thank you for setting up the cell cultures and helping with the FACS, it is a pity that the cell cultures were less enthusiastic and refused to work with us. Thanks to Hans Steenackers for the microscopy work!

Chapter 7

7 Concluding remarks

7.1 General remarks

Revealing the underlying molecular mechanisms that control a given complex phenotype is challenging, as changes in a specific phenotype may result from perturbations of many pathways, any of which may contribute very little to the observed phenotype on its own. We have used a network-based approach to search for mechanistic insights into how pyrimidine metabolism affects biofilm formation. This approach combined the vast amount of interactomics knowledge available for *Salmonella*, represented as an interactions network, with gene lists containing data of gene-expression experiments. Such an approach has various benefits. First, the interaction network aids in filtering noise from the gene expression studies. Second, the interaction networks compensate for missing information; genes relevant to the process under study that are not contained in the gene list can be recovered through their connectedness with the differentially expressed genes. Finally, integrating multiple molecular levels into an interaction network (for example protein-DNA interactions, protein-protein interactions and phosphorylation, and so forth), provides a holistic insight into the process of interest.

7.1.1 Nucleotides and biofilm formation

In this work, the regulation of *Salmonella* biofilm formation was studied, with particular focus on the role of nucleotide biosynthesis pathways. Bacteria exhibit multicellular behavior by forming biofilms. These structures provide them with protection against environmental stresses. Biofilms are problematic in industry and medicine related environments. A better understanding of the molecular processes that control biofilm formation might lead to more directed prevention and removal approaches. We reviewed the potential of repurposing nucleoside-based drugs as antibacterial agents. Many of the anti-neoplastic and antiviral drugs that are in clinical use are derived from nucleotides. Because nucleotides play such an important role in bacterial homeostasis, these drugs can impact diverse processes such as survival, growth, biofilm formation and quorum sensing, and thus would be useful weapons in our fight against pathogenic bacteria. The advantages of repurposing drugs that are already approved were discussed. In conclusion our results complement and expand observations that

advocate the therapeutic potential of interfering with pyrimidine biosynthesis to prevent the transition from free-living growth to growth as part of matrix-embedded communities.

A deeper understanding of the regulatory cascades controlling biofilm formation can aid in the identification of actors that might be candidate-targets for anti-biofilm drugs. Prior research, by other researchers, on *E. coli* and *Pseudomonas* has revealed the important role of pyrimidine biosynthesis, and here we further explored that role. Our work contributes to the current understanding of the role that nucleotides play in the regulation of biofilm formation

To gain more insight into how pyrimidine availability influences the switch to a biofilm mode of life, various techniques and assays were performed including time-lapse studies with GFP-promotor fusions, intracellular metabolite quantification and RNA-sequencing. The PheNetic algorithm was used to analyze the data. This approach enabled us to extract a core regulatory network, explaining how pyrimidine starvation affects gene transcription in *Salmonella*. The obtained regulatory network summarizes until today the most complete view on the global impact of pyrimidine starvation on enteric bacteria. Furthermore, it contributes to a better understanding of the link between metabolic processes and biofilms formation. Additionally, more general, a proof-of-principle for extracting the active regulatory network from transcriptome data was hereby delivered.

We showed that pyrimidine deficiency results in biofilm inhibition via inhibition of *csgD* transcription. Furthermore, this inhibition occurs despite an increase in intracellular c-di-GMP concentrations. We argue that the increase in c-di-GMP concentration is driven by an increase in purine nucleotide production. The downregulation of *csgD* promotor activity, despite that high levels of c-di-GMP remains unclear. An interesting link for further exploration is how changes in nucleotide levels affect the expression of the global regulator Fis, which regulates more than 20% of the genes present in the *Salmonella* genome.

7.1.2 Possible polar effects on *carB* due to *carA* deletion

Here we discuss two possible scenarios that may result from deleting *carA*. The first possibility is that transcription of *carB* is affected. The second possibility is that translation of *carB* is affected.

The $\Delta carA$ mutant was constructed by replacing the *carA* coding sequence with an antibiotic resistance cassette, and then removing the cassette according to the protocol by Datsenko and

Wanner (2000). The replaced region also include 7bp in front (partially overlapping with the Shine-Delgarno sequence) and 6bp after the coding sequence.

The genes *carA* and *carB* encode the smaller and larger subunits of the enzyme carbamoyl phosphate synthase and are transcribed from tandem promoters, P1 and P2, downstream of the *carA* coding sequence (Bouvier *et al.*, 1984). Carbamoyl phosphate synthase catalyses the synthesis of carbamoyl phosphate from bicarbonate and glutamine. The glutaminase subunit encoded by *carA* release ammonia from glutamine. The synthase subunit then uses the released ammonia and bicarbonate for the formation of carbamoyl phosphate, at the expense of one ATP. The synthase subunit can also function on its own using free ammonia as substrate (instead of glutamine).

The $\Delta carA$ mutant we constructed, retain the P1 and P2 promoters. Thus, it is possible for *carB* transcription to occur from the P1 and P2 promoters (Jensen *et al.*, 2000). Our RNA sequencing results indeed show that this occurs, because *carB* is upregulated in the mutant strain (\log_2 fold change 4.9). Transcription from P1 is negatively regulated by pyrimidines and to a lesser extent by purines, with the latter occurring by PurR-mediated repression. While transcription from P2 is negatively regulated by arginine bound to ArgR. Based on our nucleotide measurements, which show reduced levels of pyrimidine nucleotides, and the observations that we made regarding upregulation of other genes that are under PurR control, it is not a surprise to see high levels of transcription for *carB*

Nevertheless, just because transcription continues, does not mean that translation actually takes place. If the way in which the *carA* mutant was constructed, had a negative impact on the translation of *carB* mRNA, then the entire enzyme complex, instead of just one subunit would be affected and no carbamoyl phosphate, instead of very little, would be produced. This would lead to complete inhibition of *de novo* pyrimidine synthesis, as opposed to severe inhibition. The $\Delta carA$ mutant grown in TSB1/20 without added uracil does have some limited growth. This can either be due exogenously supplied pyrimidines in the medium, or due to some activity from the *de novo* pathway using free ammonia as a substrate for the first enzymatic step. However, based on the experiments that we conducted we cannot accurately say which option is true. Nonetheless, we can construct a hypothesis to explain our observations:

If the following are all true: (i) *carB* transcription is up-regulated, (ii) translation occurs, (iii) the synthase subunit can make sufficient amounts of carbamoyl phosphate from free ammonia,

(iv) and the other *de novo* pathway enzyme levels are also increased. Then it is reasonable to expect an increase in pyrimidine nucleotides via the *de novo* pathway. However, our nucleotide measurements show that pyrimidine nucleotide production is impaired. Which (given that options i and iv are true, and options ii and iii are not known) is an indication that not enough carbamoyl phosphate is produced to keep pyrimidine pools at a wild type levels.

Overexpression of *carB per se* probably does not impair biofilm formation. Rather, it is pyrimidine starvation which causes this effect, because we also observe biofilm inhibition when the other *de novo* enzymes in the pathway are deleted or replaced by kanamycin resistance cassettes. The main aim of the work presented in this thesis was to evaluate the potential of inhibiting biofilm formation by interfering with *de novo* pyrimidine biosynthesis. We feel that our results are compelling enough to confirm that this is indeed a viable strategy, regardless of which enzymatic step is targeted.

Nevertheless, there are a number of controls that one can use to determine whether knocking one gene in a operon out causes disruptions in the other genes of that operon. To test if this is the case, one can use a plasmid complementation system. If plasmid based expression of the chromosomally deleted gene does not (partially) restore the wild type phenotype, one has to consider the possibility that neighbouring genes were affected. One can use RT-PCR to check if the other genes in the operon are transcribed, or Western blotting to check if translation of the encoded proteins occurs. To prevent polar effects one can use scarless gene editing techniques to make in-frame deletions (Cox *et al.*, 2007; Blank *et al.*, 2011; Yang *et al.*, 2014; Kim *et al.*, 2014).

7.2 Future perspectives

7.2.1 Linking *fis* expression and nucleotide levels to global transcriptome changes that may impact biofilm formation

In wild type cells, transcription of the *dusB-fis* operon is predominantly initiated from +1C. The growth-phase dependent transcription from this site correlates with intracellular CTP concentration, which is high during early exponential phase and low during entry into stationary phase. Under conditions of pyrimidine starvation (where purine levels are high) transcription is initiated from -2G in a growth-phase independent manner (Walker; Osuna, 2002; Walker *et al.*, 2004). Fis regulates the transcriptional induction of RpoS by binding to a region upstream of its promoter to repress it during exponential growth (Hirsch; Elliott, 2005). In turn, RpoS is a sigma factor that is responsible for *csgD* transcription during biofilm

formation. In Chapter 5 we hypothesize that continued transcription of *fis* from -2G in the pyrimidine starved mutant is responsible for reduced transcription of *rpoS* and subsequently *csgD*. To verify the link between nucleotide dependent regulation of *fis* and transcription of *rpoS* and *csgD*, we propose to do the following experiments and hope to see the listed outcomes:

- I. Abolish growth phase regulation of *fis* transcription in the wild type and determine if biofilm formation is inhibited. This would involve replacing +1C with an A or a G. Transcription of *fis* should continue at a high level even during stationary phase. If our hypothesis is correct, *rpoS* and *csgD* should be down-regulated and the mutant should have reduced biofilm formation. Transcription of *rpoS*, *csgD* and *fis* can be measured with qRT-PCR and compared between the wild type and the relevant P_{*fis*} mutant.
- II. Reduce *fis* expression from -2G in the *carA* mutant to see if transcription of *rpoS* and *csgD* is increased and if biofilm formation is increased as well. This would involve replacing -2G with a C or a T in the Δ *carA* mutant. The transcription of *fis* would then depend on the availability of pyrimidine nucleotides and ought to be reduced during all growth phases. We expect to see increased expression of *rpoS* and *csgD*. However, increased levels of RpoS during early exponential phase might have other detrimental effects due to competition with RpoD and lead to unexpected phenotypic outputs or problems with growth.
- III. Interfere with Fis dependent repression of *rpoS* transcription in the Δ *carA* background by deleting the Fis-binding site in P_{*rpoS*}. Here we would expect that the continued high levels of Fis in the pyrimidine-starved mutant would no longer inhibit *rpoS* transcription (and subsequent *csgD* transcription). We would also expect that such a mutant would form more biofilm than the Δ *carA* mutant. However, as mentioned in point II some detrimental effects can be expected.

7.2.2 Regulatory interplay between the purine and pyrimidine pathways

The observation that pyrimidine starvation causes a “runaway” effect in purine biosynthesis is very interesting. This was something that was already observed in the 1980’s, and so far there is no complete explanation for how this happens. Based on the transcription profiles of genes in the PurR regulon, the hypothesis is that there is an unknown factor at play. It could be a protein or ligand that directly interacts with PurR to alter its activity, or it could be a transcription factor that binds the DNA in the vicinity of the Pur-box and interferes with PurR

regulation. It would also be useful to measure intracellular PRPP levels in the *carA* mutant under pyrimidine starved and pyrimidine sufficient conditions, as well as in the wild type.

7.2.3 Partitioning of nucleotide resources during biofilm formation

At any point in a metabolic pathway where a single, inevitably limiting resource (in this case UMP or a later derivative) is partitioned into two or more components (for example UTP and a UDP-sugar), there must necessarily be some decision-making mechanism in order to allow cells to match changes in substrate availability with cellular demands. It can be speculated that when the availability of pyrimidines is low, this resource would rather be partitioned towards DNA/RNA synthesis instead of matrix production. Such a partitioning of pyrimidine resources has been shown to play a role in capsulation of *Pseudomonas* (Gallie *et al.*, 2015). To further investigate how such a partitioning of pyrimidine resources could be achieved, we propose that different concentrations of isotopically labelled uracil should be added to the growth medium and that its fate be determined by measuring its incorporation into UTP, CTP and other nucleotide-derived molecules.

7.2.4 Screening NNADs

NNADs can be screened against the 12 families of bacteria that were identified by the WHO as antibiotic-resistant “priority pathogens”. The list includes *Acinetobacter*, *Pseudomonas*, *Klebsiella*, *E.coli*, *Serratia* and *Proteus*. The activities of the NNADs should be tested for their bactericidal effects, biofilm inhibitory effects, anti-virulence activities and also as adjuvants for standard antibiotic therapies.

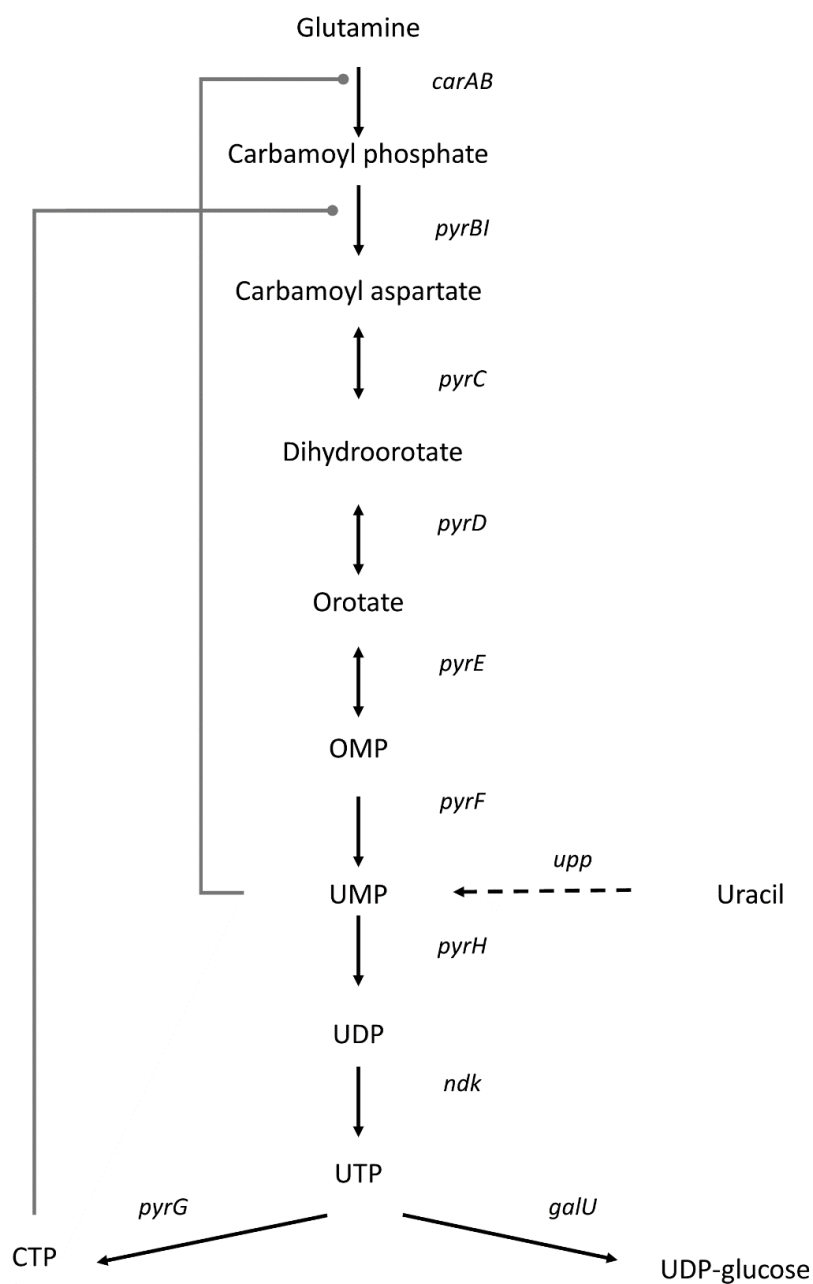
7.2.5 Effect on virulence

Given the link between biofilm formation, virulence and regulation by c-di-GMP, it would be interesting to see whether interfering with nucleotide biosynthesis, or treatment with NNADs impacts *Salmonella* pathogenicity. For this we propose cell culture assays using intestinal epithelial cells and eventually studies using animal models.

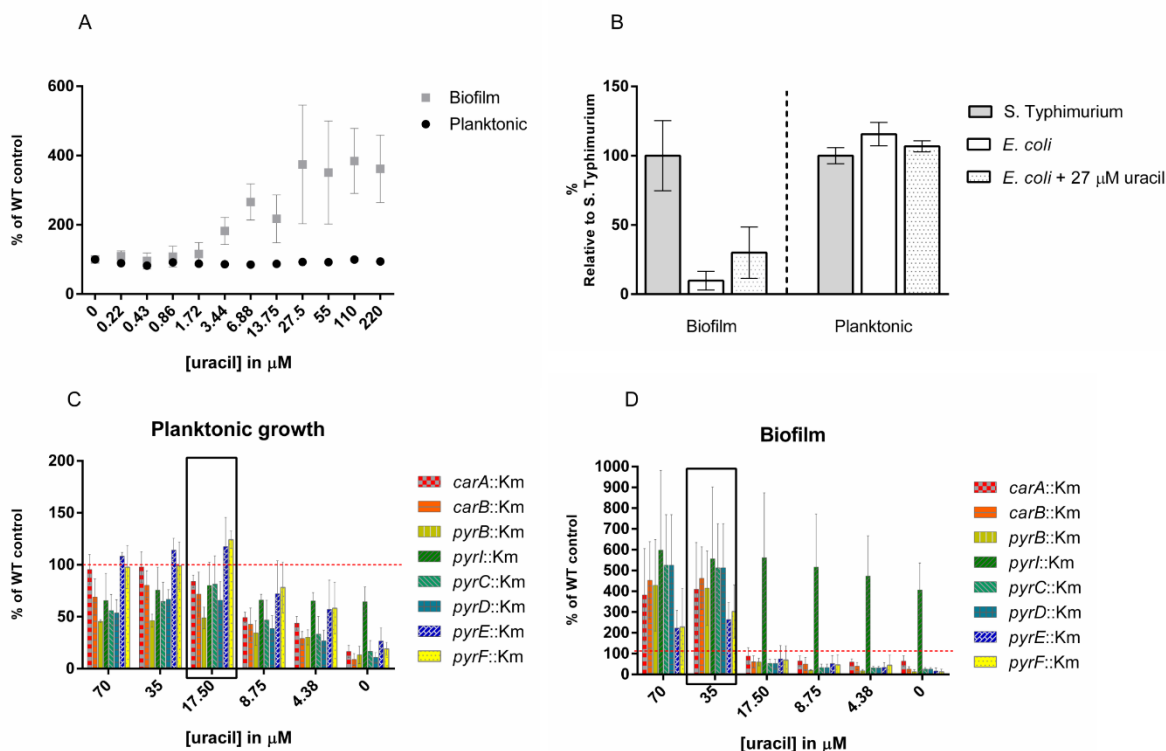
7.3 Final remarks

Recent advances in high-throughput metabolomics have enabled the detection and quantification of thousands of intracellular metabolite ions. In a recently published landmark study Fuhrer and colleagues (2017) explored the relationships between >3800 single-gene deletions and >7000 metabolite ions in *E. coli*. Their map revealed a largely unknown landscape of gene-metabolite interactions (Fuhrer *et al.*, 2017). The model that the constructed for linking genes to metabolites, and the methods which they used might be useful to predict the effects of targeting an enzyme in a particular metabolic pathway. For example, when deciding which enzymatic steps in the nucleotide biosynthesis pathway to target as a means to interfere with biofilm formation; The best candidate enzymes, to target with drugs that are designed to bind to them, can be selected based on the effects that their inhibition would have on the synthesis of biofilm matrix components

Appendix



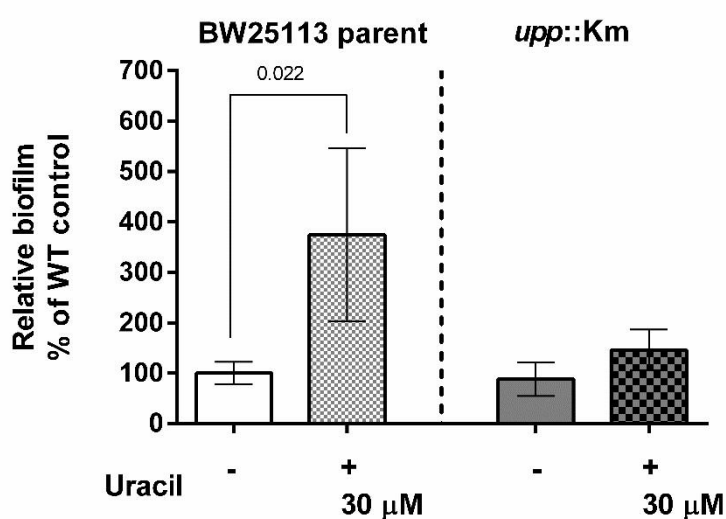
Supp. Figure 1 Diagram providing an overview of the *de novo* pyrimidine biosynthesis pathway: intermediates as well as the genes encoding enzymes responsible for catalyzing the reactions are shown. The bifurcation point where UTP is partitioned towards either CTP or UDP-glucose production is also indicated. Uracil from the growth medium can be salvaged and converted to UMP (black dotted line). Feedback inhibition of reactions by pathway end products are indicated in grey lines.



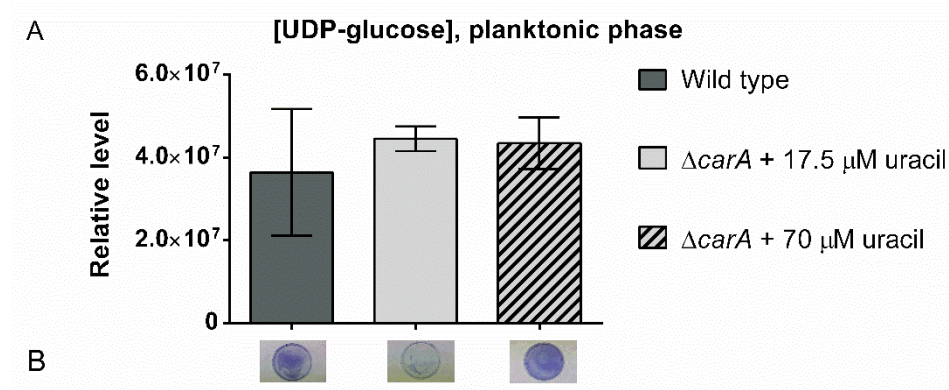
Supp. Figure 2 (Panel A) Concentration dependent induction of biofilm formation of *E. coli* BW25113 by uracil. The results are represented as percentages of the *E. coli* BW25113 control. (Panel B) Relative biofilm formation and planktonic growth of *E. coli* BW25113 (with and without added uracil) after 24 hours, compared to *S. Typhimurium* 14028. BW25113 biofilm levels are 10% of that of *S. Typhimurium* 14028. Biofilm formation of BW25113 was stimulated by 27.5 μM uracil to 30% of that of *S. Typhimurium* 14028. The planktonic phase was not affected by exogenous uracil. The *de novo* supply of pyrimidines in the parental BW25113 strain is sufficient to meet the requirements for free-living growth, but not for maximal biofilm production. (Panels C and D) Concentration-dependent restoration of planktonic growth and biofilm formation of *E. coli* BW25113 mutants that contain single gene deletions of enzymes for pyrimidine biosynthesis. The results are represented as percentages of the *E. coli* BW25113 parental control (red dotted lines). With the exception of *pyrI::Km*, all mutant strains are defective in growth and biofilm formation. Restoration of planktonic growth to the normal parental level, requires the addition of $\geq 17.5\mu\text{M}$ uracil to the medium (black box, panel C). Addition of $\geq 35\mu\text{M}$ uracil induces biofilm formation to levels that are 200 - 600% of that of the parental control (black box, panel D). The *pyrI::Km* mutant, in which the regulatory subunit of ATCase is deleted, exhibits enhanced biofilm formation together with reduced planktonic growth, irrespective of the addition of uracil to the medium. Such a mutant can still synthesize UMP via the *de novo* pathway but is insensitive to feedback inhibition by CTP and UTP leading to an unchecked production of pyrimidines. This suggests that it does not matter whether the required pyrimidine compounds are supplied via the environment or intracellularly. Experiments were performed using 3 independent overnight cultures which were used to inoculate separate multi-well plates with 2 to 3 technical repeats per condition. Error bars represent the standard deviations of the independent experiments.

Supp. Table 1 Strains from the *E. coli* BW25113 single-gene deletion Keio-collection that were used in this study (Baba *et al.*, 2006).

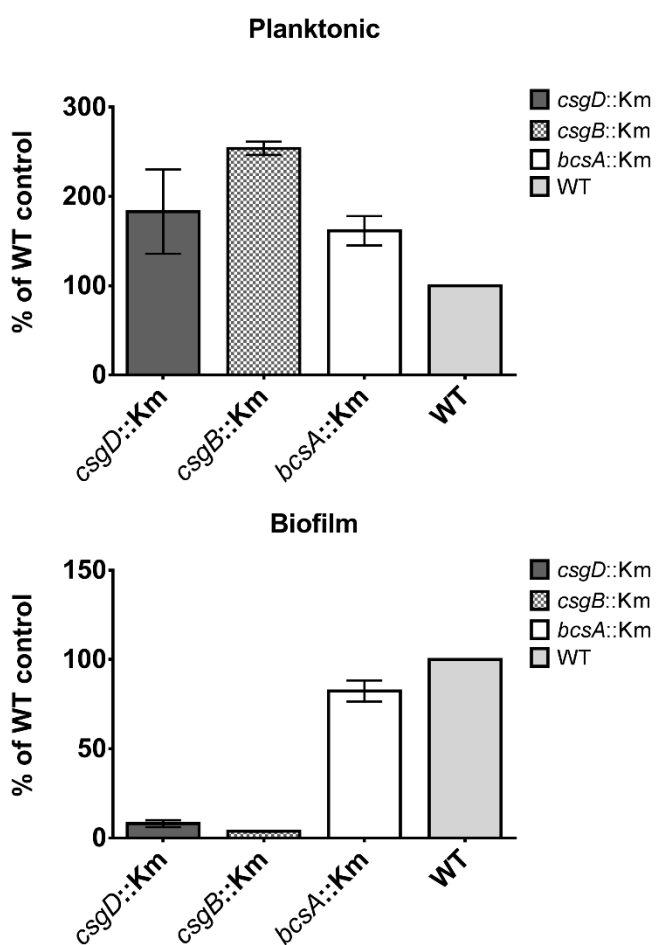
Designation	Ecogene accession numbers
BW25113	
<i>carA</i> ::Km	Eck0033
<i>pyrE</i> ::Km	Eck3632
<i>pyrI</i> ::Km	Eck4239
<i>pyrB</i> ::Km	Eck4240
<i>pyrC</i> ::Km	Eck1047
<i>pyrD</i> ::Km	Eck0936
<i>pyrF</i> ::Km	Eck1276
<i>upp</i> ::Km	Eck2494



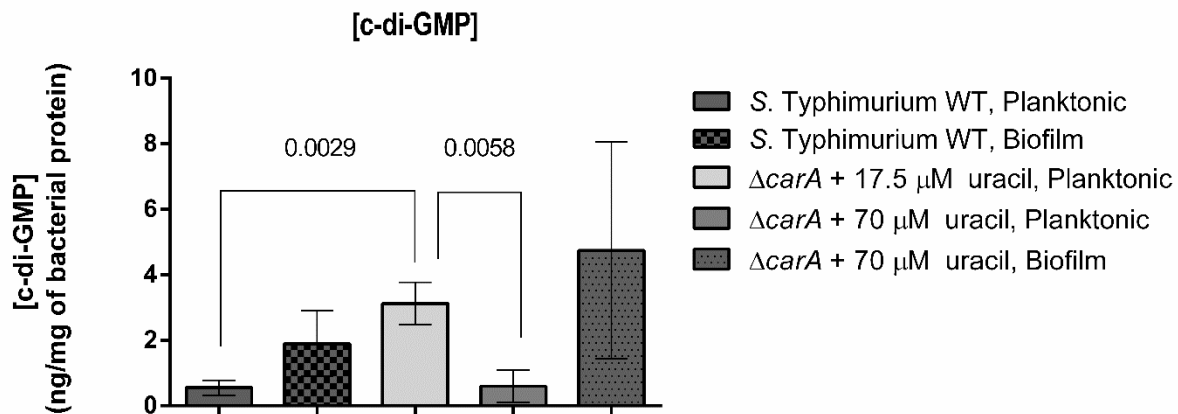
Supp. Figure 3 Relative biofilm formation of the *E. coli* BW25113 parental strain and the *upp*::Km mutant in the absence and presence of exogenous 30 μM uracil. The level of the parental control's biofilm in the absence of uracil was set to 100%. The addition of uracil significantly enhanced the parental strain's biofilm production (p value = 0.022). An insignificant increase was observed for the *upp*::Km mutant, indicating that it is less sensitive to the stimulatory effect that uracil has on biofilm formation. Data are represented as the means of independent experiments (n =3 to 4) and the error bars represent standard deviations. An unpaired t-test with a 95% confidence interval was used.



Supp. Figure 4 Panel A: Relative UDP-glucose levels from planktonic cultures under varying conditions of pyrimidine-availability were determined by mass spectrometry. For each sample, the peak area in the chromatogram was divided by the respective optical density (OD600) to obtain a normalized quantity. Samples were taken after 10 hours of incubation. There are no significant differences in intracellular UDP-glucose concentrations between the wild type control and any of the other conditions. Three biologically independent samples were used per condition. Data are represented as means \pm standard deviations. Panel B: The amount of biofilm formed on the bottom of petri-dishes after 10 hours of growth was determined with crystal violet staining. From left to right are: wild type, mutant with $17.5 \mu M$ uracil and mutant with $70 \mu M$ uracil. Photographs of only one replicate from each condition is shown.



Supp. Figure 5 The biofilm phenotypes of mutants defective in curli and/ or cellulose production (see main text for details). These results indicate that curli production is more important for biofilm formation under our experimental conditions. Data are represented as the means and standard deviations of at least 3 biological replicates.



Supp. Figure 6 Concentration of c-di-GMP from cellular extracts of *S. Typhimurium* 14028 wild type and the $\Delta carA$ mutant as determined by LC-MS/MS. Metabolites were extracted from biologically independent cultures and normalized according to sample protein content. The error bars represent standard deviations of the three independent experiments. Significant differences between samples are indicated above the bars (unpaired t-test, 95% confidence interval, p value = 0.0010). Note that normalization by protein content leads to an underestimation of c-di-GMP levels in the pyrimidine starved $\Delta carA$ mutant, when compared to normalization by optical density. This could mean that the actual protein content in the pyrimidine starved $\Delta carA$ mutant is overestimated. The BCA method is sensitive to the presence of tryptophan, tryptophan might be increased in the pyrimidine starved $\Delta carA$ mutant due to increased levels of PRPP (See the results section for details).

Supp. Table 2 Results from c-di-GMP concentration determination. The amount of c-di-GMP extracted from each sample was normalized according to the sample optical density or protein content.

Condition	Replica	Un-normalized Mass Spec data		Sample characteristics		Normalized [c-di-GMP]			
		c-di-GMP [nM]	c-di-GMP per sample (ng)	Total protein content (µg)	Optical density (OD ₆₀₀)**	ng/mg protein	Average fold change	pmol/sample/OD ₆₀₀	Average fold change
<i>Salmonella Typhimurium 14028</i>									
Wild type: Planktonic	1	1.57	0.217	453.333	0.076	0.48	1.00	4.132	1.00
	2	4.7	0.649	1776	0.138	0.37		6.812	
	3	6.53	0.901	1114.667	0.147	0.81		8.884	
Wild type: Biofilm	1	6.34	0.875	597.334	-	1.46	3.25	-	-
	2	9.19	1.268	864		1.47			
	3	19	2.622	1065.778		2.46			
Δ<i>carA</i> +17.5 µM uracil: Planktonic	1	56.6	7.812	3210.667	0.104	2.43	5.64	108.846	21.29
	2	84.2	11.621	3608	0.106	3.22		158.868	
	3	81.1	11.193	3010.667	0.105	3.72		154.476	
Δ<i>carA</i> +70 µM uracil: Planktonic	1	2.9	0.400	781.333	0.167	0.51	1.07	3.473	0.67
	2	1.77	0.245	1698.667	0.100	0.14		3.54	
	3	5.16	0.712	632	0.162	1.13		6.37	
Δ<i>carA</i> +70 µM uracil: Biofilm	1	24.9	3.437	420.444	-	8.17	8.57	-	-
	2	4.67	0.645	413.333		1.56			
	3	44.4	6.128	1364.444*		4.49			
<i>E. coli</i> BW25113									
Wild type: Planktonic	1	10.5	1.449	1095.200	0.08	1.32	1	26.25	1
	2	5.64	0.778	827.200	0.072	0.94		15.67	
	3	7.67	1.059	1063.200	0.088	1.00		17.43	
Wild type: Biofilm	1	2.72	0.375	1047.73	-	2.82	1.11	-	-
	2	4.78	0.660	1522.400		0.43			
	3	3.36	0.464	1293.067		0.36			
Δ<i>carA</i> +17.5 µM uracil: Planktonic	1	24.4	3.368	1279.200	0.104	2.63	2.09	46.92	2.19
	2	22.1	3.050	1131.200	0.095	2.70		46.53	
	3	18.6	2.567	1727.200	0.102	1.49		36.47	
Δ<i>carA</i> +140 µM uracil: Planktonic	1	11.5	1.587	1495.200	0.207	1.06	1.14	11.11	1.07
	2	26.9	3.713	2971.200	0.213	1.25		25.26	
	3	30.3	4.182	2975.200	0.224	1.41		27.05	
Δ<i>carA</i> +140 µM uracil: Biofilm	1	3.53	0.487	175.733	-	2.77	1.93	-	-
	2	3.67	0.507	290.400		1.74			
	3	4.18	0.577	321.956		1.79			

Fold changes are defined directly in terms of ratio: = (strain of interest)/(wild type) *Outlier detected with Grubbs test. **OD₆₀₀ was only measured for planktonic samples.

Supp. Table 3 Summary of Rockhopper output when the LT2 genome was used as reference for alignment

Strain	Experimental repeat	Total reads	Successfully aligned reads	Aligning sense to protein coding genes	Aligning antisense to protein coding genes	Aligning to unannotated regions
Wild type	1	5600139	5419326 (97%)	43%	43%	10%
	2	5615813	5440361(97%)	40%	41%	13%
	3	5599389	5415217 (97%)	39%	40%	15%
	4	5601998	5412869 (97%)	39%	40%	15%
$\Delta carA$	1	3683063	5387418 (96%)	33%	34%	16%
	2	5595815	5387418 (96%)	35%	36%	17%
	3	5083473	4869480 (96%)	32%	33%	21%
	4	5608974	5392786 (96%)	30%	30%	19%

Supp. Table 4 Summary of Rockhopper output when the LT2 plasmid was used as reference for alignment

Strain	Experimental repeat	Total reads	Successfully aligned reads	Aligning sense to protein coding genes	Aligning antisense to protein coding genes	Aligning to unannotated regions
Wild type	1	5600139	32926 (1%)	44%	41%	15%
	2	5615813	30046 (1%)	43%	42%	15%
	3	5599389	33903 (1%)	44%	40%	15%
	4	5601998	30017 (1%)	44%	41%	14%
$\Delta carA$	1	3683063	26472 (1%)	42%	38%	20%
	2	5595815	39157 (1%)	42%	39%	19%
	3	5083473	33035 (1%)	42%	39%	19%
	4	5608974	35347 (1%)	41%	40%	20%

Supp. Table 5 Genes with large differential expression profiles

Gene	Synonym	Product	Transcripti on Start	Transcripti on Stop	RPKM WT	RPKM <i>carA</i>	qValue vs <i>carA</i>	WT	log ₂ fold change
csgB	STM1143	minor curlin subunit	1231077	1231588	15131	98	0.00		-7.02
-	predicted RNA	antisense: <i>csgC</i> <i>csgA</i> <i>csgB</i>	1232391	1231057	14755	116	0.00		-6.75
-	predicted RNA	-	1231057	1231076	2735	22	0.00		-6.69
csgA	STM1144	major curlin subunit	1231589	1232092	23668	209	0.00		-6.60
-	predicted RNA	-	1232093	1232146	852	7	0.00		-6.52
-	predicted RNA	antisense: <i>rrsG</i>	2800146	2801555	13	495	0.00		5.39
yciE	STM1730	cytoplasmic protein	1826390	1826932	1093	24	0.00		-5.37
-	predicted RNA	antisense: <i>rrsE</i>	4396189	4394697	16	551	0.00		5.30
-	predicted RNA	antisense: <i>rrsC</i>	4101646	4100154	19	640	0.00		5.25
-	predicted RNA	antisense: <i>rrsA</i>	4197573	4196081	19	640	0.00		5.25
-	predicted RNA	antisense: <i>rrsB</i>	4352644	4351152	19	640	0.00		5.25
-	predicted RNA	antisense: <i>rrsD</i>	3570493	3571985	18	607	0.00		5.22
rrsE	STM4177	16S ribosomal RNA	4394675	4396219	16	517	0.00		5.20
rrsB	STM4132	16S ribosomal RNA	4351130	4352673	19	607	0.00		5.17
-	predicted RNA	antisense: <i>rrsH</i>	290693	289201	16	512	0.00		5.13
rrsA	STM3988	16S ribosomal RNA	4196059	4197600	19	608	0.00		5.13
rrsC	STM3889	16S ribosomal RNA	4100132	4101675	20	607	0.00		5.13
rrsG	STM2659	16S ribosomal RNA	2801660	2800118	15	444	0.00		5.10
rfbU	STM2086	O-antigen biosynthesis protein RfbU			67	1	0.00		-5.09
rrsD	STM3398	16S ribosomal RNA	3572006	3570463	19	572	0.00		5.09
rrsH	STM0249	16S ribosomal RNA	289189	290732	17	481	0.00		5.04
-	predicted RNA	-	1826334	1826389	1074	29	0.00		-5.02
csgF	STM1140	curli production assembly/transport protein CsgF	1229307	1228859	1110	30	0.00		-4.98
-	predicted RNA	antisense: <i>carB</i> <i>carA</i>	80254	76997	35	988	0.00		4.92
carB	STM0067	carbamoyl phosphate synthase large subunit	77045	80280	35	947	0.00		4.86
rfbM	STM2084	mannose-1-phosphate guanylyltransferase			76	1	0.00		-4.86
pyrB	STM4460	aspartate carbamoyltransferase catalytic subunit	4704910	4703970	34	896	0.00		4.82
-	predicted RNA	antisense: <i>codB</i>	3502208	3501985	10	272	0.00		4.82
-	STM1513	cytoplasmic protein	1592040	1592256	1952	63	0.00		-4.82
-	predicted RNA	-	1592028	1592039	525	17	0.00		-4.77
csgG	STM1139	curli production assembly/transport protein CsgG	1228858	1228025	1058	34	0.00		-4.76
-	predicted RNA	antisense: STM1513	1592281	1592027	1827	60	0.00		-4.75
-	predicted RNA	antisense: <i>prgH</i>	3017362	3017419	8	222	0.00		4.75
pyrI	STM4459	aspartate carbamoyltransferase regulatory subunit	4703969	4703426	31	759	0.00		4.73
csgC	STM1145	curli assembly protein CsgC	1232147	1232473	299	9	0.00		-4.73
-	predicted RNA	antisense: <i>rrlG</i>	2796891	2798402	26	600	0.00		4.73

Appendix

Gene	Synonym	Product	Transcripti on Start	Transcripti on Stop	RPKM WT	RPKM <i>carA</i>	qValue WT vs <i>carA</i>	log ₂ fold change
-	predicted RNA	-	1232474	1232603	242	7	0.00	-4.70
-	predicted RNA	antisense: rrlD	3567093	3568799	37	821	0.00	4.64
-	predicted RNA	antisense: rrlH	294312	292606	37	811	0.00	4.63
-	predicted RNA	antisense: rrlB	4356166	4354460	37	811	0.00	4.63
-	predicted RNA	antisense: rrlE	4399590	4397884	37	811	0.00	4.63
yciF	STM1729	cytoplasmic protein	1825763	1826333	1289	47	0.00	-4.62
-	predicted RNA	antisense: rrlC	4105007	4103301	37	807	0.00	4.62
-	predicted RNA	antisense: rrlA	4201095	4199389	37	807	0.00	4.62
-	predicted RNA	-	1229327	1229308	1029	36	0.00	-4.62
-	predicted RNA	-	75794	75845	26	584	0.00	4.59
-	predicted RNA	-	1592257	1592292	217	8	0.00	-4.55
csgE	STM1141	curli production assembly/transport protein CsgE	1229723	1229328	1160	43	0.00	-4.54
rfbV	STM2087	abequosyltransferase RfbV			90	3	0.00	-4.51
rfbN	STM2085	O antigen biosynthesis rhamnosyltransferase RfbN			73	2	0.00	-4.47
-	predicted RNA	-	77029	77044	34	698	0.00	4.45
-	predicted RNA	antisense: yciG STM1731 yciE yciF	1827833	1825513	1279	55	0.00	-4.41
-	STM1731	catalase	1826933	1827835	1089	46	0.00	-4.40
-	STM1243	cold shock-like protein CspH	1331050	1330826	4	86	0.00	4.39
rfbK	STM2083	phosphomannomutase			54	1	0.00	-4.38
rfbX	STM2088	O-antigen transferase		2168625	67	2	0.00	-4.35
-	predicted RNA	antisense: csgE csgF csgD csgG	1228015	1230502	1110	47	0.00	-4.33
-	predicted RNA	-	1230503	1230483	483	23	0.00	-4.26
-	predicted RNA	-	1228024	1228015	361	16	0.00	-4.23
pyrL	STM4461	pyrBI operon leader peptide	4705048	4704919	15	252	0.00	4.22
rfbP	STM2082	undecaprenyl- phosphate galactose phosphotransferase	2162361		56	2	0.00	-4.10
-	predicted RNA	antisense: carA	75915	75794	39	614	0.00	4.07
-	predicted RNA	antisense: pyrD	1147318	1147004	15	225	0.00	4.05
gatY	STM3253	D-tagatose-1,6- bisphosphate aldolase subunit GatY			64	3	0.00	-4.03
-	predicted RNA	-	1799796	1799828	363	21	0.00	-3.96
-	predicted RNA	-	4351031	4350964	16	227	0.00	3.95
-	predicted RNA	antisense: rrlB	4353786	4353212	44	595	0.00	3.95
-	predicted RNA	-	4100096	4099855	29	407	0.00	3.93
-	predicted RNA	antisense: STM05625	3024249	3024364	19	264	0.00	3.88
yjiG	STM4513	inner membrane protein			106	6	0.00	-3.87
rrlA	STM3991	23S ribosomal RNA	4198116	4201110	61	781	0.00	3.87
yjiH	STM4514 .S	inner membrane protein			85	4	0.00	-3.85

Gene	Synonym	Product	Transcripti on Start	Transcripti on Stop	RPKM WT	RPKM <i>carA</i>	qValue vs <i>carA</i>	WT	log ₂ fold change
rrlB	STM4135	23S ribosomal RNA	4353187	4356180	59	736	0.00		3.85
-	predicted RNA	antisense: rrlG	2799226	2799732	38	481	0.00		3.84
rrlC	STM3891	23S ribosomal RNA	4102028	4105021	58	725	0.00		3.84
rrlD	STM3396	23S ribosomal RNA	3570071	3567078	58	717	0.00		3.83
rrlE	STM4179	23S ribosomal RNA	4396611	4399604	58	713	0.00		3.82
-	predicted RNA	antisense: rrlD	3569473	3570049	38	466	0.00		3.80
-	predicted RNA	antisense: rrlE	4397210	4396634	38	466	0.00		3.80
-	predicted RNA	antisense: livJ	3734706	3734855	255	16	0.00		-3.78
-	predicted RNA	antisense: rrlH	291772	291256	57	679	0.00		3.78
csgD	STM1142	DNA-binding transcriptional regulator CsgD	1230482	1229724	1148	74	0.00		-3.74
rrlH	STM0252	23S ribosomal RNA	291244	294336	66	745	0.00		3.71
-	predicted RNA	antisense: livJ	3735499	3735515	222	16	0.00		-3.69
livJ	STM3567	high-affinity branched- chain amino acid transporter substrate- binding protein LivJ	3735599		184	13	0.00		-3.66
-	STM0562 5	hypothetical protein	3024357	3024093	15	179	0.00		3.66
yciG	STM1728	cytoplasmic protein	1825513	1825756	2313	170	0.00		-3.65
-	STM1146	hypothetical protein		1232924	139	9	0.00		-3.63
rrlG	STM2657	23S ribosomal RNA	2799764	2796755	55	570	0.00		3.57
creD	STM4590	inner membrane protein	4846401	4847901	11	128	0.00		3.54
pyrD	STM1058	dihydroorotate dehydrogenase 2	1146942	1147978	15	158	0.00		3.54
-	predicted RNA	antisense: narV	1667144	1666906	252	20	0.00		-3.53
-	predicted RNA	antisense: metW metZ	3141209	3141080	28	290	0.00		3.50
-	predicted RNA	antisense: pyrI pyrL yjfF pyrB STM4457	4702871	4705027	86	856	0.00		3.45
-	predicted RNA	-	2596997	2596843	413	33	0.00		-3.43
lysA	STM3013	diaminopimelate decarboxylase	3173967	3172469	5	50	0.00		3.41
metZ	STM2989	Met tRNA	3141064	3141140	23	222	0.00		3.41
melA	STM4298	alpha-galactosidase			125	10	0.00		-3.39
sicP	STM2879	chaperone protein SicP	3024092		5	48	0.00		3.36
-	predicted RNA	antisense: sdaA	1924330	1923352	50	469	0.00		3.33
-	predicted RNA	antisense: fliC	2047633	2049196	1985	182	0.00		-3.33
melB	STM4299	melibiose:sodium symporter			52	4	0.00		-3.32
codB	STM3333	cytosine permease	3501826		18	173	0.00		3.32
fliC	STM1959	flagellin	2049195	2047580	2083	196	0.00		-3.29
ygbJ	STM2918	3-hydroxyisobutyrate dehydrogenase	3061630		7	69	0.00		3.26
-	STM1939	glucose-6-phosphate dehydrogenase	2033021	2032538	7	61	0.00		3.25
asnT	STM2004	Asn tRNA	2084219	2084294	6	57	0.00		3.25
narW	STM1579	nitrate reductase 2 subunit delta			200	19	0.00		-3.24
prgH	STM2874	secretion system protein PrgH	3017580	3016318	4	39	0.00		3.24
-	predicted RNA	antisense: STM2786	2935411	2934578	35	316	0.00		3.24
-	predicted RNA	antisense: aceK	4405772	4405740	267	26	0.00		-3.23
-	predicted RNA	-	2596843	2596997	446	42	0.00		-3.22
-	predicted RNA	antisense: hilD	3017941	3017928	26	218	0.00		3.20

Appendix

Gene	Synonym	Product	Transcripti on Start	Transcripti on Stop	RPKM WT	RPKM <i>carA</i>	qValue WT vs <i>carA</i>	log ₂ fold change
sdhC	STM0732	succinate dehydrogenase cytochrome b556 subunit	797783		290	2396	0.00	3.19
-	predicted RNA	antisense: narY narW	1666018	1665855	295	29	0.00	-3.19
-	STM2786	tricarboxylic transport protein	2934536	2935567	34	288	0.00	3.19
sdaA	STM1826	L-serine deaminase I/L-threonine deaminase I	1923353	1924746	44	362	0.00	3.17
-	predicted RNA	antisense: rrlC	4103200	4102050	104	808	0.00	3.16
-	predicted RNA	antisense: sdhD sdhC sdhA	798734	797783	251	2034	0.00	3.15
-	predicted RNA	antisense: narW	1666399	1666304	211	21	0.00	-3.15
yibK	STM3695	tRNA (cytidine(34)-2'-O)-methyltransferase	3889589	3890064	7	69	0.00	3.15
-	predicted RNA	antisense: narZ	1663630	1663265	278	28	0.00	-3.14
sseI	STM1051	secreted effector protein SseI	1139971	1140939	5	47	0.00	3.13
-	STM2800	L-alanine exporter AlaE	2948289	2948935	41	336	0.00	3.13
metW	STM2990	Met tRNA	3141170	3141246	23	193	0.00	3.12
narV	STM1580	nitrate reductase 2 subunit gamma		1667341	223	23	0.00	-3.12
-	predicted RNA	antisense: yfiA	2808028	2807651	2467	263	0.00	-3.10
chaB	STM1770	cation transport regulator	1868991	1868750	520	54	0.00	-3.09
-	predicted RNA	antisense: ymdF	1206426	1206120	1925	211	0.00	-3.09
yfiA	STM2665	translation inhibitor protein RaiA	2807652	2808028	2254	240	0.00	-3.08
-	predicted RNA	-	2014755	2014667	182	19	0.00	-3.07
iadA	STM4512	isoaspartyl dipeptidase	4767272	4766093	171	18	0.00	-3.07
-	predicted RNA	antisense: yfiD	2786013	2786240	271	27	0.00	-3.06
-	STM4510	aspartate racemase			65	7	0.00	-3.06
narY	STM1578	nitrate reductase 2 subunit beta			242	26	0.00	-3.06
dppD	STM3627	dipeptide transporter ABC ATP-binding subunit DppD	3812333		120	13	0.00	-3.06
-	predicted RNA	antisense: narZ narY	1664825	1664398	283	30	0.00	-3.04
aceK	STM4185	bifunctional isocitrate dehydrogenase kinase/phosphatase	4405066	4408045	401	44	0.00	-3.03
ymdF	STM1121	cytoplasmic protein	1206120	1206372	2058	233	0.00	-3.03
-	predicted RNA	antisense: gcvT	3216491	3216593	26	194	0.00	3.01
hilD	STM2875	transcriptional regulator HilD	3017704	3018765	14	109	0.00	3.00
rpmE2	STM0469	50S ribosomal protein L31	526352	526612	78	8	0.00	-2.99
-	STM0759	hypothetical protein	823590	823044	2653	309	0.00	-2.97
-	predicted RNA	antisense: narY	1665731	1665159	264	30	0.00	-2.97
-	predicted RNA	-	4404982	4405065	1245	147	0.00	-2.97
-	predicted RNA	-	4195964	4195815	44	304	0.00	2.95
-	predicted RNA	antisense: STM0759	823043	823583	2264	272	0.00	-2.94
yfiD	STM2646	autonomous glycy radical cofactor	2786289	2785906	217	24	0.00	-2.94

Gene	Synonym	Product	Transcripti on Start	Transcripti on Stop	RPKM WT	RPKM <i>carA</i>	qValue vs <i>carA</i>	WT	log ₂ fold change
-	predicted RNA	antisense: mutT	162015	161539	65	451	0.00		2.91
-	predicted RNA	antisense: yfcB	2496114	2496594	46	313	0.00		2.90
-	predicted RNA	antisense: rrlD	3568900	3569399	189	1203	0.00		2.87
-	predicted RNA	antisense: rrlB	4354359	4353860	189	1203	0.00		2.87
-	predicted RNA	antisense: rrlE	4397783	4397284	189	1203	0.00		2.87
yecF	STM1949	cytoplasmic protein	2039344	2039767	50	333	0.00		2.85
rpsQ	STM3431	30S ribosomal protein S17		3591574	584	73	0.00		-2.85
aceA	STM4184	isocitrate lyase	4403659	4404981	2300	299	0.00		-2.82
rtT	STM1758	-	1852683	1852825	60	384	0.00		2.82
glyX	STM4353	Gly tRNA	4596652	4596727	582	3695	0.00		2.81
-	predicted RNA	antisense: pyrC	1248592	1249557	56	357	0.00		2.79
-	predicted RNA	-	1206373	1206425	605	82	0.00		-2.79
-	predicted RNA	antisense: tyrT tyrV	1852872	1852617	54	338	0.00		2.78
selC	STM3751	Sec tRNA	3948576	3948670	6	41	0.00		2.77
ompC	STM2267	outer membrane porin protein C	2366641	2365443	1469	198	0.00		-2.75
-	predicted RNA	antisense: rrlG	2798495	2799102	183	1081	0.00		2.75
ais	STM2296	ipopolysaccharide core heptose(II)-phosphate phosphatase	2403760	2402658	82	498	0.00		2.75
ndk	STM2526	nucleoside diphosphate kinase	2660519	2660024	227	1379	0.00		2.74
-	predicted RNA	antisense: rrlH	292505	291895	197	1156	0.00		2.74
-	predicted RNA	antisense: ompC	2365468	2366641	1379	188	0.00		-2.73
-	predicted RNA	antisense: yaiY	432864	432968	154	22	0.00		-2.73
narZ	STM1577	nitrate reductase 2 subunit alpha	1660681		209	28	0.00		-2.72
argI	STM4469	ornithine carbamoyltransferase	4712767	4711709	23	146	0.00		2.72
tyrV	STM1759	Tyr tRNA	1852858	1852942	28	170	0.00		2.71
yfhL	STM2576	ferredoxin	2721682	2721986	18	113	0.00		2.71
-	predicted RNA	antisense: narY	1665060	1664957	241	33	0.00		-2.70
-	predicted RNA	antisense: sitD	3009488	3009448	210	30	0.00		-2.70
pyrC	STM1163	dihydroorotase	1249575	1248515	59	350	0.00		2.70
lysT	STM0751	Lys tRNA	818778	818853	404	2358	0.00		2.69
-	predicted RNA	antisense: aceB aceA aceK	4405418	4401982	1806	256	0.00		-2.69
mutT	STM0137	7,8-dihydro-8- oxoguanine- triphosphatase	161496	162156	77	454	0.00		2.67
rpsS	STM3436	30S ribosomal protein S19	3593802	3593494	447	61	0.00		-2.66
yfcB	STM2385	50S ribosomal protein L3 glutamine methyltransferase	2496595	2495662	41	236	0.00		2.66
-	STM0361	cytochrome subunit II		411192	309	44	0.00		-2.66
lldD	STM3694	L-lactate dehydrogenase		3889529	11	64	0.00		2.64
-	predicted RNA	antisense: motA	2020209	2020336	188	27	0.00		-2.64
-	predicted RNA	antisense: motA	2020475	2020754	235	35	0.00		-2.63
-	predicted RNA	antisense: guaB	2625415	2625894	58	326	0.00		2.62

Appendix

Gene	Synonym	Product	Transcripti on Start	Transcripti on Stop	RPKM WT	RPKM <i>carA</i>	qValue WT vs <i>carA</i>	log ₂ fold change
yhdG	STM3384	tRNA-dihydrouridine synthase B	3555256	3556236	135	752	0.00	2.61
dppF	STM3626	dipeptide ABC transporter ATP- binding subunit DppF		3810216	104	15	0.00	-2.61
pyrF	STM1707	orotidine 5'-phosphate decarboxylase	1801340		18	105	0.00	2.60
sdhD	STM0733	succinate dehydrogenase cytochrome b556 small membrane subunit			154	852	0.00	2.60
rplV	STM3435	50S ribosomal protein L22	3593493	3593161	605	88	0.00	-2.60
-	predicted RNA	antisense: yecF	2039544	2039344	67	370	0.00	2.59
-	predicted RNA	antisense: acrB	529356	529553	306	46	0.00	-2.58
serW	STM0949	Ser tRNA	1027530	1027443	16	88	0.00	2.58
-	predicted RNA	antisense: sitC sitD	3009274	3008722	216	33	0.00	-2.57
-	predicted RNA	antisense: ndk	2659956	2660516	235	1262	0.00	2.57
-	predicted RNA	antisense: narU narZ	1660786	1660557	290	45	0.00	-2.57
-	predicted RNA	antisense: argI	4711839	4712744	26	154	0.00	2.57
-	STM1025	hypothetical protein	1113574	1112956	8	45	0.00	2.57
gltW	STM2658	Glu tRNA	2800033	2799958	28	151	0.00	2.56
-	predicted RNA	antisense: cheM	2014662	2016419	335	52	0.00	-2.55
glnU	STM0677	Gln tRNA	738523	738449	533	2837	0.00	2.55
-	predicted RNA	antisense: lysY lysW valT lysT	819295	818744	265	1394	0.00	2.54
-	predicted RNA	-	4703028	4703013	128	670	0.00	2.54
rfbJ	STM2089	CDP-abequose synthase	2170904	2169999	109	16	0.00	-2.52
gcvT	STM3055	glycine cleavage system aminomethyltransferas e T	3216703	3215563	28	146	0.00	2.52
ybgT	STM0742	outer membrane lipoprotein	812253	812380	347	55	0.00	-2.52
motA	STM1923	motility protein protein A	2021011		226	36	0.00	-2.52
-	predicted RNA	antisense: glgP	3698969	3699186	334	53	0.00	-2.50
-	predicted RNA	antisense: cydB ybgT	812372	811910	329	52	0.00	-2.50
dinP	STM0313	DNA polymerase IV	357794	358855	15	80	0.00	2.49
-	predicted RNA	antisense: suhB	2684722	2684432	81	419	0.00	2.49
rbsD	STM3881	D-ribose pyranase	4091653	4092085	16	88	0.00	2.49
glyV	STM4352	Gly tRNA	4596420	4596495	528	2672	0.00	2.49
-	STM4457	transposase	4703012	4702512	27	136	0.00	2.49
valT	STM0752	Val tRNA	818985	819060	264	1334	0.00	2.48
aceB	STM4183	malate synthase	4401979	4403658	1478	242	0.00	-2.48
-	STM1269	chorismate mutase	1349851	1350398	45	229	0.00	2.48
rfaQ	STM3723	lipopolysaccharide core biosynthesis protein			51	8	0.00	-2.48
-	predicted RNA	antisense: ydgA	1539790	1540029	274	45	0.00	-2.47
yifB	STM3899	ATP-dependent protease	4108383	4106478	8	43	0.00	2.47
-	STM1284	hypothetical protein	1361827	1360406	745	123	0.00	-2.47
-	predicted RNA	-	1868749	1868722	267	44	0.00	-2.45

Gene	Synonym	Product	Transcripti on Start	Transcripti on Stop	RPKM WT	RPKM <i>carA</i>	qValue vs <i>carA</i>	WT	log ₂ fold change
suhB	STM2546	inositol monophosphatase	2684426	2685250	51	256	0.00		2.45
rpmC	STM3432	50S ribosomal protein L29			645	107	0.00		-2.44
-	predicted RNA	antisense: glyV glyX glyY	4596954	4596240	538	2657	0.00		2.44
-	STM2011 .ln	hypothetical protein	2093957	2094232	26	134	0.00		2.44
-	STM2787	tricarboxylic transport	2935573	2936023	28	144	0.00		2.44
-	predicted RNA	antisense: yfbQ	2442242	2442025	50	244	0.00		2.44
-	predicted RNA	-	694521	694542	104	505	0.00		2.43
-	predicted RNA	antisense: sdaA	1924499	1924382	45	221	0.00		2.43
-	predicted RNA	antisense: fis yhdG	3556544	3555256	148	725	0.00		2.43
-	predicted RNA	antisense: purG	2711816	2711922	45	220	0.00		2.43
cheM	STM1919	methyl accepting chemotaxis protein II	2016427	2014756	328	55	0.00		-2.42
sitD	STM2864	Fur regulated iron ABC transporter permease SitD		3009806	196	33	0.00		-2.41
speE	STM0166	spermidine synthase	195901	195009	34	169	0.00		2.41
tyrT	STM1757	Tyr tRNA	1852569	1852653	52	253	0.00		2.41
ileT	STM3989	Ile tRNA	4197670	4197746	352	1694	0.00		2.40
ileU	STM4133	Ile tRNA	4352741	4352817	352	1694	0.00		2.40
-	predicted RNA	antisense: STM1269	1350181	1349930	59	285	0.00		2.40
rplD	STM3439	50S ribosomal protein L4	3595555		631	105	0.00		-2.40
-	predicted RNA	antisense: narZ	1661790	1661725	243	41	0.00		-2.39
-	predicted RNA	antisense: ydgA	1540230	1540543	274	47	0.00		-2.39
nrdD	STM4452	anaerobic ribonucleoside-triphosphate reductase			44	7	0.00		-2.39
-	predicted RNA	antisense: cydA	811105	810913	282	47	0.00		-2.38
-	predicted RNA	antisense: acrB	530689	530846	278	47	0.00		-2.37
-	predicted RNA	antisense: mnmA	1322466	1322672	63	297	0.00		2.37
-	predicted RNA	antisense: codB STM3334	3503090	3503039	45	212	0.00		2.37
yohL	STM3023	transcriptional repressor RcnR	3184055	3183783	7	36	0.00		2.37
-	predicted RNA	antisense: <i>ilet alaT</i>	4197941	4197647	361	1690	0.00		2.36
-	predicted RNA	antisense: <i>ileU</i> STM4134	4353012	4352718	361	1690	0.00		2.36
-	STM0360	cytochrome BD2 subunit I	408661		399	72	0.00		-2.36
priA	STM4095	primosomal protein N'	4305565	4303355	17	80	0.00		2.35
rfbA	STM2095	glucose-1-phosphate thymidyltransferase			67	11	0.00		-2.35
cadA	STM2559	lysine decarboxylase I	2699876	2702095	110	19	0.00		-2.35
-	STM3334	cytosine deaminase		3505021	23	112	0.00		2.35
glnW	STM0676	Gln tRNA	738413	738339	478	2207	0.00		2.34
-	predicted RNA	antisense: STM0362 STM0361 STM0360 STM0359	411231	408438	468	84	0.00		-2.34
-	STM3156	cytoplasmic protein		3318575	11	55	0.00		2.34
-	STM3617	endoglucanase	3798530		170	30	0.00		-2.33
dppB	STM3629	dipeptide ABC transporter permease DppB	3814407	3813243	126	22	0.00		-2.33
rplW	STM3438	50S ribosomal protein L23		3594637	707	124	0.00		-2.32

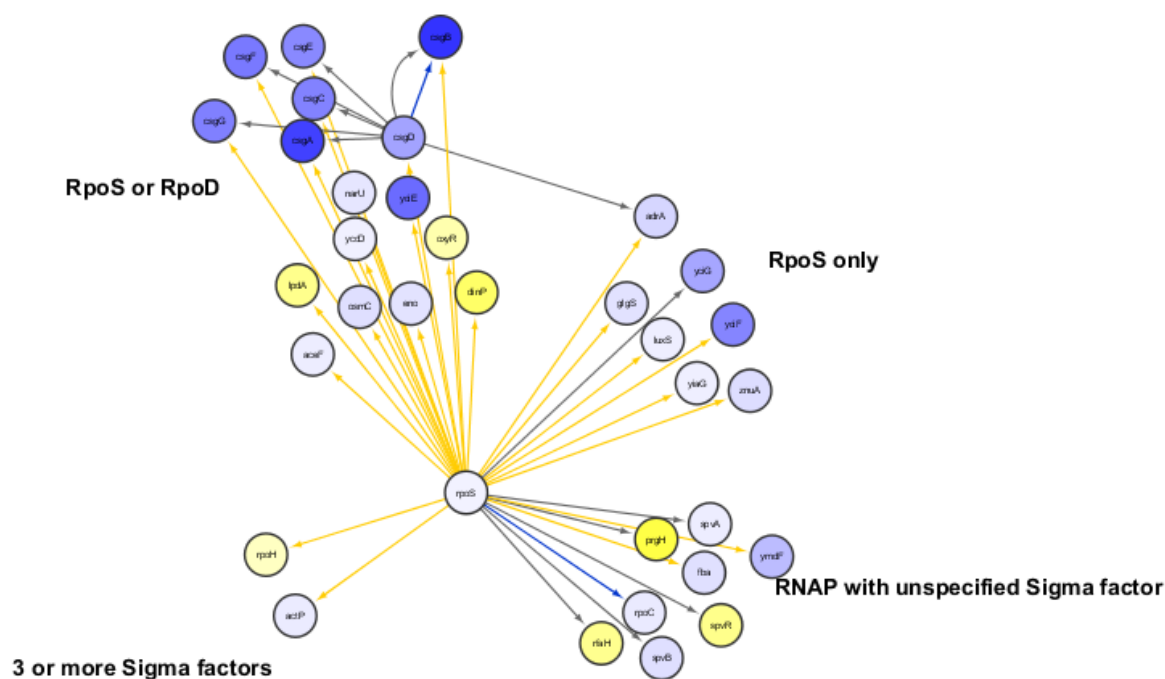
Appendix

Gene	Synonym	Product	Transcripti on Start	Transcripti on Stop	RPKM WT	RPKM <i>carA</i>	qValue WT vs <i>carA</i>	log ₂ fold change
-	predicted RNA	antisense: narZ	1662881	1662803	240	43	0.00	-2.32
-	predicted RNA	antisense: guaB	2625124	2625189	45	202	0.00	2.31
-	predicted RNA	antisense: guaC	164390	164052	68	306	0.00	2.31
rplC	STM3440	50S ribosomal protein L3	3596203	3595556	860	154	0.00	-2.31
rpsC	STM3434	30S ribosomal protein S3	3593160	3592442	535	95	0.00	-2.31
-	predicted RNA	antisense: cheR	2014306	2014351	162	30	0.00	-2.31
msgA	STM1241	virulence protein MsgA	1329716	1329446	38	173	0.00	2.31
rplB	STM3437	50S ribosomal protein L2	3594625	3593803	467	84	0.00	-2.31
glyY	STM4354	Gly tRNA	4596884	4596959	181	814	0.00	2.30
rplP	STM3433	50S ribosomal protein L16	3592441		614	111	0.00	-2.30
sdhA	STM0734	succinate dehydrogenase flavoprotein subunit		800488	94	422	0.00	2.30
lexA	STM4237	LexA repressor	4459249	4459857	97	434	0.00	2.30
-	predicted RNA	-	3814421	3814408	788	145	0.00	-2.29
tusA	STM3578	tRNA 2-thiouridine synthesizing protein TusA	3746759	3744830	52	241	0.00	2.29
-	predicted RNA	antisense: yfbE	2404801	2403916	93	416	0.00	2.29
ygdQ	STM3006	integral membrane transport protein		3164971	74	13	0.00	-2.28
-	predicted RNA	antisense: rplC rpsJ rpmC rplB rplD rplP rpsQ rpsC rpsS rplW rplV	3591604	3596679	655	119	0.00	-2.28
-	predicted RNA	antisense: STM2901	3045655	3045510	57	256	0.00	2.27
yaiY	STM0378	inner membrane protein	433067	432680	119	21	0.00	-2.27
-	predicted RNA	antisense: acrB	529892	529905	275	52	0.00	-2.27
yfbE	STM2297	UDP-4-amino-4- deoxy-L-arabinose-- oxoglutarate aminotransferase	2403907	2405110	77	343	0.00	2.27
lldP	STM3692	L-lactate permease	3885815		16	75	0.00	2.27
adrA	STM0385	diguanylate cyclase AdrA	438038	440087	248	46	0.00	-2.27
rfbB	STM2097	dTDP-glucose-4,6- dehydratase			98	18	0.00	-2.26
alaT	STM3990	Ala tRNA	4197858	4197933	232	1020	0.00	2.26
-	STM4134	Ala tRNA	4352929	4353004	232	1020	0.00	2.26
gltU	STM3890	Glu tRNA	4101759	4101834	43	189	0.00	2.26
orgA	STM2870	oxygen-regulated invasion protein OrgA			18	79	0.00	2.26
ybfE	STM0695	LexA regulated protein	758141	757785	26	116	0.00	2.25
ydgA	STM1466	periplasmic protein	1540709	1539199	242	45	0.00	-2.25
-	predicted RNA	antisense: ftnB	2027770	2027497	71	313	0.00	2.25
sitC	STM2863	Fur regulated iron ABC transporter permease SitC			181	35	0.00	-2.25
ydiY	STM1327	outer membrane protein	1406281	1407109	17	77	0.00	2.25
deaD	STM3280 .S	ATP-dependent RNA helicase DeaD	3448145	3446182	119	22	0.00	-2.24
cheR	STM1918	chemotaxis protein methyltransferase	2014647		118	22	0.00	-2.24

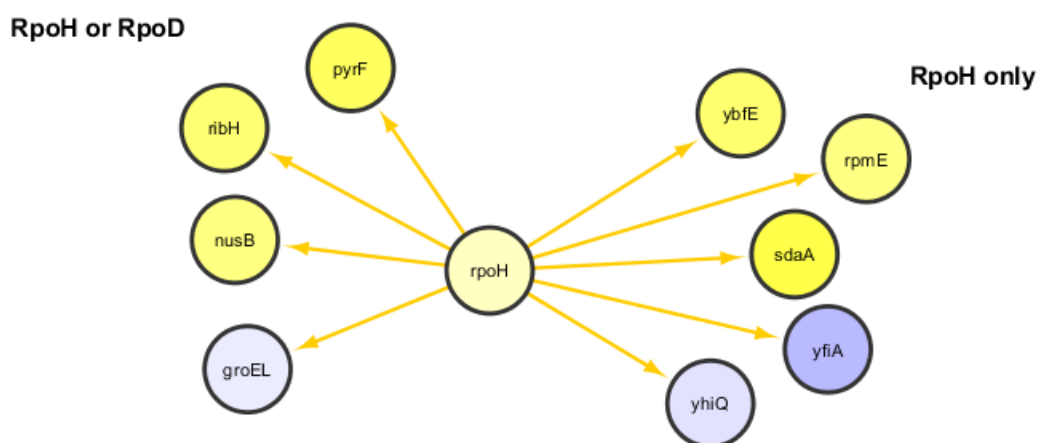
Gene	Synonym	Product	Transcripti on Start	Transcripti on Stop	RPKM WT	RPKM <i>carA</i>	qValue vs <i>carA</i>	WT	log ₂ fold change
yhfl	STM3480	outer membrane lipoprotein	3635924	3636119	27	117	0.00		2.24
-	STM3898	hypothetical protein	4106478	4107324	193	833	0.00		2.24
-	STM2449	acetyltransferase	2560120		112	21	0.00		-2.24
-	predicted RNA	-	3594636	3594626	519	98	0.00		-2.23
stpA	STM2799	DNA binding protein StpA	2947638	2946352	21	92	0.00		2.23
rsmC	STM4556	rRNA small subunit methyltransferase C	4812173	4811135	19	80	0.00		2.21
asnW	STM2012	Asn tRNA	2094236	2094161	33	140	0.00		2.21
-	predicted RNA	-	128743	128594	76	327	0.00		2.21
yjgF	STM4458	enamine/imine deaminase	4703419	4703029	299	1250	0.00		2.21
-	predicted RNA	antisense: purG	2711568	2711632	52	215	0.00		2.20
rimK	STM0875	ribosomal protein S6--L-glutamate ligase	946561	947463	27	113	0.00		2.20
metU	STM0675	Met tRNA	738323	738247	242	1012	0.00		2.20
-	STM0359	cytoplasmic protein	408443	408652	1551	315	0.00		-2.19
-	STM2901	cytoplasmic protein	3045229		58	244	0.00		2.19
yfeZ	STM2448	inner membrane protein			50	9	0.00		-2.18
nanA	STM3339	N-acetylneuraminatase	3509012		56	11	0.00		-2.18
rph	STM3734	ribonuclease PH	3927407	3926679	19	77	0.00		2.18
dppA	STM3630	dipeptide ABC transporter substrate-binding protein DppA	3816182	3814422	1508	306	0.00		-2.17
glgP	STM3534	glycogen phosphorylase	3701369	3698902	164	32	0.00		-2.17
pyrE	STM3733	orotate phosphoribosyltransferase	3926665	3925585	24	103	0.00		2.17
lamB	STM4231	maltoporin	4451991	4453437	11	48	0.00		2.17
gcvH	STM3054	glycine cleavage system protein H	3215562	3215173	35	141	0.00		2.17
-	predicted RNA	-	3596218	3596204	815	161	0.00		-2.16
yfgE	STM2496	DnaA regulatory inactivator Hda	2610585	2609220	31	128	0.00		2.16
ribH	STM0417	6,7-dimethyl-8-ribityllumazine synthase	471024	471526	22	88	0.00		2.16
-	predicted RNA	antisense: leuW metU metT glnU glnV glnW	738196	738778	478	1951	0.00		2.16
guaB	STM2511	inosine 5'-monophosphate dehydrogenase	2625925	2624452	48	194	0.00		2.15
cydB	STM0741	cytochrome d terminal oxidase polypeptide subunit II	811106	812252	235	47	0.00		-2.15
yiaJ	STM3667	IclR family transcriptional repressor	3855417	3854552	28	115	0.00		2.15
dppC	STM3628	dipeptide ABC transporter permease DppC	3813236	3812334	99	20	0.00		-2.15
-	STM2754	hypothetical protein	2892409	2893611	9	36	0.00		2.15
leuW	STM0678	Leu tRNA	738631	738547	616	2476	0.00		2.14
acrB	STM0475	RND family acridine efflux pump	532406	529247	236	48	0.00		-2.14
envE	STM1242	lipoprotein EnvE	1330422	1329896	9	38	0.00		2.14
-	predicted RNA	antisense: sdhB sdhA	801217	799195	120	482	0.00		2.13
-	predicted RNA	antisense: STM2901	3045458	3045305	71	286	0.00		2.12
-	predicted RNA	antisense: rpoC	4374073	4373723	315	65	0.00		-2.12

Appendix

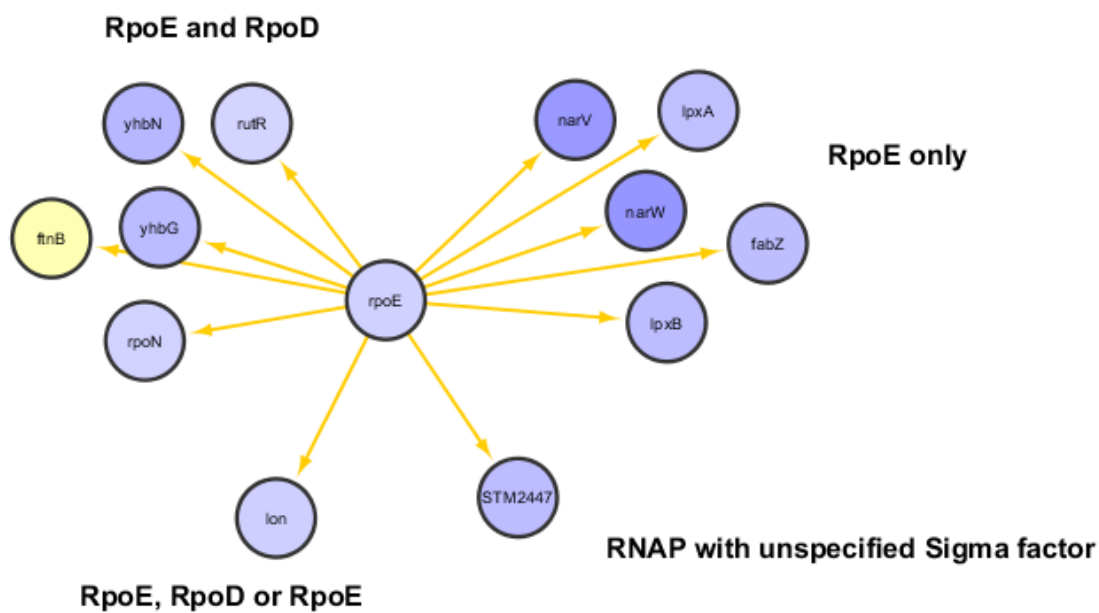
Gene	Synonym	Product	Transcripti on Start	Transcripti on Stop	RPKM WT	RPKM <i>carA</i>	qValue WT vs <i>carA</i>	log ₂ fold change
rpsJ	STM3441	30S ribosomal protein S10	3596685	3596219	836	170	0.00	-2.12
-	predicted RNA	antisense: dppA	3814268	3816179	1500	314	0.00	-2.12
-	STM1023	hypothetical protein	1112373		50	10	0.00	-2.10
-	predicted RNA	antisense: tatE	694799	694512	186	702	0.00	2.08
flgL	STM1184	flagellar hook-associated protein FlgL	1267144	1268101	219	47	0.00	-2.08
-	STM2902	cytoplasmic protein		3046044	17	68	0.00	2.08
rfbF	STM2092	glucose-1-phosphate cytidyltransferase		2173350	125	26	0.00	-2.08
-	predicted RNA	antisense: qor	4465554	4466492	351	77	0.00	-2.06
sufS	STM1373	bifunctional cysteine desulfurase/selenocysteine lyase		1457405	82	17	0.00	-2.06
-	predicted RNA	antisense: phoB	451138	451016	71	277	0.00	2.06
znuA	STM1891	zinc ABC transporter substrate-binding protein ZnuA	1987359	1986400	140	30	0.00	-2.06
qor	STM4245	quinone oxidoreductase	4466536	4465535	332	73	0.00	-2.05
-	predicted RNA	antisense: acrB	531105	531333	302	66	0.00	-2.05
yfbQ	STM2331	aminotransferase AlaT	2441969	2443211	39	149	0.00	2.05
-	predicted RNA	antisense: STM0842	910687	910534	76	287	0.00	2.05
caiF	STM0068	DNA-binding transcriptional activator CaiF			43	9	0.00	-2.04
-	STM1638	SAM-dependent methyltransferase	1729044	1729893	22	84	0.00	2.04
leuV	STM4553	Leu tRNA	4810715	4810629	86	325	0.00	2.04
holD	STM4557	DNA polymerase III subunit psi	4812263		24	89	0.00	2.03
hutH	STM0791	histidine ammonia-lyase	854896	858737	434	98	0.00	-2.03
sulA	STM1071	cell division inhibitor SulA	1162888	1162340	27	101	0.00	2.03
-	STM2610	periplasmic lysozyme inhibitor	2758320	2758781	158	34	0.00	-2.02
-	predicted RNA	antisense: fhuA	224006	223802	79	300	0.00	2.02
ynhA	STM1374	cysteine desufuration protein SufE	1457418		48	11	0.00	-2.02
-	predicted RNA	-	2660023	2659974	180	661	0.00	2.02
-	predicted RNA	antisense: flgK flgL	1268091	1265476	244	55	0.00	-2.02
ftnB	STM1932	ferritin-like protein	2027167	2027885	91	340	0.00	2.01
osmC	STM1563	peroxiredoxin OsmC	1644673	1644177	733	168	0.00	-2.01
-	predicted RNA	antisense: ydgA	1539406	1539683	273	60	0.00	-2.01
ileV	STM0250	Ile tRNA	290790	290866	106	387	0.00	2.01
-	STM4239	cytoplasmic protein		4461470	1647	377	0.00	-2.01
purG	STM2565	phosphoribosylformylglycinamide synthase	2712150	2708254	30	112	0.00	2.00
-	STM2788	tricarboxylic transport protein	2936024	2937554	25	96	0.00	2.00
nanT	STM3338	sialic acid transporter	3508047	3506467	79	17	0.00	-2.00



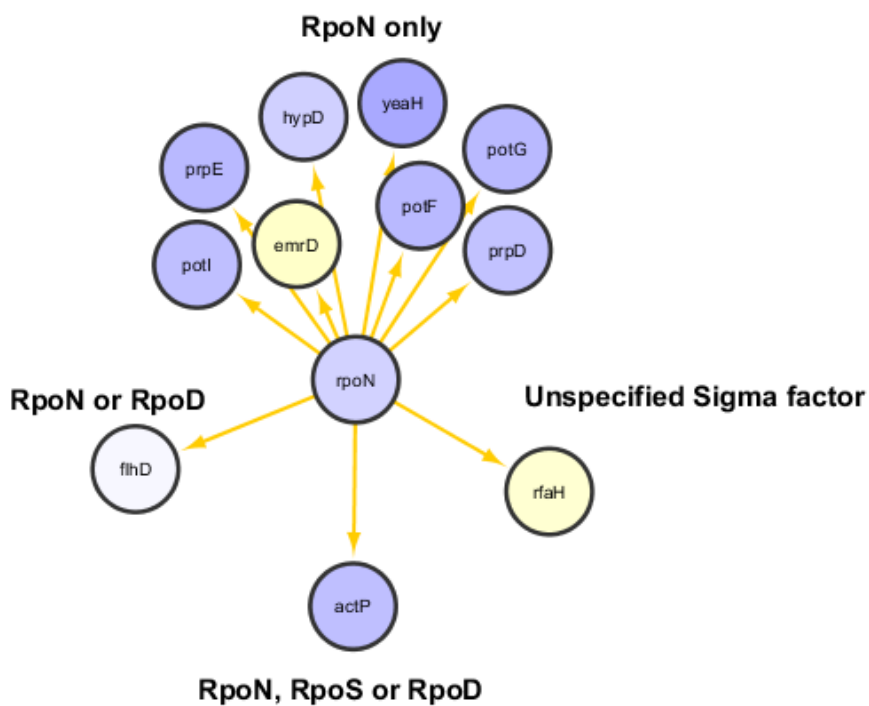
Supp. Figure 7 Sub-network extraction from our regulatory network, showing the RpoS sigmulon. Four clusters are visible: (Top left) those including genes that are transcribed by RNAP in association with RpoS or RpoD. (Top right) Those transcribed by RNAP in association with RpoS only. (Bottom left). Those transcribed by RNAP paired with any of three or more different sigma factors. (Bottom right) RNAP paired with RpoS or an unspecified sigma factor. Genes that are only transcribed by RpoS are all down regulated. BioCyc was consulted to determine which sigma factors associate with RNAP for the transcription of the various genes.



Supp. Figure 8 Sub-network extraction from our regulatory network, showing the RpoH sigmulon. Two clusters are visible: (Left). Genes that are transcribed by RNAP in association with either RpoS or RpoD. (Right) Genes transcribed by RNAP in association with RpoH. BioCyc was consulted to determine which sigma factors associate with RNAP for the transcription of the various genes.

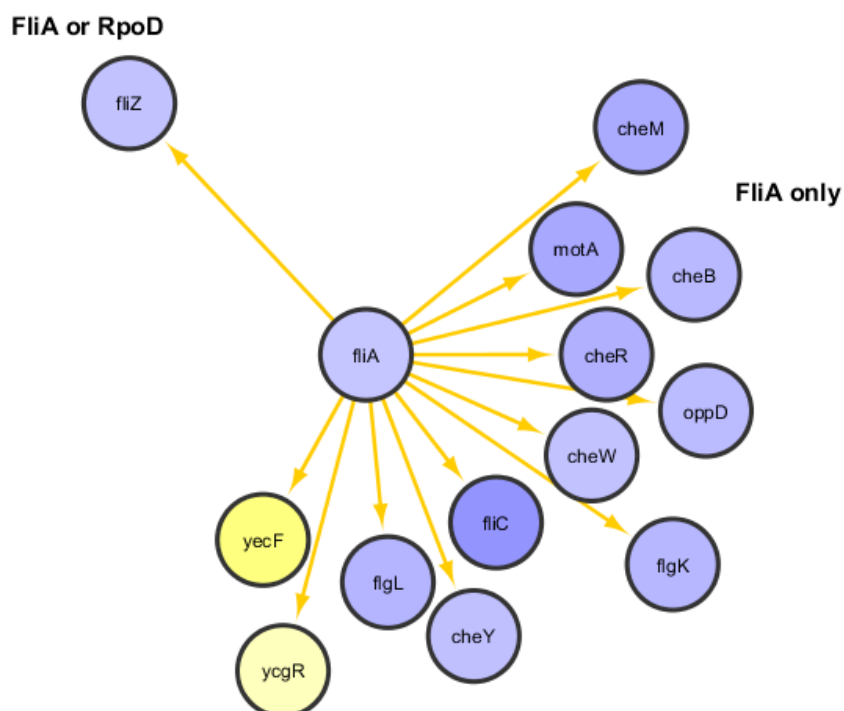


Supp. Figure 9 Sub-network extraction from our upstream-regulatory network showing the RpoE sigmulon. Genes were divided into four clusters based on the sigma factors, which associate with the core RNAP to allow their transcription. All but one gene is downregulated in the *carA* mutant. BioCyc was consulted to determine which sigma factors associate with RNAP for the transcription of the various genes.

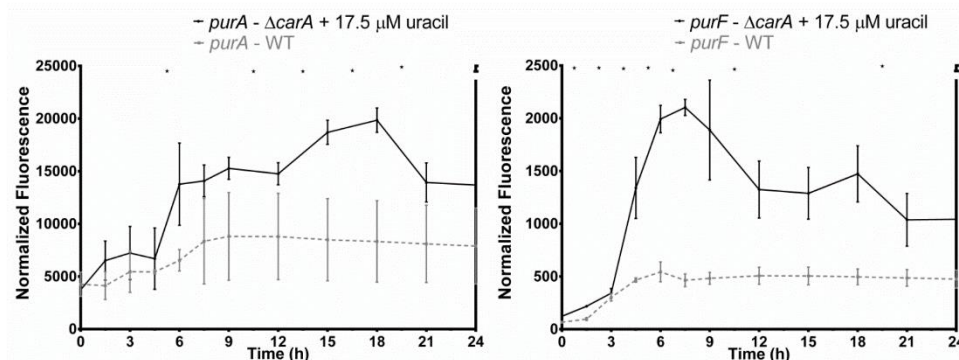


Supp. Figure 10 (previous page) Sub-network extraction from our upstream-regulatory network showing the RpoN sigmulon. Genes were divided into four clusters based on the sigma factors which associate with the core RNAP to allow their transcription. All but two genes are downregulated in the

$\Delta carA$ mutant. BioCyc was consulted to determine which sigma factors associate with RNAP for the transcription of the various genes.



Supp. Figure 11 Sub-network extraction from our upstream-regulatory network, showing the FliA and its first-neighbours that are under its direct control. Only one gene is transcribed by RNAP in complex with either FliA or RpoD, the rest are all transcribed between RNAP in complex with FliA. BioCyc was consulted to determine which sigma factors associate with RNAP for the transcription of the various genes.



Supp. Figure 12 Normalized fluorescence of the *purF* promoter (left) and the *purA* promoter (right) in the *S. Typhimurium* 14028 wild type (grey lines) and the $\Delta carA$ mutant complemented with 17.5 μM uracil (black lines), with both promoters showing a clear upregulation in the mutant. Stars indicate a significant difference in the slope of the two conditions between two time points (as determined by an unpaired t-test with a confidence interval of 95%) indicating that there is a significant difference in transcription from the promoters. The error bars represent the standard deviations between 3 technical repeats (corresponding to three wells in a multi-well plate). The experiments were repeated for a second time on a different day and similar profiles were obtained.

Supp. Table 6 Intracellular metabolite concentrations from *S. Typhimurium* 14028 wild type and $\Delta carA$ mutant in TSB1/20. The $\Delta carA$ mutant was grown in the presence of 17.5 μM uracil to complement its growth defect. Metabolite concentrations were normalized to the optical density of each sample. The experiment was conducted in triplicate.

		Normalized metabolite concentrations [pmol/sample/OD600]														
		ATP	ADP	AMP	GTP	GDP	GM P	CTP	CDP	CM P	UTP	UDP	UM P	IMP	Gua nine	Hypoxanthin e
Wild type																
1	608.9	285.5	687.5	186	64.3	63.1	172.1	258.1	236.9	48.6	61.5	359.8	114	17.2	63.7	
2	754.5	286.2	424.6	134.7	44.2	37.5	234.1	577.8	203.6	55	61.7	168.3	45	8.3	18.2	
3	460.7	236.8	656.4	106.8	37.7	49.3	144.8	433.7	267.5	36.7	41.2	284.1	74.2	11.7	127	
$\Delta carA$																
1	1925.9	1425.5	7268.5	283.3	346.3	435.2	126.9	379.6	510.2	8.9	24.7	143.5	675.9	296.3	6342.6	
2	1121.6	788.7	5322.6	137.9	161.3	229	82.3	302.4	313.7	4.8	16.5	130.7	338.7	151.6	5201.6	
3	1027.8	930.6	9166.7	142.4	193.1	318.1	87.5	285.4	456.3	5.8	18.3	138.2	506.9	314	6701.4	

Supp. Table 6 Expression patterns of genes encoding-di-GMP metabolising enzymes. Underlined genes had significant changes in their expression levels. Class I GGDEF domain proteins contain all residues that are required for catalytic activity, while Class II GGDEF domain proteins are catalytically inactive. In Class I EAL domains all residues required for c-di-GMP dependent phosphodiesterase activity are conserved. Class 2 EAL domain proteins lack the conserved loop 6, nevertheless some of these proteins have been demonstrated to possess PDE activity. Class 3 EAL domain proteins are predicted to be catalytically inactive

Name	Synonym	Product	Enzyme activity class	Effect on <i>csgD</i> expression	q-value	log fold change
adrA	STM0385	diguanylate cyclase AdrA	DGC (I)		0.00	-2.26
-	STM1697	diguanylate cyclase/phosphodiesterase domain-containing protein	No PDE (III)		0.00	1.35
gcpA	STM1987	inner membrane protein	DGC (I)	Positive	0.00	1.30
yfiN	STM2672	diguanylate cyclase/phosphodiesterase	DGC (I)		1	1.24
-	STM0343	diguanylate cyclase/phosphodiesterase domain-containing protein	PDE (I)		1	-1.04
yfeA	STM2410	diguanylate cyclase/phosphodiesterase domain-containing protein	No DGC activity, putative PDE (I, II)		1	1.04
-	STM1827.S	diguanylate cyclase/phosphodiesterase	PDE (I)	Negative	0.00	-0.68
-	STM3388	signal transduction protein	DGC (I)	Positive	1	0.58
yhdA	STM3375	regulatory protein CsrD	No PDE or DGC activity (in <i>E. coli</i>) (III, II)		1	-0.50
yeaJ	STM1283	methyl-accepting chemotaxis protein	DGC (I)		1	-0.51
rtn	STM2215	lambda/N4 phages resistance membrane protein	PDE (II)		1	0.49
yciR	STM1703	RNase II stability modulator	PDE, DGE (I, I)	Negative	1	0.43
-	STM2503	diguanylate cyclase	Probably PDE-like (I)		1	-0.42
-	STM4551	diguanylate cyclase/phosphodiesterase domain-containing protein	DGC (I)	Positive	1	0.42
yegE	STM2123	diguanylate cyclase/phosphodiesterase	DGC (I)	Positive	0.53	0.36
yjcC	STM4264	diguanylate cyclase/phosphodiesterase	PDE (I)	Negative	1	-0.35
ylaB	STM0468	diguanylate cyclase/phosphodiesterase domain-containing protein	No PDE activity (III)		1	0.34
yhjH	STM3611	diguanylate cyclase/phosphodiesterase	PDE (II)	Negative	0.05	-0.17

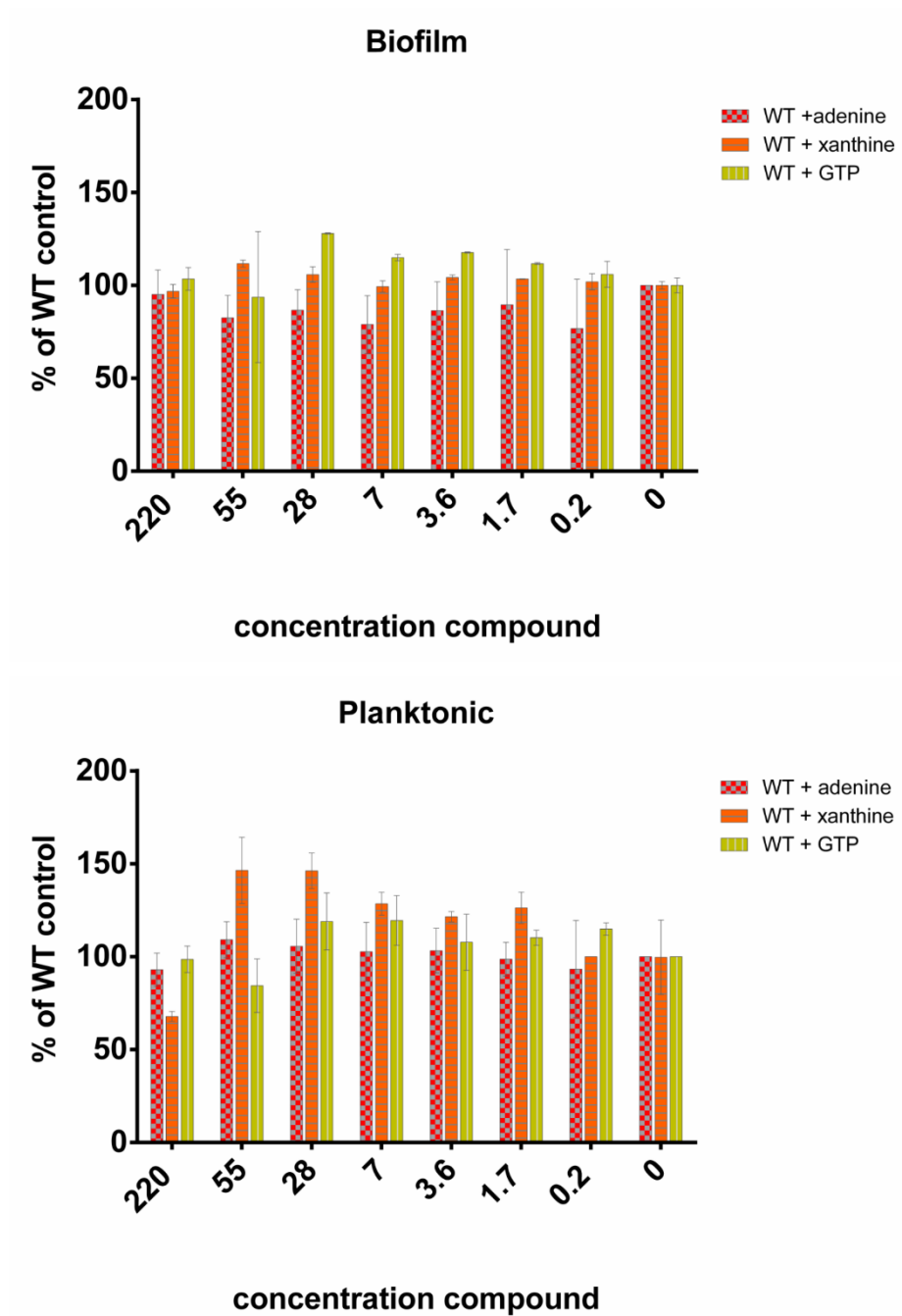
Appendix

Name	Synonym	Product	Enzyme activity class	Effect on <i>csgD</i> expression	q-value	log fold change
		terase domain-containing protein				
yhjK	STM3615	diguanylate cyclase/phosphodiesterase	Probable PDE (I)		1	0.11
ydiV	STM1344	anti-FlhC(2)FlhD(4) factor	No PDE (III)		0.03	0.04
	PSLT032	Plasmid encoded putative PDE/DGC	Unknown		0.00	-0.70

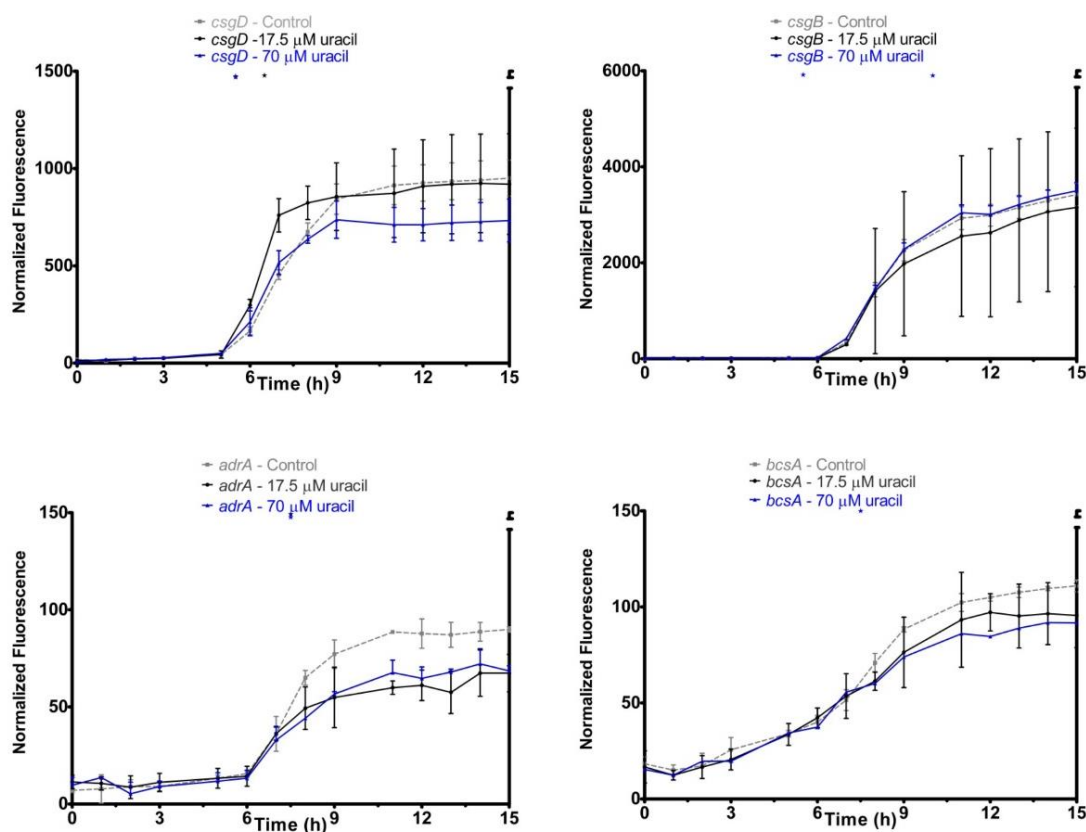
Supp. Table 7 Fold change in mRNA levels (RQ) of genes involved in adhesion and c-di-GMP metabolism

Assay	BF: Δ <i>carA</i> + 70 μ M uracil	PL: Δ <i>carA</i> + 70 μ M uracil	BF: Δ <i>carA</i> + 17.5 μ M uracil	PL: Δ <i>carA</i> + 17.5 μ M uracil	BF: Wild type	PL: Wild type
<i>adrA</i>	3.4099 \uparrow	0.6347	0.5548	0.7664	1.9588	1
<i>bcsA</i>	1.4247	0.6798	0.7285	0.8463	1.0248	1
<i>csgB</i>	5.5317 \uparrow	0.2143 \downarrow	0.0232 \downarrow	0.0116 \downarrow	3.0256 \uparrow	1
<i>csgD</i>	3.366 \uparrow	0.5153	0.2158 \downarrow	0.1986 \downarrow	1.8792	1
<i>purR</i>	0.6297	0.7557	0.683	0.709	0.5786	1
<i>gcpA</i>		0.9895		0.8973		1
STM1697		0.9685		0.9832		1
STM1827		0.8034		0.7378		1
STM2503		0.8317		1.0319		1
STM3388		0.8368		0.6268		1
<i>yciR</i>		0.7896		0.8438		1
<i>ydiV</i>		0.7489		0.7498		1
<i>yeaJ</i>		1.1564		1.2989		1
<i>yegE</i>		1.0515		1.047		1
<i>yfiN</i>		0.8836		1.1456		1
<i>yhdA</i>		0.8479		1.0521		1
<i>yhjH</i>		0.8701		1.0788		1
<i>yjcC</i>		0.8023		0.9136		1
<i>yjiE</i>		0.9355		1.3431		1

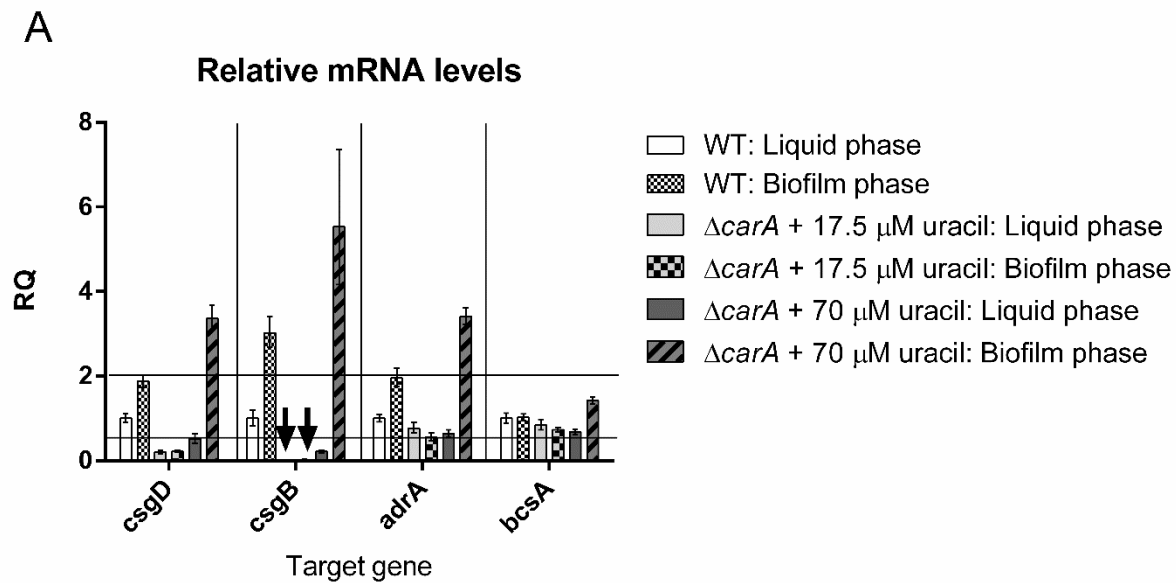
Directions of arrows indicate up or down regulation. PL and BF indicates planktonic and biofilm samples respectively.



Supp. Figure 13. Externally applied purine pathway intermediates does not have noteworthy effects on biofilm formation or planktonic growth of the wild type strain *S. Typhimurium* ATCC14028

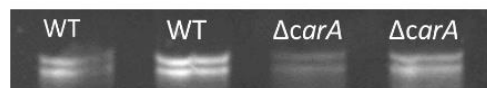


Supp. Figure 14 Normalized fluorescence of *csgD*, *csgB*, *adrA* and *bcsA* promoter fusions in the *S. Typhimurium* 14028 wild type control (light grey line) and in the presence of 17.5 and 70 μM added uracil (black line and blue line respectively), showing no noteworthy difference in transcription between the conditions. The error bars represent the standard deviations of the technical repeats (n=3). Blue starts represent significant differences between the control and 17.5 μM uracil treated condition. Black starts represent significant differences between the control and the 70 μM uracil treated condition. Experiments conducted on different occasions show similar trends.

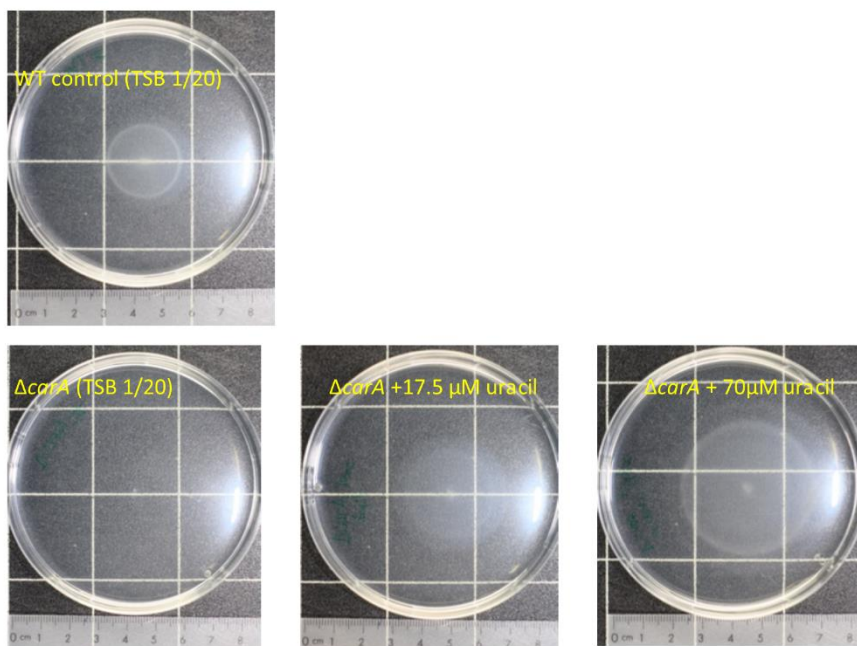


Supp. Figure 15 Relative gene expression of *csgD*, *csgB*, *adrA* and *bcsA* from free-living (planktonic) bacteria as well as surface-associated (biofilm) bacteria were determined with RT-qPCR. Panel A shows the changes in gene expression (RQ) compared to the wild type planktonic bacteria. The dotted lines indicate thresholds for fold changes. Arrows indicate that the expression of *csgB* in the pyrimidine starved $\Delta carA$ mutant was too low to be visible on the graph. The error bars in panel A represent the RQ min and max values (predicted with 95% confidence).

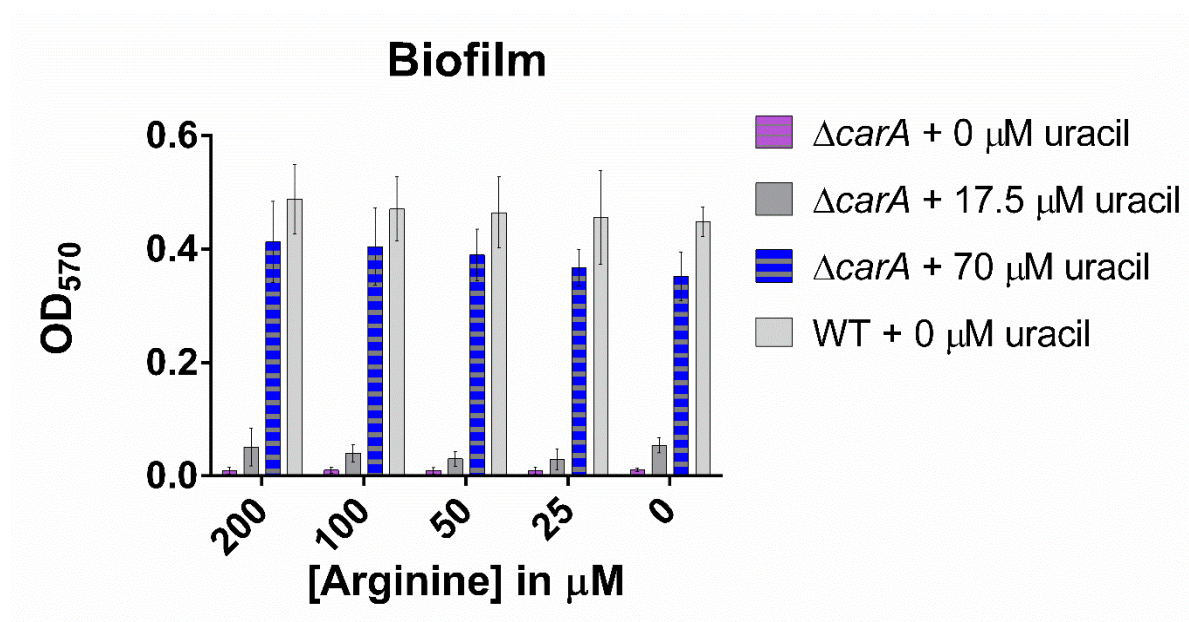
Genomic DNA fragments



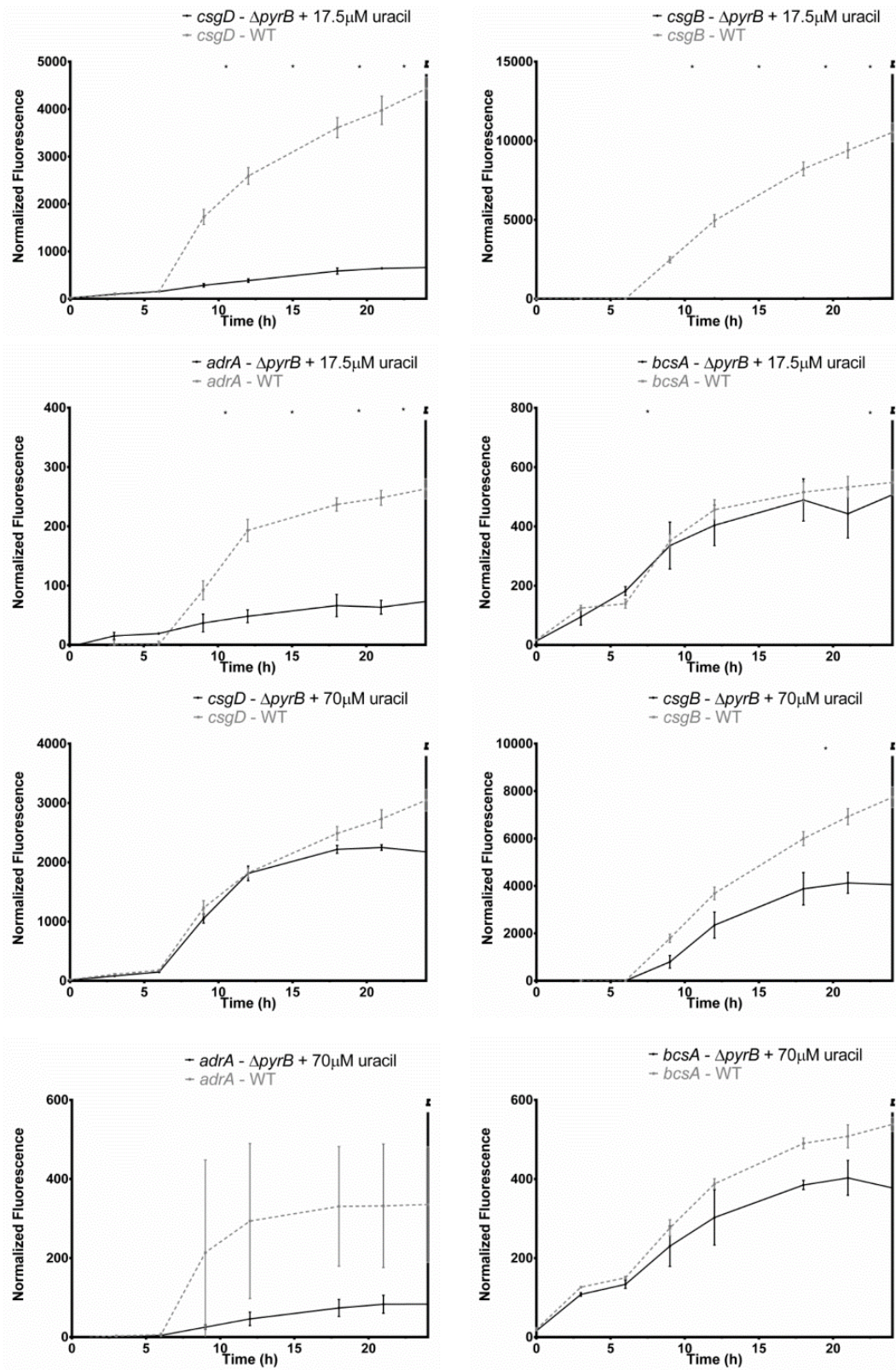
Supp. Figure 16 Fragment analysis results, obtained by amplifying the *dusB-fis* promoter region, two biological repeats were used per strain.



Supp. Figure 17 Swimming plates showing the effect of added uracil on the $\Delta carA$ mutant. Without added uracil there is very little growth and no visible swimming. When 17.5 μM was added the diameter of the colony exceeded that of the wild type control. However, the white band on the outer perimeter that is visible on the wild type colony was absent from the mutant. When 70 μM uracil was added the diameter of the colony increased even further, however, the outer white band became visible again. Medium consisting of 2% agar and TSB 1/20 were inoculated with 1 μL of normalized ONC and incubated for 24 hours at 25°C.

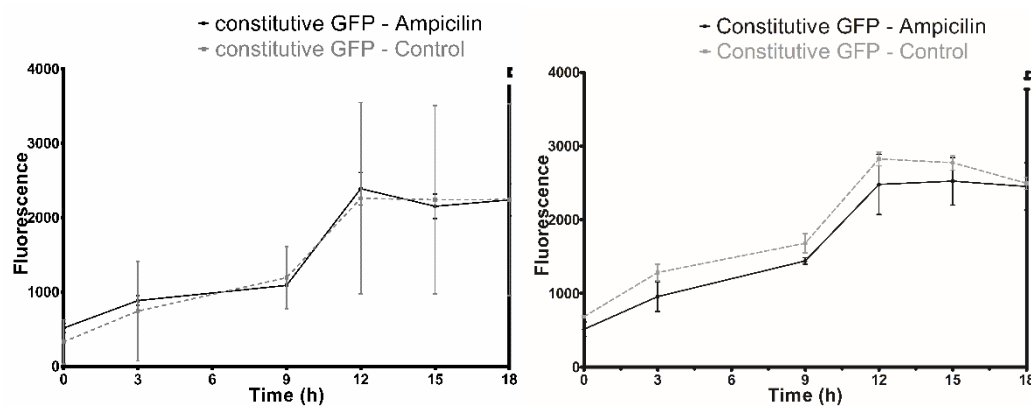


Supp. Figure 18 The addition of arginine to the wild type and the $\Delta carA$ strain does not change their biofilm phenotypes, which is a further indication that the *carA* mutants phenotype is largely determined by uracil and not by arginine. Three biological repeats for each strain were divided into three technical repeats each.



Supp. Figure 19 Normalized fluorescence of *csgD*, *csgB*, *adrA* and *bcsA* promoter fusions in the *S. Typhimurium* 14028 wild type control (WT) (light grey line) and the *S. Typhimurium* 14028 $\Delta pyrB$

mutant complemented with 17.5 μM uracil and 70 μM uracil to the mutant (black lines). These expression patterns resemble those of the *carA* mutant indicating that pyrimidine limitation affects both mutants similarly. The error bars represent the standard deviations of the technical repeats (n=3). The experiments were repeated two to four times on different days and showed similar patterns.



Supp. Figure 20 GFP was expressed constitutively from pFPV25.1. The results from the two independent experiments that are shown here indicate that the absence of ampicillin does not change the expression profile indicating that the absence of ampicillin does not negatively impact plasmid maintenance during the course of the experiment.

List of references

Abby S., and Daubin V. (2007) Comparative genomics and the evolution of prokaryotes. *Trends in Microbiology* **15**: 135-141.

Abrudan M.I., Smakman F., Grimbergen A.J., Westhoff S., Miller E.L., van Wezel G.P., and Rozen D.E. (2015) Socially mediated induction and suppression of antibiosis during bacterial coexistence. *Proceedings of the National Academy of Sciences of the United States of America* **112**: 11054-11059.

Ahmad I. (2013) PhD Thesis. Regulatory networks of c-di-GMP signalling involved in biofilm formation, motility and host pathogen interactions in *Salmonella* Typhimurium. Karolinska Institute, Sweden.

Ahmad I., Cimdins A., Beske T., and Romling U. (2017) Detailed analysis of c-di-GMP mediated regulation of *csgD* expression in *Salmonella* Typhimurium. *BMC Microbiology* **17**: 1-12.

Ahmad I., Lamprokostopoulou A., Le Guyon S., Streck E., Barthel M., Peters V., *et al.* (2011) Complex c-di-GMP signaling networks mediate transition between virulence properties and biofilm formation in *Salmonella enterica* serovar Typhimurium. *PloS One* **6**: e28351.

Alanis A.J. (2005) Resistance to antibiotics: Are we in the post-antibiotic era? *Archives of Medical Research* **36**: 697-705.

Albright L.M., Huala E., and Ausubel F.M. (1989) Prokaryotic signal transduction mediated by sensor and regulator protein pairs. *Annual Review of Genetics* **23**: 311-336.

Alhede M.a., Bjarnsholt T., Givskov M., and Alhede M. (2014) Chapter one - *Pseudomonas aeruginosa* biofilms: Mechanisms of immune evasion. *Advances in Applied Microbiology* **86**: 1-40.

Allen H.K., Moe L.A., Rodbumrer J., Gaarder A., and Handelsman J. (2008) Functional metagenomics reveals diverse beta-lactamases in a remote Alaskan soil. *The ISME Journal* **3**: 243-251.

Allen R.C., Popat R., Diggle S.P., and Brown S.P. (2014) Targeting virulence: Can we make evolution-proof drugs? *Nature Reviews Microbiology* **12**: 300-308.

Almblad H., Harrison J.J., Rybtke M., Groizeleau J., Givskov M., Parsek M.R., and Tolker-Nielsen T. (2015) The cyclic AMP-vfr signaling pathway in *Pseudomonasaeruginosa* is inhibited by cyclic di-GMP. *Journal of Bacteriology* **197**: 2190-2200.

Altier C., Suyemoto M., and Lawhon S. (2000) Regulation of *Salmonella enterica* serovar Typhimurium invasion genes by *csrA*. *Infection and Immunology* **68**: 6790-6797.

List of references

- Amikam D., and Galperin M.Y. (2006) PilZ domain is part of the bacterial c-di-GMP binding protein. *Bioinformatics* **22**: 3-6.
- Aminov R.I. (2012) The extent and regulation of lateral gene transfer in natural microbial ecosystems. In *Horizontal Gene Transfer in Microorganisms*. Francino, M.P. (ed). Caister Academic Press, pp. 93-130.
- Aminov R.I. (2010) A brief history of the antibiotic era: Lessons learned and challenges for the future. *Frontiers in Microbiology* **1**: 1-7.
- Aminov R.I. (2009) The role of antibiotics and antibiotic resistance in nature. *Environmental Microbiology Reports* **11**: 2970-2988.
- Anderson P.L., Kakuda T.N., and Lichtenstein K.A. (2004) The cellular pharmacology of nucleoside- and nucleotide-analogue reverse-transcriptase inhibitors and its relationship to clinical toxicities. *Clinical Infectious Diseases* **38**: 743-753.
- Andersson D.I., and Hughes D. (2010) Antibiotic resistance and its cost: Is it possible to reverse resistance? *Nature Reviews Microbiology* **8**: 260-271.
- Antoniani D., Rossi E., Rinaldo S., Bocci P., Lolicato M., Paiardini A., *et al.* (2013) The immunosuppressive drug azathioprine inhibits biosynthesis of the bacterial signal molecule cyclic-di-GMP by interfering with intracellular nucleotide pool availability. *Applied Microbiology and Biotechnology* **97**: 7325-7336.
- Attila C., Ueda A., and Wood T. (2009) 5-fluorouracil reduces biofilm formation in *Escherichia coli* K-12 through global regulator AriR as an antivirulence compound. *Applied Microbiology and Biotechnology* **82**: 525-533.
- Aviles B., Klotz C., Eifert J., Williams R., and Ponder M. (2013) Biofilms promote survival and virulence of *Salmonella enterica* sv. Tennessee during prolonged dry storage and after passage through an *in vitro* digestion system. *International Journal of Food Microbiology* **162**: 252-259.
- Baba T., Ara T., Hasegawa M., Takai Y., Okumura Y., Baba M., *et al.* (2006) Construction of *Escherichia coli* K-12 in-frame, single-gene knockout mutants: The Keio collection. *Molecular Systems Biology* **2**: 1-20.
- Ball C.A., Osuna R., Ferguson K.C., and Johnson R.C. (1992) Dramatic changes in Fis levels upon nutrient upshift in *Escherichia coli*. *Journal of Bacteriology* **174**: 8043-8056.
- Barak J., Gorski L., Naraghi-Arani P., and Charkowski A. (2005) *Salmonella enterica* virulence genes are required for bacterial attachment to plant tissue. *Applied and Environmental Microbiology* **71**: 5685-5691.
- Barak J.D., Liang A., and Narm K. (2008) Differential attachment to and subsequent contamination of agricultural crops by *Salmonella enterica*. *Applied and Environmental Microbiology* **74**: 5568-5570.
- Baraquet C., Murakami K., Parsek M.R., and Harwood C.S. (2012) The FleQ protein from *Pseudomonas aeruginosa* functions as both a repressor and an activator to control gene

- expression from the *pel* operon promoter in response to c-di-GMP. *Nucleic Acids Research* **40**: 7207-7218.
- Barends T.R.M., Hartmann E., Griese J.J., Beitlich T., Kirienko N.V., Ryjenkov D.A., *et al.* (2009) Structure and mechanism of a bacterial light-regulated cyclic nucleotide phosphodiesterase. *Nature* **459**: 1015-1018.
- Barker J., and Bloomfield S.F. (2000) Survival of *Salmonella* in bathrooms and toilets in domestic homes following salmonellosis. *Journal of Applied Microbiology* **89**: 137-144.
- Barner H.D., and Cohen S.S. (1954) The induction of thymine synthesis by T2 infection of a thymine requiring mutant of *Escherichia coli*. *Journal of Bacteriology* **68**: 80-88.
- Battesti A., and Bouveret E. (2006) Acyl carrier protein/SpoT interaction, the switch linking SpoT-dependent stress response to fatty acid metabolism. *Molecular Microbiology* **62**: 1048-1063.
- Bäumler A.J. (1997) The record of horizontal gene transfer in *Salmonella*. *Trends in Microbiology* **5**: 318-322.
- Beck C.F., Neuhard J., Thomassen E., Ingraham J.L., and Kleker E. (1974) *Salmonella* Typhimurium mutants defective in cytidine monophosphate kinase (*cmk*). *Journal of Bacteriology* **120**: 1370-1379.
- Beenken K.E., Dunman P.M., McAleese F., Macapagal D., Murphy E., Projan S.J., *et al.* (2004) Global gene expression in *Staphylococcus aureus* biofilms. *Journal of Bacteriology* **186**: 4665-4684.
- Beloin C., Valle J., Latour-Lambert P., Faure P., Kzreminski M., Balestrino D., *et al.* (2004) Global impact of mature biofilm lifestyle on *Escherichia coli* K-12 gene expression. *Molecular Microbiology* **51**: 659-674.
- Beraud M., Kolb A., Monteil V., D'Alayer J., and Norel F. (2010) A proteomic analysis reveals differential regulation of the S-dependent *yciGFE(katN)* locus by YncC and H-NS in *Salmonella* and *Escherichia coli* K-12. *Molecular & Cellular Proteomics* **9**: 2601-2616.
- Berleman J.E., Hasselbring B.M., and Bauer C.E. (2004) Hypercyst mutants in *Rhodospirillum centenum* identify regulatory loci involved in cyst cell differentiation. *Journal of Bacteriology* **186**: 5834-5841.
- Bernier S.P., and Surette M.G. (2013) Concentration-dependent activity of antibiotics in natural environments. *Frontiers in Microbiology* **4**: 20.
- Biaggioni I., Paul S., Puckett A., and Arzubiaga C. (1991) Caffeine and theophylline as adenosine receptor antagonists in humans. *Journal of Pharmacology and Experimental Therapeutics* **258**: 588-593.
- Bjarnsholt T., Ciofu O., Molin S., Givskov M.I., and Høiby N. (2013) Applying insights from biofilm biology to drug development -can a new approach be developed? *Nature Reviews and Drug Discovery* **12**: 791-808.

List of references

- Bjarnsholt T. (2013) The role of bacterial biofilms in chronic infections. *Acta Pathologica, Microbiologica et Immunologica Scandinavica* **121**: 1-58.
- Black R.A., Hobson A.C., and Adler J. (1980) Involvement of cyclic GMP in intracellular signaling in the chemotactic response of *Escherichia coli*. *Proceedings of the National Academy of Sciences of the United States of America* **77**: 3879-3883.
- Blackledge M.S., Worthington R.J., and Melander C. (2013) Biologically-inspired strategies for combating bacterial biofilms. *Current Opinion in Pharmacology* **13**: 699-706.
- Blair K.M., Turner L., Winkelman J.T., Berg H.C., and Kearns B. (2008) A molecular clutch disables flagella in the *Bacillus subtilis* biofilm. *Science* **320**: 1636-1638.
- Blank K., Hensel M., and Gerlach R.G. (2011) Rapid and highly efficient method for scarless mutagenesis within the *Salmonella enterica* chromosome. *PLoS One* **6**: e15763
- Bochner B.R., and Ames B.N. (1982) Complete analysis of cellular nucleotides by two-dimensional thin layer chromatography. *Journal of Biological Chemistry* **257**: 9759-9769.
- Boehm A., and Vogel J. (2012) The *csgD* mRNA as a hub for signal integration via multiple small RNAs. *Molecular Microbiology* **84**: 1-5.
- Boehm A., Steiner S., Zaehring F., Casanova A., Hamburger F., Ritz D., *et al.* (2009) Second messenger signalling governs *Escherichia coli* biofilm induction upon ribosomal stress. *Molecular Microbiology* **72**: 1500-1516.
- Boehm A., Kaiser M., Li H., Spangler C., Kasper C.A., Ackermann M., *et al.* (2010) Second messenger-mediated adjustment of bacterial swimming velocity. *Cell* **141**: 107-116.
- Bonekamp F., Clemmesen K., Karlstrom O., and Jensen K.F. (1984) Mechanism of UTP-modulated attenuation at the *pyrE* gene of *Escherichia coli*: an example of operon polarity control through the coupling of translation to transcription. *EMBO Journal* **3**: 2857-2861.
- Bordeau V., and Felden B. (2014) Curli synthesis and biofilm formation in enteric bacteria are controlled by a dynamic small RNA module made up of a pseudoknot assisted by an RNA chaperone. *Nucleic Acids Research* **42**: 4682-4696.
- Bouvier J., Patte J.C., and Stragier P. (1984) Multiple regulatory signals in the control region of the *Escherichia coli* *carAB* operon. *Proc Natl Acad Sci USA* **81**: 4139-4143.
- Boyd E.F., Wang F.S., Whittam T.S., and Selander R.K. (1996) Molecular genetic relationships of the *Salmonellae*. *Applied and Environmental Microbiology* **62**: 804-808.
- Brandl M.T., Carter M.Q., Parker C.T., Chapman M.R., Huynh S., and Zhou Y. (2011) *Salmonella* biofilm formation on *Aspergillus niger* involves cellulose--chitin interactions. *PLoS One* **6**: e25553.
- Breaker R.R. (2011) Prospects for riboswitch discovery and analysis. *Molecular Cell* **43**: 867-879.

- Brenner F.W., Villar R.G., Angulo F.J., Tauxe R., and Swaminathan B. (2000) *Salmonella* nomenclature. *Journal of Clinical Microbiology* **38**: 2465-2467.
- Brombacher E., Dorel C., Zehnder A.J.B., and Landini P. (2003) The curli biosynthesis regulator CsgD co-ordinates the expression of both positive and negative determinants for biofilm formation in *Escherichia coli*. *Microbiology* **149**: 2847-2857.
- Brophy J.A.N., and Voigt C.A. (2016) Antisense transcription as a tool to tune gene expression. *Molecular Systems Biology* **12**:854.
- Buchwald D.S., and Blaser M.J. (1984) A review of human *salmonellosis*: II. duration of excretion following infection with nontyphi *Salmonella*. *Reviews of Infectious Diseases* **6**: 345-356.
- Burhenne H., and Kaefer V. (2013) Quantification of cyclic dinucleotides by reversed-phase LC-MS/MS. In *Methods in Molecular Biology*. Gehring, C. (ed). pp. 27-37.
- Cabeza M.L., Aguirre A., Soncini F.C., and Vescovi E.G. (2007) Induction of RpoS degradation by the two-component system regulator RstA in *Salmonella enterica*. *Journal of Bacteriology* **189**: 7335-7342.
- Cai H.Y., Lu L., Muckle C.A., Prescott J.F., and Chen S. (2005) Development of a novel protein microarray method for serotyping *Salmonella enterica* strains. *Journal of Clinical Microbiology* **43**: 3427-3430.
- Campbell E.A., Westblade L.F., and Darst S.A. (2008) Regulation of bacterial RNA polymerase sigma factor activity: A structural perspective. *Current Opinion in Microbiology* **11**: 121-127.
- Cao Z., Livoti E., Losi A., and Gärtner W. (2010) A blue light-inducible phosphodiesterase activity in the cyanobacterium *Synechococcus elongatus*. *Photochemistry Photobiology* **86**: 606-611.
- Casado J.L., Valdezate S., Calderon C., Navas E., Frutos B., Guerrero A., and Martinez-Beltran J. (1999) Zidovudine therapy protects against *Salmonella* bacteremia recurrence in human immunodeficiency virus-infected patients. *Journal of Infectious Diseases* **179**: 1553-1556.
- Cegelski L., Marshall G.R., Eldridge G.R., and Hultgren S.J. (2008) The biology and future prospects of antivirulence therapies. *Nature Reviews Microbiology* **6**: 17-27.
- Center for Disease Control and Prevention. (2013) Drug resistance.) [WWW document]. URL <https://www.cdc.gov/drugresistance/pdf/ar-threats-2013-508.pdf>
- Ceri H., Olson M.E., Stremick C., Read R.R., Morck D., and Buret A. (1999) The Calgary biofilm device: New technology for rapid determination of antibiotic susceptibilities of bacterial biofilms. *Journal of Clinical Microbiology* **37**: 1771-1776.
- Chakraborty A., and Trivedi V. (2015) Streamlining the drug discovery process through repurposing of clinically approved drugs. *Austin Journal of Biotechnology and Bioengineering* **2**: 1047.

List of references

- Chan C., Paul R., Samoray D., Amiot N.C., Giese B., Jenal U., and Schirmer T. (2004) Structural basis of activity and allosteric control of diguanylate cyclase. *Proceedings of the National Academy of Sciences of the United States of America* **101**: 17084-17089.
- Chang A.L., Tuckerman J.R., Gonzalez G., Mayer R., Weinhouse H., Volman G., *et al.* (2001) Phosphodiesterase A1, a regulator of cellulose synthesis in *Acetobacter xylinum*, is a heme-based sensor. *Biochemistry* **40**: .
- Choi K.Y., and Zalkin H. (1992) Structural characterization and corepressor binding of the *Escherichia coli* purine repressor. *Journal of Bacteriology* **174**: 6207-6214.
- Chong C.R., and Sullivan D.J. (2007) New uses for old drugs. *Nature* **448**: 645-646.
- Christen M., Christen B., Folcher M., Schauerte A., and Jenal U. (2005) Identification and characterization of a cyclic di-GMP specific phosphodiesterase and its allosteric control by GTP. *Journal of Biological Chemistry* **280**: 30829-30837.
- Christen M., Kulasekara H.D., Christen B., Kulasekara B.R., Hoffman L.R., and Miller S.I. (2010) Asymmetrical distribution of the second messenger c-di-GMP upon bacterial cell division. *Science* **328**: 1295-1297.
- Clatworthy A.E., Pierson E., and Hung D.T. (2007) Targeting virulence: A new paradigm for antimicrobial therapy. *Nature Chemical Biology* **3**: 541-548.
- Coates A.R.M., Halls G., and Hu Y. (2011) Novel classes of antibiotics or more of the same? *British Journal of Pharmacology* **163**: 184-194.
- Compan I., and Touati D. (1994) Anaerobic activation of *arcA* transcription in *Escherichia coli*: Roles of *fnr* and ArcA. *Molecular Microbiology* **11**: 955-964.
- Conley M.P., Wolfe A.J., Blair D.F., and Berg H.C. (1989) Both CheA and CheW are required for reconstitution of chemotactic signaling in *Escherichia coli*. *Journal of Bacteriology* **171**: 5190-5193.
- Corrigan R.M., Campeotto I., Jeganathan T., Roelofs K.n.G., Lee V.T., and Grundling A. (2013) Systematic identification of conserved bacterial c-di-AMP receptor proteins. *Proceedings of the National Academy of Sciences of the United States of America* **110**: 9084-9089.
- Costerton J.W., Cheng K.J., Geesey G.G., Ladd T.I., Nickel J.C., Dasgupta M., and Marrie T.J. (1987) Bacterial biofilms in nature and disease. *Annual Review Of Microbiology* **41**: 435-464.
- Costerton J.W., Stewart P.S., and Greenberg E.P. (1999) Bacterial biofilms: A common cause of persistent infections. *Science* **284**: 1318-1322.
- Cox M.M., Layton S.L., Jiang T., Cole K., Hargis B.M., Berghman L.R., *et al.* (2007) Scarless and site-directed mutagenesis in *Salmonella* Enteritidis chromosome. *BMC Biotechnology* **7**: 59

- Cruickshank J.G., and Humphrey T.J. (1987) The carrier food-handler and non-typhoid salmonellosis. *Epidemiology and Infection* **98**: 223-230.
- Da Re S., and Ghigo J. (2006) A CsgD-independent pathway for cellulose production and biofilm formation in *Escherichia coli*. *Journal of Bacteriology* **188**: 3073-3087.
- Dalebroux Z.D., Svensson S.L., Gaynor E.C., and Swanson M.S. (2010) ppGpp conjures bacterial virulence. *Microbiology and Molecular Biology Reviews* **74**: 171-199.
- Dapp M.J., Clouser C.L., Patterson S., and Mansky L.M. (2009) 5-azacytidine can induce lethal mutagenesis in human immunodeficiency virus type 1. *Journal of Virology* **83**: 11950-11958.
- Dash S.S., and Gummad S.N. (2008) Inhibitory effect of caffeine on growth of various bacterial strains. *Research Journal of Microbiology* **3**: 457-465.
- Datsenko K.A., and Wanner B.L. (2000) One-step inactivation of chromosomal genes in *Escherichia coli* K-12 using PCR products. *Proceedings of the National Academy of Sciences of the United States of America* **97**: 6640-6645.
- Davey M.E., and O'Toole G.A. (2000) Microbial biofilms: From ecology to molecular genetics. *Microbiology and Molecular Biology Reviews* **64**: 847-867.
- Davies B.W., Bogard R. ., Young T.S., and Mekalanos J. . (2012) Coordinated regulation of accessory genetic elements produces cyclic di-nucleotides for *V. cholerae* virulence. *Cell* **149**: 358-370.
- Davies J. (2006a) Are antibiotics naturally antibiotics? *Journal of Industrial Microbiology and Biotechnology* **33**: 496-499.
- Davies J. (2006b) Where have all the antibiotics gone? *Canadian Journal of Infectious Diseases and Medical Microbiology* **17**: 287-290.
- Davies J., and Davies D. (2010) Origins and evolution of antibiotic resistance. *Microbiology and Molecular Biology Reviews* **74**: 417-433.
- DeLeon K., Balldin F., Watters C., Hamood A., Griswold J., Sreedharan S., and Rumbaugh K.P. (2009) Gallium maltolate treatment eradicates *Pseudomonas aeruginosa* infection in thermally injured mice. *Antimicrobial Agents and Chemotherapy* **53**: 1331-1337.
- DeMaeyer D., Weytjens B., Renkens J., DeRaedt L., and Marchal K. (2015) PheNetic: Network-based interpretation of molecular profiling data. *Nucleic Acids Research* **43**: W244-W250.
- DeMaeyer D., Renkens J., Cloots L., DeRaedt L., and Marchal K. (2013) PheNetic: Network-based interpretation of unstructured gene lists in *E. coli*. *Molecular BioSystems* **9**: 1594-1603.
- Dilmaghani M., Ahmadi M., Zahraei Salehi T., Talebi A., and Darvishzadeh R. (2010) PCR-restriction fragment length polymorphism analysis of *fljB* gene in *Salmonella enterica*

List of references

- subspecies enterica serovar Typhimurium isolated from avians. *Iranian Journal of Microbiology* **2**: 178-184.
- Doléans-Jordheim A., Bergeron E., Berezyiat F., Ben-Larbi S., Dumitrescu O., Mazoyer M., et al. (2011) Zidovudine (AZT) has a bactericidal effect on Enterobacteria and induces genetic modifications in resistant strains. *Journal of Bacteriology* **30**: 1249.
- Dombrecht B., Vanderleyden J., and Michiels J. (2001) Stable RK2-derived cloning vectors for the analysis of gene expression and gene function in gram-negative bacteria. *Molecular Plant-Microbe Interactions* **14**: 426-430.
- Drugs.com. (2017) [WWW document]. URL <http://www.drugs.com/dosage/flucytosine.html>.
- Düvel J., Bense S., Möller S., Bertinetti D., Schwede F., Morr M., et al. (2016) Application of synthetic peptide arrays to uncover cyclic-di-GMP binding motifs. *Journal of Bacteriology* **198**: 138-146.
- Düvel J., Bertinetti D., Möller S., Schwede F., Morr M., Wissing J., et al. (2012) A chemical proteomics approach to identify c-di-GMP binding proteins in *Pseudomonas aeruginosa*. *Journal of Microbiological Methods* **88**: 229-236.
- Egeblad L., Welin M., Flodin S., Gräslund S., Wang L., Balzarini J., et al. (2012) Pan-pathway based interaction profiling of FDA-approved nucleoside and nucleobase analogs with enzymes of the human nucleotide metabolism. *PloS One* **7**: e37724.
- Elwell L.P., Ferone R., Freeman G.A., Fyfe J.A., Hill J.A., Ray P.H., et al. (1987) Antibacterial activity and mechanism of action of 3'-azido-3'-deoxythymidine (BW A509U). *Antimicrobial Agents and Chemotherapy* **31**: 274-280.
- Ewald B., Sampath D., and Plunkett W. (2008) Nucleoside analogs: Molecular mechanisms signaling cell death. *Oncogene* **27**: 6522-6537.
- Fàbrega A., and Vila J. (2013) *Salmonella enterica* serovar Typhimurium skills to succeed in the host: Virulence and regulation. *Clinical Microbiology Reviews* **26**: 308-341.
- Fajardo A., and Martínez J.L. (2008) Antibiotics as signals that trigger specific bacterial responses. *Current Opinion in Microbiology* **11**: 161-167.
- Falagas M.E., Bliziotis I.A., Kasiakou S.K., Samonis G., Athanassopoulou P., and Michalopoulos A. (2005) Outcome of infections due to pandrug-resistant (PDR) gram-negative bacteria. *BMC Infectious Diseases* **5**: 1-7.
- FDA. (2008) Angiotech cvc k073520. [WWW document]. URL <https://510k.directory/clearances/K073520>.
- Figuroa-Bossi N., Uzzau S., Maloriol D., and Bossi L. (2001) Variable assortment of prophages provides a transferable repertoire of pathogenic determinants in *Salmonella*. *Molecular Microbiology* **39**: 260-272.
- Filloux A. (2012) Bacterial regulatory networks. Caister Academic Press.

- Flemming H., and Wingender J. (2010) The biofilm matrix. *Nature Reviews Microbiology* **8**: 623-633.
- Fletcher M. (1977) The effects of culture concentration and age, time, and temperature on bacterial attachment to polystyrene. *Canadian Journal of Microbiology* **23**: 1-6.
- Folkesson A., Löfdahl S., and Normark S. (2002) The *Salmonella enterica* subspecies I specific centisome 7 genomic island encodes novel protein families present in bacteria living in close contact with eukaryotic cells. *Research in Microbiology* **153**: 537-545.
- Folkesson A., Advani A., Sukupolvi S., Pfeifer J.D., Normark S., and Löfdahl S. (1999) Multiple insertions of fimbrial operons correlate with the evolution of *Salmonella* serovars responsible for human disease. *Molecular Microbiology* **33**: 612-622.
- Freeman M.W., and Dervan A.P. (2011) The path from bench to bedside: Considerations before starting the journey. *Journal of Investigative Medicine* **59**: 746-751.
- Frick M.M., Neuhard J., and Kelln R.A. (1990) Cloning, nucleotide sequence and regulation of the *Salmonella* Typhimurium *pyrD* gene encoding dihydroorotate dehydrogenase. *European Journal of Biochemistry* **194**: 573-578.
- Fuhrer T., Zampieri M., Sevin D.C., Sauer U., and Zamboni N. (2017) Genomewide landscape of gene-metabolome associations in *Escherichia coli*. *Molecular Systems Biology* **13**: .907
- Gallie J., Libby E., Bertels F., Remigi P., Jendresen C.B., Ferguson G.C., *et al.* (2015) Bistability in a metabolic network underpins the *de novo* evolution of colony switching in *Pseudomonas fluorescens*. *PLoS Biology* **13**: e1002109.
- Garau G., Di Guilmi A.M., and Hall B.G. (2005) Structure-based phylogeny of the metallo- β -lactamases. *Antimicrobial Agents and Chemotherapy* **49**: 2778-2784.
- Garavaglia M., Rossi E., and Landini P. (2012) The pyrimidine nucleotide biosynthetic pathway modulates production of biofilm determinants in *Escherichia coli*. *PloS One* **7**: e31252.
- García B., Latasa C., Solano C., Portillo F.G., Gamazo C., and Lasa I. (2004) Role of the GGDEF protein family in *Salmonella* cellulose biosynthesis and biofilm formation. *Molecular Microbiology* **54**: 264-277.
- Ge X., Kitten T., Chen Z., Lee S.P., Munro C.L., and Xu P. (2008) Identification of *Streptococcus sanguinis* genes required for biofilm formation and examination of their role in endocarditis virulence. *Infection and Immunity* **76**: 2551-2559.
- Georgellis D., Kwon O., and Lin E.C.C. (2001) Quinones as the redox signal for the Arc two-component system of bacteria. *Science* **292**: 2314.
- Gerlach P., Sogaard-Andersen L., Pedersen H., Martinussen J., Valentin-Hansen P., and Bremer E. (1991) The cyclic AMP (cAMP)-cAMP receptor protein complex functions both as an activator and as a corepressor at the *tsx*-P2 promoter of *Escherichia coli* K-12. *Journal of Bacteriology* **173**: 5419-5430.

List of references

- Gerstel U., and Römling U. (2003) The *csgD* promoter, a control unit for biofilm formation in *Salmonella* Typhimurium. *Research in Microbiology* **154**: 659.
- Gerstel U., Park C., and Romling U. (2003) Complex regulation of *csgD* promoter activity by global regulatory proteins. *Molecular Microbiology* **49**: 639.
- Giel J.L., Rodionov D.F., Liu M., Blattner F., and Kiley P.J. (2006) IscR-dependent gene expression links iron-sulphur cluster assembly to the control of O₂-regulated genes in *Escherichia coli*. *Molecular Microbiology* **60**: 1058-1075.
- Gieringer J.H., Wenz A.F., Just H.M., and Daschner F.D. (1986) Effect of 5-fluorouracil, mitoxantrone, methotrexate, and vincristine on the antibacterial activity of ceftriaxone, ceftazidime, cefotiam, piperacillin, and netilmicin. *Chemotherapy* **32**: 418-424.
- Gilbert P., and Brown M. (1995) Mechanisms of the protection of bacterial biofilms from antimicrobial agents. In *Microbial Biofilms*. Lappin-Scott, H., and Costerton, W. (eds). Cambridge: Cambridge University Press, pp. 118-131.
- Glover A.B., and Leyland-Jones B. (1987) Biochemistry of azacytidine: A review. *Cancer Treat Rep* **71**: 959-964.
- Gomelsky M., and Galperin M.Y. (2013) Bacterial second messengers, cGMP and c-di-GMP, in a quest for regulatory dominance. *EMBO Journal* **32**: 2421-2423.
- Gómez-Gómez J.M., and Amils R. (2014) Crowning: A novel *Escherichia coli* colonizing behaviour generating a self-organized corona. *BMC Research Notes* **7**: 1-10.
- Gonzalez-Escobedo G., Marshall J.M., and Gunn J.S. (2011) Chronic and acute infection of the gall bladder by *Salmonella typhi*: Understanding the carrier state. *Nature Reviews Microbiology* **9**: 9-14.
- Gordienko E.N., Kazanov M.D., and Gelfand M.S. (2013) Evolution of pan-genomes of *Escherichia coli*, *Shigella* spp., and *Salmonella enterica*. *Journal of Bacteriology* **195**: 2786-2792.
- Gotoh H., Kasaraneni N., Devineni N., Dallo S.F., and Weitao T. (2010) SOS involvement in stress-inducible biofilm formation. *Biofouling* **26**: 603-611.
- Govantes F., Albrecht J.A., and Gunsalus R.P. (2000) Oxygen regulation of the *Escherichia coli* cytochrome d oxidase (*cydAB*) operon: Roles of multiple promoters and the Fnr-1 and Fnr-2 binding sites. *Molecular Microbiology* **37**: 1456-1469.
- Gowher H., and Jeltsch A. (2004) Mechanism of inhibition of DNA methyltransferases by cytidine analogs in cancer therapy. *Cancer Biol Ther* **3**: 1062-1068.
- Grainger D.C., Hurd D., Harrison M., Holdstock J., and Busby S.J.W. (2005) Studies of the distribution of *Escherichia coli* cAMP-receptor protein and RNA polymerase along the *E. coli* chromosome. *Proceedings of the National Academy of Sciences of the United States of America* **102**: 17693-17698.

- Greenstein R.J., Su L., Haroutunian V., Shahidi A., and Brown S.T. (2006) On the action of methotrexate and 6-mercaptopurine on *M. avium* subspecies paratuberculosis. *PLoS One* **2**: e161.
- Grigg G.W. (1968) Caffeine-death in *Escherichia coli*. *Mgg* **102**: 316-335.
- Grillo-Puertas M., Rintoul M.R., and Rapisarda V.A. (2016) PhoB activation in non-limiting phosphate condition by the maintenance of high polyphosphate levels in the stationary phase inhibits biofilm formation in *Escherichia coli*. *Microbiology* **162**: 1000-1008.
- Grunberg E., Titsworth E., and Bennett M. (1963) Chemotherapeutic activity of 5-fluorocysteine. *Antimicrobial Agents and Chemotherapy* **161**: 566-568.
- Gualdi L., Tagliabue L., Bertagnoli S., Ieranò T., De Castro C., and Landini P. (2008) Cellulose modulates biofilm formation by counteracting curli-mediated colonization of solid surfaces in *Escherichia coli*. *Microbiology* **154**: 2017-2024.
- Gunn J.S., Marshall J.M., Baker S., Dongol S., Charles R.C., and Ryan E.T. (2014) *Salmonella* chronic carriage: Epidemiology, diagnosis and gallbladder persistence. *Trends in Microbiology* **22**: 648-655.
- Guttenplan S.B., and Kearns D.B. (2013) Regulation of flagellar motility during biofilm formation. *FEMS Microbiology Reviews* **37**: 849-871.
- Guzman E.C., and Martin C.M. (2015) Thymineless death, at the origin. *Frontiers in Microbiology* **6**: 499-510.
- Habazettl J., Allan M.G., Jenal U., and Grzesiek S. (2011) Solution structure of the PilZ domain protein PA4608 complex with cyclic di-GMP identifies charge clustering as molecular readout. *Journal of Biological Chemistry* **286**: 14304-14314.
- Hakala K., Van Landeghem S., Salakoski T., Van d.P., and Ginter F. (2015) Application of the EVEX resource to event extraction and network construction: Shared task entry and result analysis. *BMC Bioinformatics* **16**: S3-S3.
- Hall B.G., and Barlow M. (2004) Evolution of the serine β -lactamases: Past, present and future. *Drug Resistance Updates* **7**: 111-123.
- Hammar M., Arnqvist A., Bian Z., Olsén A., and Normark S. (1995) Expression of two *csg* operons is required for production of fibronectin- and congo red-binding curli polymers in *Escherichia coli* K-12. *Molecular Microbiology* **18**: 661-670.
- Han H.S., Anderson A.J., Yang K.Y.C., B.H., Kim K.Y., Lee M.C., Kim Y.H., and Kim C. (2006) Multiple determinants influence root colonization and induction of induced systemic resistance by *Pseudomonas chlororaphis* O6. *Molecular Plant Pathology* **7**: 463-472.
- Haneda T., Ishii Y., Danbara H., and Okada N. (2009) Genome-wide identification of novel genomic islands that contribute to *Salmonella* virulence in mouse systemic infection. *FEMS Microbiology Letters* **297**: 241-249.

List of references

- Hänsch G. (2012) Host defence against bacterial biofilms: “Mission impossible”? *ISRN Immunology* **2012**: 1-17.
- Heidelberger C., Chaudhuri N.K., Danneberg P., Mooren D., Griesbach L., Duschinsky R., *et al.* (1957) Fluorinated pyrimidines, A new class of tumour-inhibitory compounds. *Nature* **179**: 663-666.
- Hengge R. (2009) Principles of c-di-GMP signalling in bacteria. *Nature Reviews Microbiology* **7**: 262-273.
- Hensel M., Shea J.E., Bäumlner A.J., Gleeson C., Blattner F., and Holden D.W. (1997) Analysis of the boundaries of *Salmonella* pathogenicity island 2 and the corresponding chromosomal region of *Escherichia coli* K-12. *Journal of Bacteriology* **179**: 1105-1111.
- Hermans K. (2011) PhD Thesis. Functional genome-wide analysis of *Salmonella* Typhimurium biofilm formation. KU Leuven, Belgium.
- Hermans K., Nguyen T.L.A., Roberfroid S., Schoofs G., Verhoeven T., De Coster D., *et al.* (2011) Gene expression analysis of monospecies *Salmonella* Typhimurium biofilms using differential fluorescence induction. *Journal of Microbiological Methods* **84**: 467-478.
- Herth W., and Schnepf E. (1980) The fluorochrome, calcofluor white, binds oriented to structural polysaccharide fibrils. *Protoplasma* **105**: 129-133.
- Hickman J.W., and Harwood C.S. (2008) Identification of FleQ from *Pseudomonas aeruginosa* as a c-di-GMP-responsive transcription factor. *Molecular Microbiology* **69**: 376-389.
- Hirsch M., and Elliott T. (2005) Fis regulates transcriptional induction of RpoS in *Salmonella enterica*. *Journal of Bacteriology* **187**: 1568-1580.
- Hisert K.B., MacCoss M., Shiloh M.U., Darwin K.H., Singh S., Jones R.A., *et al.* (2005) A glutamate-alanine-leucine (EAL) domain protein of *Salmonella* controls bacterial survival in mice, antioxidant defence and killing of macrophages: Role of cyclic diGMP. *Molecular Microbiology* **56**: 1234-1245.
- Hosseinkhan N., Zarrineh P., Rokni-Zadeh H., Ashouri M.R., and Masoudi-Nejad A. (2015) Co-expressional conservation in virulence and stress related genes of three gammaproteobacterial species: *Escherichia coli*, *Salmonella enterica* and *Pseudomonas aeruginosa*. *Molecular BioSystems* **11**: 3137-3148.
- Houlberg U., and Jensen K.F. (1983) Role of hypoxanthine and guanine in regulation of *Salmonella* Typhimurium *pur* gene expression. *Journal of Bacteriology* **153**: 837-845.
- Hu M., Zhang C., Mu Y., Shen Q., and Feng Y. (2010) Indole affects biofilm formation in bacteria. *Indian Journal of Microbiol* **50**: 362-368.
- Huang B., Whitchurch C.B., and Mattick J.S. (2003) FimX, a multidomain protein connecting environmental signals to twitching motility in *Pseudomonas aeruginosa*. *Journal of Bacteriology* **185**: 7068-7076.

- Hussain M., Collins C., Hastings J.G.M., and White P.J. (1992) Radiochemical assay to measure the biofilm produced by coagulase-negative staphylococci on solid surfaces and its use to quantitate the effects of various antibacterial compounds on the formation of the biofilm. *Journal of Medical Microbiology* **37**: 62-69.
- Ibanez-Ruiz M., Robbe-Saule V., Hermant D., Labrude S., and Norel F. (2000) Identification of RpoS (sigma(S))-regulated genes in *Salmonella enterica* serovar Typhimurium. *Journal of Bacteriology* **182**: 5749-5756.
- Imperi F., Massai F., Facchini M., Frangipani E., Visaggio D., Leoni L., *et al.* (2013) Repurposing the antimycotic drug flucytosine for suppression of *Pseudomonas aeruginosa* pathogenicity. *Proceedings of the National Academy of Sciences of the United States of America* **110**: 7458-7463.
- Ingraham H.A., Tseng B.Y., and Goulian M. (1982) Nucleotide levels and incorporation of 5-fluorouracil and uracil into DNA of cells treated with 5-fluorodeoxyuridine. *Molecular Pharmacology* **21**: 211.
- Jacobsen A., Hendriksen R.S., Aaresturp F.M., Ussery D.W., and Friis C. (2011) The *Salmonella enterica* pan-genome. *Microbial Ecology* **62**: 487-504.
- Janga S., and Contreras-Moreira B. (2010) Dissecting the expression patterns of transcription factors across conditions using an integrated network-based approach. *Nucleic Acids Research* **38**: 6841-6856.
- Janssens J.C.A., Steenackers H., Robijns S., Gellens E., Levin J., Zhao H., *et al.* (2008) Brominated furanones inhibit biofilm formation by *Salmonella enterica* serovar Typhimurium. *Applied and Environmental Microbiology* **74**: 6639-6648.
- Jarvik T., Smillie C., Groisman E.A., and Ochman H. (2010) Short-term signatures of evolutionary change in the *Salmonella enterica* serovar Typhimurium 14028 genome. *Journal of Bacteriology* **192**: 560-567.
- Jayabalan R., Malbaša R.V., Lončar E.S., Vitas J.S., and Sathishkumar M. (2014) A review on kombucha tea—Microbiology, composition, fermentation, beneficial effects, toxicity, and tea fungus. *Comprehensive Reviews in Food Science and Food Safety* **13**: 538-550.
- Jenkins C., and Gillespie S.H. (2006) *Salmonella* spp. In Principles and Practice of Clinical Bacteriology. Gillespie, S.H., and Hawkey, P.M. (eds). John Wiley & Sons, Ltd, pp. 367-376.
- Jensen K.F. (1993) The *Escherichia coli* K-12 "wild types" W3110 and MG1655 have an *rph* frameshift mutation that leads to pyrimidine starvation due to low *pyrE* expression levels. *Journal of Bacteriology* **175**: 3401-3407.
- Jensen K.F., Neuhaard J., and Schack L. (1982) RNA polymerase involvement in the regulation of expression of *Salmonella* Typhimurium *pyr* genes. isolation and characterization of a fluorouracil-resistant mutant with high, constitutive expression of the *pyrB* and *pyrE* genes due to a mutation in *rpoBC*. *EMBO Journal* **1**: 69-74.

List of references

- Jensen K., Dandanell G., Hove-Jensen B., and Willemoës M. (2008) Nucleotides, nucleosides, and nucleobases. *EcoSal Plus* **3**: 10.1128/ecosalplus.3.6.2.
- Jensen K.F. (1988) Hyper-regulation of *pyr* gene expression in *Escherichia coli* cells with slow ribosomes. *European Journal of Biochemistry* **175**: 587-593.
- Jishage M., and Ishihama A. (1998) A stationary phase protein in *Escherichia coli* with binding activity to the major sigma subunit of RNA polymerase. *Proceedings of the National Academy of Sciences of the United States of America* **95**: 4953-4958.
- Jonas K., Edwards A.N., Ahmad I., Romeo T., Römling U., and Melefors Å. (2009) Complex regulatory network encompassing the *csr*, c-di-GMP and motility systems of *Salmonella Typhimurium*. *Environmental Microbiology Reports* **12**: 524-540.
- Jordheim L.P., Ben Larbi S., Fendrich O., Ducrot C., Bergeron E., Dumontet C., *et al.* (2012) Gemcitabine is active against clinical multiresistant *Staphylococcus aureus* strains and is synergistic with gentamicin. *International Journal of Antimicrobial Agents* **39**: 444-447.
- Jordheim L.P., Durantel D., Zoulim F., and Dumontet C. (2013) Advances in the development of nucleoside and nucleotide analogues for cancer and viral diseases. *Nature Reviews Drug Discovery* **12**: 447-464.
- Kader A., Simm R., Gerstel U., Morr M., and Römling U. (2006) Hierarchical involvement of various GGDEF domain proteins in rdar morphotype development of *Salmonella enterica* serovar Typhimurium. *Molecular Microbiology* **60**: 602-616.
- Kalia D., Merey G., Nakayama S., Zheng Y., Zhou J., Luo Y., *et al.* (2013) Nucleotide, c-di-GMP, c-di-AMP, cGMP, cAMP, (p)ppGpp signaling in bacteria and implications in pathogenesis. *Chemical Society Reviews* **42**: 305-341.
- Kanehisa M., and Goto S. (2000) KEGG: Kyoto encyclopedia of genes and genomes. *Nucleic Acids Research* **28**: 27-30.
- Kang Y., Weber K.D., Qiu Y., Kiley P.J., and Blattner F.R. (2004) Genome-wide expression analysis indicates that FNR of *Escherichia coli* K-12 regulates a large number of genes of unknown function. *Journal of Bacteriology* **187**: 1135-1160.
- Kawamukai M., Murao K., Utsumi R., Himeno M., and Komano T. (1986) Cell filamentation in an *Escherichia coli* K-12 *fic* mutant caused by theophylline or an adenylate cyclase gene (*cya*)-containing plasmid. *FEMS Microbiology Letters* **34**: 117-120.
- Keseler I.M., Mackie A., Peralta-Gil M., Santos-Zavaleta A., Gama-Castro S., Bonavides-Martínez C., *et al.* (2013) EcoCyc: Fusing model organism databases with systems biology. *Nucleic Acids Research* **41**: D605-D612.
- Khoroshilova N., Popescu C., Münck E., Beinert H., and Kiley P.J. (1997) Iron-sulfur cluster disassembly in the FNR protein of *Escherichia coli* by O₂: [4Fe-4S] to [2Fe-2S] conversion with loss of biological activity. *Proceedings of the National Academy of Sciences* **94**: 6087-6092.

- Kim J.K., Kwon J.Y., Kim S.K., Han S.H., Won Y.J., Lee J.H., *et al.* (2014) Purine biosynthesis, biofilm formation, and persistence of an insect-microbe gut symbiosis. *Applied and Environmental Microbiology* **80**: 4374-4382.
- Kim J., Sahu S., Yau Y., Wang X., Shochat S.G., Nielsen P.H., *et al.* (2016a) Detection of pathogenic biofilms with bacterial amyloid targeting fluorescent probe, CDy11. *Journal of the American Chemical Society* **138**: 402-407.
- Kim J., Webb A., Kershner J., Balaskowski S. and Copley S. (2014) A versatile and highly efficient method for scarless genome editing in *Escherichia coli* and *Salmonella enterica*. *BMC Biotechnology* **148**: 14
- Kim P.S., Zlatanovic J., Korelitz B.I., and Gleim G.W. (1999) Optimum duration of treatment with 6-mercaptopurine for Crohn's disease. *American Journal of Gastroenterology* **94**: 3254-3257.
- Kim S., Thiessen P.A., Bolton E.E., Chen J., Fu G., Gindulyte A., *et al.* (2016b) PubChem substance and compound databases. *Nucleic Acids Research* **44**: D1202-13.
- Knudsen G.M., Olsen J.E., Aabo S., Barrow P., Rychlik I., and Thomsen L.E. (2013) ClpP deletion causes attenuation of *Salmonella* Typhimurium virulence through mis-regulation of RpoS and indirect control of CsrA and the SPI genes. *Microbiology* **159**: 1497-1509.
- Kozak G.K., MacDonald D., Landry L., and Farber J.M. (2013) Foodborne outbreaks in Canada linked to produce: 2001 through 2009. *Journal of Food Protection* **76**: 173-183.
- Kozmin S.G., Wang J., and Schaaper R.M. (2010) Role for CysJ flavin reductase in molybdenum cofactor-dependent resistance of *Escherichia coli* to 6-N-hydroxylaminopurine. *Journal of Bacteriology* **192**: 2026-2033.
- Krasteva P.V., Giglio K.M., and Sondermann H. (2012) Sensing the messenger: The diverse ways that bacteria signal through c-di-GMP. *Protein Science* **21**: 929-948.
- Krishnan M.Y., Manning E.J.B., and Collins M.T. (2009) Effects of interactions of antibacterial drugs with each other and with 6-mercaptopurine on in vitro growth of *Mycobacterium avium* subspecies *paratuberculosis*. *Journal of Antimicrobial Chemotherapy* **64**: 1018-1023.
- Kröger C., Colgan A., Srikumar S., Händler K., Sivasankaran S.K., Hammarlöf D.L., *et al.* (2013) An infection-relevant transcriptomic compendium for *Salmonella enterica* serovar Typhimurium. *Cell Host and Microbe* **14**: 683-695.
- Kroupitski Y., Pinto R., Brandl M.T., Belausov E., and Sela S. (2009) Interactions of *Salmonella enterica* with lettuce leaves. *Journal of Applied Microbiology* **106**: 1876-1885.
- Kuo S.C., and Koshland D.E. (1989) Multiple kinetic states for the flagellar motor switch. *Journal of Bacteriology* **171**: 6279-6287.
- Kurtz S., Ong K., Lau E., Mowat F., and Halpern M. (2007) Projections of primary and revision hip and knee arthroplasty in the united states from 2005 to 2030. *The Journal of Bone and Joint Surgery* **89**: 780-785.

List of references

- Lamarche M.G., Wanner B.L., Crepin S., and Harel J. (2008) The phosphate regulon and bacterial virulence: A regulatory network connecting phosphate homeostasis and pathogenesis. *FEMS Microbiology Reviews* **32**: 461-473.
- Lamont I.L., Beare P.A., Ochsner U., Vasil A.I., and Vasil M.L. (2002) Siderophore-mediated signaling regulates virulence factor production in *Pseudomonas aeruginosa*. *Proceedings of the National Academy of Sciences of the United States of America* **99**: 7072-7077.
- Lamprokostopoulou A., Monteiro C., Rhen M., and Römling U. (2010) Cyclic di-GMP signalling controls virulence properties of *Salmonella enterica* serovar Typhimurium at the mucosal lining. *Environmental Microbiology Reports* **12**: 40-53.
- Landini P. (2009) Cross-talk mechanisms in biofilm formation and responses to environmental and physiological stress in *Escherichia coli*. *Research in Microbiology* **160**: 259-266.
- Landini P., Antoniani D., Burgess J.G., and Nijland R. (2010) Molecular mechanisms of compounds affecting bacterial biofilm formation and dispersal. *Applied Microbiology and Biotechnology* **86**: 813-823.
- Lapaglia C., and Hartzell P.L. (1997) Stress-induced production of biofilm in the hyperthermophile *Archaeoglobus fulgidus*. *Applied and Environmental Microbiology* **63**: 3158-3163.
- Lapierre P., and Gogarten J.P. (2009) Estimating the size of the bacterial pan-genome. *Trends in Genetics* **25**: 107-110.
- Lapouge K., Schubert M., Allain F.H.-., and Haas D. (2008) Gac/rsm signal transduction pathway of γ -proteobacteria: From RNA recognition to regulation of social behaviour. *Molecular Microbiology* **67**: 241-253.
- Latasa C., Roux A., Toledo-Arana A., Ghigo J., Gamazo C., Penadés J., and Lasa I. (2005) BapA, a large secreted protein required for biofilm formation and host colonization of *Salmonella enterica* serovar enteritidis. *Molecular Microbiology* **58**: 1322-1339.
- Latasa C., Solano C., Penadés J.R., and Lasa I. (2006) Biofilm-associated proteins. *Comptes Rendus Biologies* **329**: 849-857.
- Laventie B., Nesper J., Ahrné E., Glatter T., Schmidt A., and Jenal U. (2015) Capture compound mass spectrometry - a powerful tool to identify novel c-di-GMP effector proteins. *Journal of Visualized Experiments* e51404.
- Le Guyon S., Simm R., Rehn M., and Römling U. (2015) Dissecting the cyclic di-guanylate monophosphate signalling network regulating motility in *Salmonella enterica* serovar Typhimurium. *Environmental Microbiology Reports* **17**: 1310-1320.
- Lee E.R., Baker J.L., Weinberg Z., Sudarsan N., and Breaker R.R. (2010) An allosteric self-splicing ribozyme triggered by a bacterial second messenger. *Science* **329**: 845-848.

- Lee H., Shin J.U., and Lee K.H. (2015) The clinical efficacy of azathioprine in Korean patients with atopic dermatitis. *Annals of Dermatology* **27**: 774-775.
- Lee J., Page R., García-Contreras R., Palermino J., Zhang X., Doshi O., *et al.* (2007a) Structure and function of the *E. coli* protein YmgB: A protein critical for biofilm formation and acid-resistance. *Journal of Molecular Biology* **373**: 11-26.
- Lee K.g., Yeo W., and Roe J. (2008) Oxidant-responsive induction of the *suf* operon, encoding a Fe-S assembly system, through Fur and IscR in *Escherichia coli*. *Journal of Bacteriology* **190**: 8244-8247.
- Lee V.T., Matewish J.M., Kessler J.L., Hyodo M., Hayakawa Y., and Lory S. (2007b) A cyclic-di-GMP receptor required for bacterial exopolysaccharide production. *Molecular Microbiology* **65**: 1474-1484.
- Lele O.H., Maniar J.A., Chakravorty R.L., Vaidya S.P., and Chpudhary A.S. (2016) Assessment of biological activities of caffeine. *International Journal of Current Microbiology and Applied Sciences* **5**: 45-53.
- Lewin C.S., Allen R.A., and Amyes S.G.B. (1990a) Mechanisms of zidovudine resistance in bacteria. *Journal of Medical Microbiology* **33**: 235-238.
- Lewin C.S., Watt B., Paton R., and Amyes S.G.B. (1990b) Isolation of zidovudine resistant *Escherichia coli* from AIDS patients. *FEMS Microbiology Letters* **70**: 141-143.
- Lieb M. (1961) Enhancement of ultraviolet-induced mutation in bacteria by caffeine. *Zeitschrift Für Vererbungslehre* **92**: 416-429.
- Linares J.F., Gustafsson I., Baquero F., and Martinez J.L. (2006) Antibiotics as intermicrobial signaling agents instead of weapons. *Proceedings of the National Academy of Sciences of the United States of America* **103**: 19484-19489.
- Lipsitch M., and Samore M.H. (2002) Antimicrobial use and antimicrobial resistance: A population perspective. *Emerg Infect Diseases* **8**: 347-354.
- Lo J.C., Kazemi M.R., Hsue P.Y., Martin J.N., Deeks S.G., Schambelan M., and Mulligan K. (2005) The relationship between nucleoside analogue treatment duration, insulin resistance, and fasting arterialized lactate level in patients with HIV infection. *Clinical Infectious Diseases* **41**: 1335-1340.
- Longley D.B., Harkin D.P., and Johnston P.G. (2003) 5-fluorouracil: Mechanisms of action and clinical strategies. *Nature Reviews Cancer* **3**: 330-338.
- Lovering A.L., Capeness M.J., Lambert C., Hopley L., and Sockett R. (2011) The structure of an unconventional HD-GYP protein from *Bdellovibrio* reveals the roles of conserved residues in this class of cyclic-di-GMP phosphodiesterases. *mBio* **2**: e00163-11.
- Mah T.C., and O'Toole G.A. (2001) Mechanisms of biofilm resistance to antimicrobial agents. *Trends in Microbiology* **9**: 34-39.

List of references

- Majowicz S.E., Musto J., Scallan E., Angulo F.J., Kirk M., O'Brien S.J., *et al.* (2010) The global burden of nontyphoidal *Salmonella* gastroenteritis. *Clinical Infectious Diseases* **50**: 882-889.
- Malachowa N., Kobayashi S.D., Braughton K.R., and DeLeo F.R. (2013) Mouse model of *Staphylococcus aureus* skin infection. *Methods in Molecular Biology* **1031**: 109-116.
- Maley A., and Swerlick R.A. (2015) Azathioprine treatment of intractable pruritus: A retrospective review. *Journal of the American Academy of Dermatology* **73**: 439-443.
- Marden J.N., Dong Q., Roychowdhury S., Berleman J.E., and Bauer C.E. (2011) Cyclic GMP controls *R. centenum* cyst development. *Molecular Microbiology* **79**: 600-615.
- Marin C., Hernandez A., and Lainez M. (2009) Biofilm development capacity of *Salmonella* strains isolated in poultry risk factors and their resistance against disinfectants. *Poultry Science* **88**: 424-431.
- Martínez J.L. (2008) Antibiotics and antibiotic resistance genes in natural environments. *Science* **321**: 365-367.
- Marzan L.W., and Shimizu K. (2011) Metabolic regulation of *Escherichia coli* and its *phoB* and *phoR* genes knockout mutants under phosphate and nitrogen limitations as well as at acidic condition. *Microbial Cell Factories* **10**: 39-39.
- Massie J.P., Reynolds E.L., Koestler B.J., Cong J., Agostoni M., and Waters C.M. (2012) Quantification of high-specificity cyclic diguanylate signaling. *Proceedings of the National Academy of Sciences of the United States of America* **109**: 12746-12751.
- Max V. Ranall, Mark S. Butler, and Mark A.B.a. (2012) Resolving biofilm infections: Current therapy and drug discovery strategies. *Current Drug Targets* **13**: 1375-1385.
- McClure R., Balasubramanian D., Sun Y., Bobrovskyy M., Sumbly P., Genco C.A., *et al.* (2013) Computational analysis of bacterial RNA-seq data. *Nucleic Acids Research* **41**: e140-e140.
- McDonough K.A., and Rodriguez A. (2012) The myriad roles of cyclic AMP in microbial pathogens: From signal to sword. *Nature Reviews Microbiology* **10**: 27-38.
- McGann P., Snesrud E., Maybank R., Corey B., Ong A.C., Clifford R., *et al.* (2016) *Escherichia coli* harboring *mcr-1* and *bla*CTX-M on a novel IncF plasmid: First report of *mcr-1* in the USA. *Antimicrobial Agents and Chemotherapy* **60**: 4420-4421.
- Meng L.M., Kilstrup M., and Nygaard P. (1990) Autoregulation of PurR repressor synthesis and involvement of *purR* in the regulation of *purB*, *purC*, *purL*, *purMN* and *guaBA* expression in *Escherichia coli*. *European Journal of Biochemistry* **187**: 373-379.
- Messenger L.J., and Zalkin H. (1979) Glutamine phosphoribosylpyrophosphate amidotransferase from *Escherichia coli*. purification and properties. *Journal of Biological Chemistry* **254**: 3382-3392.

- Militello K.T., Simon R.D., Mandarano A.H., DiNatale A., Hennick S.M., Lazatin J.C., and Cantatore S. (2016) 5-azacytidine induces transcriptome changes in *Escherichia coli* via DNA methylation-dependent and DNA methylation-independent mechanisms. *BMC Microbiology* **16**: 130.
- Mitchell J.E., Oshima T., Piper S.E., Webster C.L., Westblade L.F., Karimova G., *et al.* (2007) The *Escherichia coli* regulator of sigma 70 protein, *rsd*, can up-regulate some stress-dependent promoters by sequestering sigma 70. *Journal of Bacteriology* **189**: 3489-3495.
- Morgan J.L.W., McNamara J.T., and Zimmer J. (2014) Mechanism of activation of bacterial cellulose synthase by cyclic di-GMP. *Nature Structural Molecular Biololgy* **21**: 489-496.
- Muchmore C.R.A., Krahn J.M., Smith J.L., Kim J.H., and Zalkin H. (1998) Crystal structure of glutamine phosphoribosylpyrophosphate amidotransferase from *Escherichia coli*. *Protein Science* **7**: 39-51.
- Mulas F., Li A., Sherr D.H., and Monti S. (2017) Network-based analysis of transcriptional profiles from chemical perturbations experiments. *BMC Bioinformatics* **18**: 130.
- Munck C., Gumpert H.K., Nilsson Wallin A.,I., Wang H.H., and Sommer M.O.A. (2014) Prediction of resistance development against drug combinations by collateral responses to component drugs. *Science Translational Medicine* **6**: 262ra156-262ra156.
- Musher D.M., and Rubenstein A. (1973) Permanent carriers of nontyphosa *Salmonellae*. *Archives of Internal Medicine* **132**: 869-872.
- Nazaret S., and Aminov R. (2014) Role and prevalence of antibiosis and the related resistance genes in the environment. *Frontiers in Microbiology* **5**: 520.
- Nelson J.W., Sudarsan N., Furukawa K., Weinberg Z., Wang J.X., and Breaker R.R. (2013) Riboswitches in Eubacteria sense the second messenger c-di-AMP. *Nature Chemical Biology* **9**: 834-839.
- Nelson J.W., Sudarsan N., Phillips G.E., Stav S., Lünse C.E., McCown P.J., and Breaker R.R. (2015) Control of bacterial exoelectrogenesis by c-AMP-GMP. *Proceedings of the National Academy of Sciences of the United States of America* **112**: 5389-5394.
- Nesper J., Reinders A., Glatter T., Schmidt A., and Jenal U. (2012) A novel capture compound for the identification and analysis of cyclic di-GMP binding proteins. *Journal of Proteomics* **75**: 4874-4878.
- Neuhard J., and Kelln R. (1996) Biosynthesis and conversion of pyrimidines. *Escherichia coli and Salmonella: Cellular and Molecular Biology*, **1**: 580-599
- Newell P.D., Boyd C.D., Sondermann H., and O'Toole G.A. (2011) A c-di-GMP effector system controls cell adhesion by inside-out signaling and surface protein cleavage. *PLOS Biology* **9**: e1000587.
- Nguyen Le Minh P., de Cima S., Bervoets I., Maes D., Rubio V., and Charlier D. (2015) Ligand binding specificity of RutR, a member of the TetR family of transcription regulators in *Escherichia coli*. *FEBS Open Bio* **5**: 76-84.

List of references

- Nickel J.C., Ruseska I., Wright J.B., and Costerton J.W. (1985) Tobramycin resistance of *Pseudomonas aeruginosa* cells growing as a biofilm on urinary catheter material. *Antimicrobial Agents and Chemotherapy* **27**: 619-624.
- Norizan S., Yin W., and Chan K. (2013) Caffeine as a potential quorum sensing inhibitor. *Sensors* **13**: 5117-5129.
- Nygaard P. (1983) Utilization of preformed purine bases and nucleosides. In *Metabolism of nucleotides, nucleotides and nucleobases in microorganisms*. Munch-Peterson, A. (ed). London: Academic Press, pp. 27-93.
- Nyhlén A., Ljungberg B., Nilsson-Ehle I., and Odenholt I. (2002) Bactericidal effect of combinations of antibiotic and antineoplastic agents against *Staphylococcus aureus* and *Escherichia coli*. *Chemotherapy* **48**: 71-77.
- O'Neill J. (2014) Antimicrobial resistance: Tackling a crisis for the health and wealth of nations. [WWW document]. URL <http://amr-review.org/Publications..>
- Ochman H., Lawrence J.G., and Groisman E.A. (2000) Lateral gene transfer and the nature of bacterial innovation. *Nature* **405**: 299-304.
- O'Donnell M., Langston L., and Stillman B. (2013) Principles and concepts of DNA replication in bacteria and eukarya. *Cold Spring Harbour Perspectives on Biology* **5**: 10.1101/cshperspect.a010108 a010108.
- Ogasawara H., Yamamoto K., and Ishihama A. (2011) Role of the biofilm master regulator CsgD in cross-regulation between biofilm formation and flagellar synthesis. *Journal of Bacteriology* **193**: 2587-2597.
- Oggioni M.R., Trappetti C., Kadioglu A., Cassone M., Iannelli F., Ricci S., *et al.* (2006) Switch from planktonic to sessile life: A major event in pneumococcal pathogenesis. *Molecular Microbiology* **61**: 1196-1210.
- Olszowy J., and Switzer R.L. (1972) Specific repression of phosphoribosylpyrophosphate synthetase by uridine compounds in *Salmonella Typhimurium*. *Journal of Bacteriology* **110**: 450-451.
- Oppenheimer-Shanaan S.Y., Wexselblatt E.I., Katzhendler J., Yavin E., and Ben-Yehuda S. (2011) C-di-AMP reports DNA integrity during sporulation in *Bacillus subtilis*. *EMBO Reports* **12**: 594-601.
- Osuna R., Lienau D., Hughes K.T., and Johnson R.C. (1995) Sequence, regulation, and functions of *fis* in *Salmonella Typhimurium*. *Journal of Bacteriology* **177**: 2021-2032.
- O'Toole G.A., Kaplan H.B., and Kolter R. (2000) Biofilm formation as microbial development. *Annual Review Of Microbiology* **54**: 49-79.
- O'Toole G.A., and Stewart P.S. (2005) Biofilms strike back. *Nature Biotechnology* **23**: 1378-1379.

- Otto K., and Silhavy T.J. (2002) Surface sensing and adhesion of *Escherichia coli* controlled by the Cpx-signaling pathway. *Proceedings of the National Academy of Sciences* **99**: 2287-2292.
- Park S.R., Tripathi A., Wu J., Schultz P.J., Yim I., McQuade T.J., *et al.* (2016) Discovery of cahuitamycins as biofilm inhibitors derived from a convergent biosynthetic pathway. *Nature Communications* **7**: 10710.
- Parker W.B. (2009) Enzymology of purine and pyrimidine antimetabolites used in the treatment of cancer. *Chemical Reviews* **109**: 2880-2893.
- Partridge J.D., Sanguinetti G., Dibden D.P., Roberts R.E., Poole R.K., and Green J. (2007) Transition of *Escherichia coli* from aerobic to micro-aerobic conditions involves fast and slow reacting regulatory components. *Journal of Biological Chemistry* **282**: 11230-11237.
- Passerini L., Lam K., Costerton J.W., and King E.G. (1992) Biofilms on indwelling vascular catheters. *Critical Care Medicine* **20**: 665-673.
- Patel J., and Sharma M. (2010) Differences in attachment of *Salmonella enterica* serovars to cabbage and lettuce leaves. *International Journal of Food Microbiology* **139**: 41-47.
- Paul R., Abel S., Wassmann P., Beck A., Heerklotz H., and Jenal U. (2007) Activation of the diguanylate cyclase PleD by phosphorylation-mediated dimerization. *Journal of Biological Chemistry* **282**: 29170-29177.
- Pedersen H., Sogaard-Andersen L., Holst B., and Valentin-Hansen P. (1991) Heterologous cooperativity in *Escherichia coli*. the CytR repressor both contacts DNA and the cAMP receptor protein when binding to the *deo* P2 promoter. *Journal of Biological Chemistry* **266**: 17804-17808.
- Peregrín-Alvarez J.M., Xiong X., Su C., and Parkinson J. (2009) The modular organization of protein interactions in *Escherichia coli*. *PLOS Computational Biology* **5**: e1000523.
- Pesavento C., and Hengge R. (2009) Bacterial nucleotide-based second messengers. *Current Opinion in Microbiology* **12**: 170-176.
- Pesavento C., Becker G., Sommerfeldt N., Possling A., Tschowri N., Mehliis A., and Hengge R. (2008) Inverse regulatory coordination of motility and curli-mediated adhesion in *Escherichia coli*. *Genes and Development* **22**: 2434-2446.
- Piérard A., Glansdorff N., Mergeay M., and Wiame J.M. (1965) Control of the biosynthesis of carbamoyl phosphate in *Escherichia coli*. *Journal of Molecular Biology* **14**: 23-36.
- Plunkett W., Huang P., Xu Y.Z., Heinemann V., Grunewald R., and Gandhi V. (1995) Gemcitabine: Metabolism, mechanisms of action, and self-potential. *Seminars in Oncology* **11**: 3-10.
- Poole K. (2000) Efflux-mediated resistance to fluoroquinolones in gram-negative bacteria. *Antimicrobial Agents and Chemotherapy* **44**: 2233-2241.

List of references

- Porwollik S., Santiviago C.A., Cheng P., Long F., Desai P., Fredlund J., *et al.* (2014) Defined single-gene and multi-gene deletion mutant collections in *Salmonella enterica* sv Typhimurium. *PLoS One* **9**: e99820.
- Post D.A., Hove-Jensen B., and Switzer R.L. (1993) Characterization of the *hemA-prs* region of the *Escherichia coli* and *Salmonella* Typhimurium chromosomes: Identification of two open reading frames and implications for *prs* expression. *Journal of General Microbiology* **2**: 259-266.
- Pottage A., Holt S., Ludgate S., and Langlands A.O. (1978) Fluorouracil cardiotoxicity. *British Medical Journal* **1**: 547-547.
- Pratt J.T., McDonough E., and Camilli A. (2009) PhoB regulates motility, biofilms, and cyclic di-GMP in *Vibrio cholerae*. *Journal of Bacteriology* **191**: 6632-4662.
- Pratt L.A., and Kolter R. (1998) Genetic analysis of *Escherichia coli* biofilm formation: Roles of flagella, motility, chemotaxis and type I pili. *Molecular Microbiology* **30**: 285-293.
- Projan S.J. (2003) Why is big pharma getting out of antibacterial drug discovery? *Current Opinion in Microbiology* **6**: 427-430.
- Prouty A.M., Brodsky I.E., Manos J., Belas R., Falkow S., and Gunn J.S. (2004) Transcriptional regulation of *Salmonella enterica* serovar Typhimurium genes by bile. *FEMS Immunol Med Microbiol* **41**: 177-185.
- Py B., and Barras F. (2010) Building Fe-S proteins: Bacterial strategies. *Nature Reviews Microbiology* **8**: 436-446.
- Pysz M.A., Connors S.B., Montero C.I., Shockley K.R., Johnson M.R., Ward D.E., and Kelly R.M. (2004) Transcriptional analysis of biofilm formation processes in the anaerobic, hyperthermophilic bacterium *Thermotoga maritima*. *Applied and Environmental Microbiology* **70**: 6098-6112.
- Qi Y., Rao F., Luo Z., and Liang Z. (2009) A flavin cofactor-binding PAS domain regulates c-di-GMP synthesis in AxDGC2 from *Acetobacter xylinum*. *Biochemistry* **48**: 10275-10285.
- Rae W., Burke G., and Pinto A. (2016) A study of the utility of azathioprine metabolite testing in myasthenia gravis. *Journal Neuroimmunology* **293**: 82-85.
- Rajyaguru J.M., and Muszynski M.J. (1998) Sensitization of *Burkholderia cepacia* to antibiotics by cationic drugs. *Journal of Antimicrobial Chemotherapy* **41**: 277-280.
- Rangel-Vega A., Bernstein L.R., Mandujano-Tinoco E., Garcia-Contreras S.J., and Garcia-Contreras R. (2015) Drug repurposing as an alternative for the treatment of recalcitrant bacterial infections. *Frontiers in Microbiology* **6**: 282.
- Rao F., Yang Y., Qi Y., and Liang Z. (2008) Catalytic mechanism of cyclic di-GMP-specific phosphodiesterase: A study of the EAL domain-containing RocR from *Pseudomonas aeruginosa*. *Journal of Bacteriology* **190**: 3622-3631.

- Rappu P., Shin B., Zalkin H., and Mäntsälä P. (1999) A role for a highly conserved protein of unknown function in regulation of *Bacillus subtilis purA* by the purine repressor. *Journal of Bacteriology* **181**: 3810-3815.
- Rasko D.A., and Sperandio V. (2010) Anti-virulence strategies to combat bacteria-mediated disease. *Nature Reviews Drug Discovery* **9**: 117-128.
- Reffuveille F., de la Fuente-Núñez C., Mansour S., and Hancock R.E.W. (2014) A broad-spectrum antibiofilm peptide enhances antibiotic action against bacterial biofilms. *Antimicrobial Agents and Chemotherapy* **58**: 5363-5371.
- Rinaldo S., Paiardini A., Stelitano V., Brunotti P., Cervoni L., Fernicola S., *et al.* (2015) Structural basis of functional diversification of the HD-GYP domain revealed by the *Pseudomonas aeruginosa* PA4781 protein, which displays an unselective bimetallic binding site. *Journal of Bacteriology* **197**: 1525-1535.
- Robbe-Saule V., Jaumouillé V., Prévost M., Guadagnini S., Talhouarne C., Mathout H., *et al.* (2006) Crl activates transcription initiation of RpoS-regulated genes involved in the multicellular behavior of *Salmonella enterica* serovar Typhimurium. *Journal of Bacteriology* **188**: 3983-3994.
- Robijns S.C.A., Roberfroid S., Van Puyvelde S., De Pauw B., Uceda Santamaría E., De Weerd A., *et al.* (2014) A GFP promoter fusion library for the study of *Salmonella* biofilm formation and the mode of action of biofilm inhibitors. *Biofouling* **30**: 605-625.
- Robison K., McGuire A.M., and Church G.M. (1998) A comprehensive library of DNA-binding site matrices for 55 proteins applied to the complete *Escherichia coli* K-12 genome1. *Journal of Molecular Biology* **284**: 241-254.
- Roelofs K.G., Wang J., Sintim H.O., and Lee V.T. (2011) Differential radial capillary action of ligand assay for high-throughput detection of protein-metabolite interactions. *Proceedings of the National Academy of Sciences* **108**: 15528-15533.
- Rogers G.B., Carroll M.P., and Bruce K.D. (2012) Enhancing the utility of existing antibiotics by targeting bacterial behaviour? *British Journal of Pharmacology* **165**: 845-857.
- Rogers H.J., and Perkins H.R. (1960) 5-fluorouracil and mucopeptide biosynthesis by *staphylococcus aureus*. *Biochemical Journal* **77**: 448-459.
- Roilides E., Simitopoulou M., Katragkou A., and Walsh T.J. (2015) How biofilms evade host defenses. *Microbiology Spectrum* **3**: MB-0012-2014.
- Rolfes R.J., and Zalkin H. (1990) Autoregulation of *Escherichia coli purR* requires two control sites downstream of the promoter. *Journal of Bacteriology* **172**: 5758-5766.
- Romero D., Traxler M.F., López D., and Kolter R. (2011) Antibiotics as signal molecules. *Chemical Reviews* **111**: 5492-5505.
- Römling U. (2005) Characterization of the rdar morphotype, a multicellular behaviour in enterobacteriaceae. *Cellular and Molecular Life Sciences CMLS* **62**: 1234-1246.

List of references

- Römling U., Bian Z., Hammar M., Sierralta W., and Normark S. (1998a) Curli fibers are highly conserved between *Salmonella* Typhimurium and *Escherichia coli* with respect to operon structure and regulation. *Journal of Bacteriology* **180**: 722.
- Römling U. (2009) Rationalizing the evolution of EAL domain-based cyclic di-GMP-specific phosphodiesterases. *Journal of Bacteriology* **191**: 4697-4700.
- Römling U., Galperin M.Y., and Gomelsky M. (2013) Cyclic di-GMP: The first 25 years of a universal bacterial second messenger. *Microbiology and Molecular Biology Reviews* **77**: 1-52.
- Römling U., Gomelsky M., and Galperin M. (2005) C-di-GMP: The dawning of a novel bacterial signaling system. *Molecular Microbiology* **57**: 629-639.
- Römling U., Sierralta W.D., Eriksson K., and Normark S. (1998b) Multicellular and aggregative behavior of *Salmonella* Typhimurium strains is controlled by mutations in the *agfD* promoter. *Molecular Microbiology* **28**: 249-264.
- Römling U. (2001) Genetic and phenotypic analysis of multicellular behavior in *Salmonella* Typhimurium. *Methods in Enzymology* **336**: 48-59.
- Römling U., Rohde M., Olsén A., Normark S., and Reinköster J. (2000) AgfD, the checkpoint of multicellular and aggregative behaviour in *Salmonella* Typhimurium regulates at least two independent pathways. *Molecular Microbiology* **36**: 10-23.
- Ross P., Aloni Y., Weinhouse H., Michaeli D., Weinberger-Ohana P., Mayer R., and Benziman M. (1986) Control of cellulose biosynthesis in *Acetobacter xylinum*. A unique guanyl oligonucleotide is the immediate activator of the cellulose synthase. *Carbohydrate Research* **149**: 101-117.
- Ross P., Weinhouse H., Aloni Y., Michaeli D., Weinberger-Ohana P., Mayer R., *et al.* (1987) Regulation of cellulose synthesis in *Acetobacter xylinum* by cyclic diguanylic acid. *Nature* **325**: 279-281.
- Rouf S.e., Ahmad I., Anwar N., Vodnala S., Kader A., Römling U., and Rhen M. (2011) Opposing contributions of polynucleotide phosphorylase and the membrane protein NlpI to biofilm formation by *Salmonella enterica* serovar Typhimurium. *Journal of Bacteriology* **193**: 580-582.
- Rouli L., Merhej V., Fournier P., and Raoult D. (2015) The bacterial pangenome as a new tool for analysing pathogenic bacteria. *New Microbes and New Infections* **7**: 72-85.
- Ruan J., Dean A.K., and Zhang W. (2010) A general co-expression network-based approach to gene expression analysis: Comparison and applications. *BMC Systems Biology* **4**: 8.
- Ryjenkov D.A., Simm R., Römling U., and Gomelsky M. (2006) The PilZ domain is a receptor for the second messenger c-di-GMP: the PilZ domain protein *ycgr* controls motility in Enterobacteria. *Journal of Biological Chemistry* **281**: 30310-30314.
- Salgado H., Peralta-Gil, Gama-Castro S., Santos-Zavaleta A., Muniz-Rascado L., Garcia-Sotelo J., *et al.* (2012) RegulonDB v8.0: Omics data sets, evolutionary conservation,

- regulatory phrases, cross-validated gold standards and more. *Nucleic Acids Research* **41**: 203-213.
- Sallet E., Roux B., Sauviac L., Jardinaud M., Carrare S., Faraut T., *et al.* (2013) Next-generation annotation of prokaryotic genomes with EuGene-P: Application to *Sinorhizobium meliloti* 2011. *DNA Research* **20**: 339-354.
- Salmon K., Hung S., Mekjian K., Baldi P., Hatfield G.W., and Gunsalus R.P. (2003) Global gene expression profiling in *Escherichia coli* K12: The effects of oxygen availability and FNR. *Journal of Biological Chemistry* **278**: 29837-29855.
- Sanchez-Torres V., Hu H., and Wood T. (2010) GGDEF proteins YeaI, YedQ, and YfiN reduce early biofilm formation and swimming motility in *Escherichia coli*. *Applied Microbiology and Biotechnology* **90**: 651-658.
- Sandlie I., Solberg K.t., and Kleppe K. (1980) The effect of caffeine on cell growth and metabolism of thymidine in *Escherichia coli*. *Mutation Research* **73**: 29-41.
- Sandrini M.P., Clausen A.R., On S.L., Aarestrup F.M., Munch-Petersen B., and Piškur J. (2007a) Nucleoside analogues are activated by bacterial deoxyribonucleoside kinases in a species-specific manner. *Journal of Antimicrobial Chemotherapy* **60**: 510-520.
- Sandrini M.P., Shannon O., Clausen A.R., Björck L., and Piskur J. (2007b) Deoxyribonucleoside kinases activate nucleoside antibiotics in severely pathogenic bacteria. *Antimicrobial Agents and Chemotherapy* **51**: 2726-2732.
- Sanz J.L., and Köchling T. (2007) Molecular biology techniques used in wastewater treatment: An overview. *Process Biochemistry* **42**: 119-133.
- Sat B., Reches M., and Engelberg-Kulka H. (2002) The *Escherichia coli* *mazEF* suicide module mediates thymineless death. *Journal of Bacteriology* **185**: 1803-1807.
- Sauer K., and Camper A.K. (2001) Characterization of phenotypic changes in *Pseudomonas putida* in response to surface-associated growth. *Journal of Bacteriology* **183**: 6579-6589.
- Sauer K., Camper A.K., Ehrlich G.D., Costerton J.W., and Davies D.G. (2002) *Pseudomonas aeruginosa* displays multiple phenotypes as a biofilm. *Journal of Bacteriology* **184**: 1140-1154.
- Sawers G. (1993) Specific transcriptional requirements for positive regulation of the anaerobically inducible *pfl* operon by ArcA and FNR. *Molecular Microbiology* **10**: 737-747.
- Schaefer M., Hagemann S., Hanna K., and Lyko F. (2009) Azacytidine inhibits RNA methylation at DNMT2 target sites in human cancer cell lines. *Cancer Research* **69**: 8127-8132.
- Schäfer A., Schomacher L., Barreto G., Döderlein G., and Niehrs C. (2010) Gemcitabine functions epigenetically by inhibiting repair mediated DNA demethylation. *PloS One* **5**: e14060.

List of references

- Schembri M.A., Kjærgaard K., and Klemm P. (2003) Global gene expression in *Escherichia coli* biofilms. *Molecular Microbiology* **48**: 253-267.
- Schmidt A.J., Ryjenkov D.A., and Gomelsky M. (2005) The ubiquitous protein domain EAL is a cyclic diguanylate-specific phosphodiesterase: Enzymatically active and inactive EAL domains. *Journal of Bacteriology* **187**: 4774-4781.
- Schmidt B. (2005) Methylxanthine therapy for apnea of prematurity: Evaluation of treatment benefits and risks at age 5 years in the international caffeine for apnea of prematurity (CAP) trial. *Neonatology* **88**: 208-213.
- Schmidt B. (1999) Methylxanthine therapy in premature infants: Sound practice, disaster, or fruitless byway? *Journal of Pediatrics* **135**: 526-528.
- Schonewille E., Nesse L.L., Hauck R., Windhorst D., Hafez H.M., and Vestby L.K. (2012) Biofilm building capacity of *Salmonella enterica* strains from the poultry farm environment. *FEMS Immunology and Medical Microbiology* **65**: 360-365.
- Schubert M., Lapouge K., Duss O., Oberstrass F.C., Jelesarov I., Haas D., and Allain F.H.-. (2007) Molecular basis of messenger RNA recognition by the specific bacterial repressing clamp RsmA/CsrA. *Nature Structural Molecular Biology* **14**: 807-813.
- Scott C., Partridge J.D., Stephenson J.R., and Green J. (2003) DNA target sequence and FNR-dependent gene expression. *FEBS Letters* **541**: 97-101.
- Selby C.P., and Sancar A. (1990) Molecular mechanisms of DNA repair inhibition by caffeine. *Proceedings of the National Academy of Sciences of the United States of America* **87**: 3522-3525.
- Serganov A., and Patel D.J. (2012) Metabolite recognition principles and molecular mechanisms underlying riboswitch function. *Annual Review of Biophysics* **41**: 343-370.
- Serra D.O., Richter A.M., and Hengge R. (2013a) Cellulose as an architectural element in spatially structured *Escherichia coli* biofilms. *Journal of Bacteriology* **195**: 5540-5554.
- Serra D.O., Richter A.M., Klauck G., Mika F., and Hengge R. (2013b) Microanatomy at cellular resolution and spatial order of physiological differentiation in a bacterial biofilm. *mBio* **4**: e00103-13.
- Seshasayee A.S.N., Fraser G.M., and Luscombe N.M. (2010) Comparative genomics of cyclic-di-GMP signalling in bacteria: Post-translational regulation and catalytic activity. *Nucleic Acids Research* **38**: 5970-5981.
- Shannon P., Markiel A., Ozier O., Baliga N.S., Wang J.T., Ramage D., *et al.* (2003) Cytoscape: A software environment for integrated models of biomolecular interaction networks. *Genome Research* **13**: 2498-2504.
- Shimada T., Kori A., and Ishihama A. (2013) Involvement of the ribose operon repressor RbsR in regulation of purine nucleotide synthesis in *Escherichia coli*. *FEMS Microbiology Letters* **344**: 159-165.

- Shimada T., Ishihama A., Busby S.J.W., and Grainger D.C. (2008) The *Escherichia coli* RutR transcription factor binds at targets within genes as well as intergenic regions. *Nucleic Acids Research* **36**: 3950-3955.
- Shin S.J., and Collins M.T. (2007) Thiopurine drugs azathioprine and 6-mercaptopurine inhibit *Mycobacterium paratuberculosis* growth in vitro. *Antimicrobial Agents and Chemotherapy* **52**: 418-426.
- Sideropoulos A.S., and Shankel D.M. (1968) Mechanism of caffeine enhancement of mutations induced by sublethal ultraviolet dosages. *Journal of Bacteriology* **96**: 198-204.
- Siebenhaar F., Syska W., Weller K., Magerl M., Zuberbier T., Metz M., and Maurer M. (2007) Control of *Pseudomonas aeruginosa* skin infections in mice is mast cell-dependent. *American Journal of Pathology* **170**: 1910-1916.
- Silver L.L. (2007) Multi-targeting by monotherapeutic antibacterials. *Nature Reviews Drug Discovery* **6**: 41-55.
- Simm R., Remminghorst U., Ahmad I., Zakikhany K., and Römling U. (2009) A role for the EAL-like protein STM1344 in regulation of CsgD expression and motility in *Salmonella enterica* serovar Typhimurium. *Journal of Bacteriology* **191**: 3928-3937.
- Simm R., Ahmad I., Rhen M., Le Guyon S., and Römling U. (2014) Regulation of biofilm formation in *Salmonella enterica* serovar Typhimurium. *Future Microbiology* **9**: 1261-1282.
- Simm R., Lusch A., Kader A., Andersson M., and Römling U. (2007) Role of EAL-containing proteins in multicellular behavior of *Salmonella enterica* serovar Typhimurium. *Journal of Bacteriology* **189**: 3613-3623.
- Simm R., Morr M., Kader A., Nimtze M., and Römling U. (2004) GGDEF and EAL domains inversely regulate cyclic di-GMP levels and transition from sessility to motility. *Molecular Microbiology* **53**: 1123-1134.
- Simões M., Simões L.C., and Vieira M.J. (2010) A review of current and emergent biofilm control strategies. *LWT - Food Science and Technology* **43**: 573-583.
- Singh V., Brecik M., Mukherjee R., Evans J., Svetlíková Z., Blaško J., *et al.* (2015) The complex mechanism of antimycobacterial action of 5-fluorouracil. *Chemistry and Biology* **22**: 63-75.
- Solano C., García B., Latasa C., Toledo-Arana A., Zorraquino V., Valle J., *et al.* (2009) Genetic reductionist approach for dissecting individual roles of GGDEF proteins within the c-di-GMP signaling network in *Salmonella*. *Proceedings of the National Academy of Sciences* **106**: 7997-8002.
- Soler-Garcia A., De Jesus A., Taylor K., and Brown E. (2014) Differentiation of *Salmonella* strains from the SARA, SARB and SARC reference collections by using three genes PCR-RFLP and the 2100 agilent bioanalyzer. *Frontiers in Microbiology* **5**: 147.

List of references

- Sommerfeldt N., Possling A., Becker G., Pesavento C., Tschowri N., and Hengge R. (2009) Gene expression patterns and differential input into curli fimbriae regulation of all GGDEF/EAL domain proteins in *Escherichia coli*. *Microbiology* **155**: 1318-1331.
- Song J.S., Jeon J.H., Lee J.H., Jeong S.H., Jeong B.C., Kim S.J., *et al.* (2005) Molecular characterization of TEM-type beta-lactamases identified in cold-seep sediments of edison seamount (south of Iihir Island, Papua New Guinea). *Journal of Microbiology* **43**: 172-178.
- Soo V.W., Kwan B.W., Quezada H., Castillo-Juarez I., Perez-Eretza B., Garcia-Contreras S.J., *et al.* (2016) Repurposing of anticancer drugs for the treatment of bacterial infections. *Current Topics Medicinal Chemistry* 1157-1176.
- Southey-Pillig C.J., Davies D.G., and Sauer K. (2005) Characterization of temporal protein production in *Pseudomonas aeruginosa* biofilms. *Journal of Bacteriology* **187**: 8114-8126.
- Srivastava D., and Waters C.M. (2012) A tangled web: Regulatory connections between quorum sensing and cyclic di-GMP. *Journal of Bacteriology* **194**: 4485-4493.
- Steenackers H., Hermans K., Vanderleyden J., and De Keersmaecker S.C.J. (2012) *Salmonella* biofilms: An overview on occurrence, structure, regulation and eradication. *Food Research International* **45**: 502-531.
- Stewart P.S. (2002) Mechanisms of antibiotic resistance in bacterial biofilms. *International Journal of Medical Microbiology* **292**: 107-113.
- Stickgold R.A., and Neuhaus F.C. (1967) On the initial stage in peptidoglycan synthesis. effect of 5-fluorouracil substitution on phospho-N-acetylmuramyl-pentapeptide translocase (uridine 5'-phosphate). *Journal of Biological Chemistry* **242**: 1331-1337.
- Stoodley P., Sauer K., Davies D.G., and Costerton J.W. (2002) Biofilms as complex differentiated communities. *Annual Review Of Microbiology* **56**: 187-209.
- Sudarsan N., Lee E.R., Weinberg Z., Moy R.H., Kim J.N., Link K.H., and Breaker R.R. (2008) Riboswitches in eubacteria sense the second messenger cyclic di-GMP. *Science* **321**: 411-413.
- Sun R., and Wang L. (2013) Inhibition of *Mycoplasma pneumoniae* growth by FDA-approved anticancer and antiviral nucleoside and nucleobase analogs. *BMC Microbiology* **13**: 1-12.
- Tabak M., Scher K., Hartog E., Romling U., Matthews K.R., Chikindas M.L., and Yaron S. (2007) Effect of triclosan on *Salmonella* Typhimurium at different growth stages and in biofilms. *FEMS Microbiology Letters* **267**: 200-206.
- Tarutina M., Ryjenkov D.A., and Gomelsky M. (2006) An unorthodox bacteriophytochrome from *Rhodobacter sphaeroides* involved in turnover of the second messenger c-di-GMP. *Journal of Biological Chemistry* **281**: 34751-34758.
- Tesfa-Selase F., and Drabble W.T. (1992) Regulation of the *gua* operon of *Escherichia coli* by the DnaA protein. *Molecular and General Genetics MGG* **231**: 256-264.

- Thangamani S., Younis W., and Seleem M.N. (2015) Repurposing ebselen for treatment of multidrug-resistant staphylococcal infections. *Scientific Reports* **5**: 11596.
- Timmer A., Patton P.H., Chande N., McDonald J.W.D., and MacDonald J.K. (2007) Azathioprine and 6-mercaptopurine for maintenance of remission in ulcerative colitis. *Cochrane Database of Systematic Reviews* **1**: CD000478.
- Tomasz A.B.,E. (1962) The mechanism of an osmotic instability induced in *E. coli* K-12 by 5-fluorouracil. *Biochemistry* **1**: 543-552.
- Trevino-Quintanilla L.G., Freyre-Gonzalez J.A., and Martinez-Flores I. (2013) Anti-sigma factors in *E. coli*: common regulatory mechanisms controlling sigma factors availability. *Current Genomics* **14**: 378-387.
- Trotter V., Vinella D., Loiseau L., De Choudens S.O., Fontecave M., and Barras F. (2009) The CsdA cysteine desulphurase promotes fe/S biogenesis by recruiting suf components and participates to a new sulphur transfer pathway by recruiting CsdL (ex-YgdL), a ubiquitin-modifying-like protein. *Molecular Microbiology* **74**: 1527-1542.
- Tu Y., Lu M.i., Chiang M., Huang S., Peng H., Chang H., *et al.* (2009) Genetic requirements for *Klebsiella pneumoniae*-induced liver abscess in an oral infection model. *Infection and Immunity* **77**: 2657-2671.
- Tuckerman R., Gonzalez G., Sousa E.H.S., Wan X., Saito J.A., Alam M., and Gilles-Gonzalez M. (2009) An oxygen-sensing diguanylate cyclase and phosphodiesterase couple for c-di-GMP control. *Biochemistry* **48**: 9764-9774.
- Turnbough C.L.,Jr, and Switzer R.L. (2008) Regulation of pyrimidine biosynthetic gene expression in bacteria: Repression without repressors. *Microbiology and Molecular Biology Reviews* **72**: 266-300.
- Ueda A., Attila C., Whiteley M., and Wood T.K. (2009) Uracil influences quorum sensing and biofilm formation in *Pseudomonas aeruginosa* and fluorouracil is an antagonist. *Microbial Biotechnology* **2**: 62-74.
- Ueda Y., Saito A., Fukuoka Y., Yamashiro Y., Ikeda Y., Taki H., *et al.* (1983) Interactions of beta-lactam antibiotics and antineoplastic agents. *Antimicrobial Agents and Chemotherapy* **23**: 374-378.
- Vaagland H., Blomberg B., Kruger C., Naman N., Jureen R., and Langeland N. (2004) Nosocomial outbreak of neonatal *Salmonella enterica* serotype enteritidis meningitis in a rural hospital in northern tanzania. *BMC Infectious Diseases* **4**: 35.
- Valdivia R.H., and Falkow S. (1996) Bacterial genetics by flow cytometry: Rapid isolation of *Salmonella* Typhimurium acid-inducible promoters by differential fluorescence induction. *Molecular Microbiology* **22**: 367-378.
- Valentini M., and Filloux A. (2016) Biofilms and cyclic di-GMP (c-di-GMP) signaling: Lessons from *Pseudomonas aeruginosa* and other bacteria. *Journal of Biological Chemistry* **291**: 12547-12555.

List of references

- Van Puyvelde S. (2014) PhD Thesis. Regulation of *Salmonella* biofilm formation: The role of small RNAs. KU Leuven, Belgium.
- Van Rompay A.R., Johansson M., and Karlsson A. (2003) Substrate specificity and phosphorylation of antiviral and anticancer nucleoside analogues by human deoxyribonucleoside kinases and ribonucleoside kinases. *Pharmacology and Therapeutics* **100**: 119-139.
- van Schaik W. (2015) The human gut resistome. *Philosophical Transactions of the Royal Society B: Biological Sciences* **370**: 20140087.
- Vermes A., Guchelaar H.-., and Dankert J. (2000) Flucytosine: A review of its pharmacology, clinical indications, pharmacokinetics, toxicity and drug interactions. *Journal of Antimicrobial Chemotherapy* **46**: 171-179.
- Verstraeten N., Braeken K., Debkumari B., Fauvart M., Fransaeer J., Vermant J., and Michiels J. (2008) Living on a surface: Swarming and biofilm formation. *Trends in Microbiology* **16**: 496-506.
- Vidal J.E., Ludewick H.P., Kunkel R.M., Zähler D., and Klugman K.P. (2011) The LuxS-dependent quorum-sensing system regulates early biofilm formation by *Streptococcus pneumoniae* strain D39. *Infect Immun* **79**: 4050-4060.
- Villela A.D., Sanchez-Quitian Z.A., Ducati R.G., and Basso D.S.S.a.L.A. (2011) Pyrimidine salvage pathway in *Mycobacterium tuberculosis*. *Current Medicinal Chemistry* **18**: 1286-1298.
- Vinella D., Albrecht C., Cashel M., and D'Ari R. (2005) Iron limitation induces SpoT-dependent accumulation of ppGpp in *Escherichia coli*. *Molecular Microbiology* **56**: 958-970.
- Vogel U., Pedersen S., and Jensen K.F. (1991) An unusual correlation between ppGpp pool size and rate of ribosome synthesis during partial pyrimidine starvation of *Escherichia coli*. *Journal of Bacteriology* **173**: 1168-1174.
- Vojdani J.D., Beuchat L.R., and Tauxe R.V. (2008) Juice-associated outbreaks of human illness in the united states, 1995 through 2005. *Journal of Food Protection* **71**: 356-364.
- von Hoff D.D., Slavik M., and Muggia F.M. (1976) 5-Azacytidine a new anticancer drug with effectiveness in acute myelogenous leukemia. *Annals of Internal Medicine* **85**: 237-245.
- von Wintersdorff C.J.H., Penders J., van Niekerk J.,M., Mills N.n.D., Majumder S., van Alphen L.,B., *et al.* (2016) Dissemination of antimicrobial resistance in microbial ecosystems through horizontal gene transfer. *Frontiers in Microbiology* **7**: 173.
- Walker K.A., Mallik P., Pratt T.S., and Osuna R. (2004) The *Escherichia coli* *fis* promoter is regulated by changes in the levels of is transcription initiation nucleotide CTP. *Journal of Biological Chemistry* **279**: 50818-50828.
- Walker K.A., and Osuna R. (2002) Factors affecting start site selection at the *Escherichia coli* *fis* promoter. *Journal of Bacteriology* **184**: 4783-4791.

- Walz J.M., Avelar R.L., Longtine K., Carter K.L., Mermel L.A., and Heard S.O. (2010) Anti-infective external coating of central venous catheters: A randomized, noninferiority trial comparing 5-fluorouracil with chlorhexidine/silver sulfadiazine in preventing catheter colonization. *Critical Care Medicine* **38**: 2095-2102.
- Wan X., Tuckerman J.R., Saito J.A., Freitas T.A.K., Newhouse J.S., Denery J.R., *et al.* (2009) Globins synthesize the second messenger bis-(3'-5')-cyclic diguanosine monophosphate in bacteria. *Journal of Molecular Biology* **388**: 262-270.
- Wang L., Liu J., Huang M., and Xu N. (2007) Comparison of pharmacokinetics, efficacy and toxicity profile of gemcitabine using two different administration regimens in chinese patients with non-small-cell lung cancer. *Journal of Zhejiang University Science-Biomedicine & Biotechnology* **8**: 307-313.
- Warner D.F., Evans J.C., and Mizrahi V. (2014) Nucleotide metabolism and DNA replication. *Microbiology Spectrum* **2**: 1-20.
- Warner H.R., and Rockstroh P.A. (1980) Incorporation and excision of 5-fluorouracil from deoxyribonucleic acid in *Escherichia coli*. *Journal of Bacteriology* **141**: 680-686.
- Warner J.C., Rothwell S.D., and Keevil C.W. (2008) Use of episcopic differential interference contrast microscopy to identify bacterial biofilms on salad leaves and track colonization by *Salmonella* Thompson. *Environmental Microbiology* **10**: 918-925.
- Wassmann P., Chan C., Paul R., Beck A., Heerklotz H., Jenal U., and Schirmer T. (2007) Structure of BeF₃⁻-modified response regulator PleD: Implications for diguanylate cyclase activation, catalysis, and feedback inhibition. *Structure* **15**: 915-927.
- Watson M.E., Neely M.N., and Caparon M.G. (2016) Animal models of *streptococcus pyogenes* infection. In *Streptococcus Pyogenes : Basic Biology to Clinical Manifestations*. Ferretti, J.J., Stevens, D.L., and Fischetti, V.A. (eds). Oklahoma City: University of Oklahoma Health Sciences Center, pp. 629-660.
- Weber H., Pesavento C., Possling A., Tischendorf G., and Hengge R. (2006) Cyclic-di-GMP-mediated signalling within the σ S network of *Escherichia coli*. *Molecular Microbiology* **62**: 1014-1034.
- Weigel G., Griesmacher A., DeAbreu R.A., Wolner E., and Mueller M.M. (1999) Azathioprine and 6-mercaptopurine alter the nucleotide balance in endothelial cells. *Thrombosis Research* **94**: 87-94.
- Weissborn A.C., Liu Q., Rumley M.K., and Kennedy E.P. (1994) UTP: Alpha-D-glucose-1-phosphate uridylyltransferase of *Escherichia coli*: Isolation and DNA sequence of the galU gene and purification of the enzyme. *Journal of Bacteriology* **176**: 2611-2618.
- White M.N., Olszowy J., and Switzer R.L. (1971) Regulation and mechanism of phosphoribosylpyrophosphate synthetase: Repression by end products. *Journal of Bacteriology* **108**: 122-131.
- Whiteley M. (2001) Gene expression in *Pseudomonas aeruginosa* biofilms. *Nature* **413**: 860-864.

List of references

- Whitney J.C., Colvin K.M., Marmont L.S., Robinson H., Parsek M.R., and Howell P.L. (2012) Structure of the cytoplasmic region of PelD, a degenerate diguanylate cyclase receptor that regulates exopolysaccharide production in *Pseudomonas aeruginosa*. *Journal of Biological Chemistry* **287**: 23582-23593.
- Whitney J.C., Whitfield G.B., Marmont L.S., Yip P., Neculai A.M., Lobsanov Y.D., *et al.* (2015) Dimeric c-di-GMP is required for post-translational regulation of aginate production in *Pseudomonas aeruginosa*. *The Journal of Biological Chemistry* **290**: 12451-12462.
- WHO. (2017) Global priority list of antibiotic-resistant bacteria to guide research, discovery, and development of new antibiotics. [WWW document].URL <http://www.who.int/medicines/publications/global-priority-list-antibiotic-resistant-bacteria/en/>.
- Williams I., Venables W.A., Lloyd D., Paul F., and Critchley I. (1997) The effects of adherence to silicone surfaces on antibiotic susceptibility in *Staphylococcus aureus*. *Microbiology* **143**: 2407-2413.
- Winfield M.D., and Groisman E.A. (2004) Phenotypic differences between *Salmonella* and *Escherichia coli* resulting from the disparate regulation of homologous genes. *Proceedings of the National Academy of Sciences of the United States of America* **101**: 17162-17167.
- Wissenbach U., Six S.F., Bongaerts J.F., Ternes D.F., Steinwachs S.F., and Uden G. (1995) A third periplasmic transport system for L-arginine in *Escherichia coli*: Molecular characterization of the *artPIQMJ* genes, arginine binding and transport. *Molecular Microbiology* **17**: 675-686.
- Witte G., Hartung S., Buttner K., and Hopfner K. (2008) Structural biochemistry of a bacterial checkpoint protein reveals diadenylate cyclase activity regulated by DNA recombination intermediates. *Molecular Cell* **30**: 167-178.
- Wood P.J. (1980) Specificity in the interaction of direct dyes with polysaccharides. *Carbohydrates Research* **85**: 271-287.
- Wood T.K., Hong S.H., and Ma Q. (2010) Engineering biofilm formation and dispersal. *Trends in Biotechnology* **29**: 87-94.
- Wozniak C.E., Lee C., and Hughes K.T. (2009) T-POP array identifies EcnR and PefI-SrgD as novel regulators of flagellar gene expression. *Journal of Bacteriology* **191**: 1498-1508.
- Wu H., Moser C., Wang H.Z., Høiby N., and Song Z.J. (2015) Strategies for combating bacterial biofilm infections. *International Journal of Oral Science* **7**: 1-7.
- Wu Y., and Outten F.W. (2009) IscR controls iron-dependent biofilm formation in *Escherichia coli* by regulating type I fimbria expression. *Journal of Bacteriology* **191**: 1248-57.
- Wyatt M.D., and Wilson D.M. (2009) Participation of DNA repair in the response to 5-fluorouracil. *Cellular and Molecular Life Sciences* **66**: 788-799.

- Xi H., Schneider B.L., and Reitzer L. (2000) Purine catabolism in *Escherichia coli* and function of xanthine dehydrogenase in purine salvage. *Journal of Bacteriology* **182**: 5332-5341.
- Yadav M.K., Chae S., and Song J. (2012a) Effect of 5-azacytidine on in vitro biofilm formation of *Streptococcus pneumoniae*. *Microbial Pathogenesis* **53**: 219-226.
- Yadav M.K., Go Y.Y., Chae S., and Song J. (2015) The small molecule DAM inhibitor, pyrimidinedione, disrupts *Streptococcus pneumoniae* biofilm growth in vitro. *PloS One* **10**: e0139238.
- Yadav M.K., Kwon S.K., Cho C., Park S., Chae S., and Song J. (2012b) Gene expression profile of early in vitro biofilms of *Streptococcus pneumoniae*. *Microbiology and Immunology* **56**: 621-629.
- Yadav M.K., Park S., Chae S., and Song J. (2014) Sinefungin, a natural nucleoside analogue of S-adenosylmethionine, inhibits *Streptococcus pneumoniae* biofilm growth. *Biomedical Research International* **2014**: 10.
- Yakhnin A.V., Baker C.S., Vakulskas C.A., Yakhnin H., Berezin I., Romeo T., and Babitzke P. (2013) CsrA activates *flhDC* expression by protecting *flhDC* mRNA from RNase E-mediated cleavage. *Molecular Microbiology* **87**: 851-866.
- Yang J., Sun B., Huang H., Jiang Y., Diao L., Chen B., *et al.* (2014) High-efficiency scarless genetic modification in *Escherichia coli* by using lambda red recombination and I-SceI cleavage. *Applied Environmental Microbiology* **80**: 3826-3834.
- Yeo W., Lee J., Lee K., and Roe J. (2006) IscR acts as an activator in response to oxidative stress for the *suf* operon encoding Fe-S assembly proteins. *Molecular Microbiology* **61**: 206-218.
- Yildiz F.H., and Schoolnik G.K. (1999) *Vibrio cholerae* O1 EI Tor: Identification of a gene cluster required for the rugose colony type, exopolysaccharide production, chlorine resistance, and biofilm formation. *Proceedings of the National Academy of Sciences* **96**: 4028-4033.
- Yildiz F.H., Dolganov N.A., and Schoolnik G.K. (2001) VpsR, a member of the response regulators of the two-component regulatory systems, is required for expression of *vps* biosynthesis genes and EPS(ETr)-associated phenotypes in *Vibrio cholerae* O1 EL Tor. *Journal of Bacteriology* **183**: 1716-1726.
- Yoshida T., Ueguchi C., Yamada H., and Mizuno T. (1993) Function of the *Escherichia coli* nucleoid protein, H-NS: Molecular analysis of a subset of proteins whose expression is enhanced in a *hns* deletion mutant. *Molecular Genomics and Genetics* **237**: 113-122.
- Yoshioka S., and Newell P.D. (2015) Disruption of *de novo* purine biosynthesis in *Pseudomonas fluorescens* Pf0-1 leads to reduced biofilm formation and a reduction in cell size of surface-attached but not planktonic cells. *PeerJ* **4**: e1543.

List of references

- Younis W., Thangamani S., and Seleem M.N. (2015) Repurposing non-antimicrobial drugs and clinical molecules to treat bacterial infections. *Current Pharmaceutical Design* **21**: 4106-4111.
- Yssel A.E.J., Vanderleyden J., and Steenackers H.P. (2017) Repurposing of nucleoside- and nucleobase-derivative drugs as antibiotics and biofilm inhibitors. *Journal of Antimicrobial Chemotherapy* **72**: 2156-2170.
- Zakikhany K., Harrington C.R., Nimtz M., Hinton J.C.D., and Römling U. (2010) Unphosphorylated CsgD controls biofilm formation in *Salmonella enterica* serovar Typhimurium. *Molecular Microbiology* **77**: 771-786.
- Zalkin H., and Nygaard P. (1996) Biosynthesis of purine nucleotides. In *Escherichia coli* and *Salmonella*: Cellular and Molecular Biology. Curtis, R., Ingraham, J.L., Lin, E.C.C., Brooks, K., Magasanik, L.B., Reznikoff, M., *et al* (eds). Washington, DC.: ASM Press, pp. 561-579.
- Zhang X., Shi H., Wu J.i., Zhang X., Sun L., Chen C., and Chen Z. . Cyclic GMP-AMP containing mixed phosphodiester linkages is an endogenous high-affinity ligand for STING. *Molecular Cell* **51**: 226-235.
- Zhao W., Chen J.J., Foley S., Wang Y., Zhao S., Basinger J., and Zou W. (2015) Biomarker identification from next-generation sequencing data for pathogen bacteria characterization and surveillance. *Biomarkers in Medicine* **9**: 1253-1264.
- Zheng D., Constantinidou C., Hobman J.L., and Minchin S.D. (2004) Identification of the CRP regulon using in vitro and in vivo transcriptional profiling. *Nucleic Acids Research* **32**: 5874-5893.
- Zheng Y., Sambou T., Bogomolnaya L.M., Cirillo J.D., McClelland M., and Andrews-Polymenis H. (2013) The EAL domain containing protein STM2215 (*rtn*) is needed during *Salmonella* infection and has cyclic di-GMP phosphodiesterase activity. *Molecular Microbiology* **89**: 403-419.
- Zhi-Wen Y., Yan-Li Z., Man Y., and Wei-Jun F. (2015) Clinical treatment of pandrug-resistant bacterial infection consulted by clinical pharmacist. *Saudi Pharmaceutical Journal* **23**: 377-380.
- Zogaj X., Nimtz M., Rohde M., Bokranz W., and Römling U. (2001) The multicellular morphotypes of *Salmonella* Typhimurium and *Escherichia coli* produce cellulose as the second component of the extracellular matrix. *Molecular Microbiology* **39**: 1452-1463.
- Zorraquino V., García B., Latasa C., Echeverz M., Toledo-Arana A., Valle J., *et al*. (2013) Coordinated cyclic-di-GMP repression of *Salmonella* motility through YcgR and cellulose. *Journal of Bacteriology* **195**: 417-428.

List of publications

Publications in international journals

- Yssel, A.E.J., Vanderleyden, J. & Steenackers, H.P., (2017) Repurposing of nucleoside- and nucleobase-derivative drugs as antibiotics and biofilm inhibitors, *Journal of Antimicrobial Chemotherapy*, vol. 72, no. 8, pp. 2156-2170.
- Yssel, Reva and Tastan Bishop., (2011) Comparative structural bioinformatics analysis of *Bacillus amyloliquefaciens* chemotaxis proteins within *Bacillus subtilis* group, *Applied Microbiology and Biotechnology*, vol 92, no 5, pp 997-1008.

In preparation

- A Yssel, E Peeters, D De Coster, A De Weerd, J, M Rahman, B Lories, V Kaefer, S Tschirner. Vanderleyden, H Steenackers., (2017) Pyrimidine starvation impairs biofilm formation via down-regulation of *csgD* despite high c-di-GMP levels.

Oral presentation at international meeting

- A Yssel., (2013) Tampering with purine & pyrimidine biosynthesis modulates biofilm formation of *Escherichia coli* & *Salmonella*. Oral presentation at: *Eurobiofilms*, 9-12 September 2013, Ghent, Belgium.

Poster presentations at international meetings

- A Yssel, D DeCoster, J Vanderleyden, H Steenackers., (2013) Comprehensive workflow for identifying conditionally essential genes using a T-POP transposon mutant library and Transposon directed insertion-site sequencing (TraDIS). Poster presentation at: *Applied Bioinformatics and Public Health Microbiology conference* , 15-17 May 2013, Cambridge, UK.
- A Yssel, E Peeters, J Vanderleyden, H Steenackers., (2013) Tampering with purine & pyrimidine biosynthesis modulates biofilm formation of *Escherichia coli* & *Salmonella*. Poster presentation at: *Eurobiofilms* , 9-12 September 2013, Gent, Belgium.
- A Yssel, E Peeters, H Steenackers, J Vanderleyden., (2013) Purine and pyrimidine biosynthesis are important for biofilm formation. Poster presentation at: *BIBR meeting*, Desember 2103, Lovain la Neuve, Belgium.

List of publications

- A Yssel, E Peeters, J Vanderleyden, D De Coster, A De Weerd, H Steenackers., (2014) Using a systemsbiology approach to study natural variations in ethanol tolerance in *Salmonella* and *E. coli*. Poster presentation at: *Advanced lecture series in Systems Biology*, 28 February - 5 March 2014, Innsbruck, Austria.
- A Yssel, E Peeters, D De Coster, A De Weerd, J, M Rahman, B Lories, V Kaefer, S Tschirner. Vanderleyden, H Steenackers., (2015) In spite of increased c-di-GMP levels pyrimidine starvation causes reduced biofilm formation in *Salmonella*. Poster presentation at: *c-di-GMP meeting*, 22-25 March 2015, Berlin. Germany.
- A Yssel, E Peeters, D De Coster, A De Weerd, J, M Rahman, B Lories, V Kaefer, S Tschirner. Vanderleyden, H Steenackers., (2015) *Salmonella* early stage biofilm formation is inhibited by pyrimidine starvation. Poster presentation at: *ASM conference on Biofilms*, 24- 29 October 2015, Chicago, USA.